Three-Dimensional Modelling of the Human Peri-Implantation Endometrium

Thomas Rawlings

A thesis submitted to the University of Warwick for the degree of Doctor of Philosophy.

MRC DTP in IBR

Division of Biomedical Sciences

Warwick Medical School

University of Warwick

January 2020

Contents

List of figures:

Chapter 5: EnSC-EEC interactions in complex organoid culture:

List of tables

Acknowledgements

First, I thank my supervisor Professor Jan Brosens for his invaluable advice, guidance and feedback throughout my project. Your infinite knowledge and devotion to reproductive science has continued to inspire my own passion and ambitions in the field. I also thank you for your mentorship, and for creating a wonderfully cohesive and collaborative lab group that I am so glad to be a member. In addition, to the WMS MRC DTP team, thank you for awarding me this opportunity. Being in a Doctoral Training Programme has been like having an extra safety net throughout my PhD, and I was so grateful that it was there when I did need help, so thank you.

From the lab, I first thank Dr Ruban Rex Peter Durairaj for being my first friend in the lab, for teaching me the ropes and for starting my winding PhD journey by discovering the 'ERB'. I thank Dr Emma Lucas for always knowing what to do in a crisis. Thank you for your scientific advice and scRNA-seq expertise, and for lending your office when I needed a minute of composure during a very stressful PhD. I must thank Komal Makwana, a friend for many years, for being my partner in the ever-growing Brosens' 'Team Organoid'. I appreciate your commitment to science, and for putting up with me. I thank Dr Pavle Vrljicak for his bioinformatic expertise and Dr Joanne Muter and Dr Paul Brighton for their continuous technical advice. I also thank the Implantation Clinic team for your dedication to your patients. I am above all indebted to the many hundreds of women who have donated tissue samples for our research. Without this clinic, its staff, and the generous donations from patients, I would not have been able to complete this thesis. To the whole Brosens group, I thank you all for your help, generosity, and friendship through my PhD.

In addition, to my wonderful family, thank you for your immeasurable love and support throughout my PhD. I especially thank my Mum and two sisters, Helen and Jane, for

looking after me during illness and for never giving up on me; without you, I would probably not have completed my PhD. To John, thank you for your endless love and encouragement. Thank you for always being there for me during my PhD, even when you were thousands of miles away. To my dearest friends Rebekah Jones, Emma Halling, Natasha Povey, Maria Diniz da Costa, and Komal Makwana, thank you for your unending support throughout my PhD. Finally, I thank Lady Gaga, Britney Spears, and the Spice Girls, of whom I saw live in concert during my PhD, for providing me with a soundtrack for writing this thesis.

Declaration

This thesis is submitted to the University of Warwick in support of my application for the degree of Doctor of Philosophy. It has been composed by myself and has not been submitted in any previous application for any degree apart from data presented in Figure 3.1 which was previously submitted for my MRC DTP in IBR MSc MD980 Laboratory Project 2 dissertation.

The work presented (including data generated and data analysis) was carried out by the author except in the cases outlined below:

1. The ERB model was originally developed by Dr Ruban Peter Durairaj (Peter Durairaj, 2017) and the initial preliminary data (Figure 3.1) was collected in collaboration with him, and related ERB methodologies, during my MRC DTP in IBR MSc MD980 Laboratory Project 2 dissertation.
2. Collaboration with Komal Makwana in data collection regarding the minimal differentiation medium experiment and immunohistochemical analysis of complex organoids.
3. Collaboration with Dr Emma Lucas in the preparation of the complex organoid scRNA-seq experiment and Dr Pavle Vrljicak in the bioinformatic analysis of the scRNA-seq dataset.

Abstract

Human embryo implantation is the rate-limiting step for successful pregnancy in assisted reproductive technology, and inappropriate endometrial embryo-quality biosensing is also associated with recurrent pregnancy loss. Elucidating the mechanisms underpinning the peri-implantation endometrium would enable the development of treatments for patients suffering with chronic fertility disorders. However, implantation is difficult to study. Therefore, simple *in vitro* models of human endometrial cells have been developed. However, the endometrium is a complex tissue made up of stromal cells (EnSC), epithelial glands, vasculature, and immune cells. An *in vitro* model that encompasses all aspects of the human endometrium would require a complex co-culture system. Therefore, three-dimensional (3D) culturing techniques are the most suitable. This study aimed to establish a protocol for a novel *in vitro* model of the peri-implantation endometrium by co-culturing primary EnSC and epithelial cells (EEC) using 3D culture techniques. In this study, two approaches were undertaken. The first involved the use of the Endometrial Regenerative Bodies (ERB) model, which was unsuccessful in achieving the study's aim. However, the second approach, involving the 3D co-culture of EnSC with endometrial gland organoids led to the establishment of a complex organoid culture. The growth conditions of the complex organoids were optimised by modifying the 3D matrix and medium conditions. The standard organoid growth matrix, Matrigel, a basement membrane derived hydrogel, was replaced with a purified Type I collagen hydrogel to provide a more physiological ECM for the EnSC. Direct interaction between the EnSC and EEC in the complex organoids was examined through the establishment of a minimal differentiation medium and single cell RNA-sequencing of a decidual time course of gland organoids and complex organoids. EnSC were able to induce the differentiation of EEC into a secretory phenotype in complex organoid cultures. The established complex organoid protocol offers a starting point for

developing a faithful *in vitro* model of the human peri-implantation endometrium, which will provide a step change in our collective ability to study human embryo implantation. A system that would be patient-specific, and in the long term developed into a high-throughput system for personalised medicine for the treatment of infertility.

List of abbreviations

8-bromo-cAMP	8-Bromoadenosine-3', 5'-cyclic monophosphate
ACTN1	Actinin 1
ALK	Activin-like kinase
ART	Assisted reproductive technologies
BM	Basement membrane
BSA	Bovine serum albumin
cAMP	Cyclic adenosine monophosphate
CAS	Crk-associated substrate
cEEC	Ciliated EEC
CFU	Colony forming unit
co-ExM	Complex organoid expansion medium containing E2
CRE	Camp response element
CREB	CRE binding protein
CREM	CRE modulator
Crk	Proto-oncogene c-Crk
CTB	Cytotrophoblasts
CXCL14	Cytokine chemokine (C-X-C motif) ligand 14
CXCR	Chemokine receptor type
D	Day
DCC	Dextran coated charcoal
DM	Differentiation medium containing MPA and camp
DMEM	Dulbecco's modified eagles medium
$DM_{min.}$	Minimal differentiation medium (for complex organoids)
DMSO	Dimethyl sulfoxide
$DM_{std.}$	Standard differentiation medium (for complex organoids)
DNA	Deoxyribonucleic acid
E2	Estradiol
E-cadherin	Epithelial cadherin
ECM	Extracellular matrix
EEC	Endometrial epithelial cell
EFA	Endometrial fibroblast activation
EFAM	EFA model
EGF	Epidermal growth factor
ELISA	Enzyme-linked immunosorbent assay

EnSC	Endometrial stromal cell
EpCAM	Epithelial cell adhesion molecule
ER	Estrogen receptor
ERB	Endometrial regenerative bodies
ExM	Expansion medium
FAK	Focal adhesion kinase
FBS	Fetal bovine serum
FOXO1	Forkhead box transcription factor O1
FSH	Follicle stimulating hormone
GDP	Guanosine diphosphate
GEF	Rho guanine nucleotide exchange factor
GEO	Gene expression omnibus
GIT	(GPCR)-kinase interacting protein
GTP	Guanosine triphosphate
hCG	Human chorionic gonadotropin
HGF	Hepatocyte growth factor
hPL	Human placental lactogen
IGFBP1	Insulin-like growth factor binding protein-1
IHC	Immunohistochemistry
IL	Interleukin
JAK/STAT	The Janus kinase/signal transducers and activators of transcription
k	Number of clusters
LH	Luteinising hormone
LIF	Leukaemia inhibitory factor
MACS	Magnetic-activated cell sorting
MAPK	Mitogen activated protein kinase
mg	Milligram
MLC-P	Myosin light chain phosphatase
MMP	Matrix metallopeptidases
MPA	Medroxyprogesterone acetate
MSC	Mesenchymal stem cell
MUC1	Mucin 1
MYLK	Myosin light chain kinase
MYPT1	Myosin phosphatase target subunit 1
NAC	N-acetyl L-cysteine
ncEEC	Non-ciliated EEC

NF-κB	Nuclear factor kappa-light-chain-enhancer of activated B cells
OPN	Osteopontin
P1/P2	Passage 1/2
PAEP	Progestogen-associated endometrial protein/ glycodelin
PAK	P21-activated kinase
PCR	Polymerase chain reaction
PDE	Phosphodiesterase
pg	Picogram
PGR	Progesterone receptor
PI3K	Phosphatidylinositol 3 kinase
PKA	Protein kinase A
PRL	Prolactin
PRLR	PRL receptor
PUGKO	Progestin uterine gland knockout
PVC	Perivascular stromal cells
PXN	Paxillin
QC	Quality control
RAC1	Ras-related C3 botulinum toxin substrate 1
RAG	Receptivity associated genes
RHOA	Ras homolog family member A
RNA	Ribonucleic acid
ROCK	Rho-associated, coiled-coil-containing protein kinase
RPL	Recurrent pregnancy loss
scRNA-seq	Single-cell RNA-sequencing
SD	Standard deviation
siRNA	Small interfering RNA
SNN	Shared nearest neighbour
SPP1	Secreted phosphoprotein 1
SR1	Serum replacement 1
Src	Proto-oncogene tyrosine-protein kinase Src
STB	Syncytiotrophoblasts
SUSD2	Sushi domain containing-2
TAC	Transit amplifying cell
TGFβ1	Transforming growth factor beta 1
TLN1	Talin 1
TNS1	Tensin 1

t-SNE	*T*-distributed Stochastic Neighbour Embedding
UMAP	Uniform Manifold Approximation and Projection
UMI	Unique molecular identifier
uNK	Uterine natural killer cell
VCL	Vinculin
VEGF	Vascular endothelial growth factor
αSMA	Alpha smooth muscle actin
µg	Microgram
2D	Two dimensional
3D	Three dimensional

Chapter 1:
Introduction

1.1 The human peri-implantation endometrium

The human female reproductive tract

The human internal female reproductive tract is composed of the uterus, Fallopian tubes, ovaries, cervix, and vagina. Unlike many other mammalian species, the human uterus consists of a singular uterine cavity (Spencer et al., 2012). The fetal uterus develops from the fusion of the paramesonephric (Müllerian) ducts before eight weeks gestation, forming a tubular structure consisting of a luminal epithelium enveloped by a layer of undifferentiated mesenchyme (O'Rahilly et al., 1973). The mesenchymal layer differentiates into an underlying smooth muscle layer (myometrium) and a luminal endometrial stroma at 22 weeks (Song, 1964).

The human endometrium

The human endometrium is the secretory mucosal lining of the uterus and it provides the immunoprivileged and nourishing local environment vital for embryo implantation and placentation (Tabibzadeh, 1998, Gellersen and Brosens, 2014). The endometrium consists of two major layers, the stratum basalis and the stratum functionalis (Padykula, 1991, Brenner et al., 1994) (Fig. 1.1). The functionalis, or functional layer, lies above the basalis, or basal layer, and is epithelialised (Padykula, 1991, Gray et al., 2001a). The arcuate arteries of the uterus provide the endometrial blood supply (Rogers, 1996, Farrer-Brown et al., 1970). The arcuate arteries infiltrate through the myometrium and terminate in the endometrium as spiral arteries, which supply the endometrium, and the placenta during pregnancy (Farrer-Brown et al., 1970). The human functionalis is hormone responsive and cycles through phases of proliferation, differentiation, and degradation (menstruation), in what is called the menstrual cycle, in preparation for a potential implanting embryo. However, the underlying basalis remains stable and instead functions as the endometrial germinal layer, maintaining a perivascular

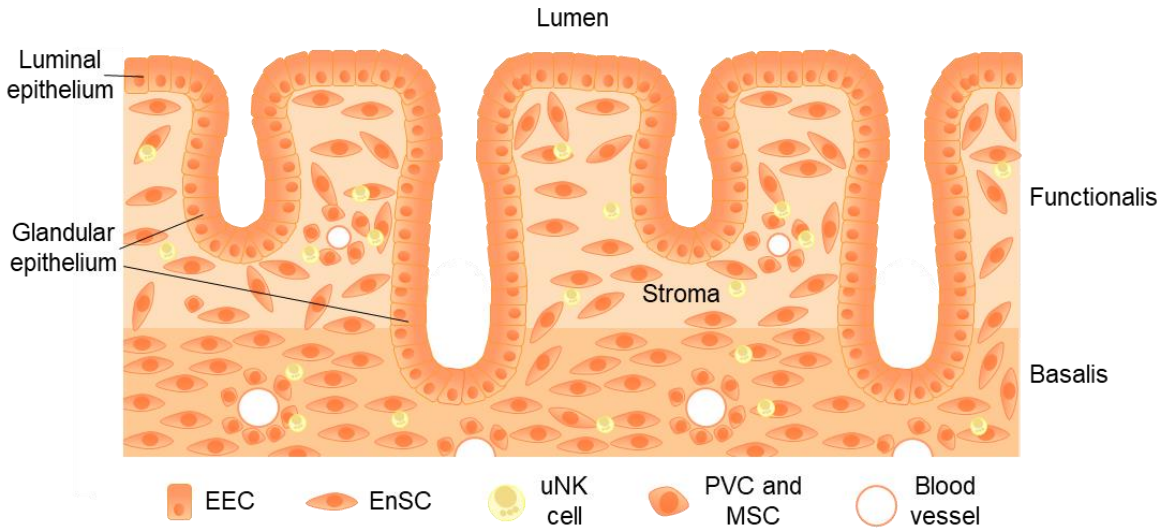

Figure 1.1. A schematic of the human endometrium. Cell types are labelled in the key below the diagram. The endometrium comprises two layers: the stratum functionalis and the stratum basalis. The functionalis is superficial and is covered in luminal epithelium. Glandular epithelium grows deep into the persistent basalis layer of the endometrium. The endometrium is vascularised and contains a population of uterine natural killer (uNK) cells. The endometrium is vascularised with spiral arteries and around these blood vessels are perivascular stromal cells (PVC) and resident mesenchymal stem cells (MSC). Adapted from (Gargett et al., 2015)

niche for resident mesenchymal stem cells (MSC) from which the functionalis regenerates each cycle (Gargett, 2006, Gargett et al., 2015).

The endometrial stroma is a highly glandular tissue (Fig. 1.1). The endometrial glands are essential in early pregnancy as they provide nutrition to the implanting embryo through secretions of glycogen and glycoproteins, collectively designated as histotroph (Gray et al., 2001a). The process of endometrial gland development, or adenogenesis, comprises of the initial budding of the luminal epithelium, followed subsequently by invagination into the stroma. Later, as the endometrial glands further develop, there is extensive branching and coiling into the underlying stroma (Cooke et al., 2013). However, despite the mesenchyme forming an endometrial stroma at 22 weeks gestation, adenogenesis at this stage is superficial (Cooke et al., 2013, Song, 1964, Valdes-Dapena et al., 1973, O'Rahilly et al., 1973). Neonates possess only sparse and shallow glandular epithelium. Indeed, much of endometrial adenogenesis occurs postnatally (Cooke et al., 2013, Gray et al., 2001a). Table 1.1 summarises a list of factors that influence endometrial adenogenesis (Gray et al., 2001a). The endometrial glands continue to develop until puberty, where they reach maturity, extending through the endometrium into the myometrium (Valdes-Dapena et al., 1973).

The structural integrity of the endometrium is maintained by its extracellular matrix (ECM). Like many tissues, the major structural component of the endometrial stromal ECM is collagen. In the stroma, collagen is deposited by endometrial cells and organised into fibrils. The major fibril-forming collagens of the endometrial ECM are collagens I, III, and V, with collagen I being the most abundant collagen species (Aplin et al., 1988, Aplin and Jones, 1989, Iwahashi et al., 1996, Kisalus et al., 1987). Microfibrils, such as collagen VI and fibrillin, associate with the bundles of larger

collagen fibrils and provide further integration and stability of the ECM (Aplin and Jones, 1989, Aplin et al., 1995).

The ECM not only provides structural support but also mediate essential cellular functions such as cell-matrix adhesion, survival, migration, proliferation, and differentiation. The ECM interacts with endometrial cells through integrins and other cell surface receptors. Several adhesive glycoproteins such as fibronectin, tenascin C, and thrombospondin 1, are found in the endometrial ECM and are important for cell adhesion and migration (Glasser et al., 1987, Aplin et al., 1988, Rider et al., 1992, Iruela-Arispe et al., 1996, Vollmer et al., 1990). Additionally, the endometrial ECM contains glycosaminoglycans (GAGs). GAGs are polar and hydrophilic heteropolysaccharides usually consisting of repetitive disaccharide units of a hexosamine with either uronic acid or galactose (Kresse and Schönherr, 2001). GAGs covalently bind to proteins and form proteoglycans (PGs). The major GAGs of the endometrial ECM are Chondroitin sulphate, dermatan sulphate, heparan sulphate and hyaluronic acid (HA) (Cidadão et al., 1990, Oliveira et al., 2015). HA is unlike other GAGs due it being not sulphated, and therefore does not form a PG (Berto et al., 2001). PGs are found on the cell surface as well as the ECM and can interact with laminins, collagens, and fibronectin as well as a variety of cytokines and growth factors. These interactions are involved in angiogenesis, cell proliferation, migration, adhesion, and differentiation (Merle et al., 2000, Couchman and Pataki, 2012, Schaefer and Schaefer, 2010, Oliveira et al., 2015).

The ECM structure surrounding the glandular and luminal epithelium, as well as blood vessels, is called the basement membrane (BM) (Wewer et al., 1985, Aplin et al., 1988, Aplin and Jones, 1989). Microfibril fibrillin 1 is associated with connecting the stromal ECM interface with the BM (Fleming and Bell, 1997). The BM contains a different assortment of proteins, including laminins, type IV collagen and heparan

sulphate PG (Faber et al., 1986, Wewer et al., 1985, Aplin et al., 1988). The structural framework of the BM is provided by a lattice of collagen IV (Timpl, 1996). Enactin, a glycoprotein, links laminin to the collagen IV lattice network (Yelian et al., 1993). In the BM surrounding epithelium, laminins are large heterotrimeric glycoproteins where they function in epithelial cell attachment, polarisation, and differentiation (Timpl, 1996).

The menstrual cycle

The functionalis of the endometrium is sensitive to ovarian hormone stimulation. This tissue cycles through periods of proliferation, differentiation and menstruation and repair (Brosens et al., 2002, Gellersen and Brosens, 2014) (Fig. 1.2). The human endometrium is exceptionally malleable and maintains its regenerative capacity through puberty until menopause. Typically, a woman from a developed nation will experience approximately 350-400 menses in their lifetime (Strassmann, 1997, Strassmann, 1999).

Proliferative phase

The proliferative phase (Cycle day: 5-13) commences following the completion of menstruation (Cycle day: 1-4) (Fig. 1.2). Endometrial regeneration is driven by the rise in estradiol levels from ovarian follicle granulosa cells. In fact, the proliferative phase endometrial estradiol concentration is 5-8 times higher than in serum (Huhtinen et al., 2012). This surge drives regeneration through intense proliferation from the underlying stable basalis. Proliferative endometrial stromal cells (EnSC) maintain a fibroblast-like morphology, including mature secretory pathway organelles, limited cytoplasm and elongated indented nuclei (Cornillie et al., 1985, Lawn et al., 1971).

Table 1.1: Factors involved in endometrial adenogenesis. Data distilled from (Gray et al., 2001a)

Factor	Role in adenogenesis	References
Epithelial-stromal interactions	• Tissue recombination studies in mice demonstrate that EnSC play a direct role in gland development	(Cunha et al., 1985, Donjacour and Cunha, 1991, Cunha and Young, 1992, Cooke et al., 1997)
ECM	• Glycosaminoglycans (GAG) affect EEC development directly and indirectly. • Mediate epithelial-stromal interactions • GAG facilitate growth factors binding to receptors on EEC • Non-sulphated GAGs such as hyaluronic acid accumulate at tips of proliferating glands • MMP affect gland development by ECM remodelling • ECM affects glandular branching morphogenesis through influencing cell cycle arrest and apoptosis	(Bartol et al., 1993, Bartol et al., 1988, Spencer et al., 1993, Werb et al., 1996)
Growth factors	• EnSC derived growth factors mediate gland development: • Fibroblast growth factor (FGF)-7 stimulates EEC proliferation • FGF-10 is essential for branching morphogenesis • Hepatocyte growth factor (HGF) induces epithelial proliferation • Insulin-like growth factor (IGF) I and II induce EEC differentiation	(Bellusci et al., 1997, Ohmichi et al., 1998, Weidner et al., 1993, Yamasaki et al., 1996, Rubin et al., 1995, Wang and Chard, 1999, Thiet et al., 1994)
Estrogen	• ERα expression is increased in proliferating gland epithelium in mice post-natally • Glandular proliferation	(Fishman et al., 1996, Greco et al., 1991, Branham et al., 1985)
Prolactin	• PRL stimulates EEC differentiation • PRLR is expressed in glands • Possibly involved in proliferation but not confirmed	(Freeman et al., 2000, Stewart et al., 2000, Telleria et al., 1998)

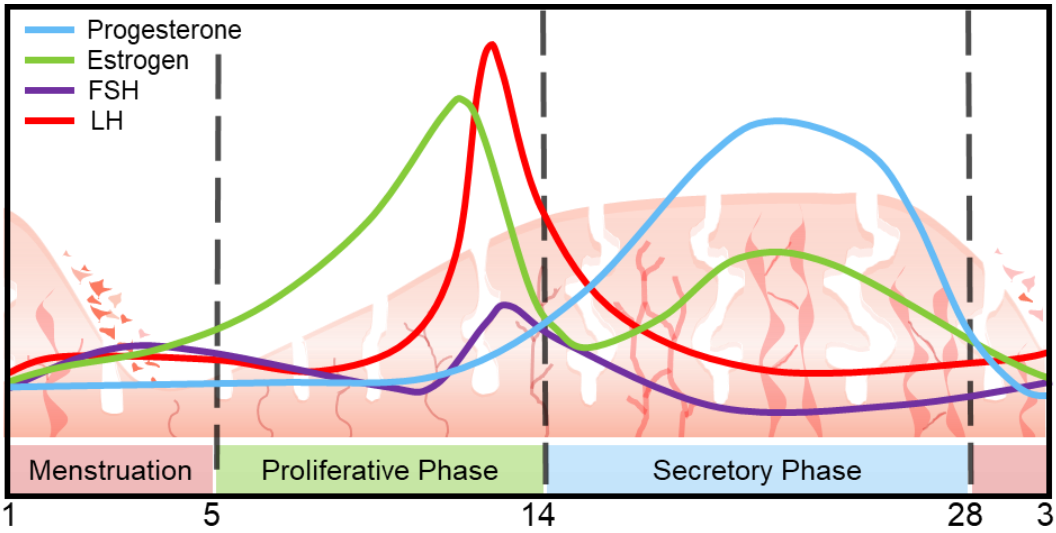

Figure 1.2. The menstrual cycle. The menstrual cycle describes the cyclic changes in ovarian hormones estrogen and progesterone. Rising estrogen leads to the proliferation of the endometrium (proliferative phase). A surge in luteinising hormone (LH) and increasing follicle stimulating hormone lead to ovulation where a mature egg cell is released from the ovary on day 14. Ovulation gives rise to the corpus luteum in the ovary which produces progesterone, where EnSC decidualise into decidual cells in preparation for an implanting embryo (secretory phase). In the absence of an implanting embryo, the ovarian hormone stimulation drops, and the endometrial tissue breaks down and sheds (menstruation). The cycle then repeats with subsequent regeneration from resident progenitor cells and rising estrogen.

The regenerative capacity of the endometrium is unsurpassed in the human body, with the thickness of the endometrium growing from approximately 4-5 mm (Cycle day: 4) to 10 mm at ovulation (Cycle day: 14) each cycle (Bromer et al., 2009). In addition, the endometrial epithelial cells (EEC) in the glands regrow, leading to the expansion of narrow tubes (Okulicz et al., 1997, Padykula et al., 1989). Unlike fetal adenogenesis, post-menstrual gland development originates from progenitor cells in the basalis and proliferates up to the luminal epithelium (Gray et al., 2001a). Endothelial cells of the spiral arteries efficiently revascularize the freshly regenerated tissue. The rising levels of estradiol ultimately induce a surge of luteinizing hormone (LH), triggering ovulation, and the completion of the proliferative phase (Gellersen and Brosens, 2014).

Secretory phase

Following ovulation, the remaining ruptured follicle transforms into the corpus luteum. This transient structure produces the steroid hormone progesterone, where rising circulatory levels inhibit EnSC proliferation (Johansson and Wide, 1969). Progesterone also induces endometrial differentiation (decidualisation). Prior to morphological changes in the EnSC, endometrial edema is observable at cycle day 18-21, before regressing by cycle day 23 (Rock and Bartlett, 1937, Gellersen and Brosens, 2014) (Fig. 1.2). At cycle day 23, morphological differentiation of EnSC bordering the terminal spiral arteries is observable (Rock and Bartlett, 1937). Decidualising EnSC become engorged with prominent cytoplasm and the nuclei enlarge (Kajihara et al., 2014). Further observable morphological changes to the EnSC include expansion of secretory organelles, accumulation of cytoplasmic glycogen and lipid droplet and an increase in nucleoli (Kajihara et al., 2014).

The composition of endometrial ECM is hormonally controlled and is extensively remodelled during decidualisation. The ratios of stromal ECM collagens III and V shift

quantitatively upon decidualisation (Iwahashi et al., 1997, Aplin et al., 1988, Aplin and Jones, 1989). In addition, BM proteins collagen IV and laminin encapsulate decidualising EnSC (Iwahashi et al., 1997). Decidualising EnSC also produce pseudopodia-like processes that extend into the ECM and to other EnSC (Lawn et al., 1971). These cells also attain phagocytic activity, enabling them to participate in the decidual remodelling of the ECM (Cornillie et al., 1985).

Cues for EnSC decidualisation

Progesterone acts upon EnSC by binding and activating its cognate nuclear receptor, the progesterone receptor (PGR). Like other nuclear receptors, PGR comprises functionally district domains to enable ligand binding, DNA binding and transcriptional regulation (Brosens et al., 2004, Beato and Klug, 2000). Progesterone is lipophilic and therefore can pass across the plasma membrane of EnSC freely and bind to PGR. Ligand binding induces a conformational change enabling the chaperone dissociation and dimerization. The bound, dimerized PGR then binds to promoters of gene targets, inducing transcription. There are two major isoforms of PGR, PGR-A and PGR-B, which derive from the same gene but are transcribed by different promoters (Kastner et al., 1990). PGR-A and -B respond differently to progesterone binding (Gellersen and Brosens, 2014). When bound to progesterone, PGR-A inhibits PGR-B activity (Vegeto et al., 1993). Furthermore, PGR-A and PGR-B expression is dynamic through the menstrual cycle. PGR-B is abundant in both EnSC and EEC in the proliferative phase, but expression falls post-ovulation (Jabbour and Critchley, 2001). PGR-A expression persists in EnSC throughout the menstrual cycle, rendering it the dominant isoform (Mote et al., 1999).

However, the lag period following rising progesterone circulation and the onset of EnSC morphological differentiation suggests that other cues are required for decidual initiation (Gellersen and Brosens, 2003). Moreover, *in vitro* studies of primary EnSC

have demonstrated that there are very few genes acutely responsive to progesterone treatment alone (Brosens et al., 1999, Aghajanova et al., 2010). There have been several *in vitro* experiments that have demonstrated that other factors are necessary for decidualisation. Table 1.2 summarises various EnSC decidual cues. Therefore, although progesterone is essential for EnSC decidualisation, these studies evidence that progesterone is insufficient to mount a decidual response in the human endometrium alone.

In addition to progesterone, there is tremendous evidence suggesting the activation of the cyclic adenosine monophosphate (cAMP) pathway is essential for decidualisation (Brosens et al., 1999). cAMP is a second messenger produced by ligand bound G protein coupled receptors (GPCR). GPCR, when bound, activate adenylyl cyclase, which catabolises adenosine triphosphate (ATP) into adenosine diphosphate (ADP) and cAMP. A major target of cAMP is protein kinase A (PKA). PKA is a holoenzyme composed of 2 regulatory and 2 catalytic subunits. The regulatory subunits can bind cAMP, which releases the catalytic subunits, enabling PKA to phosphorylate downstream targets (Skalhegg and Tasken, 2000, Kopperud et al., 2003). Targets for phosphorylation include the cAMP response element (CRE) binding protein (CREB) and CRE modulator (CREM) (Mayr and Montminy, 2001, Lamas et al., 1996). Both CREB and CREM are members of the basic region/leucine zipper (bZIP) transcriptional regulator family and bind to CRE DNA sequences in target promoters as dimers (Luscombe et al., 2000).

One study demonstrated that cAMP concentration is significantly higher in secretory phase endometrial biopsies than in proliferative samples (Bergamini et al., 1985). In addition, adenylyl cyclase activity is significantly higher in the endometrium than in

Table 1.2: Decidualisation cues and related pathways. Data distilled from (Gellersen and Brosens, 2014)

Decidual cues	Mode of action	References
Endocrine cues	• Progesterone drives differentiation of the endometrium • Lag period of 9 days post ovulation before morphological EnSC differentiation present • Relaxin enhances decidualisation in EnSC in vitro. • Prostaglandin E2 (PGE2) increases intracellular cAMP levels	(Johansson and Wide, 1969, Gellersen and Brosens, 2003, Palejwala et al., 2002, Ivell et al., 2003, Tabanelli et al., 1992, Milne et al., 2001, Salamonsen et al., 2016)
Paracrine cues	• EEC, immune cells and endothelial cells secrete cytokines, growth factors involved in decidualisation. • Removal of luminal epithelium abrogates EnSC decidualisation in rodents	(Gellersen and Brosens, 2014, Lejeune et al., 1981)
Interleukins	• Inhibition of IL-11 reduces decidual gene expression • IL-1β promotes implantation and decidualisation by upregulating integrin αvβ3. This binds ECM ligands. This upregulates cyclo-oxygenase 2 (COX-2) and therefore increases cAMP levels intracellularly. • Leukaemia inhibitory factor (LIF) is a IL-6 type cytokine. Critical in implantation and produced only by epithelial cells. Enhances decidualisation of EnSC.	(Karpovich et al., 2005, Geisert et al., 2012, van Mourik et al., 2009, Hwang et al., 2002, Tamura et al., 2002, Shuya et al., 2011)
TGFβ signalling	• Activins, inhibins and follistatin regulate decidualisation. • Morphogen bone morphogenetic protein (BMP) 2 drives expression of decidual genes.	(Jones et al., 2002, Jones et al., 2006, Li et al., 2007)
Notch signalling	• Inhibition of Notch reduces decidualisation of EnSC. • Notch receptors expressed in EnSC	(Afshar et al., 2011, Mikhailik et al., 2009)
Lipids	• Endocannabinoid system is involved in decidualisation	(Brar et al., 2001)

the myometrium (Tanaka et al., 1993). Studies have shown that *in vitro* primary EnSC cultures treated with estradiol and a progestin not only induce decidual genes but also elevate intracellular cAMP levels, albeit modestly. Furthermore, decidual gene induction is inhibited when differentiated in the presence of a PKA inhibitor. These studies indicate that cAMP signalling is essential for EnSC decidualisation (Matsuoka et al., 2010, Yoshino et al., 2003, Brar et al., 1997). Phosphodiesterases (PDE) are endogenous enzymes that degrade cAMP. The most abundant PDE in the endometrium is PDE4. Studies have shown that cAMP accumulates in EnSC when PDE4 is inhibited, and decidual gene induction is enhanced (Bartscha and Ivell, 2004, Bartsch et al., 2004). Moreover, a study reported that EnSC maintain a feed-forward mechanism to enhance PKA activity by downregulating the regulatory PKA subunits instead of using an inhibitory feedback loop (Telgmann and Gellersen, 1998).

Overall, both the cAMP and PGR pathways have been demonstrated to be essential for EnSC decidualisation. These pathways converge in order to induce the extensive decidual reprogramming of gene expression in EnSC (Gellersen and Brosens, 2014).

Decidual markers

The major decidual marker is prolactin, encoded by *PRL* (Maslar and Riddick, 1979). In pregnancy, prolactin levels peak between 18 to 26 weeks in the amniotic fluid. It was discovered prolactin is produced by the decidua and since then it has been demonstrated that decidualising EnSC induce *PRL* transcription from day 22 of the cycle (Kletzky et al., 1985, Ben-Jonathan et al., 1996). Another decidual maker is IGF-binding protein-1 (IGFBP-1), encoded by *IGFBP1* (Rutanen et al., 1985). IGFBP-1 is also enriched in amniotic fluid and peaks a few weeks before the rise of PRL (Wathen et al., 1993). *IGFBP1* transcripts are also present in non-pregnant decidualising EnSC. Studies have demonstrated that IGFBP-1 is involved in the regulation of IGF-1 bioavailability and trophoblast invasion (Gleeson et al., 2001,

Carter et al., 2004). Since, *PRL* and *IGFBP1* have become an established marker genes for the assessment of EnSC decidualisation (Gellersen and Brosens, 2014).

Other highly expressed EnSC decidual markers include left-right determination factor 2 (LEFTY2). LEFTY2 is a nodal signalling pathway inhibitor and member of the TGFβ super family. In addition, when it was first discovered, LEFTY2 named endometrial bleeding-associated factor (Kothapalli et al., 1997, Tabibzadeh, 1998). Other makers include transcription factors forkhead box protein O1 (FOXO1) and CCAAT/enhancer-binding protein-β (C/EBPβ), both induced in EnSC when treated with 8-Bromoadenosine-3', 5'-cyclic monophosphate (cAMP) *in vitro* (Christian et al., 2002).

Decidualising EnSC, acute senescence and immune surveillance

More recently, studies have purported that a proportion of decidualising EnSC differentiate into acute senescent decidual cells (Brighton et al., 2017, Lucas et al., 2018) (Fig. 1.3). These cells are progesterone resistant, secrete inflammatory mediators and express recognised senescence marker genes, such as tumour suppressor gene $p16^{INK4}$ (Brighton et al., 2017). In general, cellular senescence describes cells in permanent cell cycle arrest that secrete a combination of molecules collectively named as senescence associated secretory phenotype (SASP). Chronic senescence accumulates gradually over time through aging and cumulatively has a negative impact on organ or tissue function. However, acute senescence often involves orchestrated biological processes related to inflammation and tissue remodelling (van Deursen, 2014, Childs et al., 2017, Brighton et al., 2017). Furthermore, acute senescent cells are only transiently present in a tissue, as they are cleared by immune cells. The SASP of these acute senescent cells intensify the initial decidual inflammatory response. Therefore, these data indicate this transient

population of cells is crucial for EnSC differentiation and endometrial embryo receptivity (Brighton et al., 2017, Lucas et al., 2018).

However, in order to clear acute senescent cells from the endometrium, decidual cells recruit and activate a unique population of immune cells: the uterine natural killer (uNK) cells. The uNK cells have been shown to eliminate acute senescent cells through perforin- and granzyme-containing granule exocytosis (Brighton et al., 2017). This subpopulation of NK cells is positive for cluster of differentiation 56 (CD56) and CD16 negative (Croy et al., 2006). Post-ovulation, uNK cell numbers increase substantially in the endometrium. Decidualised EnSC produce cytokines interleukin (IL) 11, IL-15 and IL-33 which are all implicated in the proliferation and activation of uNK cells (Ashkar et al., 2003, Ain et al., 2004, Godbole and Modi, 2010, Salker et al., 2012a). In turn, uNK cells clear the acute senescent decidual population allowing for a potential embryo to implant into a tissue enriched with decidual cells (Brighton et al., 2017). Furthermore, during pregnancy uNK cells are implicated in the remodelling of the spiral arteries prior and during trophoblast invasion (Xiong et al., 2013, Chazara et al., 2011).

Endometrial gland differentiation

The post-ovulatory rise in progesterone levels also has a profound effect on endometrial glands. First, progesterone downregulates the expression of both PGR isoforms in the glands (Wang et al., 1998). The glands undergo secretory transformation by which the EEC become highly secretory and the gland lumens widen (Burton et al., 2007, Burton et al., 2010). The composition of the secretions from the endometrial glands have been studied extensively during the menstrual cycle. The glandular secretions largely consist of glycogen and glycoproteins, as well as other components such as amino acids and lipid droplets. The major glandular

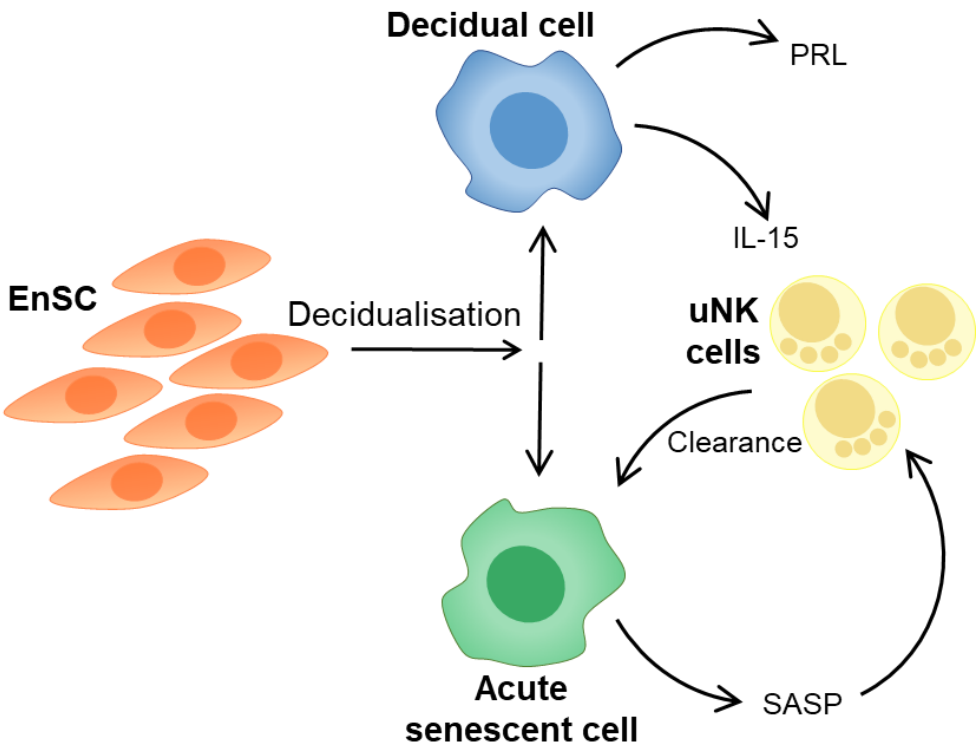

Figure 1.3. A schematic of the EnSC decidual subpopulation dynamics. It has been proposed that during decidualisation, a subpopulation of stressed EnSC do not differentiate into mature decidual cells, but instead undergo acute senescence. The acute senescent cells secrete SASP, containing many inflammatory mediators. Decidual cells secrete IL-15 which activates uNK cells to clear the acute senescent cells by granule exocytosis. The cell clearance allows for remodelling and rejuvenation of the endometrium for embryo implantation. Adapted from (Brighton et al., 2017).

product is glycodelin, a dimeric glycoprotein, also referred to as progestogen-associated endometrial protein (PAEP) and encoded by *PAEP* (Burton et al., 2002). These carbohydrate-rich secretions are referred to as histotroph as they provide nutrition for potential pre-implantation embryos as well as for an implanted conceptus (Burton et al., 2002).

Besides providing a source of nutrients for the implanting embryo, the glands induce of genes related to embryo receptivity and implantation. In humans, glandular and luminal epithelium have distinct molecular signatures. Analysis of mid-secretory phase uterine fluid as well as spent media from *in vitro* differentiated epithelial cultures has identified many types of secreted protein important for implantation such as cytokines, chemokines, growth factors, proteases and inhibitors (Salamonsen et al., 2016, Spencer et al., 2012, Hannan et al., 2010b, Hempstock et al., 2004a, Vilella et al., 2013)

Research relating to the role of the endometrial glands in implantation has been undertaken using animal model systems. For example, uterine gland knock-out (UGKO) sheep, produced by progestin-induced gland knock out, exhibit normal fertilisation. However, embryo implantation was restricted (Gray et al., 2001b). Progestin uterine gland knockout (PUGKO) mice also exhibit implantation failure. Uteri from PUGKO mice also have reduced expression of key implantation genes (Kelleher et al., 2016). These data suggest that the endometrial glands are essential for embryo implantation.

Many proteins secreted by glands implicated in endometrial receptivity are also associated with blastocyst adhesion to the luminal epithelium. For example, secreted phosphoprotein 1, encoded by *SPP1*, also termed osteopontin (OPN), is secreted by the endometrial glands and contains RGD, a tripeptide integrin-binding motif

containing amino acids arginine, glycine, and aspartate, which facilitates the adhesion of an embryo to the luminal epithelium (Singh and Aplin, 2009, Berneau et al., 2019). Furthermore, Leukaemia inhibitory factor, encoded by *LIF*, is an important protein related to blastocyst adhesion, as well as having roles in embryonic development and trophoblast differentiation (Salleh and Giribabu, 2014). Furthermore, the aforementioned glycodelin is implicated in embryonic interactions with the luminal epithelium. An *in vitro* study demonstrated that the induction of glycodelin improves trophoblast spheroid attachment to a monolayer endometrial cell line culture. Furthermore, silencing *PAEP* completely abrogated the attachment (Uchida et al., 2007).

Growth factors such as epidermal growth factor (EGF), vascular endothelial growth factor (VEGF) and transforming growth factor beta (TGFβ) are also expressed by human endometrial glands (Hempstock et al., 2004b). The cognate receptors for these growth factors are present in the trophectoderm of blastocysts. These growth factors have all been implicated in embryo implantation. For example, EGF induces proliferation of cytotrophoblasts and stimulates human chorionic gonadotropin (hCG) and human placental lactogen (hPL) secretion by syncytiotrophoblasts (Maruo et al., 1997, Ladines-Llave et al., 1991). In addition, VEGF promotes trophoblast adhesion to the luminal epithelium (Binder et al., 2014). Finally, studies have shown that TGFβ increases ECM remodelling, such as increased secretion of fibronectin, thereby facilitating endometrial adhesion for invading trophoblasts (Feinberg et al., 1994).

Regulation of endometrial gland secretions

Decidualising EnSC, the implanting embryo and the corpus luteum all regulate endometrial gland secretions (Fig. 1.4). Studies suggest that glandular differentiation by corpus luteum secreted progesterone is most likely achieved indirectly, through paracrine signalling from decidualising EnSC (Cooke et al., 1997, Arnold et al., 2001).

For example, decidualising EnSC regulate gland differentiation through the secretion of PRL. The PRL receptor (PRLR) is most highly expressed in the endometrial glands during the mid-secretory phase (Jones et al., 1998). It has been demonstrated that EnSC-secreted PRL activates the Janus kinase/signal transducers and activators of transcription (JAK/STAT) and mitogen activated protein kinase (MAPK) pathways in the endometrial glands, stimulating glandular differentiation. In parallel, the phosphatidylinositol 3 kinase (PI3K) pathway is also activated, inhibiting gland cell apoptosis (Jabbour et al., 2002).

Animal models demonstrate that uterine stroma is essential for epithelial differentiation (Cooke et al., 1997, Cunha and Young, 1992). For example, in one study, stromal and epithelial tissue from bladder and vagina were recombined and grown in intact female mice. Three weeks later an ovariectomy was performed and 1 week after this, the hosts were subjected to hormonal treatment. Bladder epithelium grown with vaginal stroma exhibited a multi-fold estrogen-induced proliferative response when compared to vaginal epithelium grown with bladder stroma. The blunted response by the vaginal epithelium could be reversed if recombined with fresh vaginal stroma. These observations demonstrated that estrogen-induced epithelial proliferation depends upon an appropriate stromal environment (Cunha and Young, 1992).

As well as the stroma, the implanting embryo regulates glandular function. In the absence of an embryo, gland secretions diminish in the late secretory phase (Dockery et al., 1988). However, in a pregnant cycle, glycogen continues to accumulate through to at least 6 weeks gestation, indicating secretion is sustained in early pregnancy by the conceptus (Spencer et al., 2004, Burton et al., 2007). Invading syncytiotrophoblasts secrete hPL, which shares 67% sequence homology with PRL,

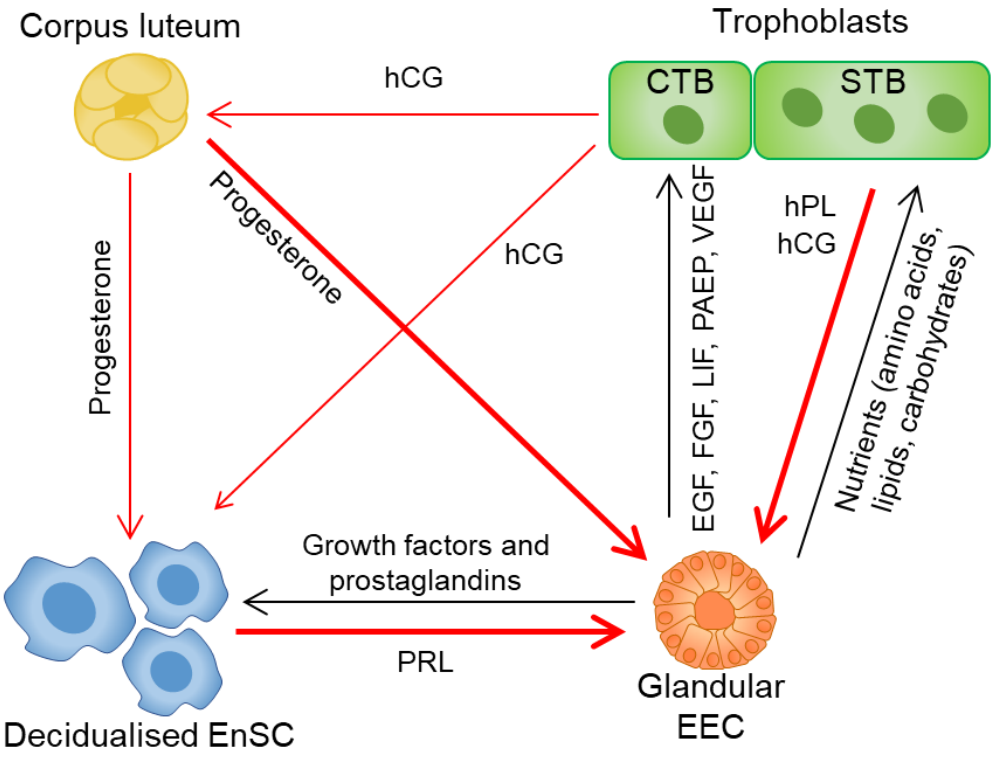

Figure 1.4. Schematic of the proposed interrelationships between endometrial glands, decidualised EnSC, corpus luteum and invading trophoblast cells during early pregnancy. In this model the invading trophoblasts (CTB: cytotrophoblasts; STB: syncytiotrophoblasts) produce hCG which maintains the corpus luteum. The corpus luteum therefore continues to produce progesterone which maintains the decidualised EnSC and differentiated gland EEC. The EnSC also secrete PRL which enacts upon the gland EEC through the PRLR to maintain a secretory phenotype. The trophoblasts also act upon the glands directly with hCG and hPL. The glands in turn produce growth factors, nutrients and receptivity markers (such as leukaemia inhibitory factor (LIF) and glycodelin (PAEP)). These secreted products in turn improve trophoblast invasion, forming a positive feedback loop. Overall, the human conceptus may be able to manipulate glandular EEC activity to further establish the pregnancy. Red arrows indicate how these cell types act upon the glands directly and indirectly. Adapted from (Burton et al., 2007, Kelleher et al., 2019)

enabling it to bind PRLR of endometrial glands and maintain gland secretions (Burton et al., 2007). A study in which PL was infused into ovine uteri increased the abundance of endometrial glands and upregulated the expression of *SPP1* (Noel et al., 2003).

The hCG receptor (LHCGR) of the endometrial glands is purportedly maximally expressed during the secretory phase (Reshef et al., 1990). A study demonstrated that treatment with exogenous hCG induced female baboons to upregulate the secretion of glycodelin (Hausermann et al., 1998). A positive feedback mechanism between the glands and the conceptus has been described. In this feedback loop, the endometrial glands secrete EGF, stimulating embryonic release of hPL and hCG by syncytiotrophoblasts. In turn, hPL and hCG induce further glandular secretion including more EGF, therefore ensuring the growth and maintenance of the implanted conceptus (Burton et al., 2007, Burton et al., 2010).

Implantation and receptivity

Embryo implantation requires both a receptive endometrium and a competent embryo to be successful. Endometrial receptivity is transient, and the 'window of implantation' is approximately 6-10 days after the LH surge (Cycle day: 20-24) (Paria et al., 2001) (Fig. 1.1). The transient nature of endometrial receptivity ensures that successful implantation requires the coordinated development of both the embryo and endometrium. This coordination reduces the risk of implanting a poor-quality embryo (Gellersen and Brosens, 2014). Clinically, assisted reproduction technologies (ART) provide sub-fertile couples the option of treatment for successful pregnancy. However, implantation failure continues to be the major rate limiting step for achieving successful pregnancy. In general, only approximately 25% of transferred embryos successfully implant (Boomsma et al., 2009, Ferraretti et al., 2012). Currently, the physiological and molecular mechanisms underpinning successful implantation and

implantation failure are only partly understood (Weimar et al., 2013). Recently, many studies have been conducted in search of identifying key molecular mechanisms and potential receptivity biomarkers. Table 1.3 summarises a list of endometrial genes implicated in receptivity (Bhagwat et al., 2013).

Traditionally, embryo implantation has been described as a consequential process of apposition, adhesion, penetration of the luminal epithelium and invasion into a passive stroma (Simón et al., 2001, Meseguer et al., 2001). Human embryo implantation involves extensive tissue remodelling and has been described as paralleling the stages of tumour invasion. However, recent evidence has described maternal endometrial cells actively encapsulating an implanting embryo (Brosens and Gellersen, 2010). Decidualised EnSC transiently attain a myo-fibroblastic phenotype, in which they become migratory and can produce ECM-degrading matrix metallopeptidases (MMP) (Anacker et al., 2011). *In vitro* studies have demonstrated primary decidualised EnSC, grown as a monolayer, can actively migrate to engulf a competent blastocyst and this process is essential for trophoblast outgrowth (Grewal et al., 2008, Grewal et al., 2010). However, the endometrium has been described as a biosensor for embryo quality. Decidualised EnSC migration has been shown to be dependent on the quality of the embryo attempting to implant (Teklenburg et al., 2010b, Brosens et al., 2014) (Fig. 1.5). Several studies have demonstrated that decidualised EnSC can sense high- and poor-quality embryos. For example, in one *in vitro* study, primary decidualised EnSC selectively migrated towards high quality human embryos only, but did not migrate towards poor quality embryos (Teklenburg et al., 2010b, Weimar et al., 2012).

Table 1.3. Human Gene Expression Endometrial Receptivity database (HGEx-ERdb) top 25 Receptivity Associated Genes (RAGs). Analysis of 84 data sets (24 studies) available on the human endometrial gene expression revealed expression of 12,099 genes during the secretory phase. These genes were scored for their expression status and also for their expression pattern in the secretory phase. Information collected from (Bhagwat et al., 2013).

Gene Symbol	Gene Name
SPP1	secreted phosphoprotein 1
GPX3	glutathione peroxidase 3 (plasma)
PAEP	progestagen-associated endometrial protein
IGFBP7	insulin-like growth factor binding protein 7
IL15	interleukin 15
CD55	CD55 molecule, decay accelerating factor for complement (Cromer blood group)
CLDN4	claudin 4
DPP4	dipeptidyl-peptidase 4
COMP	cartilage oligomeric matrix protein
LAMB3	laminin, beta 3
TIMP1	TIMP metallopeptidase inhibitor 1
DCN	decorin
LIF	leukemia inhibitory factor (cholinergic differentiation factor)
TCN1	transcobalamin I (vitamin B12 binding protein, R binder family)
C4BPA	complement component 4 binding protein, alpha
IL6ST	interleukin 6 signal transducer (gp130, oncostatin M receptor)
MAOA	monoamine oxidase A
MFAP5	microfibrillar associated protein 5
TSPAN8	tetraspanin 8
FAM148B	family with sequence similarity 148, member B
GADD45A	growth arrest and DNA-damage-inducible, alpha
S100P	S100 calcium binding protein P
IGFBP3	insulin-like growth factor binding protein 3
FXYD2	FXYD domain containing ion transport regulator 2
ABCC3	ATP-binding cassette, sub-family C (CFTR/MRP), member 3

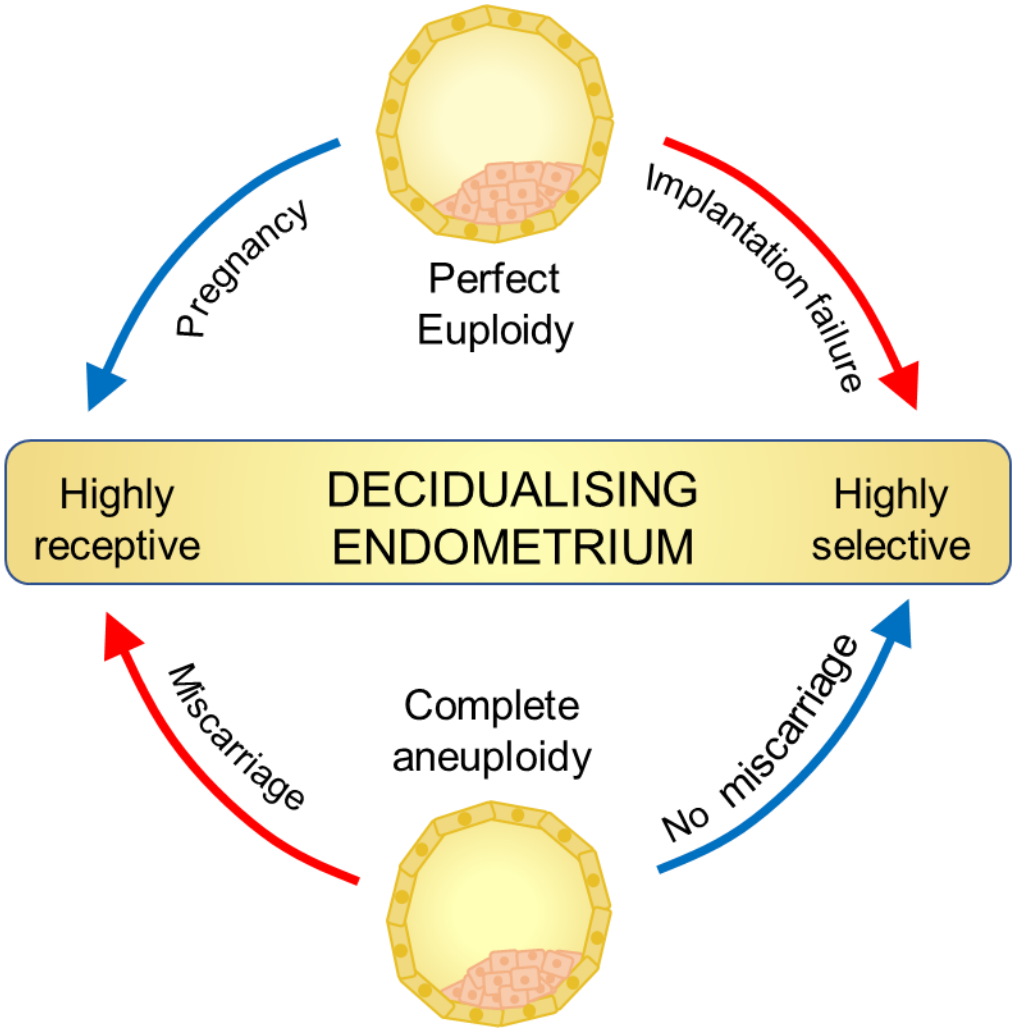

Figure 1.5. Schematic of the outcomes of differing interactions between the endometrium and implanting blastocyst. Successful pregnancy requires a high-quality embryo and a receptive endometrium. Divergence from this can lead to several different reproductive outcomes. Although blastocysts are genomically diverse and some mosaicism is common (Munne and Wells, 2017), poor quality embryos should be selected against by the endometrium, leading to no implantation. However, highly receptive endometria may still implant these blastocysts, leading to a miscarriage alter when the blastocyst development ceases prematurely, as hypothesised in RPL patients (Quenby et al., 2002). On the other hand, the endometrium may be poorly receptive, leading to high selectivity, leading it to reject high quality embryos leading to implantation failure. Adapted from (Gellersen and Brosens, 2014).

Recurrent Pregnancy Loss

Miscarriage is one of the most common pregnancy complications, with 1 in 7 recognised pregnancies ending in miscarriage within the first trimester (NHS maternity statistics). Miscarriage is defined as the spontaneous loss of pregnancy prior to fetal viability. Approximately half of all reported miscarriages are caused by embryonic chromosomal aneuploidy. In addition, the likelihood of a successful pregnancy decreases with each additional miscarriage. However, the incidence of chromosomally normal, euploidic fetal loss increases with each additional miscarriage (Gellersen and Brosens, 2014). This indicates that the endometrium may play a role in high order miscarriages. Recurrent pregnancy loss (RPL) is defined by the European Society for Human Reproduction and Embryology as two or more miscarriages (The et al., 2018). In an i*n vitro* study, primary EnSC cultures from patients with RPL were demonstrated to display a reduced decidual response. Moreover, RPL endometrium has been associated with a protracted proinflammatory response (Salker et al., 2012b). It has been hypothesised that a disordered decidual response increases the likelihood of an out-of-phase implantation event, in which embryo and endometrium are not 'in-sync' and therefore this leads inappropriate embryo implantation, and therefore miscarriage (Salker et al., 2012b, Gellersen and Brosens, 2014). Furthermore, RPL patients have a lower average abundance of MSC indicating cellular senescence, which may be a factor involved in the disordered decidual response (Lucas et al., 2013, Lucas et al., 2016).

Menstruation and repair

Implanting embryos produce human chorionic gonadotropin (hCG) which maintains the ovarian corpus luteum. Therefore, continued progesterone production maintains the integrity of the endometrium until the placenta begins producing progesterone at 6 to 8 weeks gestation (Hallast et al., 2005, Talmadge et al., 1983). However, in the absence of hCG, or an implanted competent embryo, the corpus luteum degrades

and progesterone levels drop. Progesterone withdrawal marks the degradation and shedding of the endometrial functionalis, a process called menstruation (Gellersen and Brosens, 2014). Only humans, elephant shrew, fruit bats and some old-world primates cyclically menstruate. In addition, these species are the only mammals to spontaneously decidualise, meaning decidualisation occurs without an embryo present (Emera et al., 2012, Brosens et al., 2009).

The beginning of menstruation includes a rise in inflammatory mediators produced by decidualised EnSC. Reduced progesterone levels promote nuclear factor kappa-light-chain-enhancer of activated B cells (NF-κB) leading to the activation of proinflammatory gene networks (Evans and Salamonsen, 2014). This inflammatory phenotype leads to an influx of inflammatory cells, leading to a large upregulation of matrix metalloproteinases (MMPs) (Rodgers et al., 1994, Abramson et al., 1995). MMPs are a family of zinc-dependent endopeptidases that have been demonstrated to digest a range of substrates within the endometrial ECM (Irwin et al., 1989). During menstruation, the upregulation of MMPs contribute a major role in the degradation of the endometrial functionalis. Furthermore, regulation of MMPs is through inhibition by tissue inhibitors of metalloproteinases (TIMPs) in the endometrium (Salamonsen and Woolley, 1996, Zhang and Salamonsen, 1997).

Following each menses, the endometrium must repair itself, scar-free. Endometrial regeneration is thought to be effected by endogenous resident epithelial and mesenchymal progenitor cells residing in the ovarian hormone resistant endometrial basalis layer (Chan and Gargett, 2006, Chan et al., 2004, Gargett et al., 2009, Gargett and Ye, 2012, Kanematsu et al., 2011). Both cell types are clonogenic, highly proliferative, self-renew *in vitro* and can produce mature daughter cells. At low levels, some MSC are derived from the bone marrow which migrate to the endometrium in response to uterine inflammation (Morelli et al., 2013, Cervelló et al., 2012). Specific

markers for isolating MSC have been identified. Either CD146+ PDGFRβ+ (platelet-derived growth factor receptor beta) or SUSD2^{+} (sushi domain containing-2) can be utilised to isolate perivascular EnSC which contain MSC (Schwab and Gargett, 2007, Masuda et al., 2012, Sivasubramaniyan et al., 2013).

Endometrial regeneration is still poorly understood but what is known is that the endometrium is rapidly re-epithelialised following menses (Garry et al., 2009). Studies in induced-menstruation mouse models have indicated that mesenchymal-to-epithelial transition accounts for the rapid re-epithelialisation of the endometrium. Furthermore, endometrial glands have been demonstrated to be monoclonal *in vivo*, suggesting they originate from a single epithelial progenitor cells. (Cousins et al., 2014, Ferenczy, 1976, Patterson et al., 2012, Huang et al., 2012). Overall the evidence suggests endometrial stem cells are essential for endometrial repair following menstruation.

1.2. Modelling the human peri-implantation endometrium

In vivo and in vitro models of the peri-implantation endometrium

Embryo implantation is challenging to study in humans. *In vivo* experiments studying the implantation window are unethical and impossible to perform (Weimar et al., 2013). Therefore, both *in vivo* and *in vitro* model systems have been developed. Murine, ovine, and bovine animal models have furthered our understanding of endometrial biology and pregnancy (Genbacev et al., 2003, Illera et al., 2000, Wang and Dey, 2006, Banerjee and Fazleabas, 2010). Non-human primates better replicate the human endometrium than other mammalian models and have been utilised to unravel the processes underpinning embryo implantation (Slayden and Keator, 2007, Nyachieo et al., 2007). However, the extent animal models represent human physiology may be limited due to the differences between human and animal model

reproductive systems (Lee and DeMayo, 2004). For example, human decidualisation is spontaneous and occurs cyclically without an implanting embryo present. However, in mice, for example, an implanting embryo is required for a decidual response and mouse embryos can undergo diapause (Lopes et al., 2004). Furthermore, PGR expression dynamics greatly varies between humans and mice (Teilmann et al., 2006).

Therefore, *in vitro* models using primary cells from human endometrial biopsies have been developed and established to circumvent the inter-species differences. *In vitro* endometrial models aim to represent at least certain aspects of the *in vivo* human implantation environment. In combination with a range of molecular techniques, these models act as effective tools to close the knowledge gap regarding human embryo implantation (Weimar et al., 2013). Many studies have used primary endometrial EEC or EnSC cultures, as well as endometrium-derived cell line cultures, to answer these questions.

EEC monolayer in vitro modelling

One of the first examples of an *in vitro* model utilising monolayer EEC was to study the interactions between the endometrial luminal epithelium and human embryos (Lindenberg et al., 1985). Table 1.4 and Figure 1.6 summarises the various monolayer models. One study investigated whether *in vitro* fertilisation (IVF) embryos co-cultured with an EEC monolayer prior to embryo transfer would improve the implantation rate. Embryos of women with implantation failure were cultured until blastocyst stage (day 6) on a patient matched EEC monolayer. The cultured embryos were transferred to the patients on day 6. The study reported that culturing the embryos with EEC prior to embryo transfer increased blastocyst formation as well as an increasing in the rate of implantation (Simón et al., 1999). In another study using a similar protocol, when co-cultured with embryos, the EEC upregulated expression

Table 1.4: *In vitro* human endometrial culture models of embryo implantation.
Data collected from (Weimar et al., 2013).

Model	Subtype	References
EEC Monolayer culture	EEC + human embryo	(Lindenberg et al., 1985, Simón et al., 1997, Simón et al., 1999, Meseguer et al., 2001, Caballero-Campo et al., 2002, Dominguez et al., 2003, Gonzalez et al., 2011)
	EEC + trophoblast spheroid	(Hohn et al., 2000, Galán et al., 2000, Heneweer et al., 2003, Heneweer et al., 2005, Mo et al., 2006, Uchida et al., 2007, Aboussahoud et al., 2010, Liu et al., 2011, Ho et al., 2012)
EnSC Monolayer culture	EnSC + human embryo	(Carver et al., 2003, Grewal et al., 2008, Teklenburg et al., 2010b, Weimar et al., 2012, Teklenburg et al., 2012)
	EnSC + mouse embryo	(Hanashi et al., 2003, Shiokawa et al., 1996, Grewal et al., 2010, Estella et al., 2012)
	EnSC + trophoblast spheroid	(Harun et al., 2006, Gonzalez et al., 2011, Holmberg et al., 2012, Weimar et al., 2012)
EEC + EnSC multi-layer culture	EEC + EnSC + human embryo	(Bentin-Ley et al., 1994, Bentin-Ley et al., 2000, Park et al., 2003, Petersen et al., 2005)
	EEC + EnSC + trophoblast spheroid	(Evron et al., 2011, Wang et al., 2011)

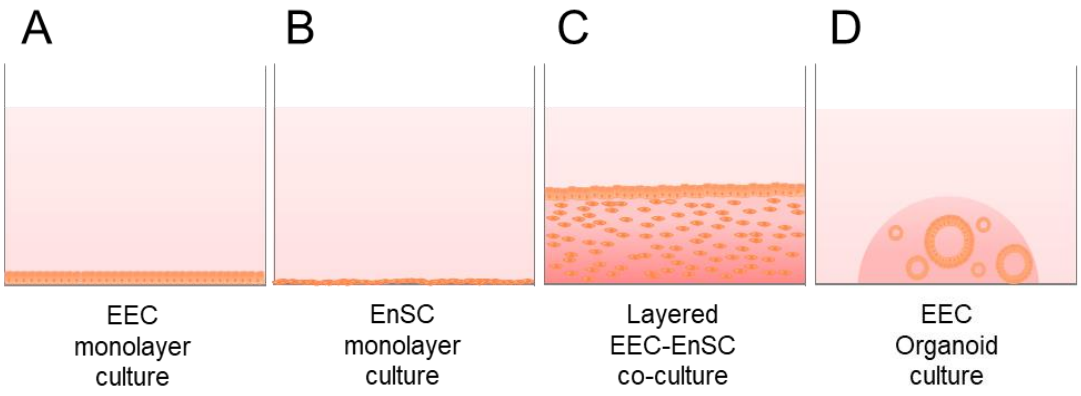

Figure 1.6. A Schematic of various *in vitro* culture methods for modelling the human endometrium.

A: Primary or cell line derived EEC monolayer cultured on cell-culture plastic grown in standard cell culture medium.

B: Primary or cell line derived EnSC monolayer cultured on cell-culture plastic grown in standard cell culture medium.

C: Primary or cell line derived stacked monolayer co-culture model. A layer of EnSC are grown in a hydrogel matrix such as Matrigel. A monolayer of EEC are grown on top of the gel to simulate the luminal epithelium. The co-culture is grown in standard cell culture medium.

D: Primary EEC derived endometrial gland organoid cultures. Glandular EEC are seeded into Matrigel droplets and grown in a complex medium of growth factors and inhibitors. EEC expand into spheroidal shaped structures that morphologically and functionally represent glandular epithelium.

of receptivity genes C-X-C chemokine receptor type 1 (CXCR1), CXCR4 and CCR5 as well as endometrial epithelial chemokine IL-8 (Dominguez et al., 2003, Caballero-Campo et al., 2002). Other studies also evidenced embryonic regulation of EEC in culture, for cell surface molecules implicated in embryo implantation, such as mucin 1 (MUC1) (Meseguer et al., 2001, Simón et al., 1997, González et al., 2000). Overall, monolayer EEC models demonstrate that preimplantation embryos can regulate the receptivity of the endometrial epithelium to prepare the endometrium for implantation. These models have also provided evidence that the EEC can support embryonic development prior to implantation (Dey et al., 2004, Teklenburg et al., 2010a). However, in comparison to EnSC, EEC have been reported to be technically challenging to grow in monolayer *in vitro*. In addition, the EEC harvested from endometrial biopsies are a mixture of both glandular and luminal EEC. As these cell types have been shown to maintain distinct gene signatures, monolayer EEC do not necessarily represent exclusively the uterine luminal epithelium interacting directly with an implanting embryo (Weimar et al., 2013).

Endometrial EEC cell lines have also been developed to reduce dependency on biopsies from donors. Cell lines should represent the cell type of origin both functionally and morphologically. Cell lines offer some benefit over primary culture. For example, a cell line will proliferate indefinitely, therefore removing the limitation of sample supply. The supply is also a consistent sample, reducing variation and improving reproducibility. They require more simple culture conditions, are inexpensive and bypass ethical concerns of using primary tissue or animal models. (Weimar et al., 2013). Table 1.5 summarises commonly used EEC cell lines. Due to their reduced culturing requirements, gene silencing experiments are often easier in cell lines than primary cells (Cervero et al., 2007). However, cell lines are immortalised cells, derived from cancers harbouring significant genetic mutations. These mutations may have secondary effects on the cells, impacting cellular

Table 1.5: Endometrial cell lines. Endometrial epithelial cell line embryo implantation characteristics. Data collected from (Hannan et al., 2010a)

Cell line	Origin	Implantation	Epithelial phenotype	Polarisation	References
ECC-1	Adenocarcinoma		Luminal	Moderate	(Satyaswaroop and Tabibzadeh, 1991)
Ishikawa	Adenocarcinoma	Adhesive	Luminal and glandular	Moderate	(Nishida et al., 1985, Heneweer et al., 2005)
HEC-1A	Adenocarcinoma	Poorly adhesive		High	(Kuramoto et al., 1972, Ball et al., 1995)
HEC-1B	Adenocarcinoma			Moderate	(Kuramoto et al., 1972)
HES		Embryotropic	luminal		(Desai et al., 1994)
RL95-2	adenosquamous carcinoma	Highly adhesive		Unpolarised	(Hohn et al., 2000, Way et al., 1983)

stimulus responses or morphology (Weimar et al., 2013). It has also been reported that cell lines can also easily become contaminated with other cell lines, confounding results (Korch et al., 2012).

EnSC monolayer in vitro modelling

Primary human endometrial EnSC are the work horse of many laboratories studying human decidualisation and the peri-implantation endometrial environment. EnSC monolayer cultures are suitable for elucidating human implantation because, *in vivo*, an implanting embryo will encounter EnSC once it penetrates the luminal epithelium.

Primary human EnSC are generally collected from secretory phase endometrial biopsies obtained with consent from donors or patients of reproductive age (Carver et al., 2003, Evron et al., 2011, Weimar et al., 2012). Endometrial cells are isolated from the tissue biopsy by mechanical digestion of the endometrial tissue, followed by enzymatic digestion using collagenase I and DNase (Barros et al., 2016). The digested suspension is filtered through a 40 µm cell sieve in which the flow through contains the EnSC, and the endometrial glands are retained in the sieve. Endometrial EnSC are cultured in standard cell culture medium supplemented with 10% fetal bovine serum (FBS) and 1 nM estradiol (Barros et al., 2016). Endometrial EnSC label positive immunohistochemically for vimentin and negative for cytokeratin. Cultured endometrial EnSC monolayers can be decidualised by treatment with cAMP and medroxyprogesterone acetate (MPA), a progestin (Brosens et al., 1999, Gellersen and Brosens, 2014).

In an initial study, a monolayer of human EnSC were co-cultured a hatched day 5 human blastocyst stage embryo for three days. (Carver et al., 2003). This implantation model demonstrated that the blastocyst could attach and implant into the EnSC monolayer. This initial system was utilised to determine the response of differentiated

and undifferentiated EnSC to the presence of embryos (Carver et al., 2003). In another study, decidualised EnSC exhibited a downregulation of expression of implantation genes when co-cultured with an arresting embryo (Teklenburg et al., 2010a). This experiment demonstrated that decidualised EnSC can act as a biosensor, detecting embryo quality. The model has also been used to investigate reproductive disorders. One study compared EnSC response to embryo quality from endometrial biopsies collected from normal fertile women and women suffering with RPL. EnSC of RPL patients failed to inhibit implantation genes when co-cultured with a poor-quality embryo (Weimar et al., 2012). This observation indicates that the endometrium of RPL patients may have defects in their embryo quality biosensing. This suggests that the endometrium of women with RPL may be less selective for embryo quality than in fertile women. This would enable a poor-quality embryo to implant, and later miscarriage. This proposed phenomenon has been described as a 'selection failure hypothesis' (Quenby et al., 2002, Teklenburg et al., 2010b, Lucas et al., 2013).

Overall, the EnSC monolayer model provides a simple and robust model for studying human early embryo implantation. However, the main disadvantage of both EnSC and EEC monolayer models is that they only include one cell type, ignoring the *in vivo* endometrial EnSC and EEC interactions, as well as the resident immune and endothelial cell populations (Weimar et al., 2013).

Colony forming unit assay

The endometrium contains resident populations of progenitor cells (Gargett et al., 2015, Chan et al., 2004, Schwab and Gargett, 2007, Gargett et al., 2009). Isolation of adult stem cells is difficult for cell culture because they reside in tissues in very small populations and usually possess very few distinguishing surface markers (Chan et al., 2004, Weissman, 2000, Robey, 2000). In other tissues, adult stem cells have

been identified by their clonogenic phenotype. Clonogenicity is defined as the ability of a single cell to produce a colony when seeded at very low densities. (Gronthos et al., 2000, Hudson et al., 2000, Pellegrini et al., 1999). Clonogenicity can be quantified using a colony forming unit (CFU) assay. The CFU assay is an *in vitro* culture assay in which cells are seeded at a defined low density on cell culture plastic and the number of colonies that form indicate the number of stem cells present in a sample as a proportion of the total population. A single colony is usually defined as consisting of at least 50 cells. Endometrial MSC were characterised using a CFU assay (Chan et al., 2004, Schwab et al., 2005, Schwab and Gargett, 2007, Masuda et al., 2012). (Chan et al., 2004). Since this discovery, there have been several studies looking at endometrial stem cells and their role in infertility. For example, patients suffering with RPL have fewer MSC than women who have normal fertile mid-secretory phase endometrium (Lucas et al., 2016).

Layered EEC and EnSC co-culture in vitro modelling

The peri-implantation environment of the endometrium involves synchronous paracrine signals, cell-cell and cell-matrix interactions between multiple cell types of the decidualising endometrium. For example, many studies have demonstrated that endometrial EnSC influence the development and differentiation of glandular EEC (Mahfoudi et al., 1992, Cunha et al., 1985, Cooke et al., 1986, Cooke et al., 1997, Cooke et al., 2013). Therefore, more recent *in vitro* models of the endometrium have been established to replicate the complexity of the *in vivo* endometrium. These more complex models are generally multi-layered co-culture models of stacked monolayers of different cell types (Bentin-Ley et al., 1994, Evron et al., 2011, Wang et al., 2011, von Arnim and Deng, 1994).

The stacked multilayer cultures consist of a layer of endometrial EnSC, which are set up in a matrix scaffold mimicking ECM, and a monolayer of EEC on top (Table 1.4)

(Fig. 6C). This scaffold is usually a ECM-derived hydrogel, such as Matrigel or collagen hydrogels (Bentin-Ley et al., 1994, Weimar et al., 2013). Matrigel is a solubilised basement membrane preparation isolated from Engelbreth-Holm-Swarm (EHS) mouse sarcoma cells. Sarcoma cells are rich in BM proteins such as laminin (a major component), collagen IV, heparin sulphate proteoglycans, entactin, and several growth factors. Collagen hydrogels tend to contain ECM proteins such as purified type I collagen.

Layered co-culture models aim to represent the complex 3D endometrial tissue architecture more closely than simple monolayer cultures grown on plastic. The monolayer of endometrial EEC is grown on top of the stromal layer to resemble a luminal epithelium above a stroma, analogous to a simplified human endometrium. In one study, the stacked multi-layered co-culture model induced EEC polarisation, resulting in embryo attachment within 48 hours (Bentin-Ley et al., 2000). Furthermore, electron scanning microscopy revealed the interactions between embryo and the polarised EEC luminal surface and penetration through the BM layer and into the underlying EnSC layer (Bentin-Ley et al., 2000). These observations presented a novel insight into the process of human embryo implantation.

In addition to this model, trans-well models for studying trophoblast invasion have been adapted to incorporate EnSC and EEC. Trophoblast invasion assays use dual chambered systems in which the trophoblast cells adhere to Matrigel-coated filter insert with 8 μm pores (Aplin, 2006, Lash et al., 2007). Adherent trophoblast cells invade the Matrigel and the number of cells that reach the surface beneath the Matrigel can be quantified. This trophoblast invasion assay has been adapted to incorporate elements of the layered co-culture model. EEC are seeded on top of the Matrigel in the trans-well prior to adding trophoblast cells and the EnSC are cultured underneath the filter (Arnold et al., 2001, Bläuer et al., 2005, Pierro et al., 2001). This

setup therefore loses the cell-cell contact between EEC and EnSC seen in other co-culture systems. However, the trans-well approach provides an easily manipulatable assay for quantifying trophoblast invasion in the presence of EnSC and/ or EEC. This model therefore provides scope for studying different parameters, such as additional endometrial cell types, or culturing cells from biopsies of women with different pathologies to assess differences in trophoblast invasion.

Organoid in vitro modelling

More recently, a new method of 3D culturing has emerged that improves upon previous monolayer approaches: organoids. Organoids are derived from stem or progenitor cells that self-organise into multicellular 3D structures that both morphologically and functionally recapitulate the tissue or organ from which the cells originate (Lancaster and Knoblich, 2014b). The progenitor cells that form organoids are derived from biopsies of adult tissue containing tissue-specific adult progenitor cells or from induced pluripotent stem cells (iPSC). Organoids exemplify the potent regenerative potential of progenitor or stem cells and by modelling the developmental processes of organogenesis, cell organisation and lineage commitment (Lancaster and Knoblich, 2014b). Organoid cultures have been established to model many different organs such as: intestine, kidney, lung, prostate, brain, stomach, and kidney (Zimmermann, 1987, Koo et al., 2012, Karthaus et al., 2014, Lancaster and Knoblich, 2014b, Lancaster and Knoblich, 2014a, Crespo et al., 2017, Bartfeld and Clevers, 2015).

Endometrial gland organoids have been recently established (Boretto et al., 2017, Turco et al., 2017) (Fig. 6D). These two pioneering studies describe protocols for the endometrial gland organoid expansion, differentiation and cryopreservation (Turco et al., 2017, Boretto et al., 2017). Turco *et al*. 2017, optimised their organoid protocol using biopsies of normal and malignant human endometrium, and Boretto *et al.* 2017,

from biopsies of normal human and mouse endometrium. The organoids are expanded by culturing dissociated endometrial glands in Matrigel. In addition, both studies optimised a defined culture medium of growth factors, inhibitors, supplements, and antioxidants that enable organoid expansion and maintenance. Table 1.6 compares the media composition from both studies. Both studies also demonstrated that human endometrial organoids are clonal and can be passaged. The organoids also recapitulate physiological responses to ovarian hormone stimulation. Treatment with estradiol increases proliferation and promotes differentiation of secretory and ciliated cells (Haider et al., 2019, Turco et al., 2017, Boretto et al., 2017). Endometrial gland organoids can also be maintained in culture long term by passaging or stored by cryopreservation, enabling the prospect of producing endometrial gland organoid biobanks (Turco et al., 2017).

There are many benefits to organoid culture over monolayer culture. First, in previous models, EEC have been cultured in monolayer, either singularly or in a stacked layered co-culture, to represent the luminal epithelium (Bentin-Ley et al., 1994, Bentin-Ley et al., 2000). However, endometrial gland organoids provide a model for glandular epithelium containing both ciliated and non-ciliated EEC when exposed to estradiol (Haider et al., 2019). Furthermore, the clonal properties of these organoids indicate that progenitor or stem cell populations can be studied using this technique. Furthermore, the organoids have already been used to develop disease models related to glandular defects which offer insight into endometrial gland biology underpinning infertility (Boretto et al., 2019). In addition, endometrial gland organoids could provide a tool for novel drug discovery for endometrial disorders. Patient-derived organoids could be used to develop personalised medicine approaches for treating infertility.

Table 1.6: A comparison of medium optimised for endometrial gland organoid expansion.

Medium component	Turco, *et al.* 2017	Boretto, *et al.* 2017	Action
Base medium	Advanced DMEM/F12	DMEM/F12 + insulin-transferrin-selenium	
NAC	✓	✓	Antioxidant
A83-01	✓	✓	Potent inhibitor of TGF-β type I receptor superfamily activin-like kinase ALK5 and its relatives ALK4 and ALK7
Nicotinamide	✓	✓	Incorporated into coenzymes NAD+ (nicotinamide adenine dinucleotide) and NADP+ (nicotinamide adenine dinucleotide phosphate) essential for metabolism
EGF	✓	✓	Promotes cell growth, proliferation and differentiation.
Noggin	✓	✓	BMP inhibitor
WNT activator	R-spondin-1	R-spondin-1 + WNT3A	Promotes canonical WNT/β catenin signalling
FGF10	✓	✓	EnSC derived. Promotes cell growth and proliferation
HGF	✓	NA	EnSC derived. Promotes cell growth and proliferation
N2 supplement	✓	✓	Supplement for serum free medium
Antibiotics	Primocin	penicillin/ streptomycin	Prevent Infection
L-Glutamine	L-Glutamine	Glutamax	Essential amino acid
B27 supplement	✓	✓	Supplement for serum free medium
SB202190	NA	✓	p38 inhibitor

Taken together, historically, the endometrial epithelium has been difficult to culture and maintain *in vitro*. Organoids provide a method of modelling glandular epithelium that is functionally and morphologically representative of the endometrium. (Deane et al., 2017). The future of endometrial gland organoid culture lies in the co-culture with EnSC and other endometrial cell types. Long term, a complex organoid co-culture model could be utilised to study embryo implantation like previous *in vitro* models, but with additional insight of the role of the glandular epithelium in early maternal-embryo interactions. The incorporation of endometrial gland organoids into a complex organoid co-culture would provide the most comprehensive *in vitro* model of the human peri-implantation endometrium to date.

1.3 Research justification and aims

Human embryo implantation is currently the rate-limiting step for achieving a successful pregnancy in ART. Inappropriate endometrial embryo-quality biosensing is also associated with RPL. Elucidating the mechanisms underpinning the peri-implantation endometrium will enable the development of treatments for patients suffering with chronic fertility disorders. However, human embryo implantation is difficult to study as it is unethical to study in women and *in vivo* animal models do not fully recapitulate the human endometrial environment. Therefore, to avoid inter-species variability, *in vitro* culture of human endometrial cells is used routinely to study implantation. However, the endometrium is a complex tissue made up of EnSC, epithelial glands, as well as a vasculature and immune cell population. An *in vitro* model that encompasses all aspects of the human endometrium requires a complex co-culture system, containing several endometrial cell types. Therefore, 3D *in vitro* culturing methods are the most suitable for developing a faithful model of human embryo implantation. The advent of endometrial gland organoids has allowed for the culture of endometrial glandular epithelium, an essential part of the peri-implantation endometrium and for embryo implantation. Currently, 3D co-cultures of endometrial gland organoids with EnSC have yet to be described in the literature. The co-culture of endometrial gland organoid and EnSC to establish complex organoids could provide a starting point for a step change in our collective ability to study human embryo implantation *in vitro*. This system will be patient specific, and in the long term be developed into a high-throughput system for personalised medicine treatments for infertility.

Thesis aims:

1. To establish and optimise a protocol for a novel *in vitro* complex organoid culture.
2. To functionally characterise the complex organoids for both morphological and functional recapitulation of the human endometrium
3. To evaluate the impact of EnSC on EEC differentiation in the complex organoids.

Chapter 2:
Materials and Methods

2.1. Materials

Cell culture materials

EnSC culture materials

Reagent	Manufacturer
Charcoal	Sigma-Aldrich
Collagenase type IA	Sigma-Aldrich
Dextran	Fisher Scientific
Deoxyribonuclease I (DNase I)	Roche
Foetal bovine serum (FBS) heat inactivated	
Insulin	Sigma-Aldrich
L-Glutamine	Gibco
Penicillin (10,000 µg/ml)- Streptomycin (10,000µg/ml) solution	Invitrogen
RNA-later	Sigma-Aldrich
Trypsin-EDTA solution	Gibco
Plastic-ware	VWR
Matrigel	Fisher Scientific
Medium 200	Gibco
Dulbecco's Modified Eagle Medium/ Ham's F-12 (DMEM)/F12 (1:1) with L-glutamine with phenol red	Fisher Scientific
DMEM/F12 (1:1) with L-glutamine, phenol free	Fisher Scientific

Organoid culture materials

Expansion medium (ExM) components

Medium component	Source	Purity/ Composition	Manufacturer
A83-01	Synthetic	≥98% (HPLC)	Sigma-Aldrich

Antibiotic-Antimycotic (100X)		10,000 units/mL of penicillin, 10,000µg/mL of streptomycin, and 25µg/mL of Fungizone™	Gibco
B27 supplement	Synthetic	Biotin, DL Alpha tocopherol acetate, DL alpha-tocopherol, BSA, catalase, human recombinant insulin, human transferrin, superoxide dismutase, corticosterone, D-galactose, ethanolamine HCl, glutathione (reduced), L-carnitine HCl, linoleic acid, linolenic acid, progesterone, putrescine 2HCl, sodium selenite, T3 (triodo-I-thryonine). Concentrations are confidential to manufacturer.	Gibco
Epidermal growth factor (EGF)	*Escherichia coli (E. coli)*	≥ 98% by SDS-PAGE gel and HPLC analyses.	Peprotech
Fibroblast growth factor 10 (FGF10)	*E. coli*	≥ 95% by SDS-PAGE gel and HPLC analyses.	Peprotech
Hepatocyte growth factor (HGF)	(BTI-Tn-5B1-4) Hi-5 Insect cells	≥ 98% by SDS-PAGE gel and HPLC analyses.	Peprotech
L-Glutamine	Synthetic	200mM L-Glutamine	Gibco
N2 supplement	Synthetic	Human transferrin 10 mg/ml; Insulin Recombinant Full Chain 500 ng/ml; Selenite 520 pg/ml; Putrescine 1.6 mg/ml; Progesterone 630 pg/ml	Gibco

N-Acetyl-Cysteine (NAC)	Synthetic	≥99% (TLC)	Sigma-Aldrich
Nicotinamide	Synthetic	≥98% (HPLC)	Sigma-Aldrich
Noggin	HEK293 cells	≥ 95% by SDS-PAGE gel and HPLC analyses.	Peprotech
R-spondin-1	CHO cells	≥ 95% by SDS-PAGE gel and HPLC analyses.	Peprotech

Organoid culture materials

Reagent	Source	Composition	Manufacturer
Advanced DMEM/F12			Gibco
Albumax II	Bovine	Purified BSA	Fisher Scientific
Cell Recovery Solution	Synthetic	nonenzymatic proprietary solution	Fisher Scientific
Collagenase type IA	*Clostridium histolyticum*	250mg of lyophilized powder. May contain caseinase, clostripain, and tryptic activities	Sigma-Aldrich
Matrigel (Growth Factor Reduced) *	See below*	See below*	Fisher Scientific
Plastic-ware			VWR
PureCol® EZ Gel solution**	See below**	See below**	Sigma Aldrich
Serum Replacement 1 50×	Bovine	Contains highly purified, heat-treated BSA, bovine transferrin and bovine insulin.	Sigma-Aldrich

TrypLE select 10x	Synthetic	Trypsin replacement; Protease concentration confidential to manufacturer	Fisher Scientific

***Matrigel (Growth Factor Reduced)**

Matrigel matrix hydrogel (Corning) is a solubilised basement membrane preparation isolated from Engelbreth-Holm-Swarm (EHS) mouse sarcoma cells. Sarcoma cells are rich in BM proteins such as laminin, collagen IV, proteoglycans, entactin, and several growth factors. The contents of the Matrigel protein preparation is approximately 60% laminin, 30% collagen IV, and 8% entactin. The typical concentration of Matrigel is 8 – 12 mg/ml. Matrigel also contains several growth factors, as seen below. In the present study, the growth factor reduced (GFR) Matrigel is used to minimise the impact of the growth factors on the cells used in experiments (Fisher Scientific).

Growth Factor	Average GF Concentration in Corning Matrigel Matrix	Average GF Concentration in GFR Corning Matrigel Matrix
EGF	0.7 ng/ml	< 0.5 ng/ml
Basic fibroblast growth factor (bFGF)	N/A	N/A
Nerve growth factor (NGF)	< 0.2 ng/ml	< 0.2 ng/ml
Platelet-derived growth factor (PDGF) Insulin-	12 pg/ml	< 5 pg/ml
like growth factor 1 (IGF-1)	16 ng/ml	5 ng/ml
Transforming growth factor beta 1 (TGF-β1)	2.3 ng/ml	1.7 ng/ml

****PureCol® EZ Gel solution**

The PureCol EZ Gel is a pre-formulated collagen hydrogel solution. The gel is a solution of 5 mg/ml purified Type I collagen in DMEM/F12 medium. It also contains a mixture of L-glutamine and L-alanine-L-glutamine dipeptide. The collagen type I is purified from bovine skin (Sigma Aldrich).

Cell culture treatments

Reagent	Concentration	Manufacturer
8-br-cAMP	0.5 mM	Sigma-Aldrich
bFGF	10 ng/ml	Merk-Millipore
Estradiol	1 nM	Sigma-Aldrich
Medroxyprogesterone acetate (MPA)	1 µM	Sigma-Aldrich
TGFβ1 (recombinant protein)	200 nM	Bio-Techne Ltd
A8301	1, 10 or 100 µM	Sigma Aldrich
Y27632	1 or 10 µM	Sigma-Aldrich
KD025	1 µM	Stratech Scientific Limited
Y15	50 µM	Stratech Scientific Limited

Chemical reagents

Reagent	Manufacturer
30% acrylamide protogel/Bis solution	Bio-rad
Ammonium Persulphate (APS)	Fisher Scientific
Bio-Rad Protein Assay Dye	Bio-Rad
Bovine serum albumin (BSA)	Sigma-Aldrich
CellTracker™ Green CMFDA Dye	Fisher Scientific
CellTracker™ Red CMTPX Dye	Fisher Scientific
Chloroform	AnalaR
cOmplete EDTA free protease inhibitors	Roche
Dimethyl sulphoxyde (DMSO)	Life Technologies
Ethylenediaminetetraacetic acid (EDTA)	Fisher Scientific

Fibronectin	Sigma-Aldrich
Formalin	Leica
Isopropanol	Sigma-Aldrich
Milk powder	AppliChem
N,N,N,N'-tetramethyl-ethane-1,2-diamine (TEMED)	Sigma-Aldrich
Phosphatase inhibitor cocktail	Sigma-Aldrich
PrecisionPlus SYBR Green Mastermix	Life Technologies
ProLong® Gold Antifade Reagent with DAPI	Cell Signaling Technology
Protein ladders	Life Technologies
RIPA	Millipore
RNase free tubes	Life-Technologies
RNase free water	Life Technologies
RNase ZAP	AMS Biotechnology
Sodium dodecyl sulphate (SDS)	Fisher Scientific
STAT-60	AMS Biotechnology
Tris base	Sigma-Aldrich
Tris HCl	Sigma-Aldrich
Tris-borate	Sigma-Aldrich
Triton X-100	Sigma-Aldrich
Tween 20	Sigma-Aldrich
β-mercaptoethanol	Fisher Scientific

Pre-Set Kits

Kit	Manufacturer
AllPrep DNA/RNA Micro Kit	Qiagen
ECL Prime Western Blotting detection system	GE Healthcare
jetPRIME Transfection Kit	VWR
QIAshredder	Qiagen
QuantiTECT Reverse Transcription Kit	Qiagen
ReadyProbes™ Cell Viability Imaging Kit, NucBlue/NucGreen	Fisher Scientific
RNase-Free DNase Set	Qiagen
RNeasy Plus Micro Kit	Qiagen

ELISA materials

ELISA Materials	Manufacturer
Clear Polystyrene Microplates	BIO-TECHNE
Human CXCL14/BRAK DuoSet ELISA	BIO-TECHNE
Human Osteopontin (OPN) DuoSet ELISA	BIO-TECHNE
Human Prolactin (PRL) DuoSet ELISA	BIO-TECHNE
Stop Solution 2N Sulfuric Acid	BIO-TECHNE
Substrate Reagent	BIO-TECHNE

Magnetic-activated cell sorting (MACS) materials

Material	Manufacturer
Anti SUSD2-PE human	MILTENYI BIOTEC
Anti-PE MicroBeads	MILTENYI BIOTEC
MACS separation columns	MILTENYI BIOTEC
MiniMACS Separator	MILTENYI BIOTEC

Buffer Recipes

TBS	*TBS-Tween (TBST)*	*TBE*
130 mM NaCl 20 mM Tris, pH 7.6	0.1% Tween in 1x TBS	0.9 M Tris-borate 2 mM EDTA, pH8.0RIPA Buffer 50 mM Tris HCl pH 7.4 1% NP40 0.5% deoxycholate 0.1% SDS 150 mM NaCl 2 mM EDTA 50 mM NaF

Western Blot Materials

Western Blot Buffer Recipes:

Running Buffer (10x)	*Transfer Buffer*	*Blocking/ Antibody Incubation Solution*
250mM Tris Base 192mM glycine 1% (w/v) SDS	250 mM Tris Base 192 mM glycine 20% (v/v) methanol	5% BSA (w/v) in TBS-Tween or 5% skimmed milk powder (w/v) in TBS-Tween (antibody dependent)

Western Blot Gel Components:

Running Gel	*Stacking Gel*
30% acrylamide Protogel 1.5 M Tris-HCL pH 8.8 H2O 10% SDS	30% acrylamide Protogel 0.5 M Tris-HCL pH H2O 10% SDS

10% APS TEMED	10% APS TEMED

Western blot antibodies

Primary Antibody	Dilution	Host	BSA/Milk	Manufacturer
αSMA	1:1000	Rabbit	5% BSA	Cell Signaling Technology
β-actin	1:10000	Mouse	5% BSA	ABCAM
MYPT1	1:1000	Rabbit	5% BSA	Cell Signaling Technology
p-MYPT1	1:1000	Rabbit	5% MILK	Cell Signaling Technology

RT-qPCR Primers

All primer efficiencies were calculated previously by the Brosens group. Purchased from Sigma-Aldrich.

Primer	Sequence (5'-)	Efficiency
L19 Forward	GCGGAAGGGTACAGCCAAT	1.98
L19 Reverse	GCAGCCGGCGCAAA	1.98
PRL Forward	AAGCTGTAGAGATTGAGGAGCAA	1.89
PRL Reverse	TCAGGATGAACCTGGCTGACTA	1.89
CXCL14 Forward	GCGACGTGAAGAAGCTGGAA	1.87
CXCL14 Reverse	TACCTGGCACGCTCTTGGT	1.87
PAEP Forward	GAGCATGATGTGCCAGTACC	1.91
PAEP Reverse	CCTGAAAGCCCTGATGAATCC	1.91
SPP1 Forward	TGCAGCCTTCTCAGCCAAA	1.95
SPP1 Reverse	GGAGGCAAAAGCAAATCACTG	1.95

Antibodies - IHC

Primary Antibody	Host	Antigen retrieval pH	Dilution	Manufacturer
EpCAM	Rabbit	6.4	1:200	New England Biolabs
E-cadherin	Rabbit	6.4	1:200	Cell Signaling Technology
Cytokeratin-18	Rabbit	6.4	1:200	ABCAM
Laminin	Rabbit	6.4	1:100	ABCAM
PR	Mouse	6.4	1:50	Agilent Technologies
Glycodelin	Rabbit	9.5	1:100	ABCAM
Ki67	Rabbit	6.4	1:200	ABCAM
Vimentin	Mouse	6.4	1:200	New England Biolabs

Secondary Antibody ***(1:500)***	Manufacturer
IgG (H+L) Cross-Adsorbed, Host-Rb, 2mg/mL, 250uL, Species Reactivity-Mouse, Polyclonal, Alexa Fluor 594,	Invitrogen
IgG (H+L) Cross-Adsorbed, Host: Gt, 2 mg/mL, 500uL, Species Reactivity: Rabbit, Alexa Fluor 488	Invitrogen

scRNA-seq Materials

Material	Manufacturer
Agencourt AMPure XP beads	Beckman Coulter
Barcoded Oligo dT primer ON Beads	Chemgenes Corporation
Bioanalyzer High Sensitivity DNA chip	Agilent
C-Chip Fuchs-Rosenthal Haemocytometer	Labtech
Droplet generation oil	Bio-Rad Laboratories
Illumina Nextera XT DNA Sample Kit	Illumina
Illumina Nextera XT Indexing Kits	Illumina
Nadia Cartridges for scRNA	The Dolomite Centre
Nadia Instrument	Blacktrace Holdings
NextSeq High Output 75 cycle V2 kit	Illumina
Qubit High Sensitivity DNA assay	ThermoFisher

Small interfering RNA

Reagent	Manufacturer
ON-TARGETplus Non-targeting Pool 1.	HORIZON DISCOVERY
ON-TARGETplus Human MYLK (4638) siRNA - SMARTpool	HORIZON DISCOVERY

2.2. Methods

Human Endometrial Biopsy Collection

Patients were recruited for endometrial biopsy from the Implantation Clinic, a research unit of University Hospitals Coventry and Warwickshire National Health Service Trust. Written informed consent was obtained from all patients in accordance with the Declaration of Helsinki 2000. The study was approved by the NHS National Research Ethics Committee of Hammersmith and Queen Charlotte's Hospital NHS Trust (1997/5065). Biopsies were all timed to the mid secretory phase, 5 to 11 days after the post-ovulatory LH surge. No patients were taking hormonal treatment for at least 3 months prior to biopsy. Processing of tissue samples is fully compliant with Human Tissue Act regulations and completed within 4 hours of collection. All experiments were conducted using primary cells isolated from human endometrial biopsies.

EnSC cell culture

DCC-FBS preparation

500 ml fetal bovine serum (FBS) was treated with dextran coated charcoal (DCC). 1.25 g charcoal and 125 mg dextran added to FBS and incubated at 57^{o}C for 2 hours, with regular mixing, to remove hormones and other factors from the FBS. FBS was centrifuged at 400 g for 30 minutes. Supernatant was sterile filtered and aliquoted for use in medium preparation.

Isolation of EnSC from endometrial biopsy.

Fresh endometrial biopsies were mechanically dissociated by finely mincing the tissue for 5 minutes by scalpel in a petri dish. The minced tissue was then enzymatically digested with collagenase I (0.5 mg/ml) and deoxyribonuclease (DNase) type I (0.1 mg/ml) in 5 ml phenol red-free Dulbecco's Modified Eagle Medium (DMEM)/F12 for 1 hour at 37°C, with regular vigorous shaking. Enzyme activity was

stopped by adding 10 ml 10% DCC-FBS supplemented DMEM/F12. 10% DCC-FBS supplemented DMEM/F12 containing 1% penicillin-streptomycin, 2 mM L-glutamine, 1 nM estradiol and 2 mg/ml insulin was used for all EnSC cell culture unless stated otherwise. Samples were flushed through a 40-µm cell sieve. EnSC and other cells (blood cells, uNK cells, endothelial cells, single EEC). Epithelial glands remained in the sell sieve. Samples were centrifuged at 400 g for 5 min. Cell pellets were resuspended in 10 ml 10% DCC-FBS supplemented DMEM/F12. Cell suspensions were plated into an appropriately sized cell culture grade flask. Cell cultures were incubated at 37°C and 5% v/v CO_2. To isolate EnSC from other cells, the medium was refreshed after 24 hours as only the EnSC attach to plastic within this time frame.

Primary EnSC cell culture

EnSC were cultured in standard cell culture incubator conditions: a humidified atmosphere, 5% v/v CO_2 and 37^{o}C. A class II microbiology safety cabinet was used for all EnSC culture. Cultures were refreshed with 10% DCC-FBS supplemented medium every 48 hours. Confluent monolayers were passaged by 1 ml trypsin-EDTA treatment for 5 minutes at 37^{o}C. Treated cell culture flasks were tapped to dislodge remaining attached cells. Trypsin activity was stopped by addition of 9 ml supplemented 10% DCC-FBS. EnSC were centrifuged at 400 g for 5 min and the cell pellet was resuspended in supplemented 10% DCC-FBS supplemented medium and split into a 1:3 ratio for further plating.

EnSC decidualisation treatment

Confluent monolayers were placed in phenol red-free 2% DCC-FBS supplemented DMEM-F12 overnight. 2% DCC-FBS supplemented DMEM/F12 contained only 1% penicillin-streptomycin and 2 mM L-glutamine. For decidualization treatment, 24 hours after medium down regulation, EnSC cultures were treated with phenol red-free DMEM/F12 containing 2% DCC-FBS with 0.5 mM 8-bromo-cAMP (cAMP) and 1

μM medroxyprogesterone acetate (MPA). For the experiment excluding either MPA or cAMP, the concentrations of the maintained factor remained the same as standard protocol. All treatments were performed in the second passage.

Isolation of stromal sub-populations

Stromal cell subtypes were isolated from endometrial tissues as described previously (Murakami et al., 2013). Following the EnSC isolation protocol, instead of plating the cells, the cell suspension was layered over Ficoll-Paque PLUS and centrifuged to remove erythrocytes. The medium/Ficoll-Paque PLUS interface, containing EnSC, was carefully aspirated, and washed with 10% DCC-FBS supplemented medium. Magnetic bead separation was performed using $SUSD2^{+}$ antibody W5C5, to isolate PVC ($W5C5^{+}$ cells) as described (Murakami et al., 2013). PVC were either cultured in a cell culture flask (PVC) or used to isolate MSC by CFU assay. $W5C5^{-}$ cells were either cultured in a cell culture flask (EnSC) or used to isolate TAC by CFU assay.

CFU-assay

CFU assay was performed by seeding EnSC or PVC at a clonal density of 50 cells/ cm^2 to ensure equal loading onto fibronectin-coated 60 mm culture dishes and cultured in 10% DCC-FBS supplemented medium supplemented with 10 ng/ml basic fibroblast growth factor (BFGF) (Murakami et al., 2013). Culture medium was not refreshed until day 7 of culture. Colonies were defined as containing ≥ 50 cells and derived from one cell. Colonies were monitored daily to ensure that they were derived from single cells. Cultures were harvested at 10 days for ERB formation assays.

ERB formation / endometrial fibroblast activation model (EFAM)

All stromal cell sub populations for ERB formation were recovered by aspirating the culture medium and washed with 1 ml sterile PBS. Cultures were subjected to trypsin-EDTA incubation for 5 minutes at 37ºC to resuspend the cells. 10% DCC-FBS

supplemented medium was added to stop trypsin enzymatic activity, and the cells were collected and resuspended in medium 200. Medium 200 was prepared by adding 1× low serum growth supplement (LSGS) to basal medium 200. The cell number was counted using an automated cell counter (LUNA). Aliquoted Matrigel (stored at -20^{o}C) was kept on wet ice. 50 µl Matrigel was pipetted using ice-cold pipette tips into a 96-well cell culture plate to form a flat plug covering the full surface of the well. The Matrigel was allowed to cure before use following method optimisation (See Chapter 3). 1×10^{5} stromal cells, suspended in medium 200, were seeded into each well on top of the Matrigel layer. The medium was topped up to 200 µl total volume per well. The plates were incubated in standard cell culture conditions for 24 hours for ERB formation to occur. For the experiment testing the collagen hydrogel, it was used the same as Matrigel.

ERB formation was designated as successful if a small mass of cells was observed 24 hours after seeding. Later experiments replaced this designation with time-lapse microscopy in which the kinetics of the contraction were observed by measuring the area of the cell mass over time (See: *Measurement of ERB area*).

ERB recombinant protein/inhibitor treatments

Transforming Growth Factor-1 (TGFβ1) recombinant protein was prepared as a 1 mM solution by being resuspended in sterile distilled water and aliquoted. For treatment, EnSC were subject to 200 nM TGFβ1 recombinant protein in medium 200 or control at the time of seeding onto Matrigel for ERB formation. The treatment was maintained for 24 hours and then the area of the ERB was measured at 24 hours post seeding (See: *Measurement of ERB area*) .

TGFβ1 superfamily activin-like kinase ALK5 inhibitor A83-01 was resuspended in DMSO (5 mg/ml) and aliquoted. EnSC were subject to 1, 10 or 100 µM A83-01 or

vehicle control diluted in Medium 200 at the time of seeding onto Matrigel for ERB formation. The treatment was maintained for 24 hours and then the area of the ERB was measured (See: *Measurement of ERB area*).

ROCK inhibitor Y-26732 was re-suspended in DMSO (5 mg/ml) and aliquoted. EnSC were subject to 1 or 10 µM Y-26732 diluted in medium 200 or vehicle control at the time of seeding onto Matrigel for ERB formation. The samples were imaged by time-lapse microscopy for 36 hours. The area of the ERB was measured every 4 hours (See: *Measurement of ERB area*).

ROCK 2 inhibitor KD025 was resuspended in DMSO (5 mg/ml) and aliquoted. EnSC were subject to 1 µM KD025 or vehicle control in 200 µl of Medium 200 at the time of seeding onto Matrigel for ERB formation. The samples were imaged by time-lapse microscopy for 36 hours. The area of the ERB was measured every 4 hours (See: *Measurement of ERB area*).

Focal adhesion kinase (FAK) inhibitor Y15 was resuspended in DMSO (5 mg/ml) and aliquoted. EnSC were subject to 50 µM Y15 or vehicle control in 200 µl of Medium 200 at the time of seeding onto Matrigel for ERB formation. The samples were imaged by time-lapse microscopy for 36 hours. The area of the ERB was measured every 4 hours (See: *Measurement of ERB area*).

Endometrial gland organoid culture

Endometrial gland organoid culture

All endometrial gland organoids were cultured in an adapted protocol first described by Turco *et al.,* 2017. As described elsewhere, fresh biopsies were digested mechanically and enzymatically and filtered through a 40-µm cell filter to separate the EnSC and endometrial gland fragments. The endometrial gland fragments were

collected by inverting the sieve onto a sterile falcon centrifuge tube and adding 10 ml phenol-free DMEM/F12 medium and centrifuged at 400 g for 5 min. The endometrial gland fragments were resuspended in 500 µl phenol-free DMEM/F12 medium in an Eppendorf microcentrifuge tube and centrifuged at 600 g for 5 minutes. The medium was removed and ice-cold neat Matrigel was added with the volume dependent on the size of the pellet (a ratio of 1:20 between pellet and Matrigel). Samples mixed in Matrigel were kept on ice until plating. 20 µl of the Matrigel suspension was aliquoted using ice cold pipette tips into a 48 well plate and allowed to cure in the cell culture incubator (37°C and 5% v/v CO_2) for 15 minutes. Expansion medium (ExM) (see table below) was then laid over the top and samples were cultured for up to 7 days and is the same formulation as Turco, et al. 2017.

ExM composition

Medium component	Final Concentration
Advanced DMEM/F12	1×
A83-01	500 nM
Antibiotic-Antimycotic (100×)	1×
B27 supplement	1×
EGF	50 ng/ml
FGF10	100 ng/ml
HGF	50 ng/ml
L-Glutamine	2 mM
N2 supplement	1×
NAC	1.25 mM
Nicotinamide	10 mM
Noggin	100 ng/ml
R-spondin-1	500 ng/ml

ExM was refreshed every 48 hours. For experiments using collagen hydrogel instead of Matrigel, the only difference is the curing time was longer, as collagen required 45 minutes of incubation before adding ExM.

Endometrial gland organoid passaging

Endometrial gland organoids were passaged 7 days after seeding. This protocol is adapted from the method described by Turco *et al.,* 2017. First, samples were collected into Eppendorf microcentrifuge tubes by scraping the Matrigel droplet. The samples were centrifuged at 600 g for 6 minutes at 4°C. Samples were resuspended in ice-cold phenol red-free DMEM/F12 and subjected to manually 300× pipetting to disrupt the organoids. The samples were centrifuged at 600 g for 6 minutes at 4°C. Samples were resuspended in ice cold additive free DMEM/F12 and subjected to a further manual 80× pipetting to further disrupt the organoids. The samples were centrifuged at 600 g for 6 minutes at 4°C again and resuspended in Matrigel and plated as described elsewhere, or for complex organoid cultures.

Complex organoid culture

Complex organoid formation and culturing

P1 EnSC and endometrial gland organoids were passaged by their respective passaging protocols described elsewhere. The EnSC and gland organoid cell pellets were mixed at a ratio of 1:1. Ice cold collagen hydrogel added was dependent on the size of the pellet (a ratio of 1:20 between EnSC and gland organoid mixture and Collagen hydrogel). Samples were kept on ice until plating. 20 µl of the mixed suspension was aliquoted using ice cold pipette tips into a 48 well plate and allowed to cure in the cell culture incubator (37°C and 5% v/v CO_2) for 45 minutes. Complex organoid expansion medium (co-ExM) containing 1 nM estradiol was then laid over the top and samples were cultured for up to 7 days. Co-ExM was refreshed every 48 hours. See Chapter 4 for further details.

Complex organoid growth medium optimisation

Complex organoid cultures from three independent biopsies were aliquoted into a 48 well plate such that there were duplicate wells of cultures for each growth medium composition. Samples were subjected to the different media for 8 days to allow for growth and expansion. On day 8, all samples were imaged and observed for visual signs of expansion.

Complex organoid decidualisation treatment

Complex organoid cultures were grown in co-ExM for 4 days to allow for growth and expansion. On day 4, samples were treated with differentiation medium (DM) containing 0.5 mM 8-bromo-cAMP and 1 µM MPA for 4 days or maintained in co-ExM as control. After 4 days of differentiation, all samples were harvested for RNA. On D0, D2 and D4 of differentiation, spend media was collected, and DM was replaced.

Complex organoid minimal differentiation medium optimisation

Complex organoid cultures from three independent biopsies were aliquoted into a 48 well plate such that there were duplicate wells of cultures for each DM composition. All samples were grown in co-ExM for 4 days to allow for growth and expansion. On day 4, each sample was subject to the different DM compositions (See Chapter 4 for specific compositions) or co-ExM as control. After 4 days of differentiation, all samples were harvested for RNA.

Microscopy

Brightfield microscopy

All microscopy was performed on the EVOS FL Auto Imaging System instrument. For ERB formation studies, brightfield images were captured using 2× objective in brightfield. For ERB formation studies using time-lapse microscopy, EnSC were seeded onto Matrigel as described in a 96-well cell culture plate, and then mounted

onto microscope vessel holder contained in a sealed environment chamber maintained at 37^{o}C with humidified 5% v/v CO_2. Brightfield images were taken every 4 hours for 36 hours.

Live cell tracker stain microscopy

Co-cultured ERB containing EnSC and EEC were stained with CellTracker Green CMFDA and CellTracker Red CMPTX dyes, respectively, prior to being mixed and seeded onto Matrigel. CellTracker dyes were resuspended in DMSO to a final concentration of 10 mM. The CellTracker dye working solutions were prepared by diluting the CellTracker stock solutions to 25 µM in serum free phenol free DMEM/F12, exactly by the manufacturer's instructions. Cultured EnSC were harvested with Trypsin-EDTA as described previously. Fresh, patient matched cryopreserved EEC were thawed by first warming the sample until almost fully thawed and adding 8 ml 10% DCC-FBS supplemented DMEM/F12 into a 14 ml Falcon centrifuge tube. Both EnSC and EEC were centrifuged separately and resuspended in their respective CellTracker working solution. Samples were incubated at 37^{o}C for 30 minutes and then centrifuged at 400 g for 5 minutes and resuspended in Medium 200. The ERB forming assay was performed as described above. However, for co-culture with EEC, 1x10^{4} CellTracker stained EEC were either mixed with 1x10^{5} CellTracker stained EnSC prior to seeding onto 50 µl Matrigel or 1x10^{4} EEC were seeded 24 hours after seeding the EnSC onto Matrigel (original method) (See Chapter 3 for optimisation details). Red fluorescence was imaged by the EVOS Auto TxRed colour cube (Excitation: 585/29 nm, Emission: 628/32 nm) (CellTracker™ Red CMTPX Dye excitation/emission spectra (577/602 nm maxima)) and green fluorescence was imaged by the GFP colour cube (Excitation: 470/22 nm, Emission: 525/50 nm) (CellTracker Green CMFDA excitation/emission spectra (492/517 nm maxima)).

Live/ dead stain microscopy

ERB were measured for live and dead cells following formation. ERB were stained with NucBlue (Excitation/Emission: 360/460 nm) and NucGreen (Excitation/Emission: 504/523 nm) 24 hours after EnSC were seeded onto Matrigel exactly as described by the manufacturer's instructions. NucBlue is a dye that can diffuse across cellular membranes and bind DNA and stain live cells, representing the live cell population. NucGreen cannot pass through cellular membranes and therefore can only stain cells of which their membranes have been disrupted, as an indicator of cell death. Images were taken 1, 2 and 4 days after EnSC seeding onto Matrigel. Blue fluorescence was imaged by the EVOS DAPI light cube (Excitation: 357/44 nm, Emission: 447/60 nm). and the green fluorescence was imaged by the EVOS GFP light cube (Excitation: 470/22 nm, Emission: 525/50 nm).

Immunohistochemistry

Complex organoids were harvested by peeling the gel off the well plate with tweezers carefully to maintain the droplet in one piece and placed into a bijou tube. Samples were washed in PBS and formalin fixed in the tube for 15 minutes. Samples were washed three times with PBS and stored for use. The samples were then dehydrated by being subjected to increasing concentrations of ethanol (70%, 90% and 100%) for 1 hour each. Samples were then transferred to a glass tube and resuspended in xylene for 1 hour. Samples were then paraffin embedded and placed on an ice-cold surface to set. Embedded samples were sectioned into 5 µm slices by microtome and mounted onto microscopy slides and stored at 4^{o}C.

For immunohistochemistry (IHC) studies, sections were then subjected to a series of hydration steps of xylene, 100% isopropanol, 70% isopropanol and distilled water. Samples were then subject to antigen retrieval by being submerged in buffer (pH dependent on antibody) and placed in a Pickcell pressure cooker for ~1 hour, allowing

further time for the instrument to cool fully. Slides were then placed into a dark moisture chamber and wash with distilled water. Following this step, a hydrophobic pen (PAP) was used to mark a border around the sample. For samples to be immunolabelled for internal markers, samples were permeabilised by triton x-100 for 30 minutes. Samples were then washed with PBS and blocked in 2% BSA/ TBST for 30 minutes. Primary antibodies were diluted (See antibodies table) in 2% BSA/ TBST overnight at 4^{o}C. Samples were then washed in TBST three times and secondary rabbit and mouse antibodies conjugated to Alexa Fluor 488 or 594, respectively, (See antibodies tables) diluted 1:500 in 2% BSA/ TBST were added for 2 hours at room temperature. Samples were then washed in TBST three times and mounted in Vectashield with DAPI for nuclear counterstain. Samples were visualised using the EVOS Auto system using the GFP, TxRed and DAPI cubes to visualise Alexa Fluor 488 and 594, and DAPI, respectively. The microscopy parameters (LED intensity, camera gain, and exposure) for imaging were set the same for all images and maintained throughout image acquisition (See IHC Microscopy Parameters table on the next page).

IHC Microscopy Parameters

EVOS Light Cube	**LED intensity**	**Camera gain** (dB)	**Exposure** (ms)
DAPI	6	0.0	28
TxRed	25	1..0	65
GFP	35	1.2	88

Image analysis

ERB area measurement

Image analysis program ImageJ was utilised for all image analysis. Images of ERB were processed by converting the image to an 8-bit and then a threshold was manually used to highlight the ERB. The images were assigned a scale by using the

‘Set Scale’ command and manually drawing over the pre-set scale bar from the EVOS Auto system and assigning it the measurement provided by the EOVS. This scale was set as the ‘global’ scale for all images being analysed, as all images were imaged using the same objective. The area highlighted was measured by using the ‘Measure’ command, ensuring ‘Area’ was checked in the ‘Set Measurements’ box.

Immunohistochemistry

The EVOS Auto system saves individual channel data as .TIF images. In ImageJ, the images were merged into a single colour image using the ‘Merge Channels’ tool and saved as jpeg files. Brightness and contrast were enhanced in images that were being compared to each other to the same degree.

Protein analysis

Protein extraction

Cultures of EnSC were subject to whole cell protein extraction by direct lysis using RIPA buffer. The RIPA buffer was supplemented with cOmplete EDTA-free protease inhibitor. For extraction, cell culture medium was aspirated from the cultures. EnSC were washed with PBS twice. RIPA buffer solution (60 µl) was added per 6-well plate well. Plates were scraped using a silicon scraper to detach any unlysed cells. The solution was collected into microcentrifuge tubes per sample. For ERB cultures, Matrigel was first removed by harvesting the ERB and gel plugs into a microcentrifuge tube per sample and centrifuging the samples 400 g for 5 min at 4^{o}C. The samples were washed three times with ice cold PBS and centrifuged in between each wash until there was a visible cellular pellet and Matrigel removed. RIPA buffer solution (60 µl) was added per in triplicate ERB sample. All samples were centrifuged at 12000 g for 15 min at 4°C. Supernatants were collected (containing extracted protein) and stored at -80°C.

Protein concentration quantification

Extracted protein concentration was determined by Bradford assay. The Bradford assay reagent contains Coomassie blue dye. The assay is a colorimetric assay in which the Coomassie blue changes absorbance when bound to certain protein residues (As seen by a colour change from brown to blue, visible by eye). Stock Bovine Serum Albumin (BSA) was diluted to produce a concentration curve of 0 to 3.5 µg in 0.5 µg increments in a clear 96 well plate. Bio-Rad protein assay dye reagent (20 µl) was added to each well for both the standard curve and samples, in duplicate. Whole cell protein extract samples were diluted 1:400 in distilled water and added to the sample wells. PheraStar microplate reader measured the plate at 595 nm absorbance. Protein concentrations were determined by reference to the constructed concentration curve.

SDS-PAGE

Samples were diluted to 20-40 µg protein in 3.5 µl 1 M DTT, 8.75 µl NuPage buffer as well as distilled water topped up to a total volume of 35 µl. Protein solutions were heated to 70^{o}C and then placed rapidly on wet ice and briefly mixed and centrifuged. SDS-Page gels were prepared in disposable plastic cassettes. The lower resolving gel was prepared to pH 8.8. The percentage of acrylamide protogel used was dependent on the size of the protein of interest. The upper stacking gel was always prepared to pH 6.8 and 5% acrylamide protogel. Gel polymerisation was initiated by TEMED and 10% APS. First, the resolving gel was poured into the cassette and overlaid with 100% isopropanol. Once set, the isopropanol was rinsed off with distilled water and the stacking gel was poured on top and the 10-well comb was inserted. Once fully cast, gel cassettes with the comb removed were inserted into Invitrogen XCell SureLock Mini-cell and then into the electrophoresis tank with running buffer. Equal volumes of the prepared protein solutions were loaded into the wells as well as a pre-stained molecular weight ladder. A 100V constant voltage was applied until

protein separation occurred. After electrophoresis, gel cassettes were removed and opened to remove the gel for Western blot immunoprobing.

Western blot

Resolved protein sample gels were transferred to nitrocellulose membrane for antibody immunoprobing using a wet-blot method. The sample gel and pre-soaked nitrocellulose membrane were placed on top of pre-soaked blotting pads and Whatman filter paper, followed by more filter paper and blotting pads to form a gel/membrane sandwich. The sandwich was rolled to remove bubbles, which can interfere with visualisation. The assembled chamber was placed into a transfer tank with transfer buffer. Transfer was performed at a constant voltage of 280 mA for 1 hour 50 minutes. Following transfer, the nitrocellulose membrane was blotted and transferred to a 50 ml Falcon centrifuge tube and blocked in 5% milk or BSA in TBST for 1 hour at room temperature on a roller, antibody dependent. The membrane was subsequently incubated with the primary antibody diluted in 5% milk or BSA in TBST overnight on a roller at 4˚C. The membrane was washed in TBST three times. The membrane was then incubated with a secondary antibody conjugated to horseradish peroxidase in 5 % milk TBST for 1 hour on a roller at room temperature. The secondary antibody needs to be immunoreactive for the primary antibody host species. The membrane was washed in TBST three times. Finally, the ECL Plus solution was prepared and pipetted immediately onto the blotted membrane and incubated at room temperature for 5 minutes and visualised by G-Box for luminescence.

ELISA

Solid Phase Sandwich enzyme-linked immunosorbent assay (ELISA) kits were used for the detection of PRL, OPN and CXCL14. For detection of PRL in Chapter 3, total protein lysate was used and harvested as previously described. For detection of PRL,

OPN and CXCL14 in Chapter 4, spend medium from complex organoid culture was used. Spent medium was collected every two days during a 4-day decidual time course. ELISA were performed exactly as per manufacturer's instructions (DuoSet ELISA kits for PRL (DY682), OPN (DY1433), CXCL14 (DY866), Bio-Techne, Abingdon, UK). Once completed, the colour development was stopped using the stop solution and a PheraStar microplate reader was used to measure absorbance at 450 nm and background absorbance measured at 540 nm. Protein concentration was obtained using a 4-paramenter logistic regression analysis and interpolation from the curve. The data were normalised to total protein concentration, explained elsewhere.

Transient transfection

Primary EnSC cultures were transiently transfected using the jetPRIME PolyPlus transfection kit following the manufacturer's instructions. All siRNA were resuspended to 25 µM, aliquoted and stored at -20^{o}C. For transfection, siRNA was diluted in the jetPRIME buffer to a concentration of 55 nM and briefly vortexed. Then, 4 µl jetPRIME reagent was added per 200 µl jetPRIME buffer used, briefly vortexed and centrifuged and incubated at room temperature for 10 minutes. 200 µl of the transfection solution was added per 2 ml of 10% DCC-FBS supplemented DMEM/F12 (used per well of a 6 well plate). This medium was then added dropwise to the ~80% confluent EnSC culture. Media was refreshed after 24 hours with 10% DCC-FBS supplemented DMEM/F12. All targeted siRNA used were Dharmacon SMARTpool siRNA, and the Dharmacon Non-Targeting siRNA Pool 1 was used as a non-targeting (NT) control.

RNA extraction

RNA extraction of EnSC and ERB cultures

For all RNA extraction procedures, RNase-free plastic-ware and nuclease free water were utilised, and surfaces and pipettes were cleaned with RNase ZAP, in order to minimize RNA degradation. Per well of a 6-well plate, 400 µl of STAT-60 reagent was

added to ensure full coverage and incubated for 5 minutes at room temperature. A cell scraper was used to disrupt any remaining attached cells. The solution was transferred to RNase-free 1.5 ml Eppendorf microcentrifuge tubes on wet ice or snap frozen and stored at -80ºC. For RNA extraction, 20% volume of ice-cold chloroform was added to the STAT-60 solution and briefly vortexed. The STAT-60/chloroform mixtures were centrifuged at 12000 g at 4°C for 30 minutes to separate out the aqueous and organic phases. The aqueous phase, containing the RNA, was transferred to an Eppendorf microcentrifuge tube containing 0.5× volume ice-cold 100% isopropanol and incubated for 10 minutes at room temperature. The RNA was pelleted by configuration at 12000 g at 4°C for 15 minutes. The RNA pellet was then washed twice with 1 ml ice cold 75% ethanol and centrifuged at 12000 g at 4°C for 5 minutes between wash steps. The RNA pellet was then allowed to air dry and then resuspended in nuclease free water. RNA concentration and purity were determined by Nano-Drop. RNA samples with values of ≥ 1.80 on the 260/280 absorbance scale were used for downstream analyses. All RNA samples were stored at -80°C.

RNA extraction of complex organoid cultures

For all RNA extraction procedures, RNase-free plastic-ware and nuclease free water were utilised, and surfaces and pipettes were cleaned with RNase ZAP, in order to minimize RNA degradation. Gland organoid cultures were recovered scraping the samples into RNase-free 1.5 ml Eppendorf microcentrifuge tubes. Samples were centrifuged at 600 g for 6 minutes. The cellular pellet was resuspended in 500 µl 500 µg/ml collagenase I and incubated at 37ºC for 10 minutes (See Chapter 5 for method optimisation). Samples were centrifuged at 600 g for 6 minutes and resuspended in PBS for washes (repeated 2 times) and then cellular pellets were either snap frozen or placed into lysis buffer for RNA extraction. RNA extraction was performed using the RNeasy Micro Kit (Qiagen) exactly following manufacturer's instructions. RNA concentration and purity were determined by Nano-Drop. RNA samples with values

of ≥ 1.80 on the 260/280 absorbance scale (were used for downstream analyses. All RNA samples were stored at -80°C.

cDNA synthesis

cDNA was reverse transcribed from the collected mRNA using a QuantiTect Reverse Transcription Kit following manufacture's instruction. In brief, all reagents were first thawed on wet ice and briefly vortexed and centrifuged. Then, for to up to 1 µg of sample RNA, 2 µl of 7× gDNA Wipeout buffer was added to each sample. However, for most simple and complex organoid samples 1 µg was not possible, and therefore instead the lowest concentration of RNA across the samples was used for all samples. This solution was then made to a total volume of 14 µl with RNase-free water and incubated at 42°C for 2 minutes to remove any genomic DNA. After, the samples were quickly placed and kept wet ice. Per sample, 1µl of Quantiscript Reverse Transcriptase (RT), 4 µl 5x Quantiscript RT Buffer and 1 µl RT Primer Mix were added while kept on ice. For RT negative controls, the Quantiscript RT was replaced with nuclease free water. Samples were incubated at 42°C for 30 minutes and then the RT was inactivated by sample incubation at 95˚C for 3 minutes.

Real time quantitative polymerase chain reaction

Real time quantitative polymerase chain reaction (RT-qPCR) was used to determine relative mRNA abundance of genes of interest, as a method of measuring relative gene expression. Genes of interest were amplified using PrecisionPlus detection reagent, premixed with SYBR Green. The qPCR master mix contained 10 µl PrecisionPlus 2× master mix, 0.3 µl of forward and reverse primer (20 µM) and 8.4 µl nuclease free water to total 19 µl, per reaction. For a reaction, 1 µl of cDNA was added to 19 µl of RT-qPCR master mix per well in triplicate for a total of 20 µl per 96-well. Non-template controls replaced cDNA with nuclease free water. The plate was sealed, briefly centrifuged and placed into the RT-qPCR machine (ABI PRISM 7500

Sequence Detection System). The thermocycling conditions were: 50^{o}C for 2 minutes, 95°C for 10 minutes, 95°C for 15 seconds and 60°C for 1 minute for 40 cycles.

The SYBR green of the PrecisionPlus detection reagent binds to double stranded DNA and produces a fluorescent signal. This signal is measured at each cycle, allowing the DNA to be quantified and assigned a Ct (cycle threshold) value. The Ct value represents the cycle in which the fluorescent signal reaches above background noise. Ct values were normalised to housekeeping gene *L19* and the Pffafl method was employed to account for variable primer efficiencies (see Primer table in Materials section). The normalised data was then directly compared to control samples to provide relative fold change of expression between the treatment and control samples.

Data mining

The dataset 'Endometrium through the menstrual cycle: GDS2052' from the GEO repository was data-mined for gene expression data in Chapter 3. ScRNA-seq data from Lucas *et al.* (2018) was data-mined for gene expression data through an *in vitro* primary EnSC 8-day decidual time course. In addition, genes of interest related to fibroblast activation in Chapter 3 were plotted onto the previously constructed co-regulated gene networks produced by Lucas *et al.* (2018).

Statistical analysis

Data were analysed using GraphPad Prism. All data were given as mean ± standard deviation (SD). For paired, non-parametric significance testing between two groups, the Wilcoxon matched-pairs signed rank test was used. For paired, non-parametric significance testing between multiple groups, the Friedman test and Dunn's multiple

comparisons *post hoc* test were performed. Only values of $P < 0.05$ were considered statistically significant.

Single cell RNA sequencing

Sample preparation

A single human endometrial biopsy was cultured as both simple and complex organoid cultures at passage 2. For both the simple and complex organoids, 10 technical replicates per time point were grown to ensure enough mRNA material for scRNA-seq. The samples were grown for 4 days in co-ExM and then harvested on day D0, D2 and D4 of decidualisation with minimal differentiation medium ($DM_{min.}$). Harvest was by collagenase I treatment, described as previous, and 5× TrypLE Select treatment (See Chapter 5 for method optimisation) to ensure a single cell suspension for droplet generation and single cell RNA sequencing (scRNA-seq).

Droplet generation and scRNA-seq.

The harvested single cell suspensions were loaded into a cartridge and placed into the microfluidic system (Nadia Instrument). The transcriptomes of single cells in simple and complex organoid cultures were captured in aqueous droplets containing barcoded beads according to the manufacturer's instructions and the Drop-Seq method described by Macosko, *et al.* (2015).

cDNA synthesis

Following droplet formation, the droplets were broken, and the beads were isolated. Reverse transcription of the bound mRNA was performed exactly as described by Macosko and Goldman (Drop-Seq Laboratory Protocol version 3.1). AMPure XP beads were used for PCR clean-up as described by Illumina RNA-seq protocols. The reverse transcribed cDNA was eluted in 12 µl. cDNA quality was measured by a Bioanalyzer High Sensitivity DNA chip.

Library preparation and Sequencing

XT DNA sample and indexing kits were used to produce tagmented libraries from the cDNA, as previously explained in Lucas. *et al*, 2018. AMPure XP beads were used for DNA clean up, as described elsewhere. A Bioanalyzer High Sensitivity DNA chip was used to assess quality and determine library size. Sample concentration was measured by Qubit High Sensitivity DNA assay. The library was sequenced using a NextSeq High Output 75 cycle V2 kit.

Data analysis and quality control

Data processing was performed initially as described by Nemesh, as previously explained in Lucas. *et al*, 2018. In brief, differential gene expression analysis was performed using the Seurat v2 68 package. Quality control (QC) was performed by only including genes that appear in at least three cells, and cells that express ≥ 200 genes. Only cells with ≤ 6000 genes and < 10% mitochondrial genes were included, to minimize inclusion of data from doublets and low-quality (broken or damaged) cells, respectively. In addition, cell-cycle regression was applied to the dataset. Principal component (PC) analysis was performed and the first 10 PC were utilised for clustering by shared nearest neighbour (SNN) and Uniform Manifold Approximation and Projection (UMAP) algorithms. This produced a visual representation of the cell aggregation, colour coded by statistically significant clusters. Marker genes for each cell state cluster in the UMAP representation were identified using the Seurat function 'FindAllMarkers'.

Gene ontology (GO) analysis using the Gene Ontology Consortium database (Ashburner et al., 2000, The Gene Ontology Consortium, 2018, Mi et al., 2013) was performed on significantly differential genes ($P < 0.05$ with Bonferroni-correction), where genes were clustered by annotated biological process categories. The GO

terms generated were further summarised using REVIGO, a web server that groups redundant GO terms by semantic similarity (Supek et al., 2011)

Chapter 3:

Endometrial Regenerative Bodies

3.1 Introduction

The human endometrium undergoes defined cycles of proliferation and differentiation in order to prepare for the embryo implantation (Gellersen and Brosens, 2014). In the absence of an implanting embryo, the upper layer of the human endometrium is sloughed off at menstruation in preparation for another cycle. Tissue repair, rapid growth and angiogenesis encompass the proliferative phase of the next cycle, under the influence of estradiol (Gellersen and Brosens, 2014). This rapid regeneration is principally due to a population of bone marrow-derived mesenchymal stem cells (MSC) that reside in the perivasculature of the basal layer of the endometrium (Schwab and Gargett, 2007, Chan and Gargett, 2006, Gargett et al., 2015).

As the MSC drive the rapid proliferation of the endometrial stroma, the main structural support of the endometrium, it was reasonable to utilize these cells as a starting point for developing a 3D model of the endometrium *in vitro*. Isolation of endometrial MSC and other sub-populations of the endometrial stroma have been described in the literature (Chan et al., 2004, Schwab et al., 2005). Perivascular endometrial stromal cells (PVC) express a specific surface antigen, called Sushi domain-containing 2 (SUSD2), which can be used to isolate them from a mixed population of cells by Magnetic-Activated Cell Sorting (MACS) (Masuda et al., 2012, Sivasubramaniyan et al., 2013) (Fig. 3.1). In this study, mixed populations of endometrial stromal cells (EnSC) are incubated with the antibody for SUSD2, originally named the W5C5 antibody (Masuda et al., 2012, Murakami et al., 2013), conjugated to a magnetic bead. The suspension is passed through a magnetic column, which retains $SUSD2^{+}$ cells only. However, the MSC represent only a fraction (approximately 4%) of the total PVC, which in turn is approximately 4% of total EnSC (Masuda et al., 2012). MSC are highly clonal as demonstrated by a colony forming unit (CFU) assay (Masuda et al., 2012). The $SUSD2^{-}$ EnSC fraction also contains clonal cells (Masuda et al., 2012),

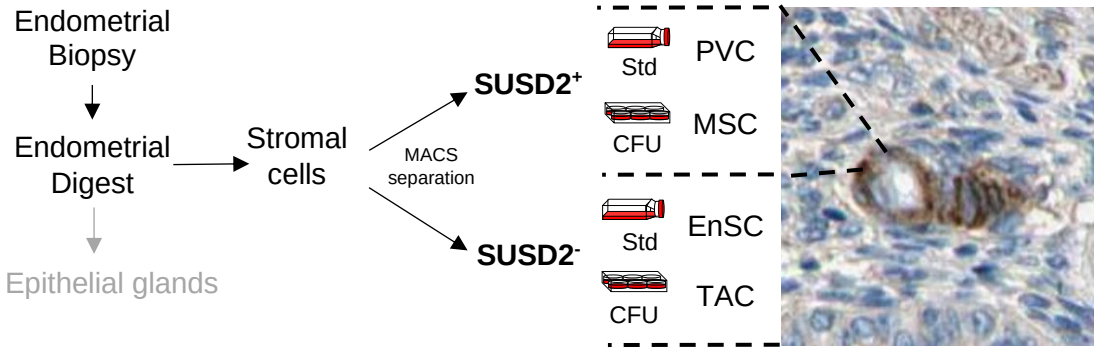

Figure 3.1: Schematic of the protocol for culturing endometrial stromal cell subtypes. Endometrial biopsies are enzymatically and mechanically dissociated. EnSC are separated from the mixture by a 40 µm cell sieve. MACS is performed using SUSD2^{+} antibody (W5C5). SUSD2^{+} and SUSD2^{-} cell fractions are cultured as standard culture (Std) or by CFU. Right Panel: Immunohistochemistry image of SUSD2^{+} immunolabelling of PVC around endometrial blood vessels. (Human Protein Atlas, SUSD2 Antibody HPA004117, Human Endometrium 1, Patient id: 2941, https://www.proteinatlas.org/ENSG00000099994-SUSD2/tissue/endometrium, Uhlén et al., 2015)

which are referred to here as transit amplifying cells (TAC). TAC are the undifferentiated but committed daughter cells of stem cells, which are found outside the stem cell niche. They are highly proliferative and exhibit clonal properties, like MSC (Gargett, 2006).

While investigating the angiogenic potential of the MSC, a former PhD student of Professor Brosens observed that MSC rapidly reorganise into singular tissue-like structures overnight when seeded onto Matrigel and cultured in an angiogenic medium (Medium 200) (Peter Durairaj, 2017). These tissue structures were designated Endometrial Regenerative Bodies (ERB), due to the presumed regenerative capacity of MSC (Peter Durairaj, 2017). ERB formation was purportedly a MSC-specific phenomenon; fresh unseparated EnSC failed to reorganise into the same tissue-like mass, further emphasizing the regenerative potential of endometrial MSC. ERB responded to ovarian hormone stimulation and expressed decidual marker genes upon differentiation by cAMP and MPA (Peter Durairaj, 2017). Therefore, the ERB provided a starting point to develop a 3D *in vitro* model of the endometrium.

In this chapter, I aimed to develop the ERB into a novel 3D *in vitro* model of the endometrium. This was to be achieved by completing the following objectives:

1. To establish a protocol for co-culturing the MSC-derived ERB with epithelial cells.

2. To study ERB growth and differentiation.

3. To elucidate the mechanisms underpinning the rapid cellular reorganisation.

3.2 Results

Endometrial Regenerative Bodies

Previous observations indicate that ERB are formed when MSC are seeded on top of Matrigel (Fig. 3.2A). Overnight, MSC form a singular 3D triangular mass (Peter Durairaj, 2017) (Fig. 3.2B). First, to investigate the MSC specificity, ERB formation was assessed in MSC and TAC and freshly isolated EnSC. Freshly isolated EnSC failed to form ERB, therefore confining ERB formation to progenitor cells. ERB formation was reported in MSC cultures (64% formation efficiency), and to a lesser extent in TAC cultures (12% formation efficiency). However, freshly isolated EnSC failed to form ERB (0% formation efficiency) (Fig. 3.2C) (Peter Durairaj, 2017). This indicated ERB formation was a specific phenomenon of the endometrial progenitor cells. It was therefore hypothesised that this process was regenerative in nature, and that these could form the basic cellular scaffold for developing a 3D *in vitro* model of the endometrium for human embryo implantation studies.

To further characterise the ERB, we previously investigated their ability to differentiate upon treatment of 8-bromo-cAMP (cAMP) and medroxyprogesterone acetate (MPA), a progestin. The MSC of three independent patient biopsies were isolated by MACS followed by CFU assay. The MSC from each biopsy were then subjected to ERB formation followed by differentiation with cAMP and MPA for 8 days in triplicate. By RT-qPCR, we demonstrated the induction of *PRL*, encoding decidual prolactin, by ERB treated with cAMP and MPA, establishing their ability to differentiate in response to deciduogenic cues (Fig. 3.2D).

Additionally, ERB (Day 1 ERB) from three independent patient biopsies were co-cultured with patient-matched endometrial epithelial cells (EEC) overnight and then fixed in formalin and paraffin embedded for sectioning. The sectioned ERB where

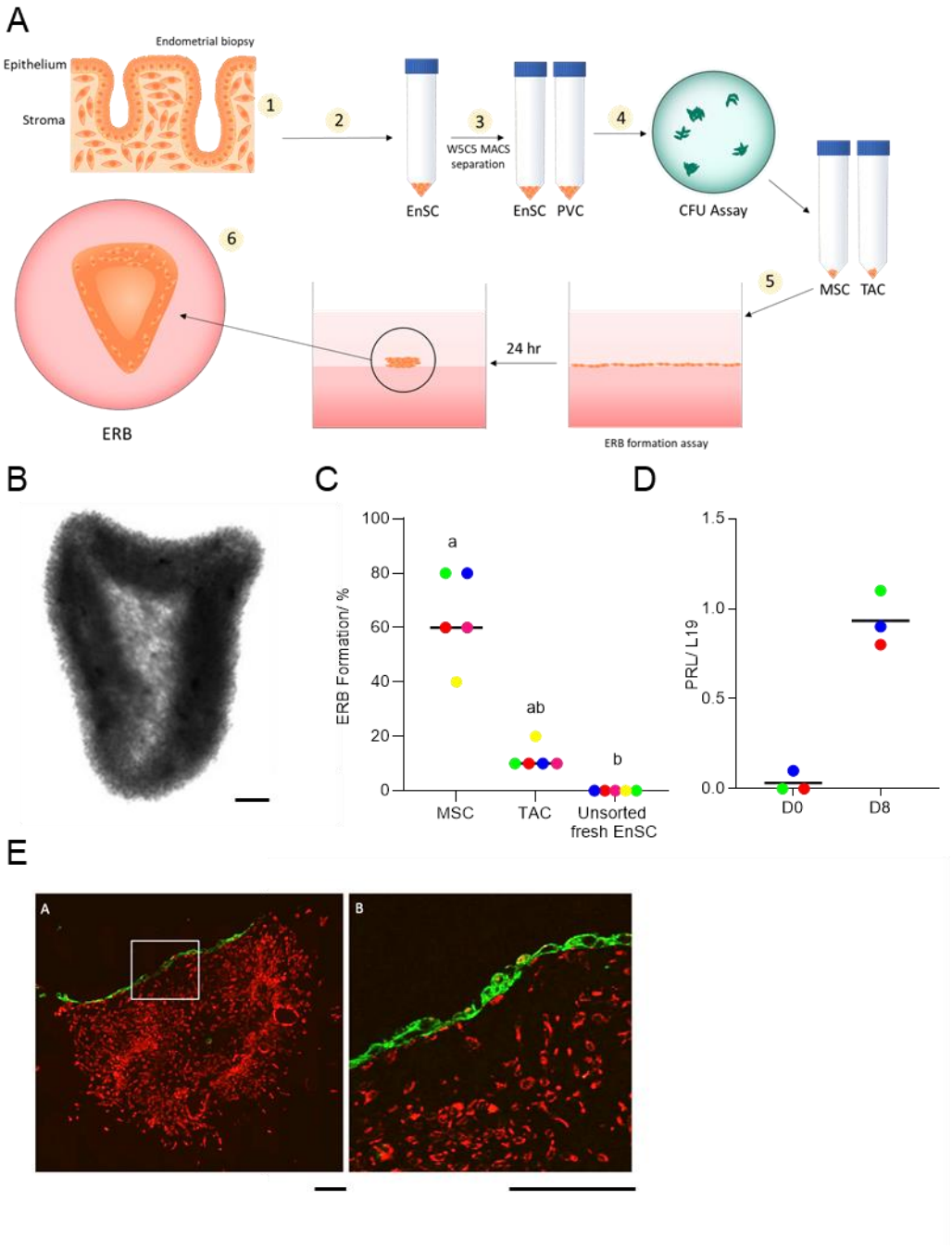

Figure 3.2: Initial characterisation of the ERB.

A: Schematic of ERB formation methodology: 1. Human endometrial biopsies are processed mechanically and enzymatically. 2. EnSC are separated from the epithelial glands. 3. MACS separation by SUSD2 antibody W5C5. 4. CFU assay of SUSD2^{+} cells. 5. ERB formation protocol performed by seeding 5×10^{4} MSC onto Matrigel. 6. A representative schematic of a formed ERB.

B: Brightfield image of an ERB 24 hours after seeding MSC onto Matrigel, representative of three biological replicates in triplicate. Scale bar = 500 µm.

C. The data show the percentage ERB formation by MSC, TAC and unsorted fresh EnSC, 24 hours after seeding onto Matrigel. Five biological replicates were tested in triplicate. Different letters above the error bars represent statistical difference from other groups at $P < 0.05$. Group comparison by Friedman test and Dunn's Multiple Comparison *post hoc* test.

D. The data show individual *PRL* transcript levels measured in ERB after being decidualised for 8 days with MPA and cAMP (D8) compared to control (D0). *PRL* expression was normalised to housekeeping gene *L19* mRNA levels. $P > 0.05$ (Wilcoxon matched pairs signed rank test).

E. Immunofluorescence image of a sectioned epithelialised ERB, representative of three biological replicates. ERB were formalin fixed and paraffin embedded and sectioned. Channels were visualised by epifluorescent microscopy (EVOS FL Auto Imaging System) using a secondary antibody conjugated to Alexa 488 and 594, depicted in green and red, respectively. Nuclei were counterstained with DAPI, depicted in blue. Cytokeratin (green) labelled the epithelial cells and vimentin (red) labelled the EnSC. (Scale bar: 100 μm).

The ERB model was developed by Dr Ruban Peter Durairaj (Peter Durairaj, 2017) and the initial preliminary data was collected in collaboration with Dr Ruban Rex Peter Durairaj during my MRC DTP in IBR MSc MD980 Laboratory Project 2 dissertation.

immunolabelled with vimentin (red) and cytokeratin (green) to visualise the MSC and EEC of the co-culture, respectively, by immunohistochemistry (IHC). The IHC revealed epithelialisation of the ERB along the external surface (Fig. 3.2E). These initial data further evidenced that ERB could potentially serve as a 3D model of the endometrium exemplified by the ability of these cells to differentiate and be re-epithelialised in co-culture with primary EEC.

Epithelialisation of ERB

The initial co-culture protocol produced an externally epithelialised ERB. However, epithelialisation of the internal surface of the ERB would better recapitulate the *in vivo* endometrium. In addition, a previous study demonstrated that EEC form a monolayer epithelium when seeded on top of cultured EnSC grown in 3D culture (Bentin-Ley et al., 1994). The initial ERB co-culture protocol seeded EEC on a formed ERB, 24 hours after seeding MSC on Matrigel. The external layer of epithelial cells suggested the EEC were unable to penetrate the ERB. Therefore, EEC were mixed with MSC and then seeded together on Matrigel on Day 0 (pre-formation) (Fig. 3.3A). Cells were stained with live cell tracker stains (MSC: red, EEC: green) and ERB were visualised by epifluorescence microscopy 24 hours after seeding. All ERB formed, however, the EEC were in the centre of the ERB, with the MSC surrounding the outside (Fig. 3.3B). However, a monolayer of EEC on the inward facing surface of the ERB was not observed suggesting co-culturing for 24 hours may not have been sufficient for ERB re-epithelialisation.

Next, using three independent patient biopsies, I performed a time-course to investigate whether the EEC would reorganise themselves into a monolayer epithelium along the inner surfaces of the ERB. However, unexpectantly, over the course of 10 days, the ERB continued to contract down into a small, tight mass of

A

Method	Day 0	Day 1	Day 2	Expected Outcome
External	Add MSC	Add EEC	**Co-cultured ERB**	
Internal	Add MSC + EEC	**Co-cultured ERB**		

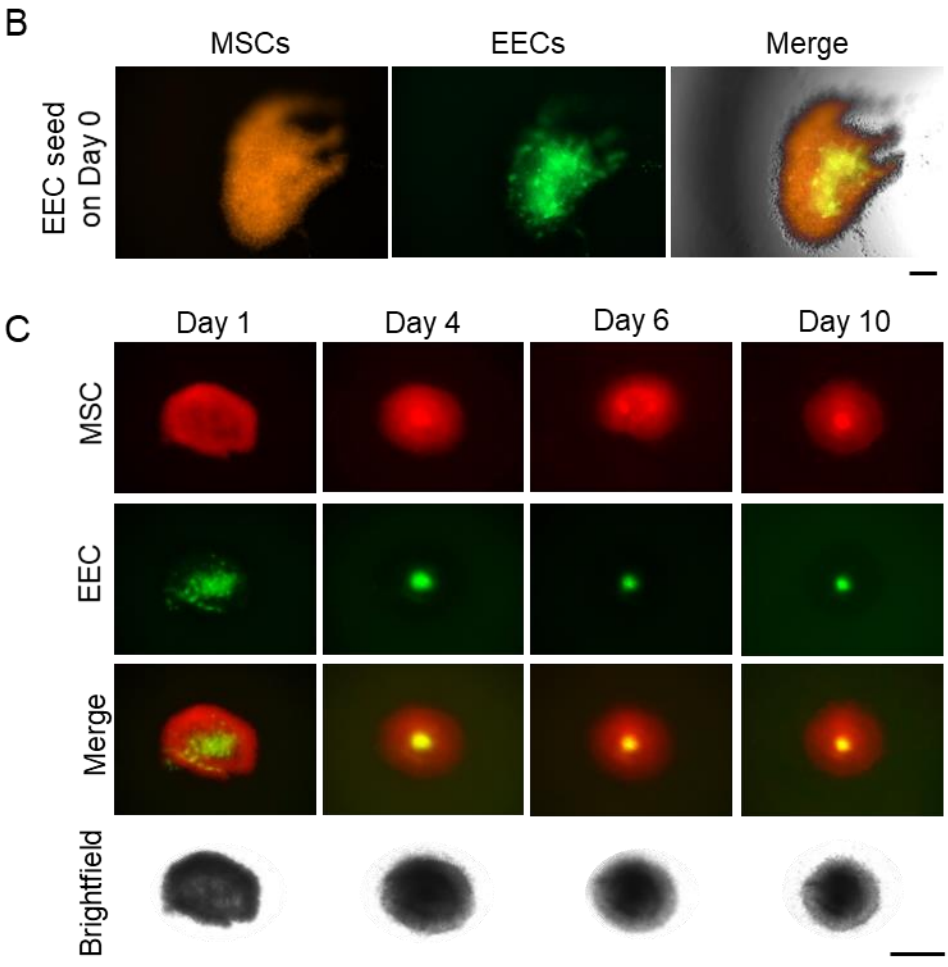

Figure 3.3: Re-epithelialisation of the ERB.

A: Table of ERB re-epithelialisation methods. Day 0 represents day of seeding onto Matrigel, and so on. Schematics of hypothesised ERB organisation are included. MSC were stained with Red CellTracker CMTPX and EEC were stained with CellTracker Green CMFDA. Scale bar = 100 μm.

B: Epifluorescence images of the ‘internal method.’ Representative images of three biological replicates in triplicate are shown. MSC were stained with Red CellTracker CMTPX and EEC were stained with CellTracker Green CMFDA. Scale bar = 500 μm. C. Epifluorescence images of ERB formation using the ‘Internal method’ over 10 days. Representative images of three biological replicates performed in triplicate are shown. MSC were stained with Red CellTracker CMTPX and EEC were stained with CellTracker Green CMFDA. Scale bar = 500 μm.

cells, compressing EEC into the centre of the structure (Fig. 3.3C). This evidenced that the ERB are short-lived structures and unable to support long-term growth.

Method development

Following initial characterisation, ERB formation efficiency was still sub-optimal and it was unclear if this lack of reproducibility was due to technical issues or the patient-specific characteristics, as assumed previously (Peter Durairaj, 2017). To test this, I developed an alternative protocol in which the Matrigel was plated and pre-incubated without cells before seeding (Fig. 3.4A). The hypothesis was that standardising the Matrigel curing time would reduce experimental inconsistencies. ERB formation following this new protocol was 100% efficient in five independent MSC cultures (Fig. 3.4B and 3.4C). In comparison, the previous method formed ERB with 46% efficiency. Thus, this novel protocol was utilised for all subsequent experiments.

ERB form from all cultured stromal cell subtypes.

As the new method had improved ERB formation to a 100% efficiency, it was essential to confirm the previous observation that ERB formation is specific to MSC. Instead of freshly isolated EnSC, cultured EnSC and PVC were subjected to ERB formation to compare directly to the cultured CFU-derived MSC and TAC. ERB formation was imaged under time-lapse microscopy for 36 hours following the new protocol and the area of the cell mass was measured every 4 hours to ensure the full formation was captured (Fig. 3.5A). The images were then analysed by ImageJ in order to measure the area of the ERB at each time point to map the contraction kinetics of each stromal cell subtype (Fig. 3.5B). Surprisingly, all subpopulations, including the non-CFU-derived fractions (EnSC and PVC), formed ERB in what appeared to be by a cellular contraction phenomenon. However, at 16 hours, the MSC had contracted further than the PVC (Area ± standard deviation (SD) = 0.12 ± 0.02 cm^2 versus 0.52 ± 0.14 cm^2, respectively). Similarly, the clonal TAC had also

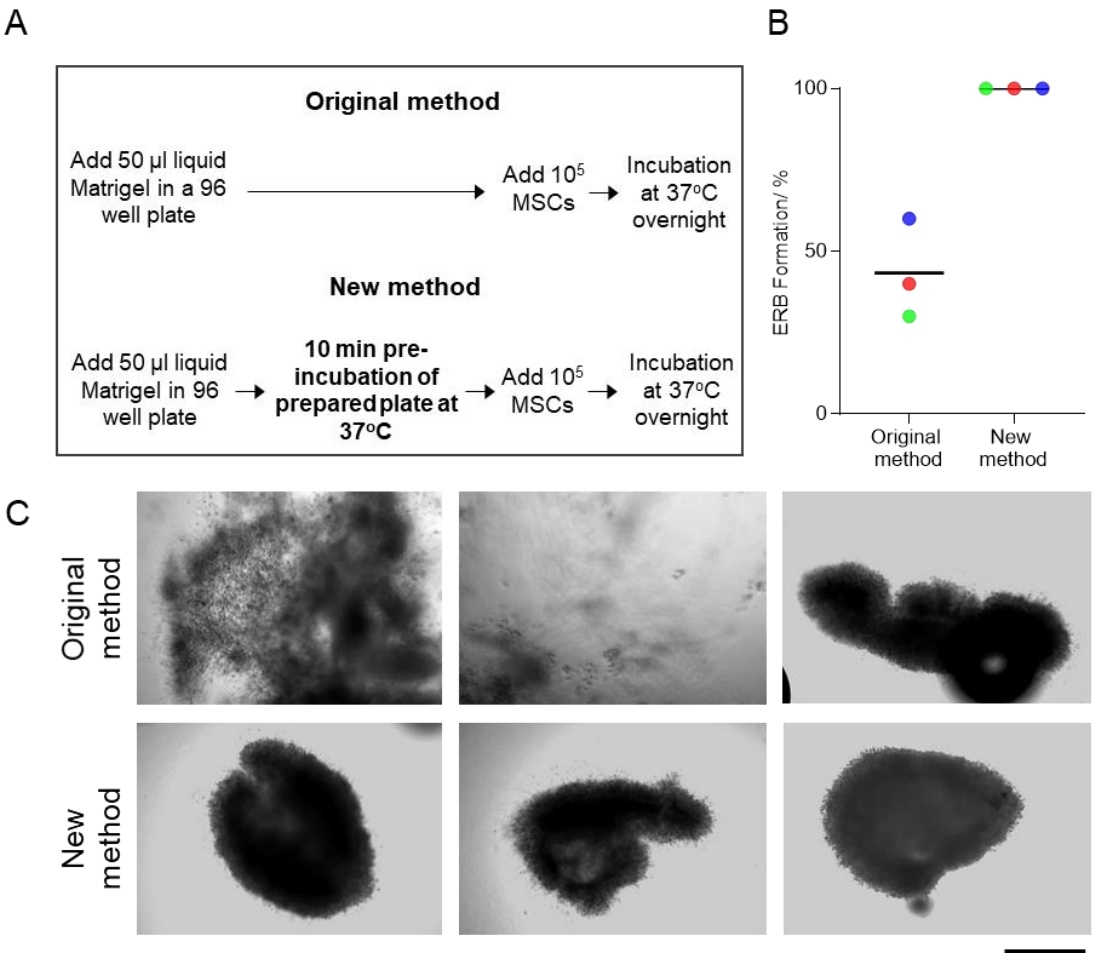

Figure 3.4: ERB method optimisation.

A: A schematic comparing the original and proposed methods for ERB formation.

B: The data show percentage ERB formation in MSC, TAC and unsorted fresh EnSC 24 hours after seeding onto Matrigel. The colours represent the three individual cultures. The line represents the mean. ERB formation was performed on three independent primary cultures in triplicate. $P > 0.05$ (Wilcoxon matched pairs signed rank test).

C. Brightfield images of ERB formation using the two methods, representative of five biological replicates in triplicate. Scale bar = 500 µm.

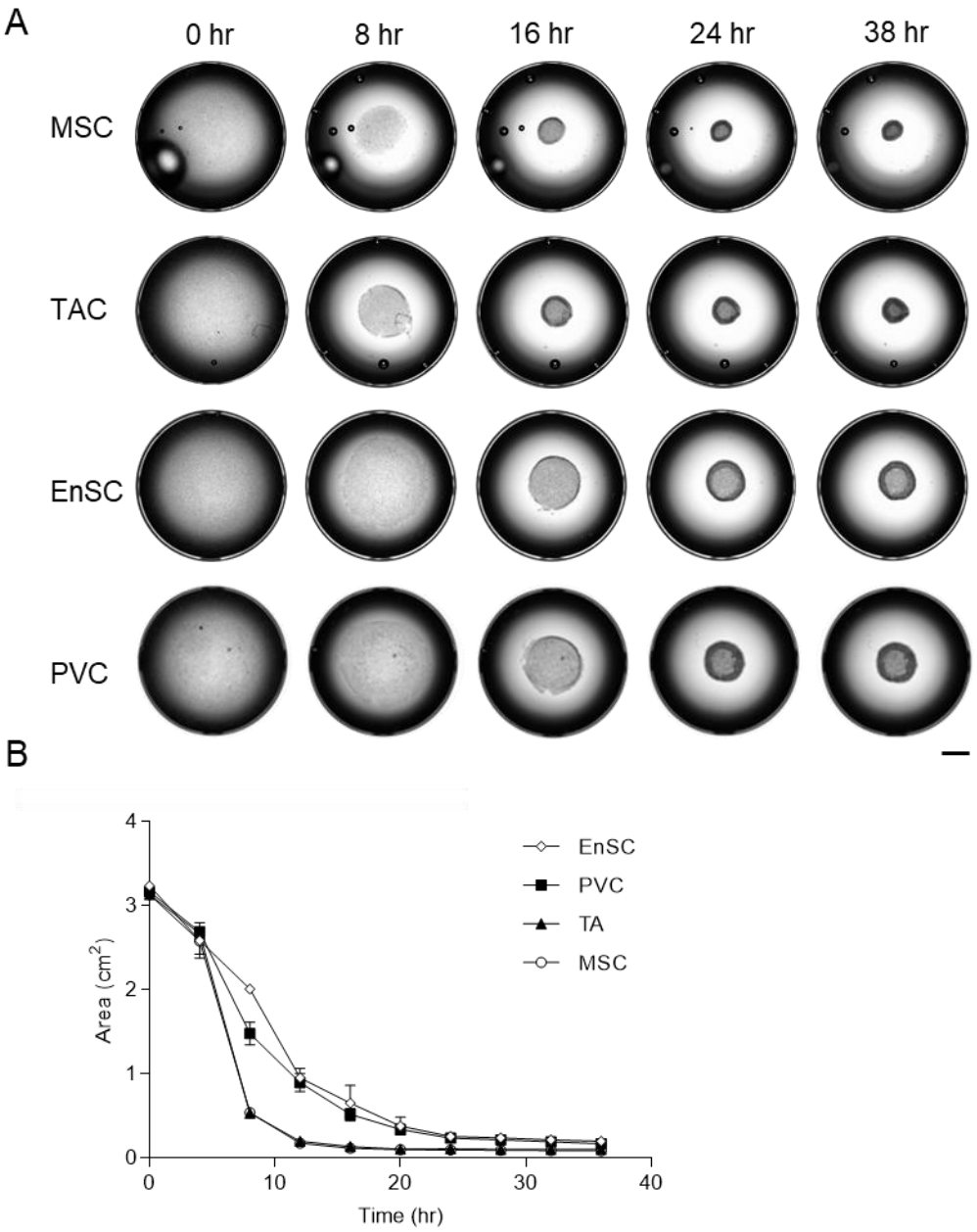

Figure 3.5: Time-lapse imaging of ERB formation in endometrial stromal subtypes.

A: Representative brightfield images of ERB formation using different stromal subtypes (MSC, TAC, EnSC, and PVC) over a period of 38 hours. ERB formation was performed on three matched independent primary cultures in triplicate for each stromal subtype.

B: Data show the contraction kinetics of ERB formation using the different stromal subpopulations over 38 hours. The data show area ± standard deviation of the cellular mass measured every 4 hours. The ERB formation was performed on three matched independent primary cultures in triplicate for each stromal subtype.

contracted further than the EnSC (Area ± SD = 0.14 ± 0.01 cm^2 versus 0.65 ± 0.05 cm^2, respectively). However, by 24 hours, both PVC and EnSC reached a similar area to their clonal counterparts and ceased to contract further (Area ± SD = 0.23 ± 0.01 cm^2 and 0.26 ± 0.01 cm^2, respectively). Hence, ERB formation was deemed not a stem cell-specific, regenerative process. Therefore, due to their greater availability, EnSC were used instead of MSC for all further experiments.

Fibroblast activation

From the time-lapse microscopy data, it was clear that these cellular aggregates were contracting, instead of reorganising, and that this was a characteristic of all i*n vitro* propagated endometrial stromal subtypes when cultured on Matrigel. I hypothesised that this contraction was due to fibroblast activation. Fibroblasts are known to attain a myo-fibroblastic contractile phenotype when activated (Tampe and Zeisberg, 2013, Zeisberg and Zeisberg, 2013, Kalluri, 2016). Transforming growth factor beta 1 (TGFβ1), a growth factor and cytokine, is a major regulator of fibroblast activation (Rønnov-Jessen, 1993, Kalluri, 2016). TGFβ1 is also involved in the upregulation of extracellular collagen production during fibroblast activation-associated ECM remodelling (Kalluri, 2016). Therefore, three independent cultures were subjected to either recombinant TGFβ1 or with A83-01, a potent inhibitor of activin-like kinase 5 (ALK5), ALK4 and ALK7 from the TGFβ1 receptor superfamily (Tojo et al., 2005a). EnSC from three independent cultures were plated onto Matrigel and subjected to either 200 nM recombinant TGFβ1 treatment or vehicle control (DMSO). At 24 hours, the cultures treated with recombinant TGFβ1 were more contracted than matched vehicle control cultures (Area ± SD = 0.22 ± 0.04 cm^2 versus 0.29 ± 0.02 cm^2, respectively (Fig. 3.6A). This suggests that the added recombinant TGFβ1 was able to accelerate EnSC contraction. In addition, when three independent cultures were treated with either 1 or 10 μM A83-01 when seeded onto Matrigel, a significant dose response was observed. Treatment with 10 μM A83-01 maintained a significantly

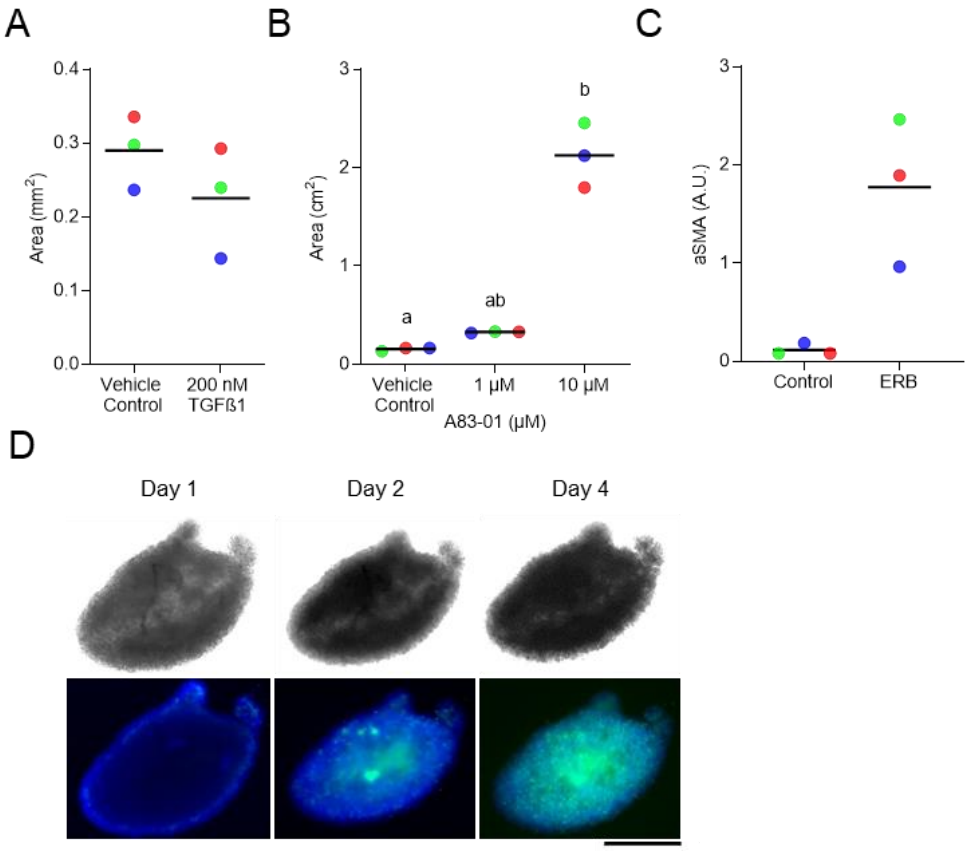

Figure 3.6: Characterisation of fibroblast activation in ERB.

A: Area of ERB formation from EnSC treated with 200 nM TGF-β1 or vehicle control (DMSO). The data show the area of ERB formed from three biological replicates performed in triplicate 24 hours after seeding on Matrigel. The colours represent the three individual cultures. The line represents the mean. $P > 0.05$ (Wilcoxon matched pairs signed rank test).

B: Data show the area of ERB from EnSC of three biological replicates in triplicate 24 hours after seeding on Matrigel treated with 1 or 10 µM A83-01 or vehicle control (DMSO). The colours represent the three individual cultures. The line represents the mean. Normalised to Western blot probed for β-actin to ensure equal loading. Different letters above the error bars represent statistical difference from other groups at $P < 0.05$. Group comparison by Friedman test and Dunn's Multiple Comparison *post hoc* test.

C: The densitometry from western blots probed for αSMA from three biological replicates of standard EnSC culture (Control) and ERB (36 hours after seeding on Matrigel). The colours represent the three individual cultures. The line represents the mean. $P > 0.05$ (Wilcoxon matched pairs signed rank test).

D: A representative image of an ERB stained with NucBlue Live/ NucGreen dead stain following formation at Day 1 (24 hours from seeding), and 48 hours (Day 2) and 96 hours (Day 4) later. Scale bar = 200 μm.

larger area when compared to the vehicle control (DMSO) at 24 hours (Area ± SD = 0.31 ± 0.02 cm^2 and 0.15 ± 0.001 cm^2 versus 2.15 ± 0.14 cm^2, respectively, $P < 0.05$, Friedman test and Dunn's Multiple Comparison post hoc test) (Fig. 3.6B). This suggests that A83-01 treatment inhibited EnSC contraction. Taken together, these data indicated that TGFβ1 signalling is implicated in the contraction of the ERB.

I also measured, alpha smooth muscle actin (αSMA), a key cytoskeletal hallmark of fibroblast activation (Micallef et al., 2012, Rønnov-Jessen, 1993, Kalluri, 2016). Analysis of three independent primary cultures showed that αSMA was upregulated at protein level following ERB formation, indicating cytoskeletal remodelling (Fig. 3.6C). Activated fibroblasts are also known to apoptose after contraction as part of the normal wound healing process (Kalluri, 2016, Tomasek et al., 2002). Following ERB formation, EnSC were stained for live (NucBlue dye; blue nuclei) and dead cells (NucGreen dye; green nuclei). Following 4 days of progression, many of the cells were stained green, indicating they were dead (Fig. 3.6D). Overall, these data provided evidence that EnSC undergo endometrial fibroblast activation (EFA) when subjected to ERB formation. Therefore, ERB formation was renamed as the endometrial fibroblast activation model (EFAM).

Decidualisation silences fibroblast activation

Next, the effect of decidualisation on EFA was investigated. Three independent cultures of EnSC were pre-treated with MPA and cAMP for four days to induce decidualisation prior to performing the EFAM protocol. Previous studies have reported that cAMP alone can induce contraction in fibroblasts (Ehrlich et al., 1986, Kamio et al., 2007, Schiller et al., 2010). Therefore, cultures were pre-treated with MPA and cAMP, either alone or in combination. Cultures were imaged under time-lapse microscopy for 36 hours and the area of the cell mass was measured every 4 hours (Fig. 3.7A). The area of cell mass was measured using ImageJ every 4 hours

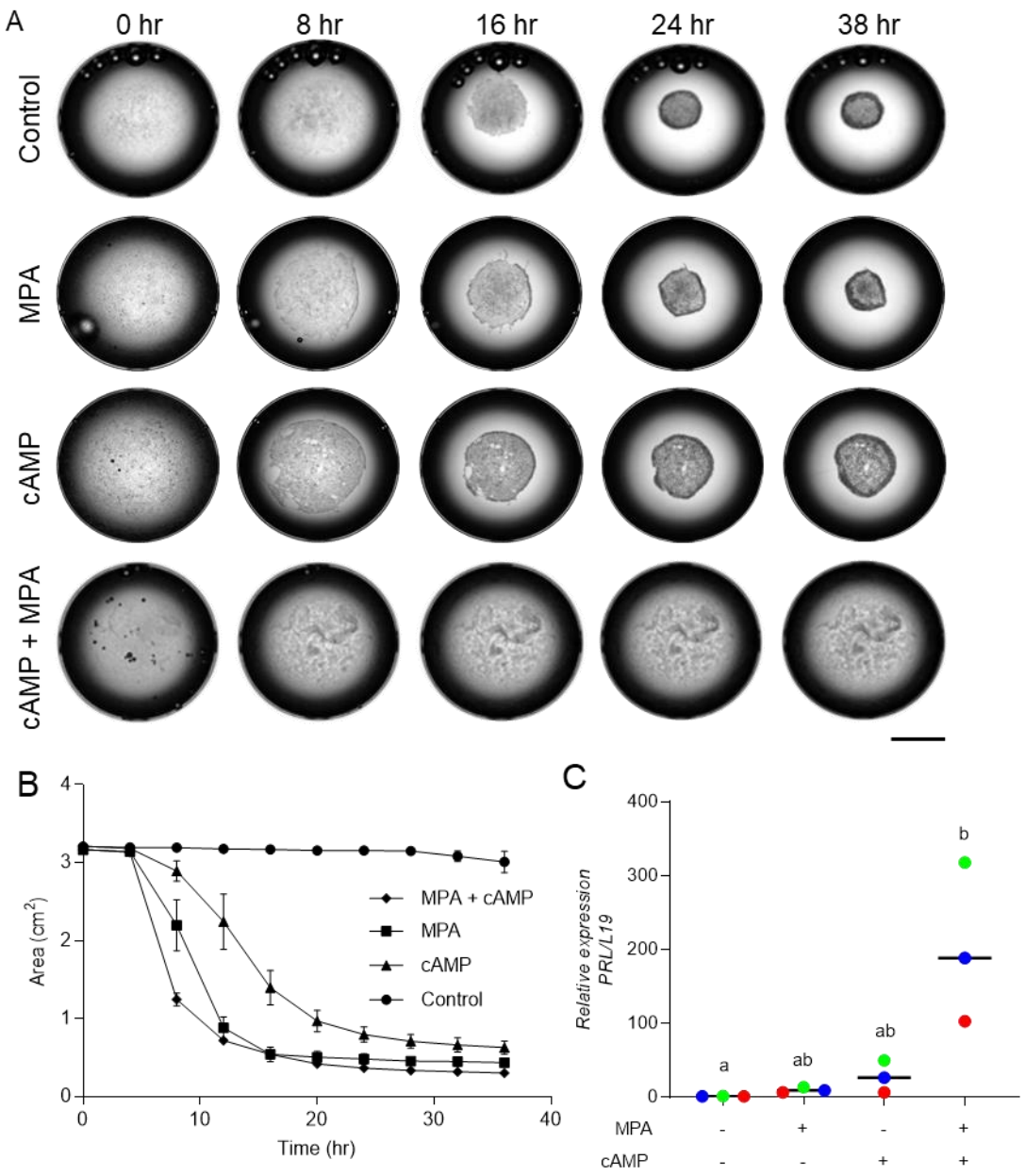

Figure 3.7: ERB formation from pre-decidualised EnSC.

A: Representative brightfield images of EFAM contraction over 38 hours of three independent cultures pre-treated with either MPA or cAMP or both as well as vehicle control (DMSO) for 4 days. Scale bar = 500 µm.

B: The data show the contraction kinetics of the three independent EnSC cultures subjected to the EFAM over 38 hours when pre-treated with either MPA or cAMP or both as well as vehicle control (DMSO) for 4 days. Area was measured every 4 hours. Error bars represent standard deviation.

C: Stromal decidual gene *PRL* transcript levels were measured for each pre-treatment group to test for decidual response in three independent cultures performed in triplicate. The colours represent the three individual cultures. The line represents the

mean. Expression was normalised to *L19* mRNA levels. Different letters above the error bars represent statistical difference from other groups at $P < 0.05$. Group comparison by Friedman test and Dunn's Multiple Comparison *post hoc* test.

to map the contraction kinetics under each treatment (Fig 3.7B). At 24 hours, EFA, as measured by the area of contraction, was attenuated in response to cAMP signalling when compared to MPA treatment or vehicle control (DMSO) (Area ± standard deviation = 0.79 ± 0.1 cm^2 versus 0.48 ± 0.08 cm^2 and 0.36 ± 0.02 cm^2, respectively). However, EFA was abolished by the combination of cAMP and MPA (Area ± standard deviation = 3.5 ± 0.01 cm^2). Therefore, these observations indicated that the inhibition of EFA was mediated by a synergistic effect between MPA and cAMP. As shown in Figure 3.7C, cAMP and MPA also had a synergistic effect on the induction of EnSC decidual marker gene *PRL*, as reported previously (Brosens et al., 1999). Taken together, this suggested that decidualisation of EnSC inhibits EFA.

Reprogramming of the ROCK pathway upon decidualisation

The rho-associated, coiled-coil-containing protein kinase (ROCK) pathway is involved in cellular contraction (Amano et al., 2010). Myosin II, a key component of the cytoskeleton for cellular contraction, is switched to an active state upon phosphorylation of regulatory myosin light chain (MLC) by myosin light chain kinase (MYLK) (Fig. 3.8A) (Amano et al., 2010, Totsukawa et al., 2000, Kamm and Stull, 1985). Active myosin II cross-bridges with actin, thereby initiating cellular contraction. (Choi et al., 2008, Amano et al., 2010). Myosin II is deactivated by dephosphorylation of the MLC by myosin light chain phosphatase (MLC-P). ROCK1 can inhibit MLC-P by phosphorylating myosin phosphatase target subunit 1 (MYPT1). Therefore, ROCK1 potentiates contraction by inhibiting MLC-P. (Narayanan et al., 2016). ROCK2 is an isoform that is believed to have a similar role to ROCK1 (Yoneda et al., 2005), a claim disputed more recently (Amano et al., 2010, Jerrell and Parekh, 2016).

A high-throughput single-cell RNA-sequencing (scRNA-seq) reconstruction of the decidual pathway in cultured primary EnSC indicates a switch in expression of key

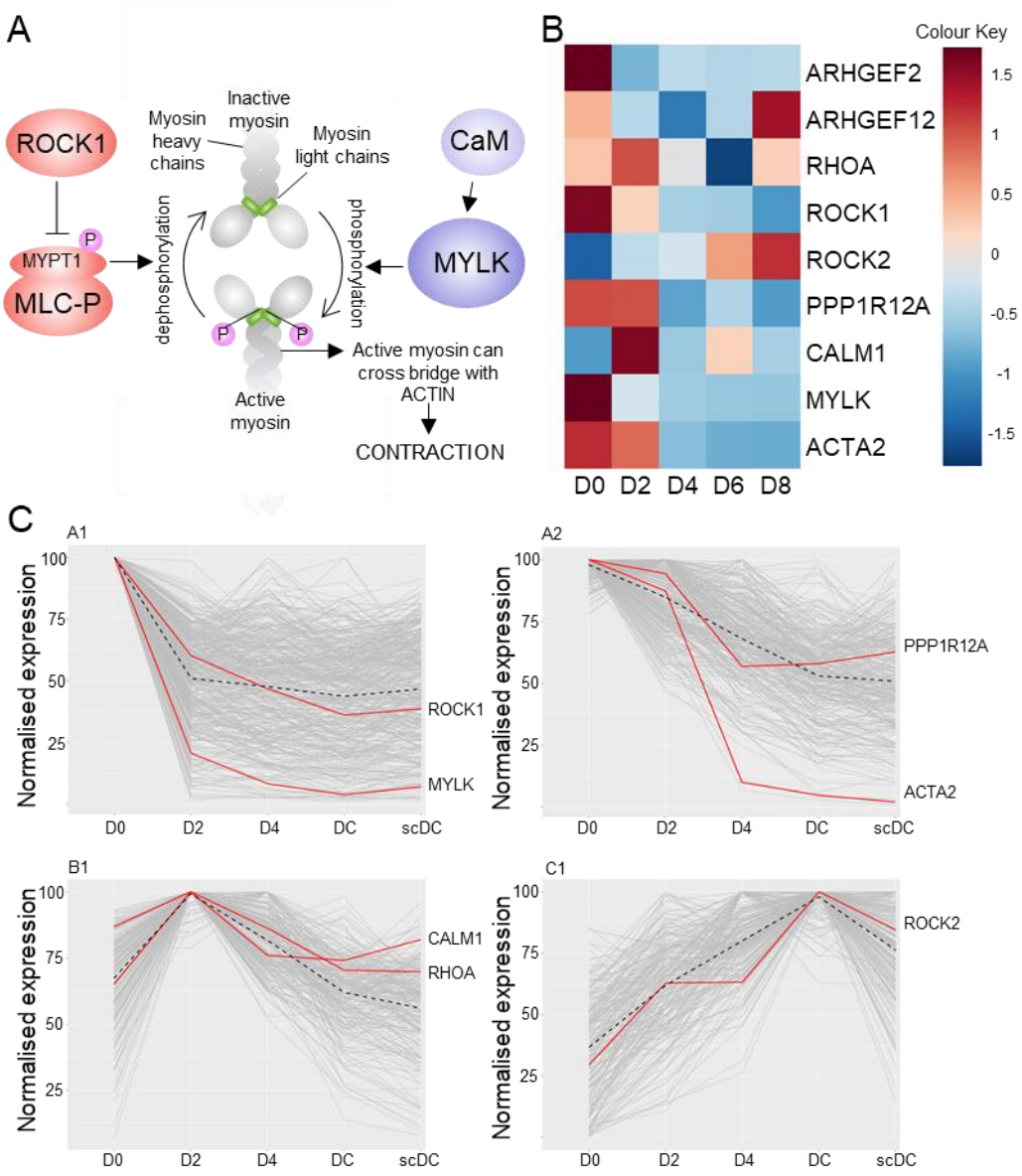

Figure 3.8: Temporal expression of the ROCK pathway genes through decidualisation. A: A schematic of the opposing control myosin light chain phosphorylation, regulating cellular contraction.

B: A heat map showing the relative expression (z-score) of key genes involved in the ROCK pathway over a decidual time course of EnSC (D0-D8) of treatment with cAMP and MPA from published scRNA-seq data (Lucas et al., 2018).

C. K-means cluster analysis of 1,748 differentially expressed genes across an *in vitro* EnSC decidual time course (Lucas et al., 2018). Data show normalised expression for decidualising EnSC progress through intermittent transcriptional states between D0 and D4, after which they emerge as either decidual cells (DC) or senescent decidual cells (scDC) (Lucas et al., 2018, Lucas et al., 2019). The analysis revealed that genes related to the ROCK pathway were in four co-regulated decidual gene

networks. Networks are annotated for key genes involved in ROCK pathway. These data were collected and presented in collaboration with Dr Pavle Vrljicak.

genes in the ROCK pathway (Lucas et al., 2018). *MYLK, ROCK1* and *ACTA2* (αSMA) are significantly reduced in expression upon decidualisation (Fig. 3.8B). *CALM1* and *PPP1R12A* (MYPT1) do not change significantly in expression. *ROCK2* mRNA expression increases upon decidualisation, suggesting a possible switch in ROCK isoforms upon differentiation. Although Ras homolog family member A (*RHOA)* is largely unaffected by decidualisation at the RNA level, transcript levels for both Rho guanine nucleotide exchange factors (GEF) *ARHGEF2* (GEF-H1) and *ARHGEF12* (LARG), which activate RhoA-GDP to RhoA-GTP, upstream of ROCK1, were downregulated upon decidualisation (Guilluy et al., 2011).

In addition, from the scRNA-seq decidual pathway reconstruction, k-means cluster analysis, where k is the number of clusters, revealed that the decidual *pathway in vitro* is underpinned by seven networks of uniquely co-regulated genes (Lucas et al., 2018, Lucas et al., 2019) (Fig. 3.8C). Cross referencing showed that several genes associated with the ROCK pathway belong to four of the networks. *MYLK* and *ROCK1* are in the first gene network (termed A1), which include genes that are rapidly 'switched off' upon decidualisation, perhaps suggesting progesterone-dependent repression. *ACTA2* and *PPP1R12A* are in a separate gene network (termed A2), which include genes from the decidual time course that decrease in expression at a slower rate. *CALM1* and *RHOA* are in gene network B1, which peak during the initial phase of the decidual pathway. Collectively, these data demonstrate that the ROCK pathway is largely switched off upon endometrial stromal cell differentiation into decidual cells. However, *ROCK2* is in gene network C1, which include genes that are most highly expressed in decidual cells.

The reprogramming of ROCK pathway underlies the loss of fibroblast activation in decidual cells

Next, I tested the hypothesis that the silencing of signal intermediates in the ROCK pathway caused the loss of contraction in decidualised EnSC. The activity of the ROCK pathway was measured by assessing the phosphorylation status of MYPT1 in undifferentiated cells and cells decidualised for 4 days from three independent cultures. Total protein lysates were subjected to Western blot analysis using both total and phospho-specific MYPT1 antibodies. In addition, β-actin was probed to ensure equal loading. As shown in Figure 3.9A, decidualisation abolished the phosphorylation of MYPT1.

Furthermore, to confirm whether MYLK was involved in the EnSC contraction, three independent primary cultures were transfected with either MYLK small interfering RNA (siRNA) or a non-targeting (NT) control siRNA for 24 hours. Transfected cells were then subjected to the EFAM. At 24 hours post-seeding onto Matrigel, the MYLK knock down group failed to contract as a single contractile mass when compared to cells transfected with NT control siRNA (Area ± SD = 1.5 ± 0.03 cm^2 versus 0.31 ± 0.09 cm^2, respectively) (Fig. 3.9B) implicating its involvement in ERB associated contraction.

In order to determine if ROCK1 was involved the contraction, three independent cultures of EnSC were subjected to Y-27632, a ROCK inhibitor (Narumiya et al., 2000, Ishizaki et al., 2000). At 24 hours, treatment of cultures with 1 µM Y-27632 attenuated EFA, but treatment with 10 µM Y-27632 completely abrogated EFA when compared to vehicle control (DMSO) (Area ± SD = 0.73 ± 0.07 cm^2 and 2.89 ± 0.22 cm^2 versus 0.67 ± 0.10 cm^2, respectively) (Fig. 3.9C).

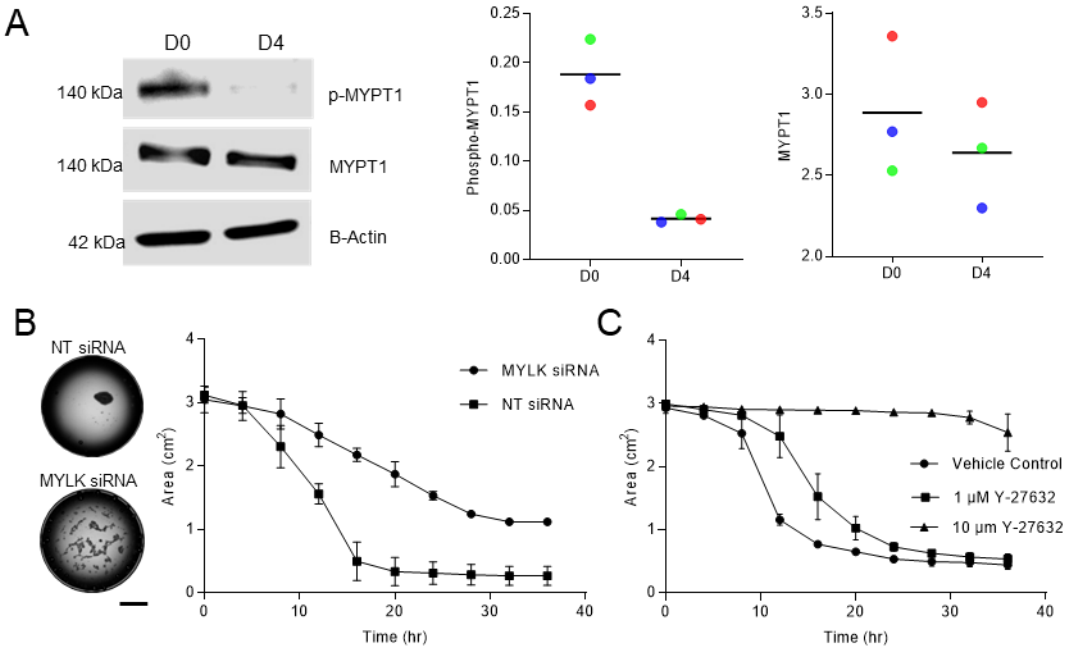

Figure 3.9: The ROCK pathway is essential for ERB formation.

A: Representative Western blot probed for both total MYPT1 (MYPT1) and phosphorylated MYPT1 (p-MYPT1) antibodies to assess the phosphorylation status of MYPT1 in three independent EnSC cultures that were either undifferentiated (D0) or decidualised for 4 days with MPA and cAMP (D4). β-actin was probed to ensure equal loading. The data show the densitometry for D0 and D4. The colours represent the three individual cultures. The line represents the mean. $P > 0.05$ (Wilcoxon matched pairs signed rank test).

B: Three independent EnSC cultures were transfected with either non-targeting siRNA (NT) or siRNA targeting MYLK (MYLK siRNA) for 24 hours. EnSC were collected and subjected to the EFAM. Representative images of the EFAM from EnSC transfected with NT or MYLK siRNA. Data show the area of EFA (mean ± SD) over time for both NT and MYLK siRNA EFAM cultures measured every 4 hours. $P > 0.05$ (Wilcoxon matched pairs signed rank test).

C: Three independent EnSC cultures were subjected to the EFAM in the presence of 1 or 10 µM ROCK inhibitor Y-27632 or vehicle control (DMSO). Data show the average area of EFA (mean ± SD), measured every 4 hours and plotted.

The scRNA-seq data indicated that *ROCK2* was upregulated upon decidualisation, in contrast to the downregulation of *ROCK1* (Lucas et al., 2018). To investigate the role of ROCK2, three independent cultures were subjected to the EFA protocol in the presence of the ROCK2-specific inhibitor KD-025. By 24 hr, KD-025 has no effect on EFA in undifferentiated EnSC compared to control (Area ± SD = 3.02 ± 0.05 cm^2 versus 3.02 ± 0.05 cm^2, respectively) (Fig. 3.10A). The decidual response of EnSC cultured in the presence of KD-025 were also measured. Three independent cultures of EnSC were subjected to cAMP and MPA for eight days, with or without KD-025. Secreted PRL was measured by enzyme-linked immunosorbent assay (ELISA). KD-025 partially reduced secreted prolactin suggesting an impaired decidual response when ROCK2 is inhibited (Fig. 3.10B).

Taken together, these data support the hypothesis that the ROCK pathway is essential for EFA, and the downregulation of this pathway upon decidualisation is likely the cause of the loss of contractibility in decidual cells. In addition, ROCK2 appears to have a different role to ROCK1, as it was not implicated in EFA, but instead it is possibly involved in EnSC decidualisation.

Focal adhesions are required for EFA.

As stated previously, fibroblast activation is a wound healing response to damage or cellular mechanical stress (Kalluri, 2016). Therefore, fibroblast activation requires a mechano-sensing pathway in order to sense the mechanical stress. Previous studies have shown that change in tension between the cell and the ECM can trigger fibroblast activation through cell-matrix adhesions (Petrie and Yamada, 2012). Adhesions are found in locations where molecular interactions between a cell and the surrounding ECM occur. They can assemble or disassemble in response to extracellular cues, such as mechanical stress. Adhesions are formed of a dynamic

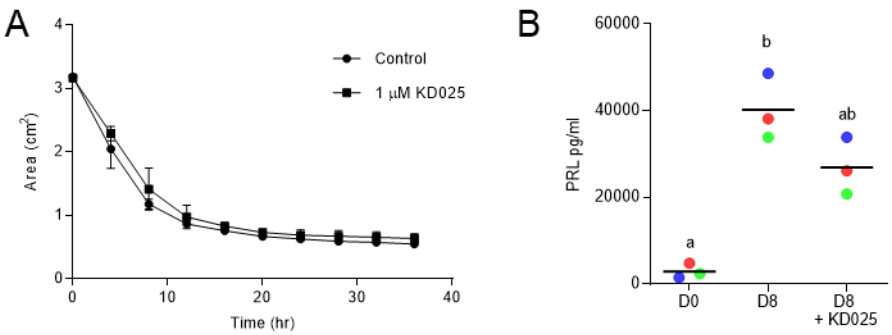

Figure 3.10: ROCK2 is not essential in ERB formation.

A: Three independent EnSC cultures were subjected to the EFAM in the presence of 1 µM ROCK2 inhibitor KD025 or vehicle control (DMSO). The data show the contraction kinetics of EFA (mean ± SD) subjected to KD025 or control, measured every 4 hours.

B: Data show PRL levels measured by ELISA in spent media of three independent EnSC cultures. The colours represent the three individual cultures. The line represents the mean. EnSC cultures were either undifferentiated (D0) or treated with cAMP and MPA for 8 days with or without KD-025 (D8 + KD025 and D8, respectively). Different letters above the error bars represent statistical difference from other groups at $P < 0.05$. Group comparison by Friedman test and Dunn's Multiple Comparison *post hoc* test.

multi-protein complex that include proteins such as focal adhesion kinase (FAK), Proto-oncogene tyrosine-protein kinase Src (Src), paxillin (PXN), proto-oncogene c-Crk (Crk), Crk-associated substrate (CAS), Ras-related C3 botulinum toxin substrate 1 (RAC1), p21-activated kinase (PAK) and (GPCR)-kinase interacting protein (GIT). (Vicente-Manzanares et al., 2005) (Fig. 3.11A). Other proteins such as actinin 1 (ACTN1), vinculin (VCL), tensin 1 (TNS1), talin 1 (TLN1) are also involved. Adhesion protein complexes bind to integrins. Integrins are a family of cell surface adhesion receptors. They are formed of heterodimers of alpha and beta subunits that connect the ECM to the cellular actin cytoskeleton. (Marjoram et al., 2014, Hynes, 2002).

Under mechanical stress, Rho GTPases, such as RhoA are activated by adhesions and aid in adhesion maturation (Vicente-Manzanares et al., 2005). RhoA is also upstream of the ROCK pathway, which leads to cellular cytoskeletal contraction, as seen in fibroblast activation. Mechanical stress-induced RhoA activation has been demonstrated to be enacted through the GEFs (Guilluy et al., 2011). GEFs activate Rho-GTPases, such as RhoA, by exchanging GDP with GTP. Guilley *et al.* identified that force applied to β1 integrins on fibroblasts activates two GEFs, GEF-H1 and LARG, encoded by *ARHGEF2* and *ARHGEF12*, respectively. LARG is activated downstream of a Src kinase and GEF-H1 is activated by the phosphorylation of ERK (Guilluy et al., 2011) (Fig. 3.11A). This therefore suggests that these proteins couple the perceived mechanical stress to EFA.

In addition to this, FAK, encoded by *PTK2* (protein tyrosine kinase 2), is a key protein in establishing cell-matrix adhesions. (Moore et al., 2010, Petrie and Yamada, 2012, Mitra et al., 2005). To confirm that cell-matrix adhesions are indeed essential for contraction, three independent cultures were subjected to the EFAM protocol in the presence of FAK inhibitor Y15 (Golubovskaya et al., 2008). By 24 hours, exposure of Y15 abolished EFA compared to vehicle control (DMSO) (Area ± SD = 3.02 ± 0.05

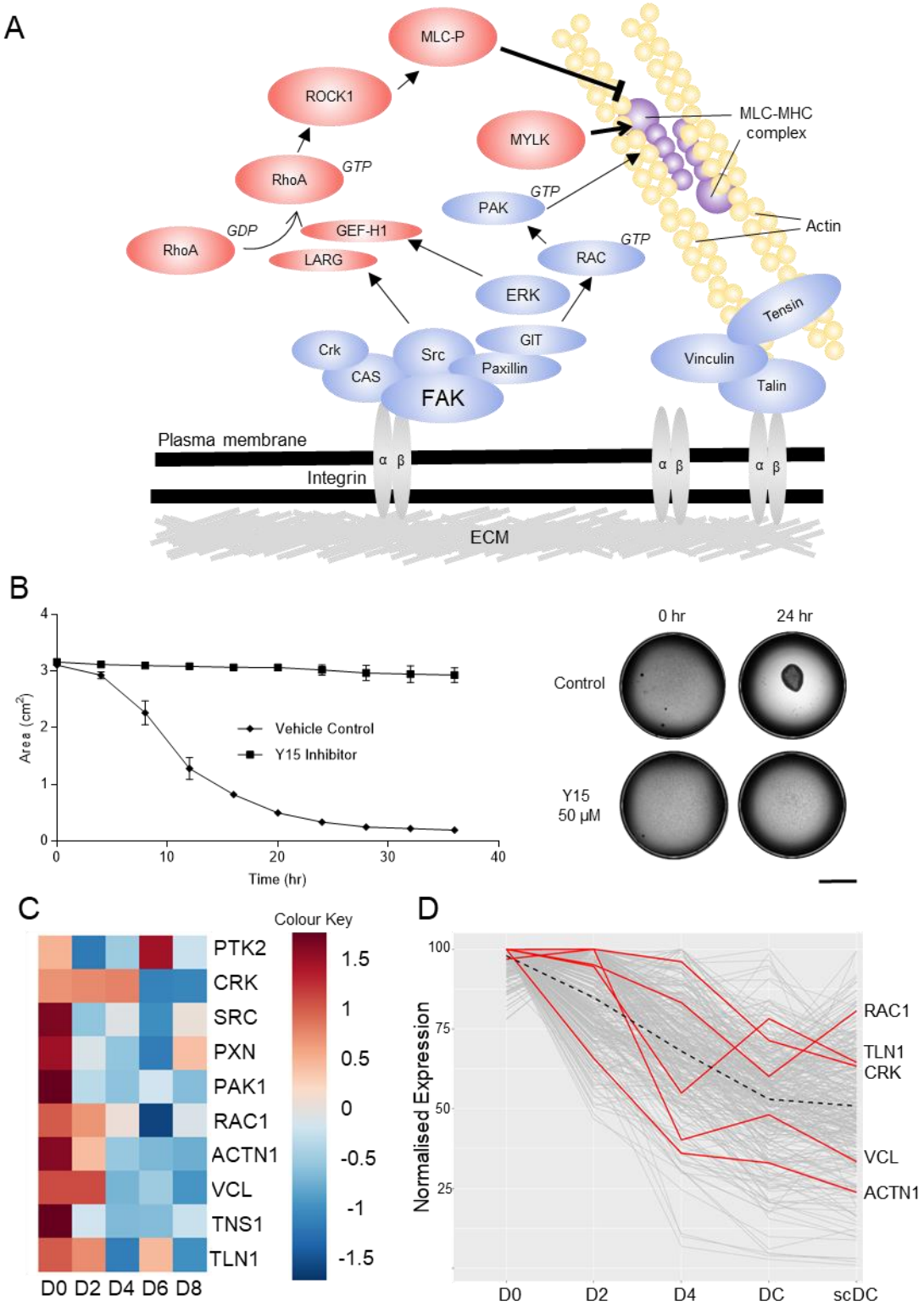

Figure 3.11: Focal adhesion kinase is essential for ERB formation.

A: Schematic representation of the link between cell-matrix adhesions and contraction. Cell-matrix adhesion complex proteins are coloured blue. Integrins coloured grey. ROCK pathway proteins coloured in red. Pointed arrowheads

represent activation, blunt arrowheads represent inhibition. Acto-myosin chain is represented in yellow and purple.

B: Three independent EnSC cultures were subjected to the EFAM in the presence of 50 μM Y15 (FAK inhibitor) or vehicle control (DMSO). The data show the average area of EFA (mean ± SD) for the treatment and control groups, measured every 4 hours. Right: Representative images of EFAM at 0 hours and 24 hours from cultures treated with Y15 and vehicle control (DMSO). Scale bar = 200 μm.

C: A heat map showing the relative expression (z-score) of key genes involved in the cell-matrix adhesion complex over a 8 day decidual time course of EnSC from scRNA-seq data (Lucas et al., 2018)

D. K-means cluster analysis of 1,748 differentially expressed genes across an *in vitro* EnSC decidual time course (Lucas et al., 2018). Data show normalised expression for decidualising EnSC progress through intermittent transcriptional states between D0 and D4, after which they emerge as either decidual cells (DC) or senescent decidual cells (scDC) (Lucas et al., 2018, Lucas et al., 2019). This analysis revealed that several genes involved in cell-matrix adhesions were found in a single co-regulated decidual gene. The network is annotated for key genes involved in cell-matrix adhesion complex formation. These data were collected and presented in collaboration with Dr Pavle Vrljicak.

cm^2 versus 0.33 ± 0.01 cm^2, respectively) (Fig. 3.11B). This therefore confirmed that cell-matrix adhesions are essential for cellular contraction.

As decidualised EnSC are resistant to EFA, I examined the expression of genes related to the adhesion complex. Data mining of the scRNA-seq data identified multiple genes implicated in cell-matrix adhesions that are downregulated upon decidualisation. (Fig. 3.11C) (Lucas et al., 2018, Lucas et al., 2019). Furthermore, k-means cluster analysis revealed that many of these genes belong to a single network containing genes that are progressively downregulated in decidualising EnSC (Fig. 3.11D) (Lucas et al., 2018). This therefore indicates that adhesions may be less likely to occur in decidual cells. Taken together, these data suggest that multiple mechanisms render decidualising EnSC resistant to fibroblast activation, including genes involved in sensing mechanical stress.

3.3 Discussion

Initial characterisation

The aim of this study was to reconstruct the endometrium *in vitro* using 3D cell culture techniques. Here, I used a model referred to as Endometrial Regenerative Bodies (ERB) (Peter Durairaj, 2017). ERB were assumed to be progenitor cell-derived tissue-like structures that formed within 24 hours when seeded on Matrigel. In collaboration, I initially demonstrated that this model could respond to deciduogenic cues and be re-epithelialised. However, with further characterisation, it became apparent that early interpretations of the data were erroneous and further investigation was required.

First, in order to serve as a 3D model of the endometrium, after initial formation, the ERB were required to maintain their structure and form an epithelium when in co-culture with EEC. A previous study has shown that EEC form a monolayer when seeded on top of a layer of cultured EnSC grown in a hydrogel (Bentin-Ley et al., 1994). When MSC and EEC were seeded together on Matrigel, the EEC appeared to preferentially move to the centre of the ERB, as shown by cell tracker stains. However, co-cultured ERB cultured for more than 24 hours showed signs of contraction, and after 10 days were contracted completely. Hence, this questioned the initial interpretation that EEC preferentially move to the centre of the mass, but instead it was more likely these cells were compressed by collective cell contraction. This was the first evidence that the ERB were formed by contraction, rather than cellular reorganisation.

Furthermore, initially, it was assumed that ERB formation was a patient-specific phenomenon, with only a percentage of independent primary MSC cultures capable of ERB formation (Peter Durairaj, 2017). However, the method optimisation revealed that this initial interpretation was erroneous, but instead, all primary cultured EnSC

form ERB. The key issue driving the previously inconsistent data was the unstandardized Matrigel curing time. The time lapse microscopy data provided further evidence that ERB formation was due to a collective contraction of the cells into the centre of the well, not cellular reorganisation or regeneration into a tissue-like structure.

A shift in the paradigm

As the original hypotheses were incorrect, a change of paradigm was required to understand these new observations. EnSC are fibroblastic and therefore I hypothesised that the contractile phenotype exhibited by these cells when cultured on Matrigel was due to the activation of a wound healing response. In other tissues, fibroblasts have been shown to undergo a morphological differentiation process when subjected to mechanical stress or physical damage, called fibroblast activation (Kalluri, 2016, Tampe and Zeisberg, 2013, Zeisberg and Zeisberg, 2013). Activated fibroblasts were first observed in healing wounds in skin tissue, where it was hypothesised that they were responsible for the closure of dermal wounds by cellular contraction (Croft and Tarin, 1970, Tomasek et al., 2002, Driskell and Watt, 2015). Since this discovery, the sustained presence of activated fibroblasts in a tissue has been established as a morphological marker of fibrosis (Kalluri, 2016, Monaco and Lawrence, 2003, Gurtner et al., 2008).

In addition to their contractility, activated fibroblasts acquire a myo-fibroblast phenotype, including cytoskeletal remodelling (production of αSMA), and ECM remodelling through collagen deposition by TGFβ1 signalling (Tomasek et al., 2002). Therefore, to test the hypothesis of fibroblast activation, TGFβ1 signalling was manipulated. The ALK5 inhibitor A83-01 impeded contraction of MSC in a dose dependent manner. In addition, a cytoskeletal hallmark of fibroblast activation, αSMA

(Rønnov-Jessen, 1993, Kalluri, 2016), was significantly increased at the protein level in the ERB further substantiating the fibroblast activation hypothesis.

Another characteristic of wound healing-associated fibroblast activation is cell death or de-differentiation after contraction (Tomasek et al., 2002). Initially, activated fibroblasts contract and mass produce ECM proteins such as collagens to aid in closing the wound. However, in normal wound healing, activated fibroblast cell death or de-differentiation follows contraction (Kalluri, 2016, Tomasek et al., 2002). This is an essential step in the later stages of wound healing, to ensure excessive ECM is not produced. I demonstrated that most cells in the ERB died by 4 days in culture. Collectively, the evidence indicated that ERB formation was due to fibroblast activation, and not due to MSC tissue regeneration. Therefore, henceforth the ERB was renamed the endometrial fibroblast activation model (EFAM).

Next, the impact of decidualisation of EnSC on EFA was investigated. Pre-decidualising EnSC with MPA and cAMP for 4 days inhibited EFA. Analysis of published decidual time course scRNA-seq data revealed that many genes involved in the ROCK pathway are downregulated upon decidualisation (Lucas et al., 2018). The ROCK pathway has been described previously as a key pathway in cellular contraction (Amano et al., 2010). Validation of key genes indicated the ROCK pathway is essential in ERB formation. The MYLK knockdown inhibited the previously observed collective contractile phenotype, therefore implicating MYLK in EFA. At protein level, MYPT1, the phosphorylation target of ROCK1, was unphosphorylated in decidualised EnSC. This observation correlated with the downregulation of ROCK1 upon decidualisation observed in the decidual time course scRNA-seq data (Lucas et al., 2018). Therefore, it is likely that the silencing of this pathway impedes EFA in decidualised EnSC.

These observations support a previous study showing that contraction of EnSC seeded in a hydrogel is suppressed when decidualised (Tsuno et al., 2009). This study also identified the ROCK1 pathway as being a major pathway involved in their observed cellular contraction. Curiously, they presented data showing that both ROCK1 and ROCK2 were down regulated upon decidualisation. This opposes the scRNA-seq data presented in this study, in which ROCK2 is upregulated upon decidualisation. Additionally, when ROCK2 was inhibited there was no effect on EFA. Instead, inhibiting ROCK2 reduced prolactin secretion, indicating a different role in EnSC to ROCK1. Historically, it has been reported that the two ROCKs have similar roles, but recent studies in cardiac and embryonic fibroblasts indicate an opposing role for ROCK1 and ROCK2 (Shi et al., 2013, Jerrell and Parekh, 2016, Satoh et al., 2018, Hartmann et al., 2015). Shi *et al*., demonstrated that ROCK1 in essential for actin destabilisation, whereas ROCK2 maintains actin stability, indicating opposing roles in cell-cell and cell-matrix attachment properties (Shi et al., 2013). Taken together, this suggests that the ROCKs maintain different and opposing roles in cell attachment and contraction in the endometrium.

Furthermore, inhibition of FAK by inhibitor Y15 impeded EFA in EnSC. This therefore indicates that cell-matrix adhesions are essential for EFA. Adhesions and contractility have been linked through the ROCK pathway by Rho guanine nucleotide exchange factor proteins GEF-H1 and LARG (Heck et al., 2012, Guilluy et al., 2011, Petrie and Yamada, 2012). GEF-H1 and LARG activate in response to changes in matrix rigidity or mechanical stress from the ECM. Changes in matrix rigidity can be sensed due to basal actomyosin contractility tension held by cell-matrix adhesions (Lo et al., 2000, Moore et al., 2010, Jerrell and Parekh, 2016). Therefore, when activated, GEF-H1 and LARG activate RhoA by exchanging a GDP with an activating GTP. Active Rho can then act on ROCK1, leading to contractility. However, for decidualised EnSC, the scRNA-seq data evidenced that despite FAK remaining stable over the decidual time

course, the ROCK pathway is downregulated, including both GEF-H1 and LARG (Fig. 3.8) (Lucas et al., 2018). In addition, many genes related to the adhesion complex were shown to be downregulated upon decidualisation in the scRNA-seq data further suggesting mechanosensing is impeded. This discrepancy between FAK and the ROCK pathway suggests there is an uncoupling of the ROCK pathway from cell-matrix adhesions and therefore there is no EFA in decidual EnSC when challenged by the EFAM protocol (Fig. 3.12).

Clinical relevance

Human endometrial decidual cells have been shown previously to be programmed to resist a range of stressors, thus ensuring integrity of the interface and survival of the conceptus (Kajihara et al., 2006, Jones et al., 2006, Leitao et al., 2011, Muter et al., 2015, Muter et al., 2016, Muter et al., 2017, Shah et al., 2013). Therefore, it is likely that the silencing of the ROCK pathway upon decidualisation is another feature of this programmed resistance to external stress. Excessive fibroblast activation can cause scaring and fibrosis of tissues and scarring of the endometrium, such as in Asherman's syndrome, significantly decreases fertility and the chance of successful pregnancy (Yu et al., 2008). Therefore, it is possible that fibroblast activation has been silenced during the evolution of decidualisation and menstruation in order to protect the cycling endometrium from fibrosis and the healing of the endometrium scar free (Evans et al., 2011, Salamonsen, 2003).

Furthermore, endometriosis is a disorder in which endometrial tissue grows outside of the endometrium, such as in the ovaries, Fallopian tubes or peritoneal cavity. It is often characterised by lesions that are highly painful and contain scar tissue. It has been proposed that retrograde 'breakthrough' bleeding in premenarcheal and adolescent women could be a cause of endometriosis in some patients

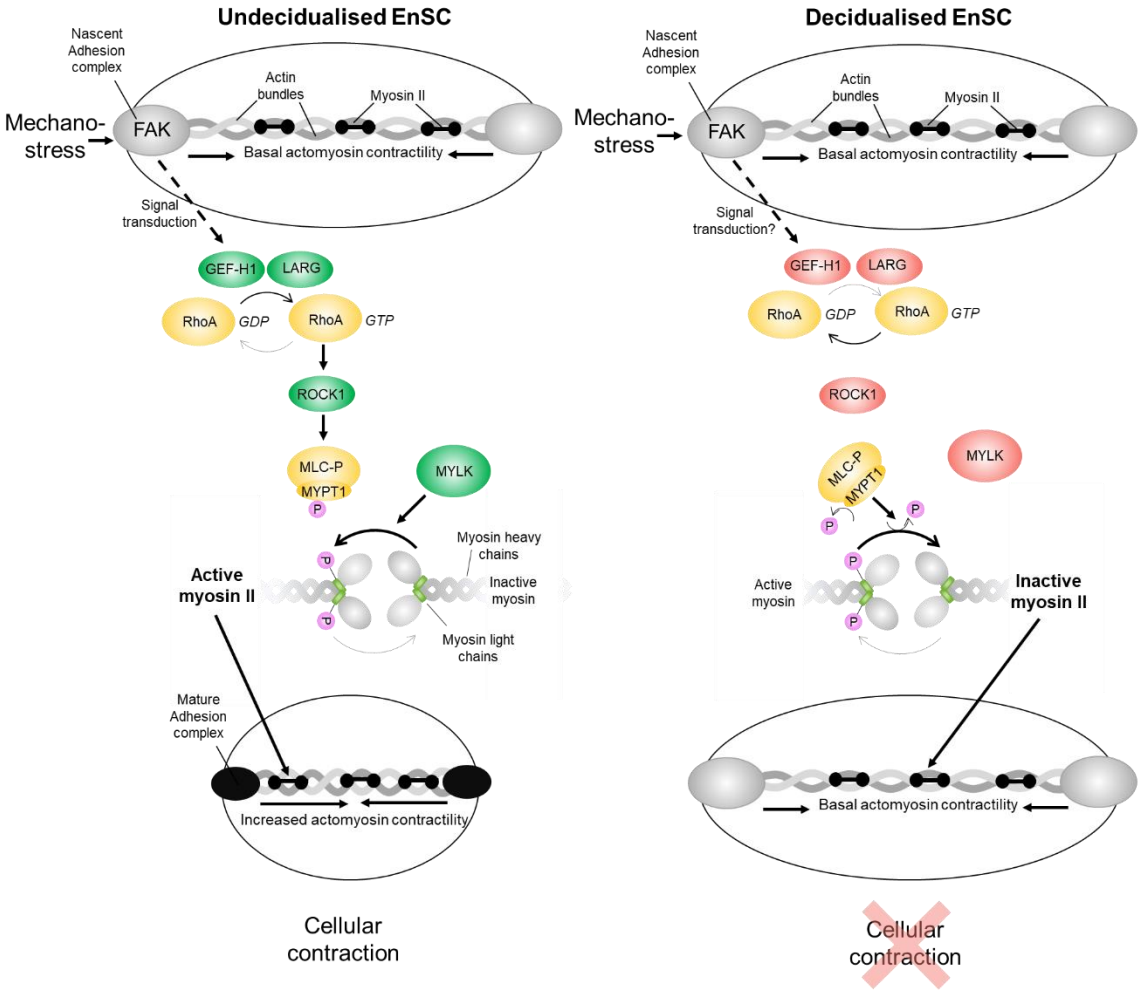

Figure 3.12: Proposed model of mechano-sensing of matrix rigidity and contraction in undecidualised and decidualised stromal cells. A schematic depicting the relationship between cellular adhesions and the ROCK pathway and subsequent contraction in undecidualised EnSC (left) and decidualised EnSC (right). Myosin II maintains a basal tension on actin fibres that is coupled to the matrix by cell-matrix adhesions. Changes in tension are sensed by myosin II and activate GEF-H1 and LARG, which activate RhoA, which then activates ROCK1. ROCK1 phosphorylates MYPT1 of the Myosin light chain phosphatase complex (MLC-P). MLC-P is therefore inhibited. MYLK phosphorylates Myosin light chain, activating the myosin for contraction. This cascade is inhibited in decidualised cells, and MLC-P, by MTP1, removes phosphate groups from myosin light chain, inactivating the myosin II. Green circles represent proteins upregulated at the RNA level; red circles represent proteins downregulated at the RNA level. Yellow circles represent genes not significantly different at RNA level in undecidualised and decidualised stromal cells. Arrows indicate the direction of action of the proteins.

(Brosens et al., 2013b, Brosens et al., 2013a, Brosens and Benagiano, 2016, Brosens et al., 2016, Gargett et al., 2014). Breakthrough bleeding is non-menstruation-stimulated bleeding into the peritoneal cavity, usually before menarche or in adolescence (Brosens et al., 2013a, Brosens and Benagiano, 2016). Cells within a breakthrough bleed are not decidualised at the point of contact with the peritoneum. Therefore, it could be speculated cells that may seed and develop into lesions may retain their capacity for fibroblast activation, possibly resulting in lesions that are more likely to form inflammatory scar tissue. Further investigation into the differences between undifferentiated and differentiated cell seeding of endometriotic lesions may lead to better understanding of how they develop, and therefore how endometriosis can possibly be treated or even prevented in some circumstances.

Impact in modelling the human endometrium in vitro

Although this model failed to form the basis of a 3D model of the endometrium, it did provide key information for further study. This study highlights the potential drawback of using Matrigel as a scaffold for 3D *in vitro* culture of EnSC. As these cells activated upon contact with Matrigel, it is likely that they are not functioning physiologically as in the normal undamaged stroma. Hydrogels that maintain the physiological quiescent phenotype of the undifferentiated stromal cell would be better choices for 3D modelling, possibly such as collagen hydrogels (Bentin-Ley et al., 1994, Anguiano et al., 2017, Arnold et al., 2001). Moving forward, it was clear that alternatives to Matrigel were required to ensure appropriate support for EnSC growth and differentiation in future 3D models of the human endometrium.

Conclusion

In this study, despite being unable to meet the aim of developing a 3D model of the endometrium *in vitro*, I demonstrated clear evidence that all subgroups of endometrial

stromal cells possess the capacity to mount a wound healing response through fibroblast activation and that this capacity is lost upon differentiation. From *in silico* analysis of published *in vitro* single cell RNA sequencing data, I observed a strong divergence in the expression profiles of the ROCK pathway between undifferentiated and decidualised EnSC. I have gone on to confirm this pathway is functionally implicated in the contraction of these cells on Matrigel by both small molecule inhibitors and gene knock down by siRNA, indicating this is this pathway that underpins this phenomenon. These data highlight a possible example of the evolution of human decidual cell stress resistance and their ability to shut off normal cellular pathways to help maximise the chances of successful pregnancy. Future work with this model could be to further investigate EFA in the context of other hydrogels for 3D culturing or to further investigate the role of pre-menarche breakthrough bleeding and the onset of endometriosis.

Chapter 4:

Complex Organoid Culture

4.1 Introduction

The endometrial glands are an essential component of studying human embryo implantation as they provide the nutritional support essential for the growth and survival of an implanting conceptus in human pregnancy (Burton et al., 1999, Bazer, 1975, Kane et al., 1997). However, modelling endometrial epithelial glands *in vitro* has been challenging, with the major focus of *in vitro* endometrial studies being traditionally focused on EnSC. Recently, *in vitro* modelling of the endometrial glands has become possible due to the development of 3D organoid culture. Organoids are named due to their spheroidal 'organ-like' morphology and function (Lancaster and Knoblich, 2014b, Zimmermann, 1987). Organoids form from stem cells or progenitor cells that are grown in a 3D scaffold, such as Matrigel. Differentiation of progenitor cells into organoids is driven by a complex medium containing a specified formulation of growth factors and inhibitors intended to replicate the niche or cell environment *in vivo* (Lancaster and Knoblich, 2014b). There are many published examples of organoids from organs and tissues such as the brain, retina, liver, kidney, and intestine (Xinaris et al., 2012, Luni et al., 2014, Xia et al., 2013, Lancaster and Knoblich, 2014a, Ramsden et al., 2013). However, the most pertinent to this area of research is the endometrial gland organoid (Turco et al., 2017, Boretto et al., 2017).

Two protocols, first published in 2017, now enable the formation of endometrial gland organoids that recapitulate *in vivo* endometrial glandular epithelium, both morphologically and functionally (Turco et al., 2017, Boretto et al., 2017). Spheroid-shaped organoids expand when EEC are seeded in Matrigel and grown in a chemically defined medium containing growth factors and inhibitors called expansion medium (ExM). Single EEC expand into organoids reaching 200-500 μm in diameter when cultured for 4-8 days. Organoids can be maintained long-term by passaging in which cultures are dissociated mechanically and plated into fresh Matrigel for re-

expansion. Furthermore, endometrial gland organoids maintain genomic stability over many passages and can be cryopreserved, enabling the possibility of long-term biobanking (Turco et al., 2017, Boretto et al., 2017).

Endometrial gland organoids label positively with EEC markers such as epithelial cell adhesion molecule (EpCAM), cytokeratin, and epithelial cadherin (E-cadherin). The cells polarise, and electron microscopy has demonstrated that a proportion of the cells become ciliated along the luminal apical surface when exposed to estradiol (Turco et al., 2017, Haider et al., 2019). The endometrial gland organoids differentiate, at least partially, when exposed to MPA and cAMP, as demonstrated by the induction of genes related to glandular differentiation and embryo receptivity, such as *PAEP, LIF, DPP4, HSD17B2*, and secretion of glycogen and glycoproteins, such as mucins (Turco et al., 2017, Boretto et al., 2017).

Endometrial gland organoids therefore provided an alternative basis for developing a 3D *in vitro* model of the human endometrium. This study aimed to optimise a protocol for developing a 'complex organoid' system that consist of both primary gland organoid EEC with patient matched EnSC to establish a novel *in vitro* 3D model of the endometrium.

The objectives of this study were:

1. To determine the gel matrix conditions required to support of complex organoid growth
2. To establish a medium suitable to support growth of complex organoids.
3. To characterise functionally and morphologically differentiating complex organoids

4.2 Results

Establishing the growth conditions for a complex organoid culture

In chapter 3, I described a protocol for studying EFA using Matrigel. In brief, cultured EnSC activate when plated on Matrigel and contract into a central mass. I concluded that Matrigel is not suitable for modelling the normal physiology of EnSC *in vitro*. However, the established protocol for organoid formation uses Matrigel (Turco et al., 2017) (Fig. 4.1). In brief, endometrial biopsies are enzymatically digested, and the epithelial gland fraction is isolated using a cell sieve. The dissociated glands are mixed with Matrigel (ratio 1:20) and plated into 20 µl droplets and grown in ExM. The discrepancy in gel requirements between EnSC and EEC therefore posed an important hurdle.

Previous studies have used a layered co-culture model culturing EnSC in a collagen-based hydrogel overlaid with a monolayer of EEC (Bentin-Ley et al., 1994, Mardon et al., 2007). I examined EFA on an equivalent formulation of collagen hydrogel (PureCol® EZ Gel solution) in comparison to standard Matrigel (Fig. 4.2A). EnSC from three independent patient biopsies were seeded in duplicate either on top of 50 µl Matrigel or 50 µl collagen hydrogel and cultured in Medium 200 and imaged over 16 hours by time-lapse microscopy. On Matrigel, the EnSC contracted as predicted (mean area ± SD at 16 hours = 0.7 ± 0.03 cm^3). However, on collagen hydrogel, the EnSC did not contract (mean area ± SD at 16 hours = 2.7 ± 0.12 cm^3). This observation indicated that collagen hydrogel is more suitable at maintaining physiological EnSC morphology.

Next, organoid expansion was tested in collagen hydrogel. Following the protocol from Turco *et al*. 2017, endometrial gland organoids from three independent patient biopsies were expanded in Matrigel. Passages 0 (P0) and 1 (P1) organoid cultures

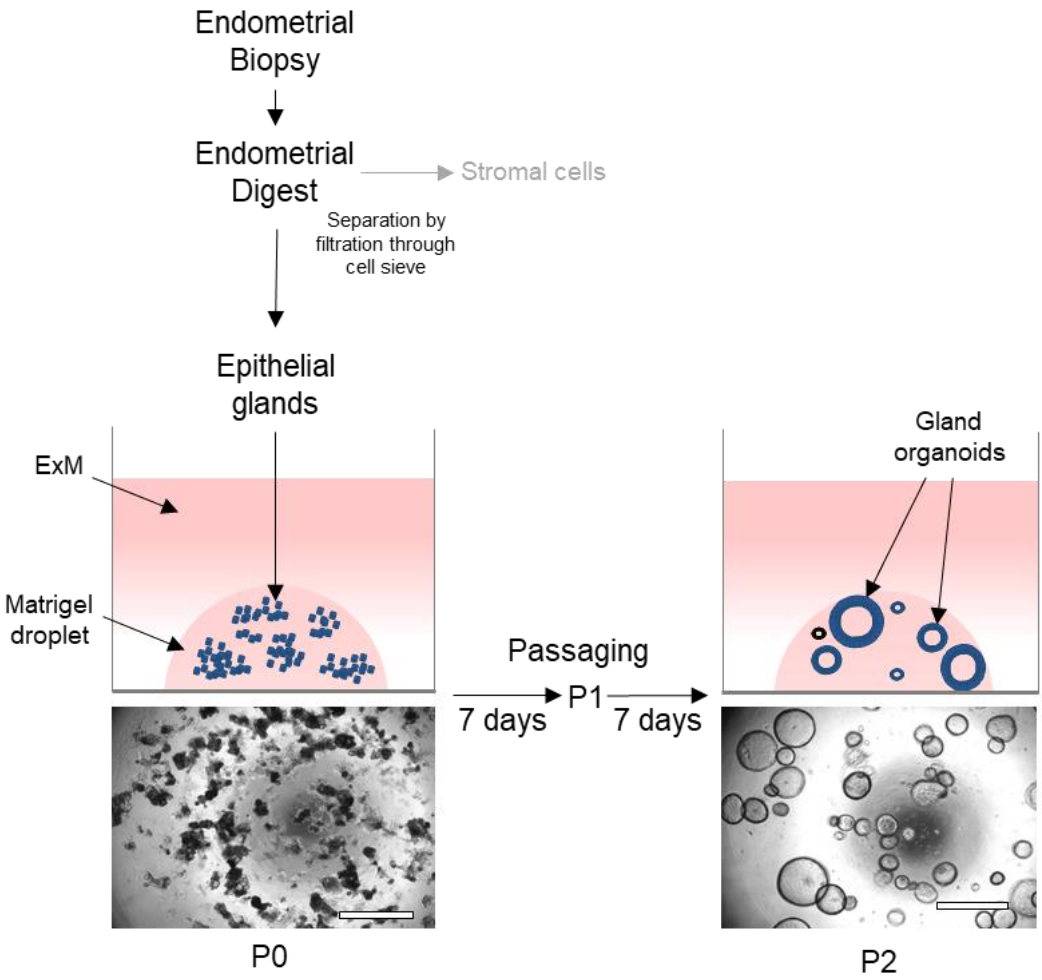

Figure 4.1: Schematic representation of endometrial gland organoid formation and culture *in vitro*. Fresh human endometrial biopsies are dissociated mechanically and enzymatically, and the glandular epithelial fraction is separated by size by a 40 µm cell sieve. The epithelial gland fraction is mixed with Matrigel at a 1:20 ratio and aliquoted into 20 µl droplets in a 48 well plate and cured at 37^{o}C for 15 min. ExM (200 µl) is added and cultures are grown for 7 days with medium refreshed every 48 hours (P0). By the end of P0 (day 7) very few organoids form, instead clumps of glandular cells can be observed. Cultures are then passaged and grown for a second 7 days (P1). Cultures are passaged again to P2 where the recognisable spheroid shaped organoids form. Images visualised by brightfield microscopy. Scale bar: 500 µm. Protocol adapted from Turco, *et al*. 2017.

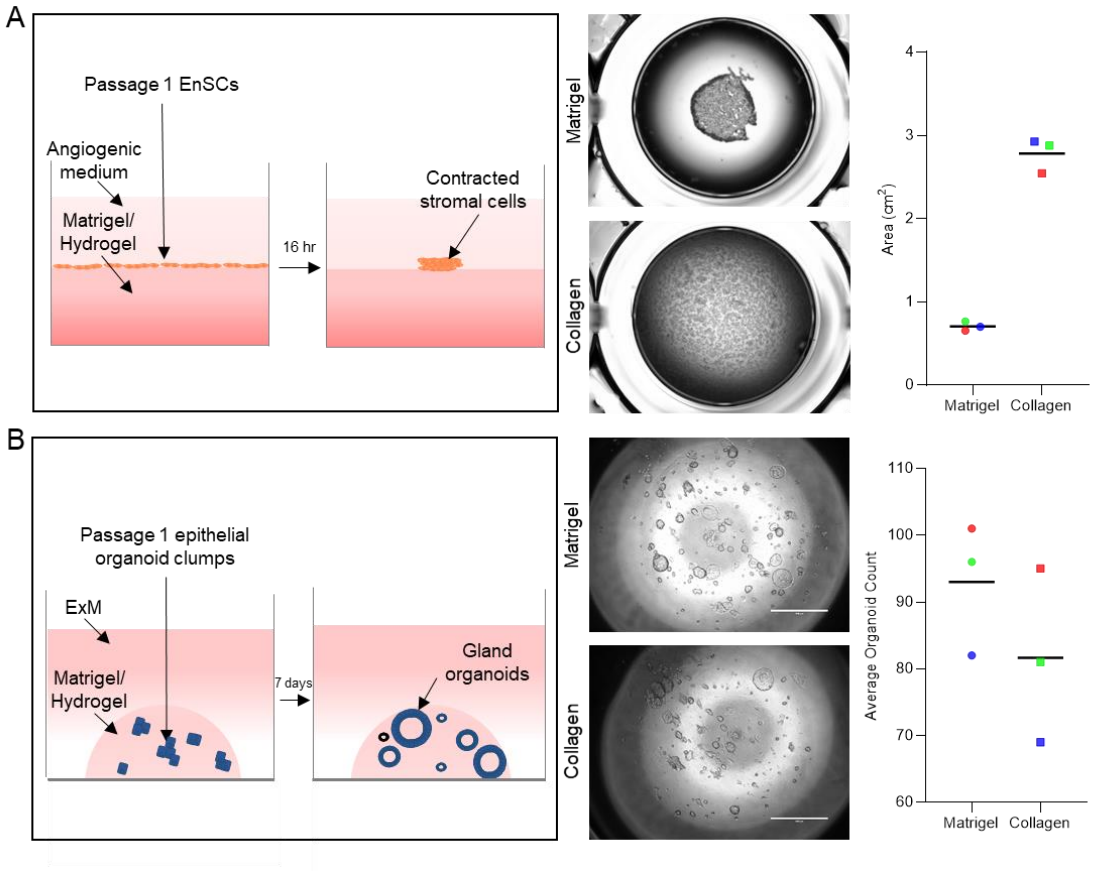

Figure 4.2: Determining a suitable hydrogel for *in vitro* culture of EnSC and endometrial gland organoids.

A: Left: A schematic of the EFAM protocol. In brief, passaged EnSC are seeded onto Matrigel and over 24 hours contract into a mass. Middle: Representative images of EFAM performed on Matrigel and collagen hydrogel at 24 hours from three independent cultures in triplicate, visualised by brightfield microscopy. Right: Data show area of EnSC 24 hours after seeding onto Matrigel or collagen. This experiment was performed on three independent cultures in triplicate. The colours represent the three individual cultures. $P > 0.05$ (Wilcoxon matched pairs signed rank test).

B: Left: A simplified schematic of endometrial gland organoid protocol as in Fig. 4.1. Middle: Representative images of the organoid protocol performed on Matrigel and collagen hydrogel at 8 days from three independent cultures in triplicate, visualised by brightfield microscopy Right: Data show absolute number of endometrial gland organoids formed after 8 days of culture from three independent samples. The colours represent the three individual cultures. The line represents the mean. $P > 0.05$ (Wilcoxon matched pairs signed rank test).

contain semi-intact glands and cellular debris whereas at P2 pure organoid cultures emerged (Fig. 4.1). Therefore, experiments were undertaken at P2. Briefly, P1 organoids were passaged after a growth period of 7 days by mechanical dissociation. Dissociated gland organoids were mixed into the gels (neat) at a 1:20 volume ratio (final gel concentration 95%) and aliquoted into 20 µl droplets in a 48 well plate and grown in ExM (Fig. 4.2B). After 4 days in culture, the number of organoids were counted. Organoids expanded in both gels to similar numbers (Fig 4.2B).

Finally, I compared Matrigel and collagen hydrogel in complex organoid culture. In order to produce complex organoids, I mixed the standard volume of pelleted P1 dissociated gland organoid EEC (1:20 volume ratio) with the same volume of pelleted EnSC into the gels in ExM (final gel concentration 90%). The aim of producing the complex organoid culture was for it to structurally resemble a simplified endometrium with a stroma interspersed with glandular structures, in three dimensions (Fig. 4.3A). Therefore, a successful complex organoid must adhere to the following criteria when seen under a light microscope:

1. Gland organoid expansion present
2. A well distributed mesh-like matrix of spindle-shaped EnSC around the gland organoids
3. No indication of EnSC-driven hydrogel contraction

In both Matrigel and collagen hydrogel, the gland organoid structures were able to form (Fig 4.3B). However, as previously described, in Matrigel, the EnSC contracted to the edges of the gel droplet (Fig. 4.3B, black arrows). In collagen hydrogel, the EnSC were able to form a matrix-like morphology without EnSC-driven hydrogel contraction. Collectively, these data demonstrated collagen hydrogel was able to fulfil

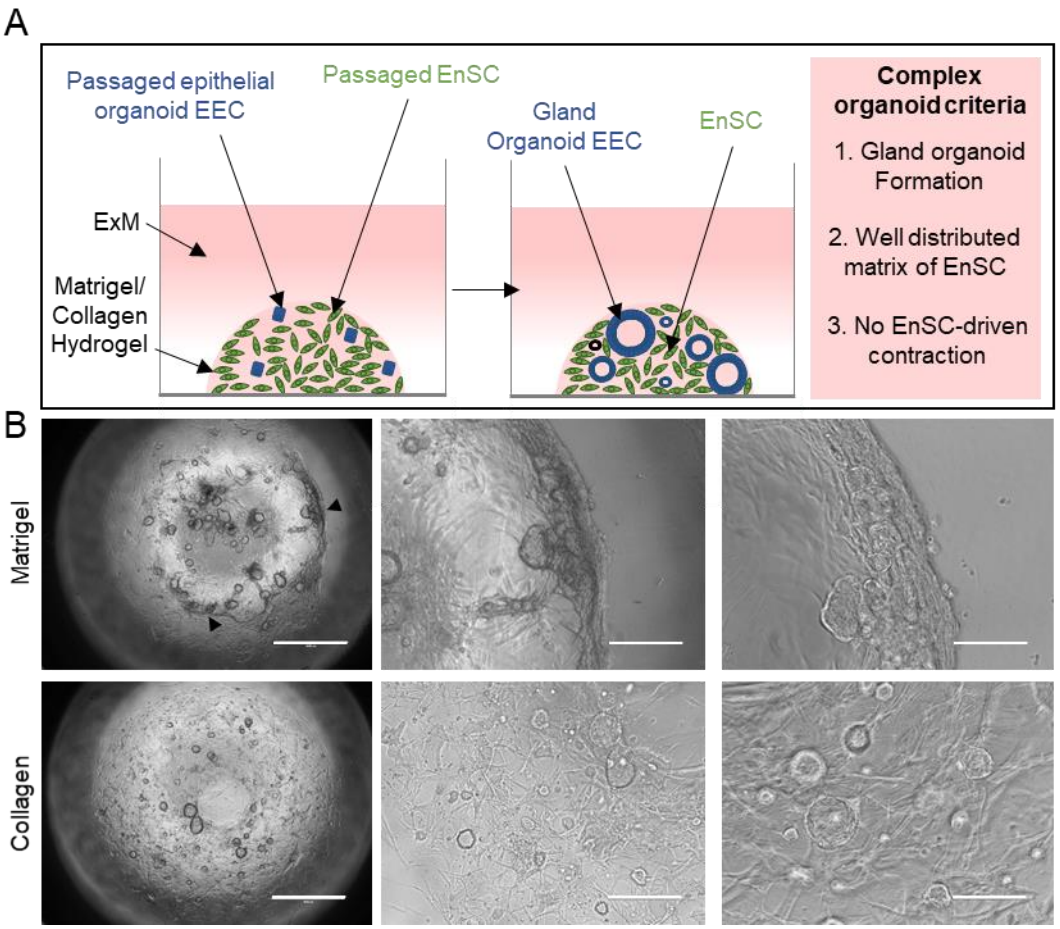

Figure 4.3: Determining a suitable hydrogel for *in vitro* complex organoid culture.

A: A schematic of the complex organoid protocol. Equal volume of EnSC and dissociated gland organoid EEC were added to Matrigel or collagen hydrogel at a ratio of 1:20 each and aliquoted into 20 µl droplets in a 48 well plate and cured at 37^{o}C for 15 min. ExM (200 µl) is added and cultures are grown for 8 days with medium refreshed every 48 hours. The criteria for a complex organoid is included on the right to be used when visualising the complex organoids by light microscopy.

B: Representative images of complex organoids grown in Matrigel or collagen hydrogel from three independent cultures in triplicate visualised by brightfield microscopy. Left: 2× magnification. Black arrows indicate areas of EnSC contraction. Scale bar: 1000 µm. Middle: 10× magnification. Scale bar: 100 µm. Right: 20× magnification. Scale bar: 200 µm.

the complex organoid criteria and therefore was more suitable for complex organoid culture and hence used for all further experimentation.

Optimising the growth medium for an endometrial complex organoid culture.

The medium was the next component of the complex organoid to optimise. For the initial experiments, the previously defined ExM was used (Turco et al., 2017). The use of collagen hydrogel had alleviated the criterion issue of EnSC-driven gel contraction. However, visual observation indicated that the EnSC matrix when cultured in ExM was sparse and without indication of EnSC expansion. Monolayer EnSC are cultured routinely in medium containing E2 and serum, such as fetal bovine serum (FBS) (Barros et al., 2016, Irwin et al., 1989). E2 is an ovarian steroid hormone essential for proliferation of EnSC during the proliferative phase of the human menstrual cycle (Gellersen and Brosens, 2014). FBS provides a source of amino acids for EnSC growth and proliferation.

The ExM does not contain serum or E2. Instead, ExM contains N2 and B27, which are both commercial chemically defined supplements suitable for cell proliferation in serum free media (Brewer et al., 1993, Bottenstein and Sato, 1979, Turco et al., 2017). Both were originally formulated for neuronal stem cell culture. B27 includes human insulin and transferrin, antioxidants, hormones, fatty acids, and amino acids (Bottenstein and Sato, 1979, Romijn, 1988). N2 is similar in composition, containing human insulin, hormones, putrescine, a precursor to polyamine biosynthesis, selenite, an antioxidant (Bottenstein and Sato, 1979, Needham et al., 1987).

Therefore, I examined the effect of the adding E2 to the ExM on EnSC expansion. Additionally, I examined the growth of EnSC in complex organoids in ExM supplemented serum replacement 1 (SR1) and Albumax II would benefit EnSC growth. SR1 contains highly purified, heat-treated bovine serum albumin (BSA), heat-

treated bovine transferrin and bovine insulin (Chase and Firpo, 2007). Albumax II is purified BSA (Ichikawa, 2010). These commercial serum replacements were chosen in order to maintain a chemically defined medium (Gstraunthaler, 2003). FBS was not tested because of its unspecified composition.

Three independent complex organoid cultures were grown in triplicate in each of the tested ExM formulations for 8 days and cultures were visually examined. Complex organoid EnSC were rounded in standard ExM, indicating cell death (Fig. 4.4A). However, EnSC grown in ExM containing 1nM E2 expanded to confluency in the collagen hydrogel and formed a dense, well distributed matrix around the gland organoids when grown in this medium (Fig. 4.4B). There was no observed additional EnSC expansion with the addition of SR1 (1×) (Fig. 4.4C). The addition of Albumax II (2%) had the greatest effect in EnSC expansion visually, however it inhibited gland organoid expansion (Fig. 4.4D). Instead, large holes in the gel were observed indicating EnSC contraction.

In summary, the medium composition chosen for complex organoid culture was defined as ExM supplemented with 1 nM E2. This formulation produced complex organoids that best suited the criteria set with a well distributed stroma and epithelial organoids present. In order to distinguish this medium from standard ExM, medium supplemented with E2 was designated as co-ExM as it is optimised for complex organoid culture.

To examine whether proliferation was improved by co-ExM, complex organoids were immunolabelled for the proliferation marker Ki67 by IHC. Ki67 is expressed at the protein level in all active phases of the cell cycle but absent in quiescent cells (Mertens et al., 2002). Complex organoids from three independent patient biopsies grown in

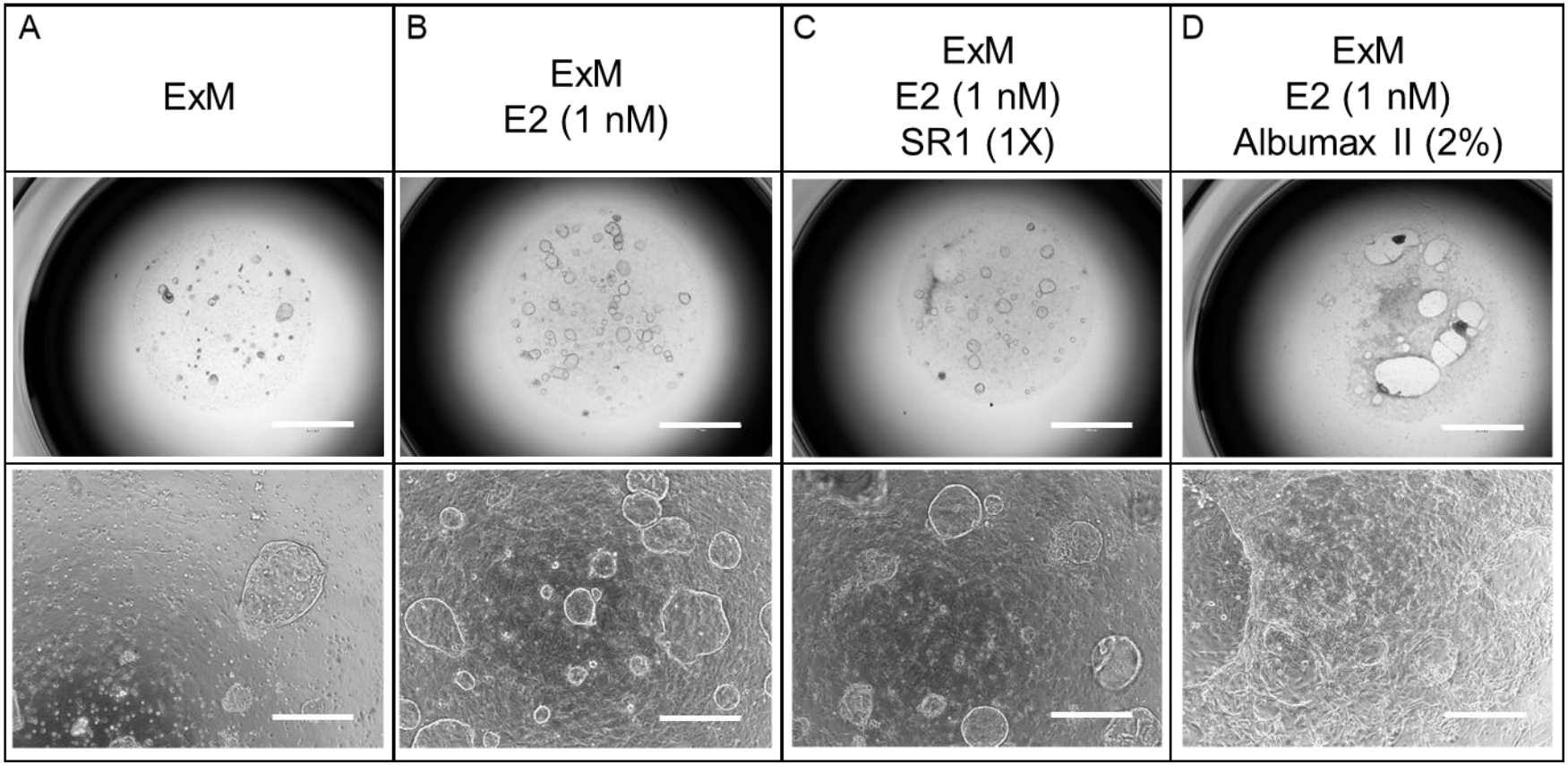
A
ExM
B
ExM
E2 (1 nM)
C
ExM
E2 (1 nM)
SR1 (1X)
D
ExM
E2 (1 nM)
Albumax II (2%)

Figure 4.4: Determining the optimal growth medium for complex organoid cultures. Complex organoids from three independent cultures in triplicate were grown in the various growth medium formulations for 7 days (A-D). Top Row: Growth medium formulations. Middle Row: Representative brightfield images of complex organoids at day 7 of culture. Magnification= 2×. Scale bar: 1000 μm. Bottom Row: Representative images of complex organoids grown in above medium. Magnification: 10×. Scale bar: 100 μm. Images visualised by brightfield microscopy.

ExM or co-ExM were fixed with formalin, paraffin embedded and sectioned. These sections were immunolabelled for Ki67 by IHC (Fig. 4.5). In the ExM samples, only the EEC were labelled positively for Ki67 (labelled by white dotted lines). However, in co-ExM, some EnSC also expressed Ki67. Thus, the IHC demonstrated that EnSC do not proliferate in standard ExM. However, co-ExM induces some EnSC proliferation, although the response is partial.

Differentiation of complex organoids

In order to establish a functional complex organoid culture, I had to determine whether the gland organoids and the EnSC could differentiate within the optimised conditions presented in this study. Harvesting RNA from the complex organoids for RT-qPCR analysis required optimisation. The standard procedure for RNA collection from Matrigel involves melting the gel at 4^{o}C, followed by mechanical dissociation for retrieval of cells from the gel, and then addition of RNA lysis buffer (Turco et al., 2017). However, collagen hydrogel forms covalent bonds when set at 37^{o}C and so will not melt back into a liquid when chilled to 4^{o}C, unlike Matrigel (Yahia et al., 2015). Instead the hydrogel requires enzymatic digestion with collagenase I to release the cells.

Three independent complex organoid cultures were harvested with RNA lysis buffer and manual dissociation (300× pipetting) along with, or without, pre-treatment of collagenase I (500 µg/ml for 10 min at 37^{o}C) (Fig. 4.6). Pre-treatment of collagenase I digestion improved RNA yield compared to control (mean ± SD: 36.0 ± 8.54 ng/µl versus 2.76 ± 0.33 ng/µl, respectively). Hence, collagenase I was utilised for all subsequent RNA harvests from collagen hydrogel.

Next, to test complex organoid differentiation, three independent patient-matched cultures were first grown for four days in co-ExM. Following expansion, the complex organoids were subjected to differentiation medium (DM), composed of ExM with

Merge
Ki67
DAPI
ExM
co-ExM

Figure 4.5: Immunohistochemistry for Ki67 in sectioned complex organoids grown in ExM or co-ExM. Complex organoids from three independent cultures in triplicate were grown for 4 days in either ExM or co-ExM. Cultures were formalin fixed and paraffin embedded and sectioned. Channels were visualised by epifluorescent microscopy using a secondary antibody conjugated to Alexa 488, depicted in green. Nuclei were counterstained with DAPI, depicted in blue. Ki67 (Alexa 488, red; nuclei DAPI, blue) was present and localised in EEC in both ExM and co-ExM (inside the white dotted circle). Ki67 was also present in some EnSC in co-ExM. (Scale bar: 50 μm).

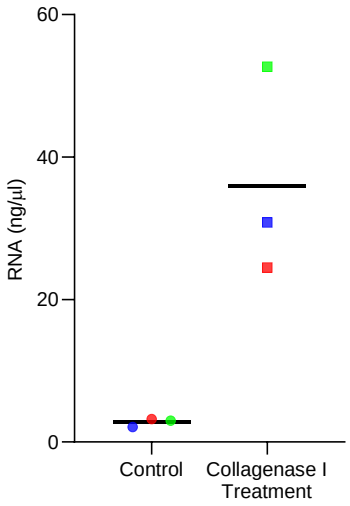

Figure 4.6: Optimisation of RNA extraction protocol in complex organoids using collagenase I. Three independent patient cultures were grown as complex organoids for 7 days before being harvested for RNA isolation. Three replicate complex organoids of each sample were harvested by RNA lysis buffer alone, and three replicate complex organoids of each sample were harvested by first adding 200 µl collagenase I and incubating at 37°C for 10 min. Samples were pelleted by centrifugation and RNA lysis buffer was added. RNA extraction was performed, and RNA quantity was measured by a NanoDrop spectrophotometer (ng/µl). Data show RNA quantity of three independent complex organoid cultures. The colours represent the three individual cultures. The line represents the mean. $P > 0.05$ (Wilcoxon matched pairs signed rank test).

cAMP and MPA, for four days. Undifferentiated control cultures were maintained in co-ExM (Fig. 4.7A). Treatment with cAMP and MPA in the absence of E2 was chosen based on previous *in vitro* studies of EnSC decidualisation (Brighton et al., 2017, Lucas et al., 2019, Muter et al., 2016, Brosens et al., 1999). Treated complex organoids (D4) and untreated control cultures (D0) were harvested for RNA for RT-qPCR analysis. A panel of genes (*PAEP, CXCL14, SPP1, PRL*) was used to examine the complex organoids' response to DM. The panel was curated in accordance with previous literature (Turco et al., 2017, Gellersen and Brosens, 2014). Cell-type specificity of each gene from the panel was confirmed by published *in vivo* scRNA-seq data (Fig 4.7B) (Lucas et al., 2018). Gland-specific differentiation markers *PAEP* and *SPP1* encode proteins glycodelin and osteopontin, respectively, which are secreted by differentiated endometrial glands *in vivo* (von Wolff et al., 2001, Turco et al., 2017). Expression of *CXCL14,* encoding cytokine chemokine (C-X-C motif) ligand 14, is also upregulated during the secretory phase but by both the glandular EEC and EnSC (Díaz-Gimeno et al., 2011). Finally, *PRL,* encoding prolactin, is a canonical EnSC decidual marker gene in culture, despite its modest expression *in vivo* (Gellersen and Brosens, 2014, Garrido-Gomez et al., 2017, Brosens et al., 1999).

RT-qPCR analysis was used to measure the induction of the four marker genes (Fig 4.7C). Relative expression of all genes increased in complex organoids treated with DM. Relative expression of *CXCL14* increased 10.3-fold and *PAEP* increased 8.6-fold when compared to the undifferentiated control D0. Relative expression of *SPP1* increased 8.5-fold. *PRL* exhibited the highest increase in relative expression by 36.7-fold compared to matched undifferentiated control samples. However, there was considerable variability in the level of induction between different complex organoid cultures.

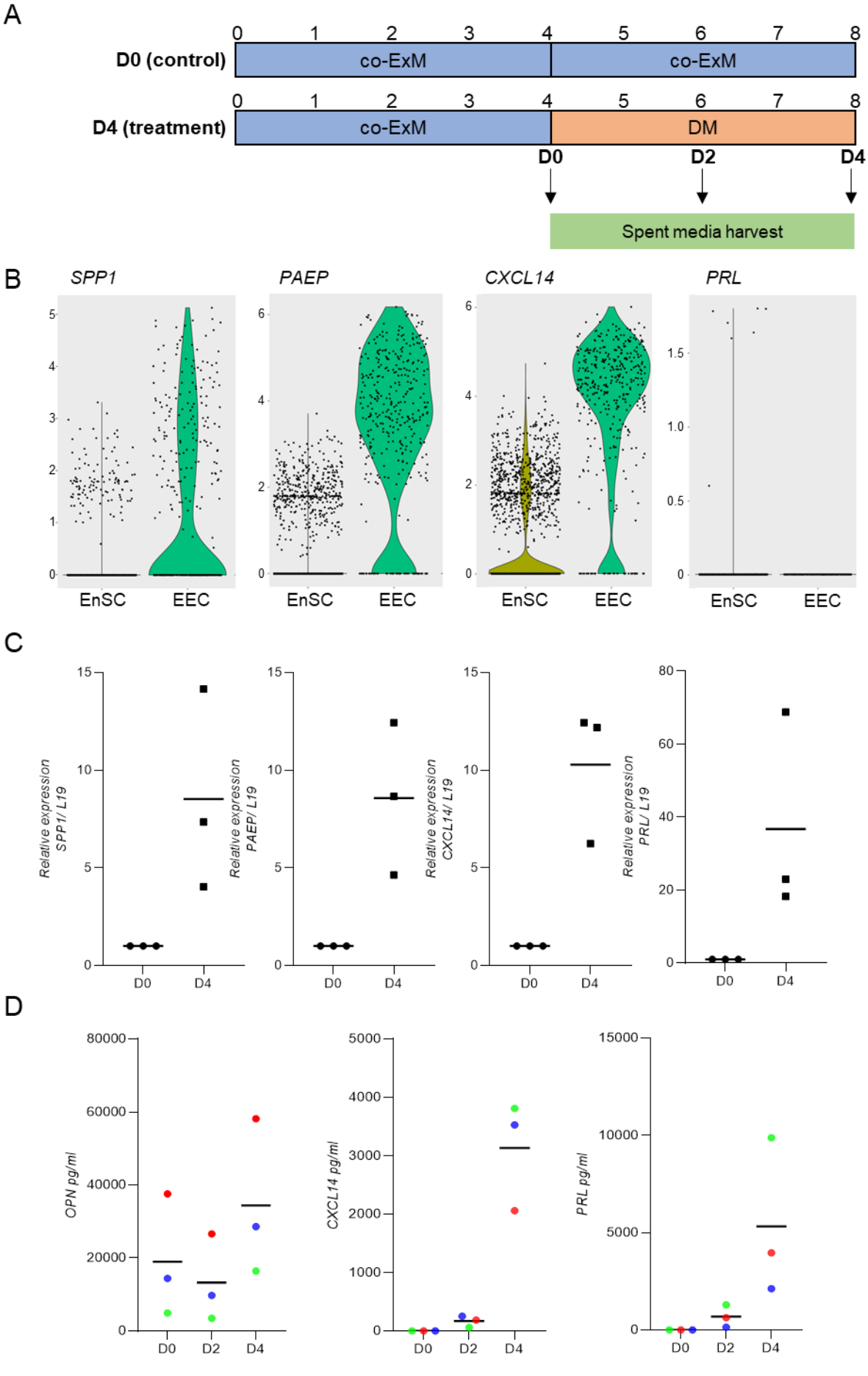
A
0 1 2 3 4 5 6 7 8
D0 (control)
co-ExM
co-ExM
0 1 2 3 4 5 6 7 8
D4 (treatment)
co-ExM
DM
D0
D2
D4
Spent media harvest
B
SPP1
PAEP
CXCL14
PRL
EnSC
EEC
C
Relative expression SPP1/ L19
Relative expression PAEP/ L19
Relative expression CXCL14/ L19
Relative expression PRL/ L19
D0
D4
D
OPN pg/ml
CXCL14 pg/ml
PRL pg/ml
D0
D2
D4

Figure 4.7: Differentiation of the complex organoid cultures.

A: A schematic of the differentiation protocol. Three independent complex organoid cultures were grown in duplicate for both control and treatment groups. Control group (D0) was grown in co-ExM for 8 days. Treatment group were grown in co-ExM for 4 days (D4), and then DM for 4 days. RNA was harvested at day 8 of culture. Spent media was collected on day 0 (D0), day 2 (D2) and day 4 (D4) of differentiation.

B: Expression data of the four marker genes (*SPP1*, *PAEP*, *CXCL14*, *PRL*) chosen for differentiation analysis in EnSC and EEC from *in vivo* scRNA-seq data (Lucas et al., 2018). Data collected in collaboration with Dr Pavle Vrljicak.

C: *SPP1*, *PAEP*, *CXCL14*, *PRL* transcript levels were measured in complex organoids at D0 and D4 from three independent cultures in duplicate. Gene expression was normalised to housekeeping gene *L19* mRNA levels. The data show gene expression relative to D0 in three independent cultures. The line represents the mean. $P > 0.05$ (Wilcoxon matched pairs signed rank test).

D: Secreted OPN, CXCL14 and PRL from the spent media of complex organoids collected at D0, D2 and D4 of differentiation was measured by ELISA. Data show secreted levels measured from three independent cultures in duplicate. The colours represent the three individual cultures. The line represents the mean. These experiments were performed in collaboration with Komal Makwana.

ELISA were performed on the spent culture media samples to measure the concentration of CXCL14, OPN (encoded by *SPP1*) and PRL secreted by the cultures (Fig. 4.7D). Average OPN protein concentration increased at D4 when compared to D0 (mean ± SD: 34000 ± 12400 pg/ml versus 18000 ± 9700 pg/ml, respectively, but decreased at D2 (mean ± SD: 13000 ± 6910 pg/ml). Average CXCL14 protein concentration was undetectable at D0. Increase in CXCL14 average protein concentration was small at D2 (mean ± SD: 170 ± 56 pg/ml). However, CXCL14 protein concentration increased at D4 (mean ± SD: 3100 ± 543 pg/ml). Average PRL protein concentration was also undetectable at D0, and low at D2 (mean ± SD: 610 ± 332 pg/ml), but at D4, average protein concentration increased to 5300 ± 2340 pg/ml (mean ± SD). Again, the magnitude of PRL secretion by the complex organoids varied between cultures.

Immunohistochemical analysis of complex organoids

Finally, the aim of this study was to develop a model that not only functionally but also morphologically recapitulated the human endometrium. Therefore, the morphology of undifferentiated and differentiated complex organoids was examined in addition by IHC. Three independent cultures were grown for four days in co-ExM and then differentiated in DM for a further 4 days or maintained undifferentiated in co-ExM. Complex organoids were then harvested, formalin fixed, paraffin embedded and sectioned. First, antibodies for gland-specific structural markers cytokeratin, EpCAM and E-cadherin were tested (Fig. 4.8). All three antibodies labelled the endometrial gland organoid cells positively at the plasma membrane. The IHC revealed that undifferentiated EEC gland structures were small and spherical, whereas upon differentiation they were widened and contorted. This recapitulates the morphology of glands in the human endometrium (Gray et al., 2001a). Furthermore, the EnSC were labelled with a vimentin antibody (Fig. 4.8). Upon differentiation, the EnSC produced a dense matrix of decidualising stroma surrounding the gland organoids.

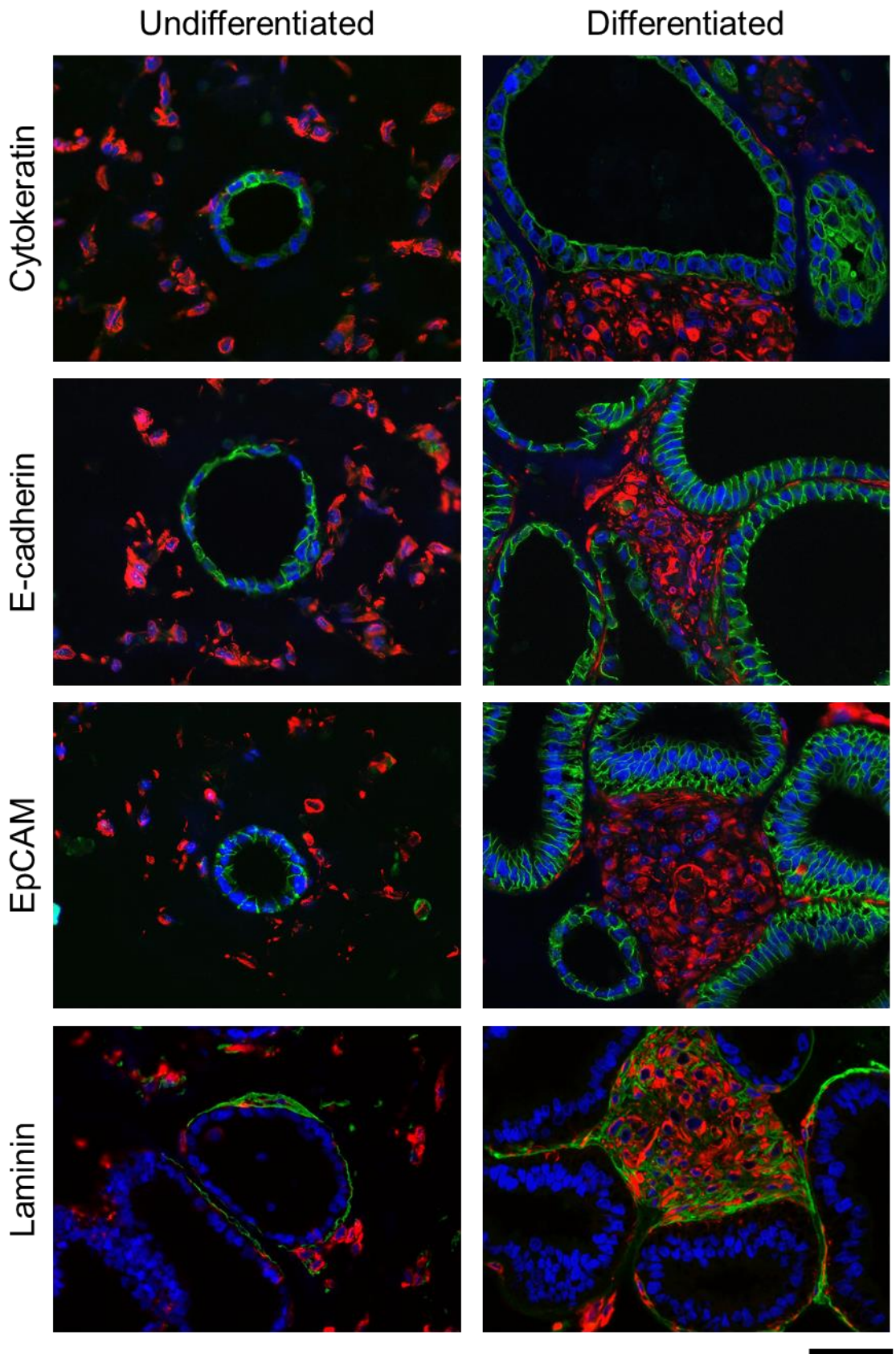
Undifferentiated
Differentiated
Cytokeratin
E-cadherin
EpCAM
Laminin

Figure 4.8: Immunohistochemistry for EEC structural markers in undifferentiated and differentiated complex organoids. Complex organoids from three independent cultures in triplicate were grown for 4 days in co-ExM and then differentiated in DM for a further 4 days (Differentiated) or maintained in co-ExM (Undifferentiated). Cultures were formalin fixed and paraffin embedded and sectioned. Channels were visualised by epifluorescent microscopy using a secondary antibody conjugated to Alexa 488, depicted in green. EnSC were immunolabelled with vimentin antibody and visualised using secondary antibody conjugated to Alexa 594, depicted in red. Nuclei were counterstained with DAPI, depicted in blue. Cytokeratin, E-cadherin and EpCAM (green) localised to the plasma membrane of endometrial gland organoid epithelial cells. Laminin (green) localised to the BM between the EnSC and EEC. (Scale bar: 50 μm). Data collected in collaboration with Komal Makwana.

Laminin was also labelled positively in a thin layer between the gland organoids and surrounding EnSC indicating BM formation. In differentiated samples, laminin also localised to the ECM surrounding the EnSC. Taken together, these data demonstrate complex organoids recapitulate some aspects of human endometrial morphology.

Furthermore, the complex organoids were also labelled with a PGR antibody (Fig. 4.9). Undifferentiated cultures exhibited localisation of PGR in the nuclei of both EEC and EnSC. However, upon differentiation, the labelling of PGR was reduced in all cultures. In addition, the complex organoids were labelled with a glycodelin antibody (Fig. 4.10). Undifferentiated samples did not label positively for glycodelin. However, differentiated samples displayed localisation of glycodelin to the luminal surfaces of the EEC. This indicated that the EEC were polarised and were actively secreting glycodelin into their luminal cavities. This is further evidenced by the positive labelling of glycodelin in the luminal cavities. Finally, in addition to antibody labelling, the secondary antibodies were tested on same samples to account for any non-specific binding of the fluorophores (Fig. 4.11).

Overall the RT-qPCR, ELISA and IHC confirm that the complex organoids not only functionally respond to deciduogenic cues but in addition to this attain a morphology that partially recapitulates the human endometrium under the conditions optimised in this study. Figure 4.12 is a schematic summary of the established protocol for culturing complex organoids.

Merge
PGR
DAPI
Undifferentiated
Differentiated

Figure 4.9: Immunohistochemistry for PGR in undifferentiated and differentiated complex organoids. Complex organoids from three independent cultures in triplicate were grown for 4 days in co-ExM and then differentiated in DM for a further 4 days (Differentiated) or maintained in co-ExM (Undifferentiated). Cultures were formalin fixed and paraffin embedded and sectioned. Channels were visualised by epifluorescent microscopy using a secondary antibody conjugated to Alexa 594, depicted in red. Nuclei were counterstained with DAPI, depicted in blue. PGR (red) localised to the nuclei of EnSC and gland organoids in undifferentiated samples. (Scale bar: 50 μm) Data collected in collaboration with Komal Makwana.

Merge
Glycodelin
DAPI
Undifferentiated
Differentiated

Figure 4.10: Immunohistochemistry for glycodelin in undifferentiated and differentiated complex organoids. Complex organoids from three independent cultures in triplicate were grown for 4 days in co-ExM and then differentiated in DM for a further 4 days (Differentiated) or maintained in co-ExM (Undifferentiated). Cultures were formalin fixed and paraffin embedded and sectioned. Channels were visualised by epifluorescent microscopy using a secondary antibody conjugated to Alexa 488, depicted in green. Nuclei were counterstained with DAPI, depicted in blue. Glycodelin (green) localised to the apical plasma membrane and lumen of endometrial gland organoids. (Scale bar: 50 μm) Data collected in collaboration with Komal Makwana.

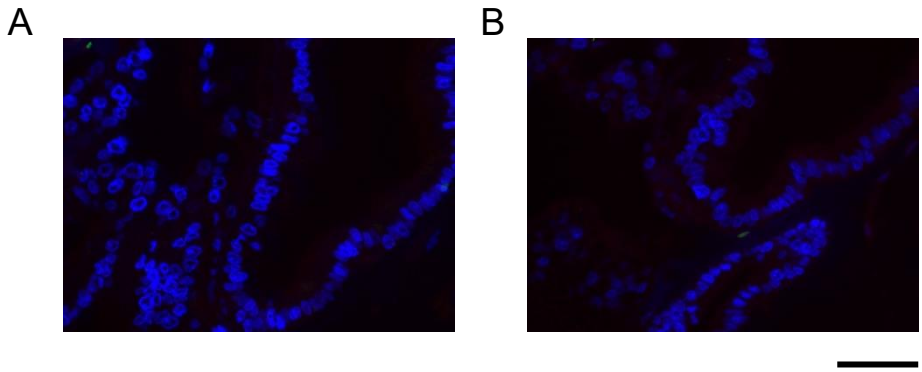

Figure 4.11: Negative control for immunohistochemistry of undifferentiated and differentiated complex organoids. Complex organoids from three independent cultures in triplicate were grown for 4 days in co-ExM and then differentiated in DM for a further 4 days (Differentiated) or maintained in co-ExM (Undifferentiated). Cultures were formalin fixed and paraffin embedded and sectioned. IHC in Figure 4.5, 4.9 and 4.10 were performed concurrently.

A: Channels were visualised by epifluorescent microscopy using a secondary antibody conjugated to Alexa 594 only, depicted in red. Nuclei were counterstained with DAPI, depicted in blue. .

B: Channels were visualised by epifluorescent microscopy using a secondary antibody conjugated to Alexa 488 only, depicted in green. Nuclei were counterstained with DAPI, depicted in blue. (Scale bar: 50 μm).

Data collected in collaboration with Komal Makwana.

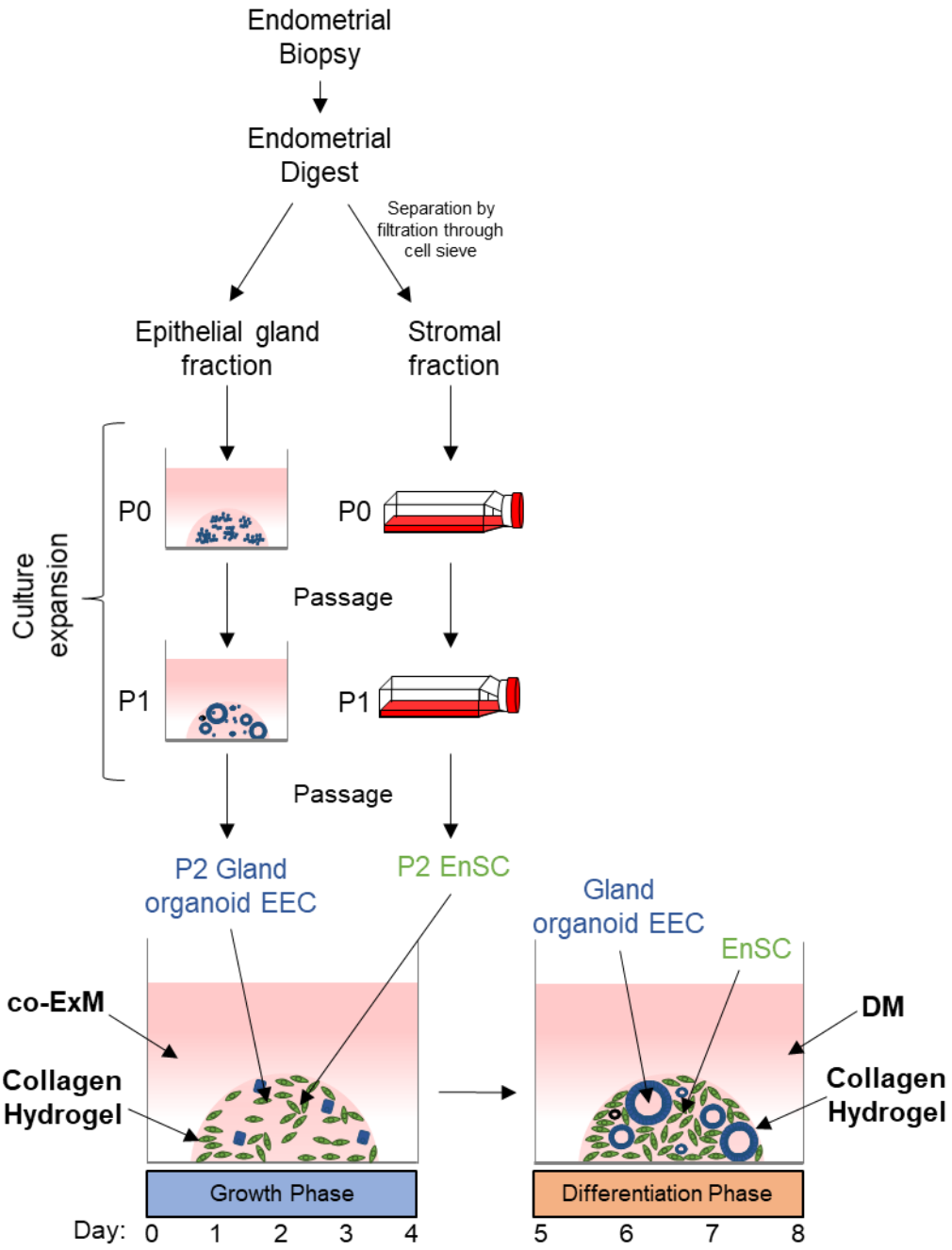

Figure 4.12: A schematic representation of the optimised protocol for producing an endometrial complex organoid culture. Endometrial biopsies are dissociated mechanical and enzymatic digestion. The endometrial digest is separated into gland and stromal fractions by a 40 µm cell sieve. For P0-1, gland organoids and EnSC are grown separately to expand the number of cells in both cultures. At P2, dissociated gland organoid EEC and EnSC are mixed in a collagen hydrogel at a ratio of 1:20 each and aliquoted into 20 µl droplets in a 48 well plate at let to cure at 37°C for 45 min. co-ExM (200 µl) is added and cultures are grown for 4 days (growth phase) with medium refreshed every 48 hours. At day 4, medium is replaced with

differentiation medium (DM) for a further 4 days (differentiation phase) for differentiation studies. DM is refreshed every 48 hours. At Day 8, complex organoid cultures are harvested for downstream analyses.

4.3 Discussion

Determining the hydrogel matrix suitable complex organoid culture

The aim of this study was to establish a protocol for an *in vitro c*omplex organoid system by culturing endometrial gland organoids with EnSC. The development of this system required the optimisation of the growth conditions to accommodate both the organoids and EnSC. The published endometrial gland organoid protocol used Matrigel for expansion, as it is derived from BM matrix that consists largely of BM proteins including laminins, collagen V and entactin (Kleinman and Martin, 2005). Therefore, Matrigel is a suitable gel for anchoring EEC and establishing cellular polarisation, essential for endometrial epithelial gland differentiation (Bentin-Ley et al., 1994, Classen-Linke et al., 1997). In the context of the endometrial gland organoids, the basal surface is in contact with Matrigel, and the apical surface lines the internal lumen. Endometrial gland organoid polarisation has been previously demonstrated in Matrigel (Turco et al., 2017).

However, in Chapter 3, I demonstrated that Matrigel was inappropriate for EnSC culture. Instead, a previous study used collagen hydrogels for culturing fibroblasts in 3D *in vitro* (Bentin-Ley et al., 1994). In the present study, EnSC failed to contract on collagen hydrogel with subjected to the EFAM protocol. Previous studies have demonstrated that stiffer ECM, or even cell culture plastic, is more likely to activate fibroblasts into a myo-fibroblast-like phenotype (Balestrini et al., 2012, Lambricht et al., 2014). Collagen gels have been reported as being less stiff than Matrigel (Motte and Kaufman, 2013, Anguiano et al., 2017). Therefore, the failure of the EnSC to activate on the collagen hydrogel is likely attributed to the relative softness of the gel. In addition, collagen, particularly types I, III and VI, are the primary constituents of the stromal ECM of the endometrium (Iwahashi et al., 1997). This suggests the collagen

hydrogel, consisting of purified collagen I, recapitulates the endometrial ECM more faithfully than the BM-derived Matrigel and is therefore more suitable for culture.

In addition to the EnSC findings, gland organoids expanded in the collagen hydrogel despite it being softer and containing a different ECM composition. EnSC and EEC can induce the production of ECM components essential for BM formation, such as laminins, *in vivo* (Classen-Linke et al., 1997, Wewer et al., 1986). The IHC revealed that laminin is present and localised between organoids and EnSC indicating that the complex organoids can produce a BM when cultured in collagen hydrogel. The presence of a BM suggests that the organoids polarised in the collagen hydrogel. Hence, these findings suggest that the EnSC support the development of EEC gland structures in complex organoids.

Optimising the growth medium for complex organoids.

The standard ExM medium published by Turco, *et al*., used for expanding gland organoids does not contain E2 during initial expansion (Turco et al., 2017). In this study, when complex organoids were cultures in ExM, the EnSC failed to show any visual sign of expansion. E2 is known to drive endometrial proliferation in the menstrual cycle. In this study, it was demonstrated that E2 is essential for EnSC proliferation, as evidenced by the EnSC morphology and some positive labelling of proliferation marker Ki67 in both complex organoid EEC and EnSC. Therefore, this complex organoid medium was designated co-ExM.

However, unexpectedly, the additional serum replacements did not improve the proliferation of the complex organoids. Standard EnSC medium contains FBS which supports EnSC proliferation. However, FBS is known to contain an unspecified composition, including hormones and growth factors. These hormones can be stripped by dextran-coated charcoal (DCC) treatment; however, the specific

composition of FBS is not consistent (Gstraunthaler, 2003). Therefore, it was important to use a serum replacement such as serum replacement 1 (SR1) and Albumax II to maintain a defined medium to maintain consistency of culture. Both are purified BSA. SR1 had no visual effect on EnSC morphology or proliferation at 1× concentration when in combination with E2. Also, although Albumax was able to improve EnSC proliferation, it inhibited organoid expansion. BSA is a natural carrier protein that binds to peptides such as growth factors in the circulatory system, as well as used as a carrier protein for long term storage of growth factors *in vitro* (Kragh-Hansen, 1981, Friedrichs, 1997, Merlot et al., 2014). Therefore, it is possible that the Albumax quenched growth factors from the ExM, removing them from suspension in the medium and therefore inhibiting organoid expansion. As neither additive was beneficial to the complex organoids, they were not included in the final co-ExM formulation. In addition, previous studies have demonstrated that N2 and B27 alone are effective at increasing cell proliferation equivalent to FBS in organoid-based cell cultures (Crespo et al., 2017), substantiating that further serum replacement was unnecessary for this medium when E2 is present.

Comparing the complex organoid cultures to the in vivo endometrium

The aim of this study was to establish an optimised *in vitro* model that functionally and morphologically recapitulates the human endometrium. In this study, I have demonstrated that both the EnSC and EEC respond to DM treatment in complex organoid cultures. The EEC gland structures induced key gland-specific differentiation genes *PAEP* and *SPP1* as well as *CXCL14*. In addition, at the protein level, the EEC secreted OPN and CXCL14 into the medium when differentiated, recapitulating endometrial glandular secretions *in vivo* (von Wolff et al., 2001, Díaz-Gimeno et al., 2011). These findings are in agreement with endometrial gland organoid studies (Turco et al., 2017, Boretto et al., 2017). This demonstrates that gland organoids can respond to deciduogenic stimulation when grown in collagen

hydrogel and in complex organoids. In addition, EnSC were also able to decidualise in DM, demonstrated by the induced expression of *PRL*, and the subsequent secretion of PRL. Thereby demonstrating the EnSC can differentiate when grown in collagen hydrogel and in the presence of organoids.

This study demonstrated that the complex organoids partially recapitulate the human endometrium morphologically. Previous studies have established layered co-culture systems that have positively stained for epithelial, stromal and BM markers (Bentin-Ley et al., 1994). However, no published studies have yet described this complex organoid culture. In this present study, endometrial EEC-specific structural markers such as EpCAM, cytokeratin and E-cadherin labelled positively along the plasma membrane of the gland organoids. This confirms that in complex organoids, the gland organoid structures remain epithelial. These observations agree with previous gland organoid studies (Turco et al., 2017). Additionally, the EnSC, labelled positively with vimentin and negative for the gland-specific markers, formed a dense cellular matrix around the glands upon differentiation, recapitulating the structure of the *in vivo* endometrium (Cloke et al., 2008, Gellersen and Brosens, 2014). Furthermore, a positive labelling of laminin between the EnSC and EEC indicate BM formation at the basal surface of the EEC in the collagen hydrogel. Furthermore, the localisation of laminin surrounding decidualising EnSC recapitulates the ECM of the human decidua (Iwahashi et al., 1997, Aplin et al., 1995).

Furthermore, differentiated complex organoids lost PGR expression, in keeping with *in vivo* expression (Jabbour et al., 2002, Mote et al., 1999). However, previous gland organoid studies have demonstrated PGR expression to be maintained in EEC, but these organoids were not cultured with EnSC (Turco et al., 2017). This may possibly suggest that the gland organoids require EnSC for differentiation. EnSC induced differentiation of EEC has been observed *in vivo* (Cooke et al., 1997, Arnold et al.,

2001). The EEC in complex organoid cultures secreted glycodelin when differentiated, further demonstrating their secretory potential. Taken together, these data indicate that the complex organoids morphologically and functionally recapitulate the *in vivo* human endometrium.

Conclusion

Overall, the aim of this study was to establish a complex organoid model by coculturing the endometrial gland organoids and EnSC. The purpose of this model is to be the first step in bringing about a step-change improvement in the *in vitro* modelling of the human peri-implantation endometrium. In this study, I have established and optimised a protocol for complex organoid culture. The endometrial gland organoid protocol from Turco, *et al.* 2017*,* was modified by replacing Matrigel with a collagen hydrogel and by adding E2 to ExM (co-ExM) to best accommodate both EnSC and EEC proliferation. I have demonstrated complex organoids both morphologically and functionally recapitulate the stroma and glands of the human endometrium. The next step in the optimisation of this system was to determine to what extent the EnSC can replace the components of the co-ExM in supporting the differentiation of the EEC in order to produce a more physiological *in vitro* model of the endometrium.

Chapter 5:

EnSC-EEC interactions in complex organoid culture

5.1 Introduction

EnSC are pivotal to the development, growth and differentiation of the overlaying epithelium (Bigsby and Cunha, 1986, Cooke et al., 1986). In human endometrium, gland differentiation is regulated *via* paracrine signalling by EnSC in response to rising progesterone levels (Cooke et al., 1997, Kurita et al., 1998). Simple *in vitro* models of human EnSC and EEC have demonstrated the regulatory role of the stroma (Arnold et al., 2001). In this particular study, EnSC and monolayer EEC were grown either in mono- or a layered co-culture, cultured either in Matrigel or on plastic, and either in contact with the other cell type or separated by an insert. Co-cultures grown in contact and in Matrigel induced a multi-fold increase in differentiation response of the EEC when compared to other conditions, substantiating that EnSC paracrine regulation of EEC differentiation can be modelled *in vitro* (Arnold et al., 2001). Other studies have characterised further the impact of EnSC on the differentiation of EEC through the menstrual cycle *in vitro* (Evron et al., 2011, Cook et al., 2017).

Unlike previous studies using EEC monolayers, which are grown from a mixture of luminal and glandular EEC, endometrial gland organoids specifically model endometrial glands (Turco et al., 2017, Boretto et al., 2017). EnSC regulation of the differentiation endometrial glandular epithelium has yet to be described using human endometrial gland organoids. Following the establishment of the complex organoid system in the Chapter 4, the subsequent step was to assess the impact of EnSC on the glandular EEC of the gland organoids. However, unlike monolayer EEC, endometrial gland organoids are grown in a complex medium (ExM) (Turco et al., 2017) with multiple growth factors and inhibitors that maintain an artificial environment for the organoids that permits glandular differentiation without EnSC regulation (Table 5.1). Therefore, I hypothesised that a minimal differentiation medium ($DM_{min.}$), consisting of only essential factors, would be necessary to observe EnSC-EEC

Table 5.1: A List of components of Expansion Medium (ExM). For each medium component, the concentration and function are stated alongside relevant references. The recipe taken from Turco, *et al.,* 2017.

Component	Concentration	Function	References
Advanced DMEM/F12	1X	Base medium suitable for reduced serum media formulations	(Turco et al., 2017)
A83-01	500 nM	Potent inhibitor of TGF-β type I receptor superfamily activin-like kinase ALK5 and its relatives ALK4 and ALK7	(Gurung et al., 2015, Tojo et al., 2005b, Sato et al., 2011, Karthaus et al., 2014, Bartfeld et al., 2015)
R-spondin1	500 ng/ml	Promotes canonical WNT/β catenin signalling	(Binnerts et al., 2007)
Nicotinamide	10 mM	Incorporated into coenzymes NAD+ (nicotinamide adenine dinucleotide) and NADP+ (nicotinamide adenine dinucleotide phosphate) essential for metabolism	(Inoue et al., 1989, Mitaka et al., 1991, Koo et al., 2012)
N-acetyl-L-cysteine (NAC)	1.25 mM	Antioxidant	(Zafarullah et al., 2003, Circu and Aw, 2008)
Noggin	100 ng/ml	BMP (Bone morphogenetic protein) inhibitor	(Krause et al., 2011, Au - Bartfeld and Au - Clevers, 2015, Sato et al., 2009)
Fibroblast Growth Factor 10 (FGF10)	100 ng/ml	Promotes cell growth and proliferation	(Chen et al., 2000, Chung et al., 2015)
Hepatocyte Growth Factor (HGF)	50 ng/ml	Promotes epithelial cell growth and proliferation	(Sugawara et al., 1997, Bartfeld et al., 2015)
Epidermal Growth Factor (EGF)	50 ng/ml	Promotes cell growth, proliferation and differentiation.	(Suzuki et al., 2010, Abud et al., 2005)

N2	1X	Supplement for serum free medium	(Bottenstein and Sato, 1979)
B27	1X	Supplement for serum free medium	(Brewer et al., 1993)
Antibiotic-Antimycotic	1X	Prevent Infection	(Barros et al., 2016)
L-glutamine	2 mM	Essential amino acid	(Eagle et al., 1956)

interactions. When differentiated in this defined DM_{min}, EnSC may replace the factors in the standard DM ($DM_{std.}$) and produce the necessary cues for gland organoid differentiation.

In this study, scRNA-seq was performed after 2 and 4 days of decidualisation of complex and simple organoids to determine the impact of decidualising EnSC on EEC differentiation in DM_{min}. Standard RNA-seq was deemed inappropriate as it does not yield information on changes in gene expression in different cell types of the complex organoids. Therefore, scRNA-seq was chosen as the method of RNA sequencing (Macosko et al., 2015). In this protocol, samples are digested to single cells and flowed through a microfluidic device. Individual cells are encapsulated into single aqueous droplets containing a nanoparticle bead, each bound with unique PCR primers that 'barcode' each cell. Within the droplet, the cell is lysed, and the messenger RNA (mRNA) is released and binds to the barcoded PCR primer. Each primer contains a PCR handle, a cell barcode that is unique to the bead, and a unique molecular identifier (UMI), which is unique to each primer. In addition, a 30-base pair oligo-dT sequence allows for mature mRNA poly(A) tail to bind. The mRNA-bound beads are collected, and subjected to a series of processes: reverse transcription, amplification, libraries generation and sequencing (Macosko et al., 2015). The transcription profiles of individual cells can be identified by their unique barcodes from the scRNA-seq dataset (Macosko et al., 2015).

The mRNA profiles are mapped graphically by *t*-distributed Stochastic Neighbour Embedding (*t*-SNE) or Uniform Manifold Approximation and Projection (UMAP) algorithms (van der Maaten and Hinton, 2008, Kobak and Berens, 2018, Becht et al., 2018b, McInnes et al., 2018). These are examples of nonlinear dimensionality reduction techniques where high-dimensional data such as RNA sequencing data can be visualised graphically in a 2D space. Each point on the graph represents a single

cell transcriptome, where nearby points are transcriptionally similar and distant points are transcriptionally different. In this present study, the UMAP algorithm was utilised due to its faster speed and more biologically meaningful aggregation of cell clusters with regard to cell type and subtypes (Becht et al., 2018a). The shared nearest neighbour (SNN) algorithm was performed also in parallel and groups the data into clusters of transcription profiles based on similarity. The SNN algorithm assumes that if two points share several neighbours in common, they are more likely to be similar (Xu and Su, 2015). The SNN clusters are represented graphically by coloured groupings in *t*-SNE or UMAP plots. Points that share the same colour are defined as being transcriptionally similar (Xu and Su, 2015).

The aim of this chapter was to model EnSC-EEC interactions in my established complex organoid co-culture, demonstrating it to be a working model of the endometrium. The objectives to achieve this aim were:

1. To define the $DM_{min.}$ that enables decidualisation of endometrial gland organoids in the complex gland organoid system.
2. To determine the impact of EnSC on the transcriptional responses in endometrial gland organoids in decidualising complex organoids.

5.2 Results

Defining the Minimal Differentiation Medium

The first objective was to define the $DM_{min.}$ required to model EnSC-induced EEC differentiation in the complex organoids. Three independent patient samples were used to grow gland (simple) organoids alone or complex organoids with patient matched EnSC, as described in Chapter 4. These cultures were grown for 4 days in co-ExM (Growth Phase) (Fig 5.1A). On Day 4, cultures were subjected to differentiation medium in which a single growth factor or inhibitor was omitted one at a time (Differentiation Phase). The media formulations are listed in Figure 5.1B, where one growth factor or inhibitor was removed per medium, as well as complete DM. All cultures were harvested on day 8 for RNA extraction.

RT-qPCR was used to measure the induction of EEC-specific differentiation markers (*SPP1* and *PAEP*), the canonical EnSC decidual marker prolactin (*PRL*), as well as *CXCL14*, which is expressed in both decidualising EnSC and EEC. (Fig. 5.2). Relative expression of both *SPP1* and *PAEP* was consistently higher in simple organoids (red bars) than in matched complex organoids (blue bars) for all DM formulations (Fig. 5.2A and 5.2B). There was large variation in relative expression of *CXCL14* in the samples, but expression was similar in both simple and complex organoid cultures (Fig. 5.2C). There was a trend towards higher expression of *PRL* upon removal of A83-01 (-A83-01) (Fig. 5.2D); however, removal of all other components reduced expression of *PRL* in complex organoid cultures. Therefore, removing any single factor from the DM was not sufficient to inhibit differentiation in simple organoids while still being able to enable the EnSC to induce EEC differentiation in the complex organoids. Therefore, a different approach was required to achieve this aim.

A

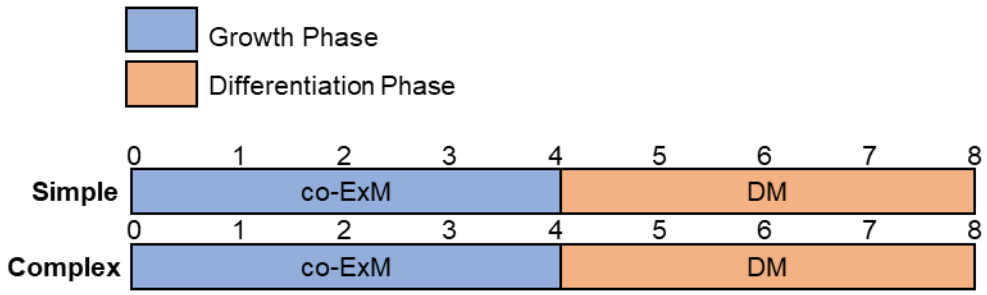

B

Medium Components	DM									
	co-ExM (control)	Complete	-NAC	-A83-01	-Nicotinamide	-EGF	-Noggin	-R-spondin	-FGF10	-HFG
Advanced DMEM/F12	✓	✓	✓	✓	✓	✓	✓	✓	✓	✓
NAC	✓	✓		✓	✓	✓	✓	✓	✓	✓
A83-01	✓	✓	✓		✓	✓	✓	✓	✓	✓
Nicotinamide	✓	✓	✓	✓		✓	✓	✓	✓	✓
EGF	✓	✓	✓	✓	✓		✓	✓	✓	✓
Noggin	✓	✓	✓	✓	✓	✓		✓	✓	✓
R-spondin-1	✓	✓	✓	✓	✓	✓	✓		✓	✓
FGF10	✓	✓	✓	✓	✓	✓	✓	✓		✓
HGF	✓	✓	✓	✓	✓	✓	✓	✓	✓	
N2 + B27	✓	✓	✓	✓	✓	✓	✓	✓	✓	✓
Antibiotic + Antimycotic	✓	✓	✓	✓	✓	✓	✓	✓	✓	✓
L-Glutamine	✓	✓	✓	✓	✓	✓	✓	✓	✓	✓
E2	✓									
cAMP + MPA		✓	✓	✓	✓	✓	✓	✓	✓	✓

Figure 5.1: Experimental plan for defining the minimal differentiation medium by the systematic removal of ExM components.

A: A schematic timetable of simple and complex organoid differentiation. The growth phase (blue) lasts from day 0 to day 4 and ExM medium is used. Day 4 to day 8 is the differentiation phase (orange) and DM is used.

B: A table of DM formulations. Blue represents growth medium co-ExM, orange represents DM formulations. Ticks in white boxes indicate the component is present. Grey boxes indicate the component is absent from the medium.

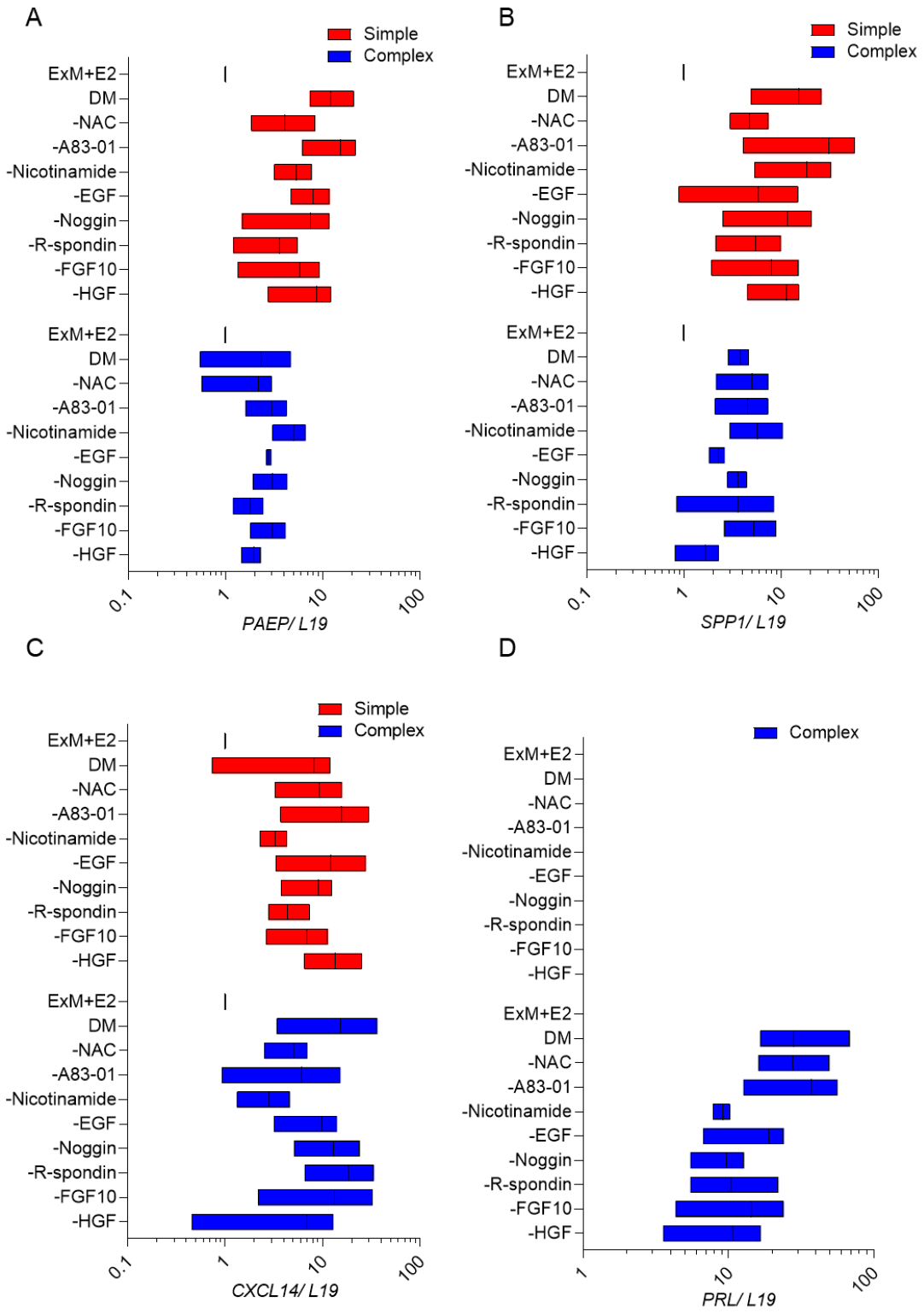

Figure 5.2: Expression of selected decidual marker genes upon removal of specific growth factors/ inhibitors in simple and complex organoids.

SPP1, *PAEP*, *CXCL14*, *PRL* transcript levels were measured in simple and complex organoid cultures after 4 days of differentiation in the various DM formulations from

three independent cultures in duplicate. Red bars represent min-max values for simple organoid relative expression. Blue bars represent min-max values complex organoid relative expression. Gene expression was normalised to housekeeping gene *L19* mRNA levels and relative to simple or complex organoid undifferentiated control (co-ExM), respectively $P > 0.05$ for all comparisons respective to undifferentiated control (Group comparison by Friedman test and Dunn's Multiple Comparison post hoc test). A: *PAEP* relative expression. B: *SPP1* relative expression. C: *CXCL14* relative expression. D: *PRL* relative expression. Data collected in collaboration with Komal Makwana.

The next strategy to define a $DM_{min.}$ was to remove all growth factors and inhibitors from the $DM_{std.}$ and then to add back systematically one factor at a time. Three independent patient biopsies were used to expand simple and complex organoids. Figure 5.3 lists the various DM formulations tested. All cultures were harvested on day 8 for RNA extraction.

The addition of any single factor to the DM was not sufficient to induce significant *PAEP* expression in simple organoid cultures (red bars). However, for complex organoid cultures (blue bars), *PAEP* expression was significantly induced in the complete DM (DM) or the DM containing NAC (+NAC) when compared to the undifferentiated control (ExM + E2) ($P < 0.05$, Friedman test and Dunn's Multiple Comparison *post hoc* test) (Fig. 5.4A). Furthermore, the addition of any single factor was not sufficient to induce significant *SPP1* expression in simple organoid cultures (Fig. 5.4B). However, *SPP1* expression was significantly induced for complex organoid cultures treated with DM containing NAC or nicotinamide (+Nicotinamide) when compared to undifferentiated control ($P < 0.05$, Friedman test and Dunn's Multiple Comparison *post hoc* test). Overall, expression of *SPP1* was higher in complex organoids for all DM treatments in comparison to matched simple organoid expression. Similarly, the addition of any single factor resulted in lower *CXCL14* expression for both simple and complex organoids (Fig 5.4C). However, relative expression of *CXCL14* was consistently higher in complex organoids than in matched simple organoid cultures. There were no significant differences in relative expression of *PRL* when any of the factors were added back systematically to the DM ($P > 0.05$, Friedman test and Dunn's Multiple Comparison *post hoc* test) (Fig 5.4D).

Taken together, these observations indicated that it may be beneficial to retain only NAC in the DM_{min}. All other growth factors and inhibitors appeared to be dispensable

Medium Components	DM										
	co-ExM (control)	Complete	Null	+NAC	+A83-01	+Nicotinamide	+EGF	+Noggin	+R-spondin	+FGF10	+HFG
Advanced DMEM/F12	✓	✓	✓	✓	✓	✓	✓	✓	✓	✓	✓
NAC	✓	✓		✓							
A83-01	✓	✓			✓						
Nicotinamide	✓	✓				✓					
EGF	✓	✓					✓				
Noggin	✓	✓						✓			
R-spondin-1	✓	✓							✓		
FGF10	✓	✓								✓	
HGF	✓	✓									✓
N2 + B27	✓	✓	✓	✓	✓	✓	✓	✓	✓	✓	✓
Antibiotic + Antimycotic	✓	✓	✓	✓	✓	✓	✓	✓	✓	✓	✓
L-Glutamine	✓	✓	✓	✓	✓	✓	✓	✓	✓	✓	✓
E2	✓										
cAMP + MPA		✓	✓	✓	✓	✓	✓	✓	✓	✓	✓

Figure 5.3: Experimental plan for defining the minimal differentiation medium by the systematic addition of ExM components. A table of various DM formulations with all growth factors/ inhibitors removed and replaced one at a time. Blue represents growth medium co-ExM, orange represents DM formulations. Ticks in white boxes indicate the component is present. Grey boxes indicate the component is absent from the medium.

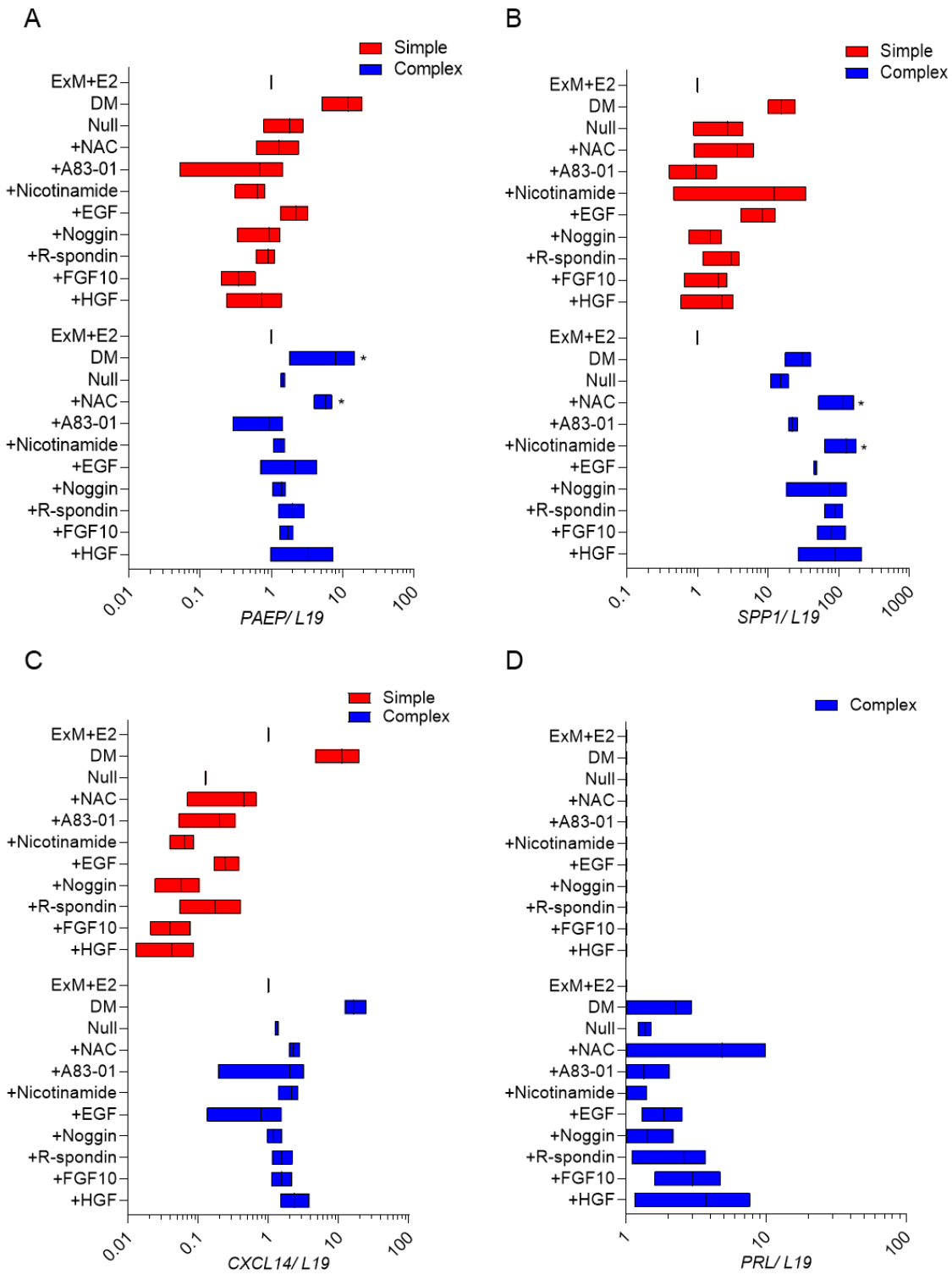

Figure 5.4: Expression of selected decidual marker genes upon addition of specific growth factors/ inhibitors in simple and complex organoids.

SPP1, *PAEP*, *CXCL14*, *PRL* transcript levels were measured in simple and complex organoid cultures after 4 days of differentiation in the various DM formulations from three independent cultures in duplicate. Red bars represent min-max values for

simple organoid relative expression. Blue bars represent min-max values for complex organoid relative expression. Gene expression was normalised to housekeeping gene *L19* mRNA levels and relative to simple or complex organoid undifferentiated control (co-ExM), respectively. * indicate $P < 0.05$ when compared to its respective undifferentiated control (Group comparison by Friedman test and Dunn's Multiple Comparison post hoc test). A: *PAEP* relative expression. B: *SPP1* relative expression. C: *CXCL14* relative expression. D: *PRL* relative expression. Data collected in collaboration with Komal Makwana.

for the decidualisation of complex organoids when NAC was present. Therefore, DM containing NAC was selected as the $DM_{min.}$ for future work.

scRNA-seq of decidualising simple and complex organoids in $DM_{min.}$

In order to perform scRNA-seq on the complex organoid cultures, the protocol for digestion of samples to a single cell suspension required optimisation. Previously, I optimised recovering RNA from collagen hydrogel by collagenase I. However, I observed that collagenase I treatment and manual digestion were sufficient for passaging, but not to produce a single cell suspension (See Chapter 4). TrypLE reagent is a trypsin alternative that is less damaging to cell surface epitopes. It has been used in intestinal organoid digestion previously (Grün et al., 2015). Three independent biopsies were grown as complex organoids for 7 days and then subjected to various digestion protocols. I examined whether the addition of 1× and 5× TrypLE reagent would produce a single cell suspension when used in addition to collagenase I and manual digestion (Fig. 5.5). The 1×TrypLE reagent produced a suboptimal single cell suspension (mean ± SD: 2.70 $x10^4$ ± 0.47 $X10^4$). However, 5× TrypLE reagent provided improved average single cell counts compared to control (mean ± SD: 9.93 $x10^4$ ± 0.63 $X10^4$ versus 1.60 $x10^4$ ± 0.23 $x10^4$, respectively, $P < 0.05$, Friedman test and Dunn's Multiple Comparison *post hoc* test). Hence, 5× TrypLE reagent was included into the protocol for single cell harvesting. The final protocol for single cell harvest including the 5× TrypLE reagent is illustrated in Figure 5.5B.

Next, simple and complex organoids expanded from a single biopsy were cultured for 4 days in co-ExM and then treated with $DM_{min.}$ for a further 4 days (Fig. 5.6). At D0, D2 and D4 of $DM_{min.}$ treatment, respectively, cultures were recovered and subjected to high-throughput scRNA-seq (Macosko *et al*., 2015). Unfortunately, the number of cells captured and sequenced per time-point varied (Fig. 5.7A). There was also

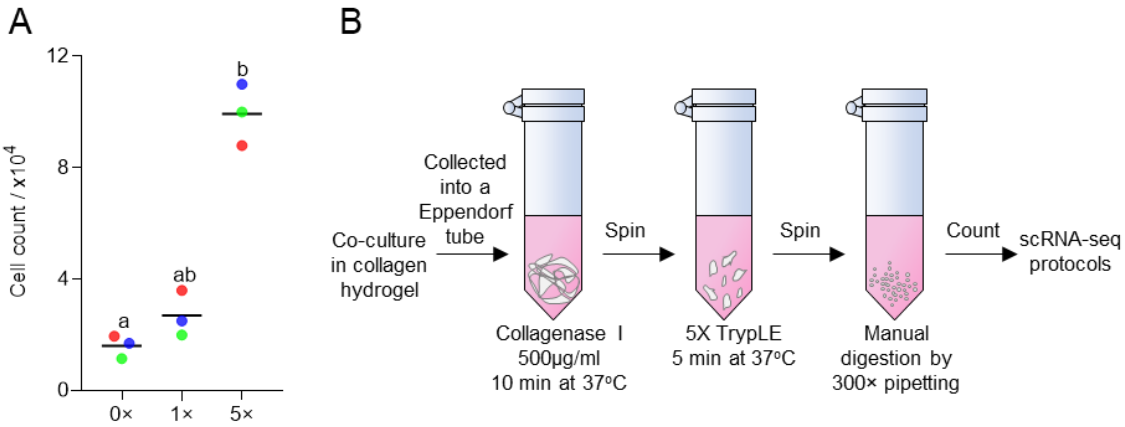

Figure 5.5: Optimisation of complex organoid digestion to single cell suspension.

A: Three independent patient biopsies were grown as complex organoid cultures for 8 days and then digested by collagenase I (500 µg/ml, 10 min at 37°C) and then split into three fractions and further digested by either manual digestion alone (0×), or with an additional step before manual digestion of a 5 min incubation with either 1× or 5× TrypLE reagent at 37°C. Single cells from each fraction of each sample were counted by haemocytometer. The colours represent the three individual cultures. The line represents the mean. Different letters above the error bars represent statistical difference from other groups at $P < 0.05$. Group comparison by Friedman test and Dunn's Multiple Comparison post hoc test.

B: A schematic of the final protocol for digestion to single cell suspension. Droplets of complex organoids cultured in hydrogel are scraped off the plastic well plate and collected into an Eppendorf tube. Collagenase I (500 µg/ml) is added, and the sample is placed in a water bath for 10 min at 37°C. The samples are centrifuged and pelleted. Samples are resuspended in 5× TrypLE reagent for 5 min at 37°C. The samples are centrifuged and pelleted. Samples are manually dissociated by 300× pipetting. Single cells are then counted by haemocytometer and used for downstream scRNA-seq protocols.

A

Medium Components	Medium	
	co-ExM	$DM_{min.}$
Advanced DMEM/F12	✓	✓
NAC	✓	✓
A83-01	✓	
Nicotinamide	✓	
EGF	✓	
Noggin	✓	
R-spondin-1	✓	
FGF10	✓	
HGF	✓	
N2 + B27	✓	✓
Antibiotic + Antimycotic	✓	✓
L-Glutamine	✓	✓
E2	✓	
cAMP + MPA		✓

B

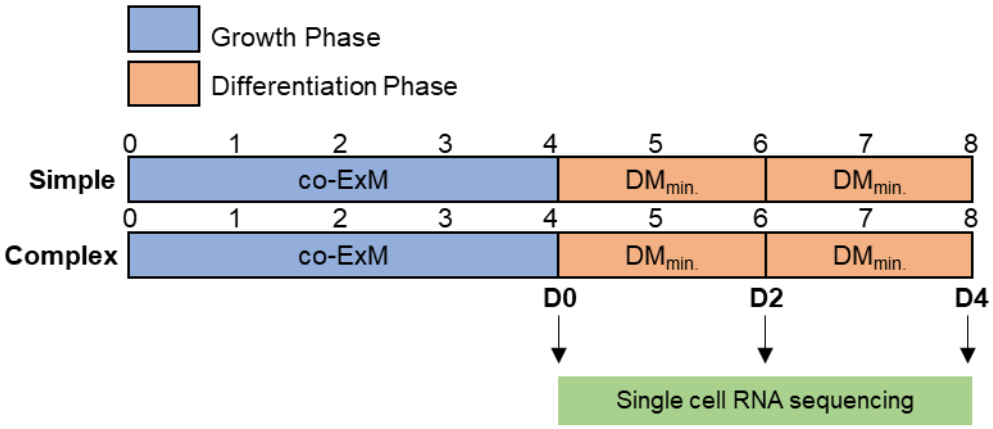

Figure 5.6: Experimental plan for comparing simple and complex organoid differentiation in $DM_{min.}$ by scRNA-seq.

A: A table of media formulations used for growth and differentiation of simple and complex organoids. Blue represents growth phase medium ExM, orange represents differentiation phase medium $DM_{min.}$. Ticks in white boxes indicate the component is present. Grey boxes indicate the component is absent from the medium.

B: A schematic timetable of experimental plan for scRNA-seq of differentiated simple and complex organoids. The growth phase (blue) lasts from day 0 to day 4 and ExM medium is used. Day 4 to day 8 is the differentiation phase (orange) and DM is used. D0, D2 and D4 represent 0, 2 and 4 days of $DM_{min.}$ treatment, respectively. At these time points, samples were harvest for scRNA-seq.

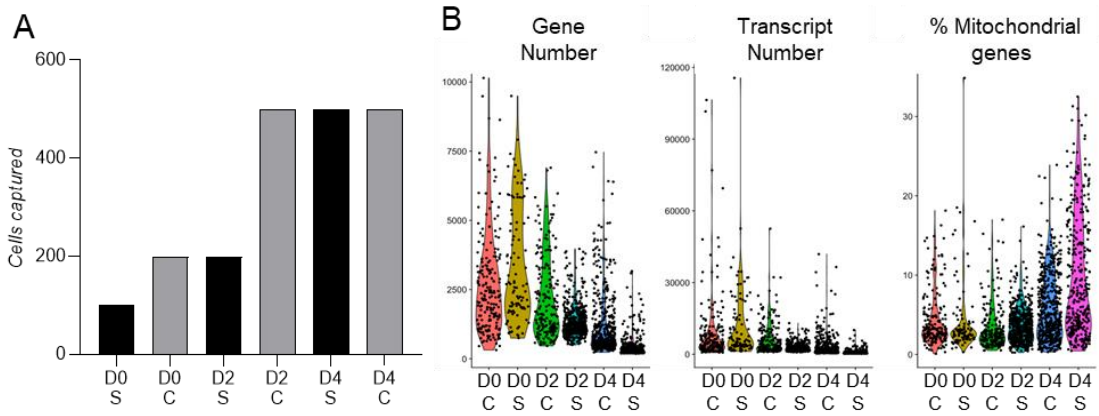

Figure 5.7: Quality control of differentiated simple and complex organoid culture scRNA-seq data.

A: The number of cells captured per sample from the scRNA-seq.

B: Violin plots of the number of genes, number of transcripts and the percentage mitochondrial DNA per cell from a decidual time course of 4 days (D0-4) of patient matched simple (S) and complex (C) organoid culture.

All data collected and analysed in collaboration with Dr Emma Lucas and Dr Pavle Vrljicak. Panel figure B produced by Dr Pavle Vrljicak.

variation in the average number of transcripts and genes per cell (Fig 5.7B), which decreased over the time course. Conversely, the percentage of mitochondrial genes increased over the time-course (Fig. 5.7B). Quality control (QC) was performed by only including genes that appear in ≥ 3 cells, and cells that express ≥ 200 genes. Only cells with ≤ 6000 genes and < 10% mitochondrial genes were included, to minimize inclusion of data from doublets and low-quality (broken or damaged) cells, respectively.

After this quality control filtering, a total of 1518 cells were graphed computationally by the UMAP algorithm (Fig. 5.8A). Combined with the SNN method, the cells were computationally assigned to 7 transcriptionally discrete cell states (Fig. 5.8B). Using these clusters, a heatmap of the most differentially expressed genes of each cluster was generated (Fig. 5.8C). Three cell types were assigned to the clusters (EnSC, ECC1, and ECC2) (Fig. 5.8D). Clusters 0-4 represented transcription profiles of ECC1. Cluster 5 represented transcription profiles of EnSC and Cluster 6 represented transcription profiles of ECC2. EEC2 expressed genes such as *CCDC19*, *SPAG17* and *MNS1* indicating that these were ciliated EEC (cEEC) (Zhou et al., 2012, Osinka et al., 2019, Teves et al., 2013, Lucas et al., 2018). Overall, following the QC, a total of 103 EnSC were captured, from complex organoid samples only. In addition, the EEC1 cluster contained the largest number of cells (n=1368). However, only 47 cEEC were captured, with the majority originating from simple organoids (Fig. 5.8E).

To investigate the impact of the EnSC on EEC differentiation, I focused in on the EEC1, non-ciliated EEC (ncEEC) fraction of the scRNA-seq data. Classifying the initial clusters by cell type permitted the removal of EnSC and ciliated EEC transcription profiles from the dataset. This was essential as the purpose of this experiment was to compare the EEC transcription profiles from simple and complex organoids directly. Figure 5.9A is a UMAP plot of the ncEEC transcription profiles

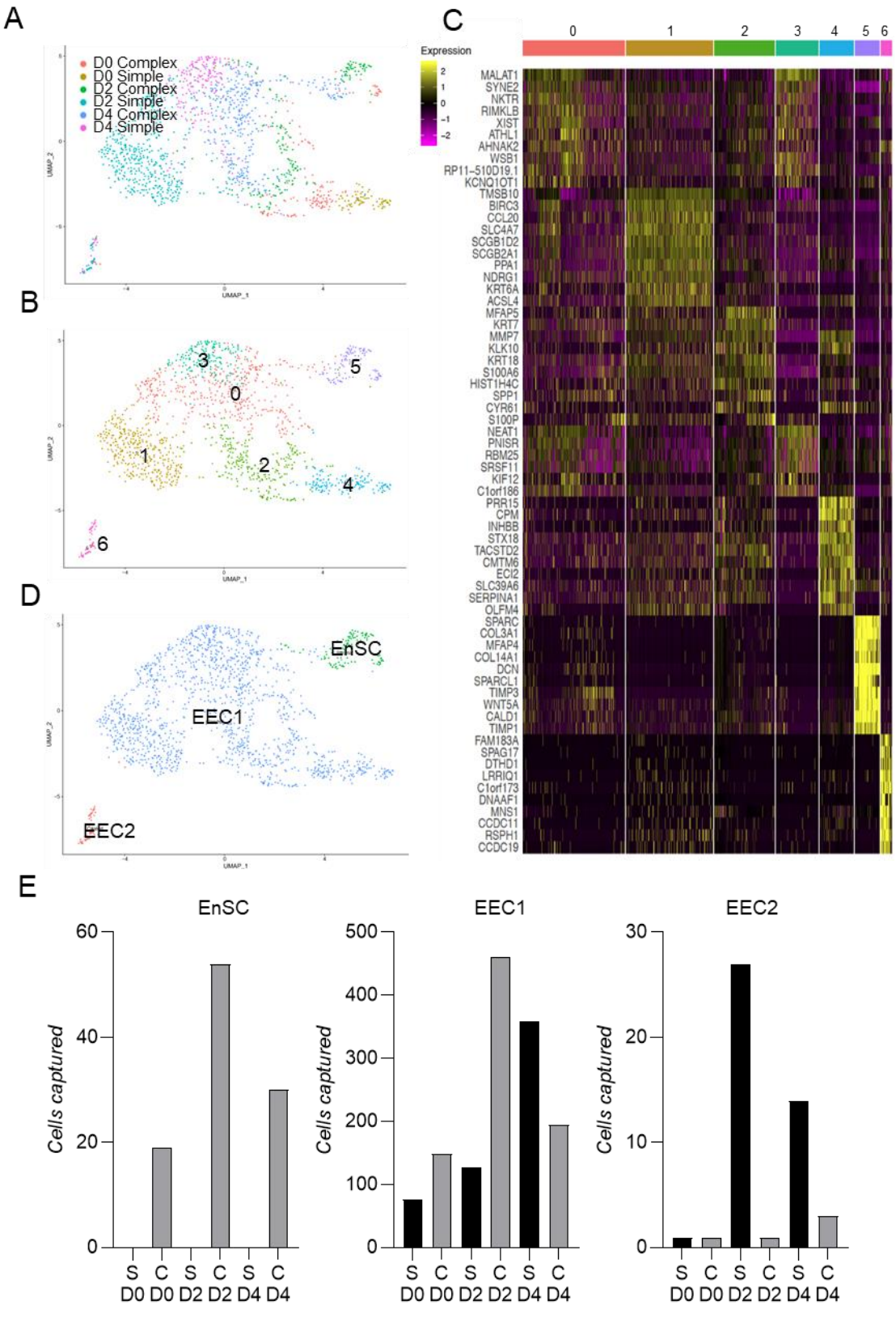

Figure 5.8: scRNA-seq cell type analysis of simple and complex organoids.

A: UMAP plot with cells colour-coded by sample, labelled by day and culture type after quality control analysis.

B: UMAP plot with cells colour-coded by transcriptional state.
C: A corresponding heat map of upregulated differentially expressed marker genes from the transcriptional states produced in the UMAP plot in panel B.
D: UMAP plot with cells colour-coded by cell type determined from heat map in panel C. Transcriptional states 0-4 represent EEC1 (non-ciliated EEC, ncEEC), transcriptional state 5 represents EnSC and transcriptional state 6 represents EEC2 (ciliated EEC, cEEC). Two EEC subpopulations were found (ncEEC and cEEC), as well as EnSC from complex organoid cultures.
E: The number of cells in each cell type state by sample sequenced.
All data collected and analysed in collaboration with Dr Emma Lucas and Dr Pavle Vrljicak. Panel A-D figures produced by Dr Pavle Vrljicak.

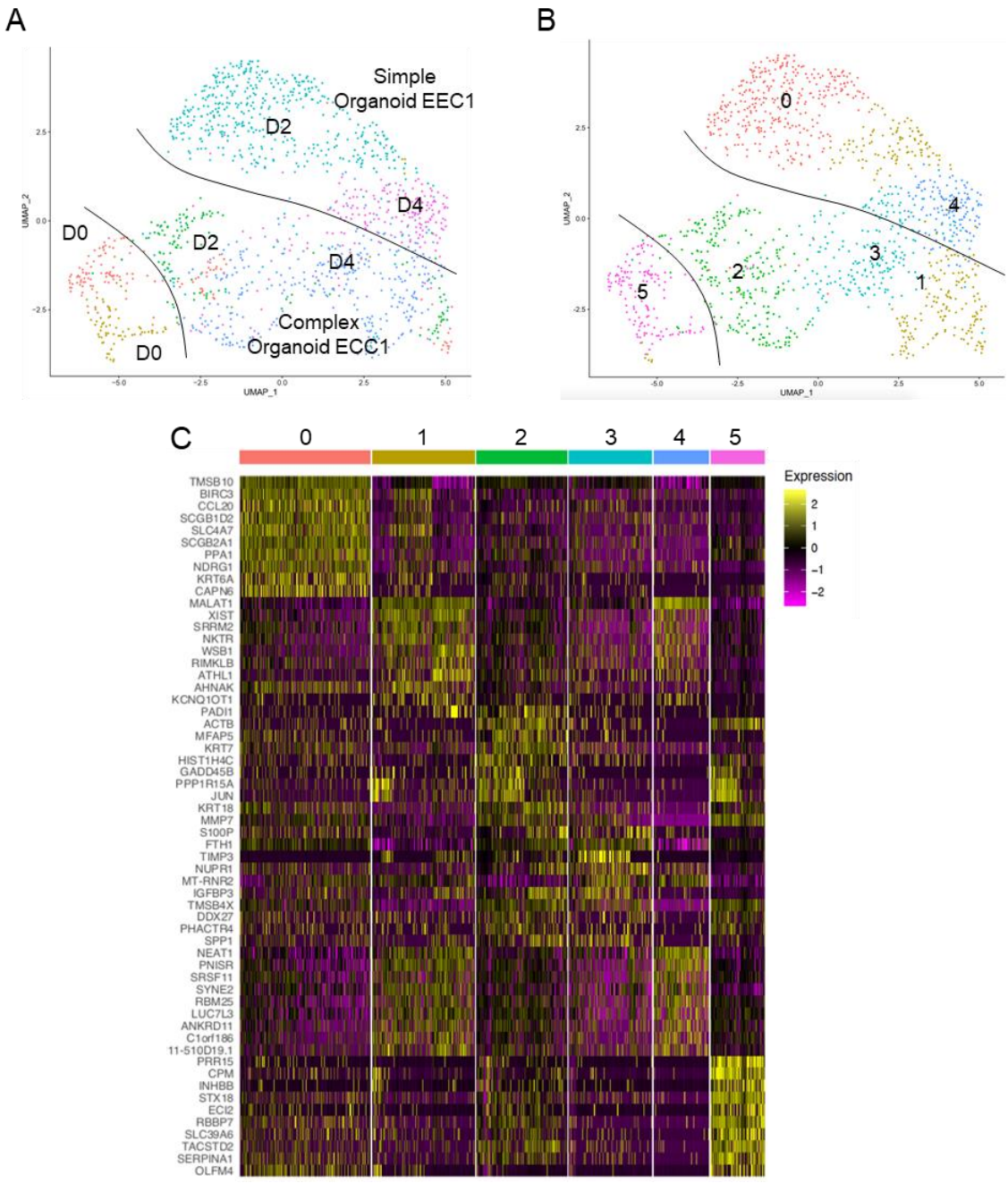

Figure 5.9: scRNA-seq analysis of ncEEC only in simple and complex organoids

A: UMAP plot with ncEEC in both simple and complex organoids colour-coded by sample, labelled by day and culture type.

B: UMAP plot with ncEEC in both simple and complex organoids colour-coded by transcriptional state.

C: A heat map of marker genes of transcriptional states of ncEEC in both simple and complex organoids.

All data collected and analysed in collaboration with Dr Emma Lucas and Dr Pavle Vrljicak. Panel figures produced by Dr Pavle Vrljicak.

from simple and complex organoids. Figure 5.9B is colour-coded by SNN cluster analysis labelling discrete transcriptional states. Both D0 samples of ncEEC from both simple and complex organoid clustered together in cluster 5, indicating their transcription profiles were not significantly different. However, the ncEEC D2 and D4 samples were divergent in simple and complex organoids, with cluster 2 representing the D2 complex organoid ncEEC and cluster 0 representing the D2 simple organoid ncEEC. D4 simple organoid ncEEC were contained largely in cluster 4. Genes in cluster 4, such as *LUC7L3*, *RBM25*, *ANKRD11* and *PNISR* do not change in expression over the menstrual cycle indicating these are not genes associated with differentiation (GEO Profiles, GDS2052). However, D4 complex organoid ncEEC were represented by two clusters: 3 and 1. Cluster 3 genes included classical endometrial gland differentiation genes *SPP1*, *IGFBP3* and *TIMP3* indicating this cluster represented differentiated EEC. However, cluster 1 also represented some of the D2 simple organoid ncEEC indicating there were some shared genes in between simple and complex organoid EEC such as *RIMKLB* and *AHNAK*, both induced in the secretory phase of the menstrual cycle (GEO Profiles, GDS2052). This suggested therefore there was some differentiation in the simple organoid cultures.

Further analysis was performed by comparing the most highly expressed genes in the complex organoid ncEEC at each time-point. First, as simple and complex organoid D0 ncEEC clustered together, the most highly expressed genes at D0 represented ncEEC in both simple and complex organoids (Fig. 5.10). Figure 5.10A is a heat map representing the most differentially expressed genes at D0 when compared to the other time points. These genes were compared to *in vivo* data from microarray data deposited in the Gene Expression Omnibus (GEO Profiles, GDS2052) to map the genes to the menstrual cycle (Fig. 5.10B). The genes at D0

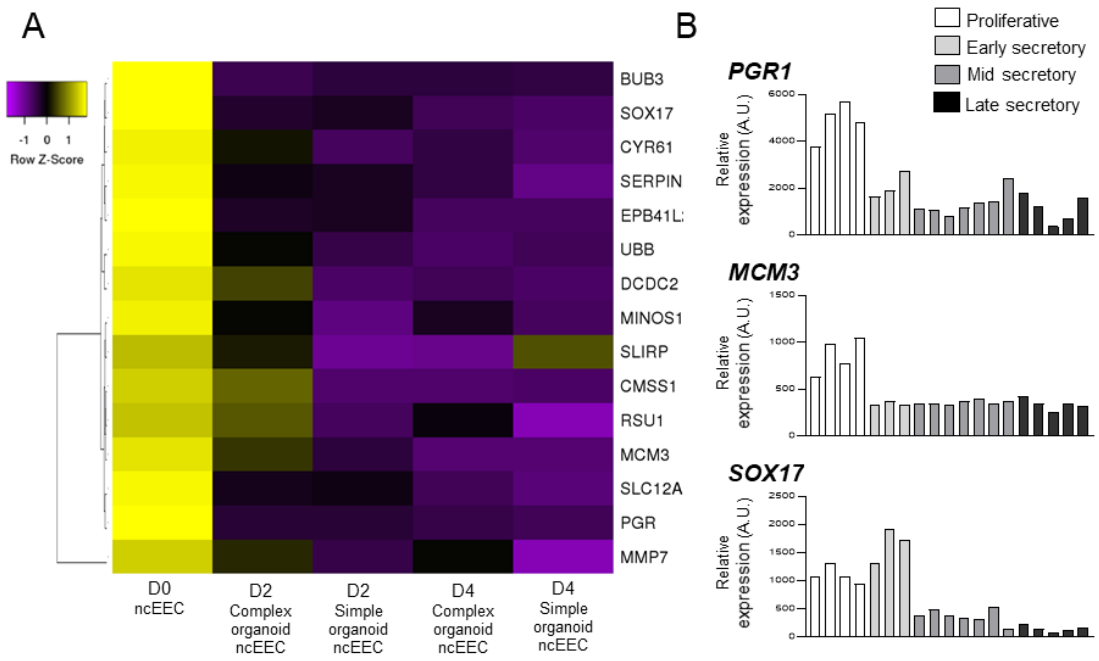

Figure 5.10: Analysis of the most differentially expressed genes in D0 organoid ncEEC.

A: A heat map of the most differentially expressed genes in D0 ncEEC compared to the other ncEEC samples in simple and complex organoids.

B: Expression of three representative expressed genes in D0 ncEEC across the menstrual cycle, across the proliferative phase and early, mid and late secretory phase as seen in colour key. Each bar represents relative expression data from an individual biopsy. PGR1 encodes progesterone receptor 1, *MCM3* encodes minichromosome maintenance complex component 3, and *SOX17* encodes SRY-Box Transcription Factor 17. The data were retrieved from microarray data deposited in the Gene Expression Omnibus (GEO Profiles, GDS2052).

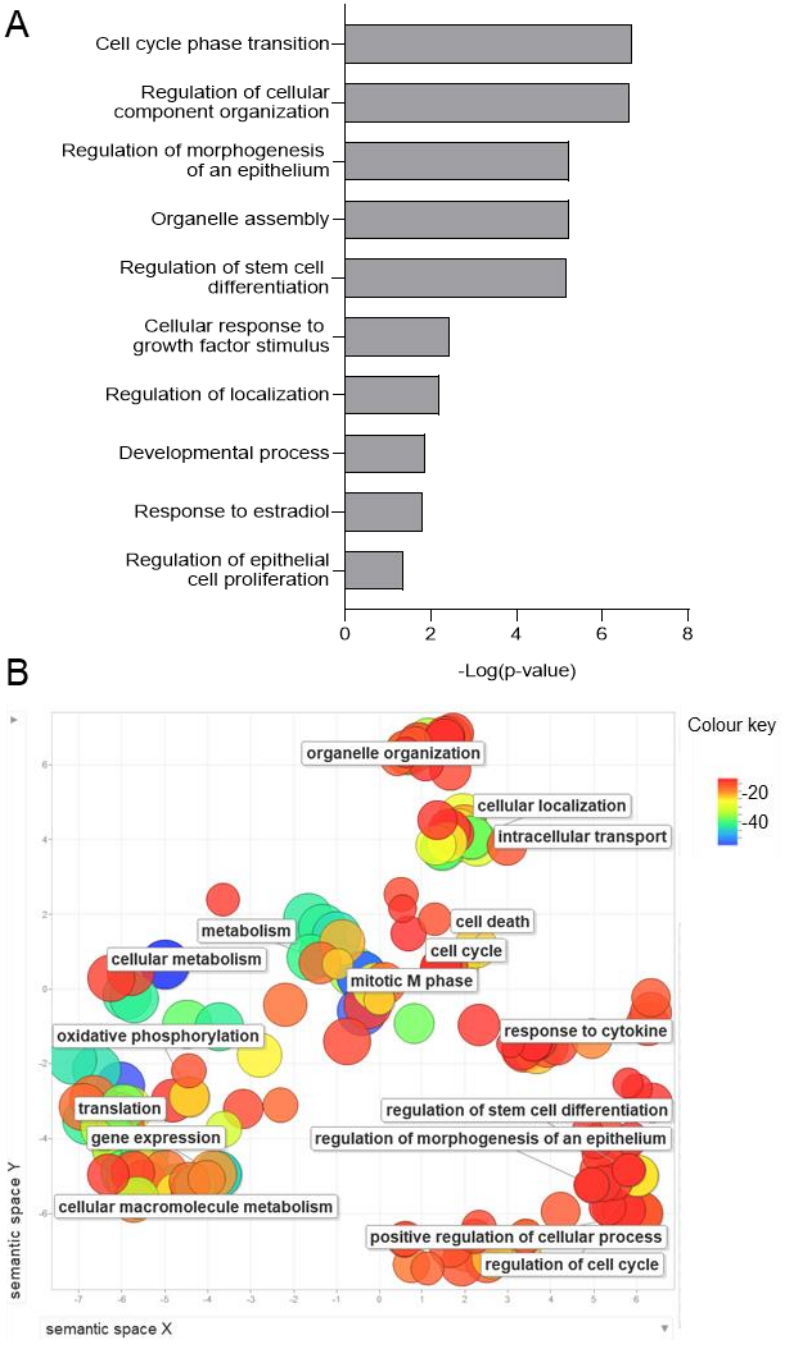

Figure 5.11: Gene ontology analysis of differentially expressed genes in D0 organoid ncEEC.

A: Significant GO terms (P < 0.05) of differentially upregulated genes in D0 organoid ncEEC using the Gene Ontology Consortium database.

B: REVIGO visualization of semantic clustering of significant GO terms (*P* < 0.05) of differentially upregulated genes in D0 organoid ncEEC. The colour of the circle indicates the log10 *P* value. Colour key is present on the right. Circle size is representative of the number of genes in each GO term.

were most highly expressed in proliferative phase transcription profiles. Gene ontology (GO) analysis using the Gene Ontology Consortium database (Ashburner et al., 2000, The Gene Ontology Consortium, 2018, Mi et al., 2013) was performed, where significantly differential genes ($P < 0.05$ with Bonferroni-correction) were clustered by annotated biological process categories (Fig 5.11A). The GO terms generated were further summarised using REVIGO, a web server that groups redundant GO terms by semantic similarity (Supek et al., 2011) (Figure 5.11B). Many of the statistically significant GO terms related to endometrial gland proliferation, such as 'response to estradiol', 'regulation of epithelial cell proliferation' and 'cell cycle phase transition'. Other GO terms involved stem cell differentiation, indicating that genes at D0 related to glandular development as seen in the expansion of the organoids.

The D2 ncEEC transcription profiles of simple and complex organoids diverged. Therefore, D2 complex organoid ncEEC were compared to D2 simple organoid ncEEC, and the most significantly expressed genes of the D2 complex organoid ncEEC compared to the other samples were plotted on a heat map (Fig. 5.12A). These genes mapped to the early secretory phase of the menstrual cycle when compared to *in vivo* data (GEO Profiles, GDS2052) (Fig 5.12B). GO analysis of these genes further demonstrated that the D2 co-culture organoid gland cells responded to the deciduogenic cues of the $DM_{min.}$ (Fig. 5.13A and 5.13B).

However, the differentiation gene signature was more pronounced at D4 in complex organoid ncEEC. D4 complex organoid ncEEC were compared to D4 simple organoid ncEEC and the most significantly expressed genes of the D4 complex organoid ncEEC are shown in a heatmap (Fig. 5.14A). These genes mapped to the mid- and late- secretory phase of the menstrual cycle when compared to *in vivo* data (GEO Profiles, GDS2052) (Fig 5.14B). For D4 complex organoid ncEEC, there was a clear

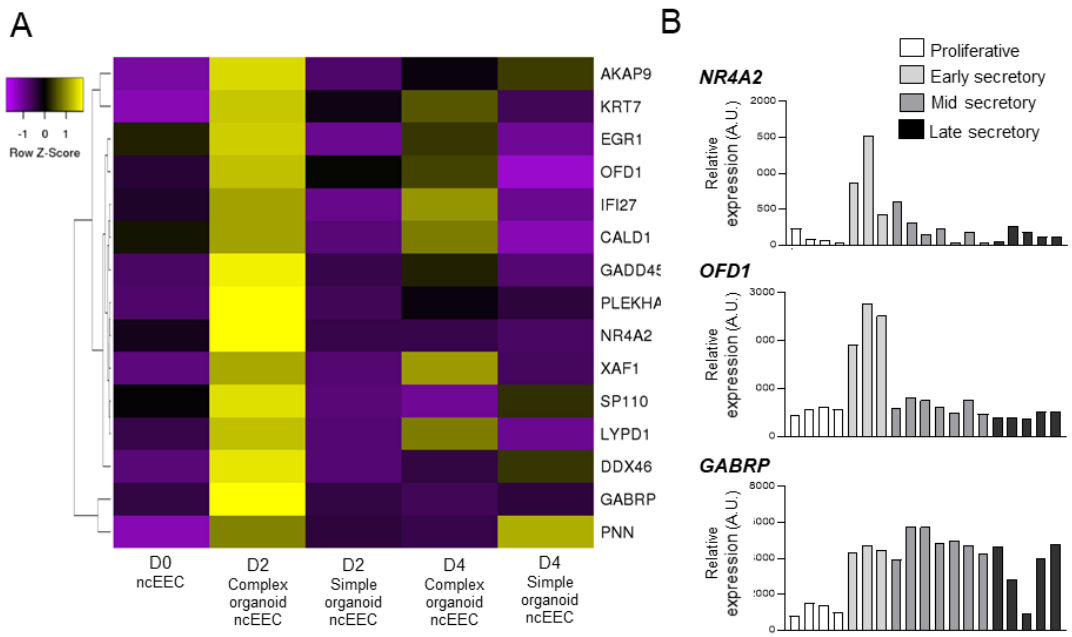

Figure 5.12: Analysis of the most differentially expressed genes in D2 complex organoid ncEEC when compared to simple organoids.

A: A heat map of the most differentially up-regulated genes in D2 complex organoid ncEEC compared to the other ncEEC samples in simple and complex organoids.

B: Expression of three representative up-regulated genes in D2 complex organoid ncEEC across the menstrual cycle, across the proliferative phase and early, mid and late secretory phase as seen in colour key. Each bar represents relative expression data from an individual biopsy. *NR4A2* encodes nuclear receptor related 1, *OFD1* encodes oral-facial-digital syndrome 1, and *GABRP* encodes gamma-aminobutyric acid receptor subunit pi. The data were retrieved from microarray data deposited in the Gene Expression Omnibus (GEO Profiles, GDS2052)

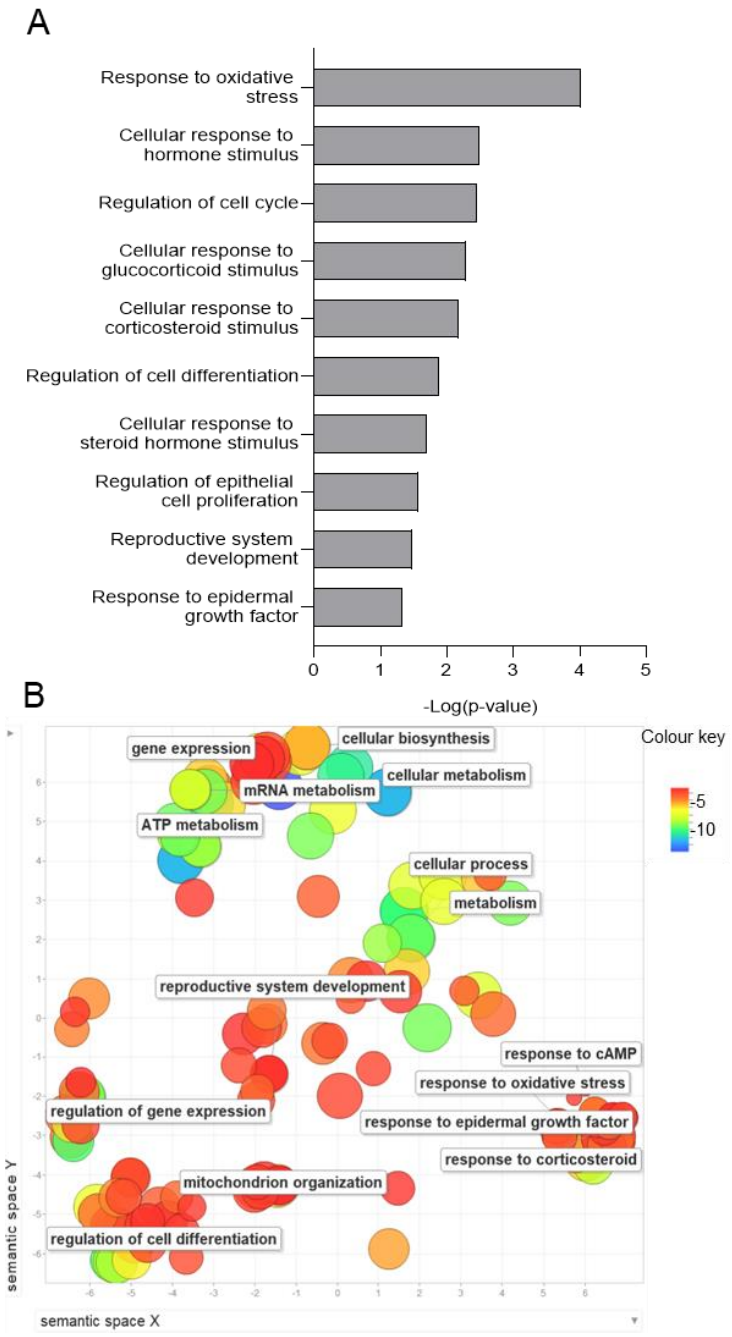

Figure 5.13: Gene ontology analysis of differentially expressed genes in D2 complex organoid ncEEC when compared to ncEEC in simple organoids.

A: Significant GO terms ($P < 0.05$) of differentially upregulated genes in D2 complex organoid ncEEC when compared to ncEEC in simple organoids using the Gene Ontology Consortium database.

B: REVIGO visualization of semantic clustering of significant GO terms ($P < 0.05$) of differentially upregulated genes in D2 complex organoid ncEEC when compared to ncEEC in simple organoids. The colour of the circle indicates the log10 *P* value. Colour key is present on the right. Circle size is representative of the number of genes in each GO term.

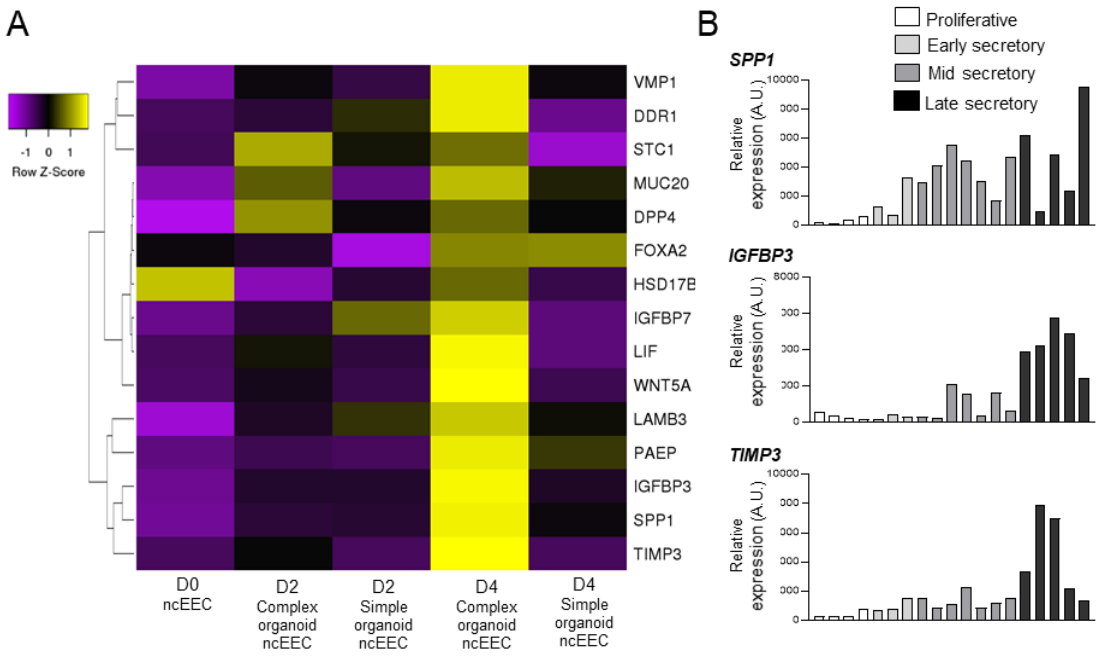

Figure 5.14: Analysis of the most differentially expressed genes in D4 complex organoid ncEEC when compared to ncEEC in simple organoids.

A: A heat map of the most differentially up-regulated genes in D4 complex organoid ncEEC compared to the other samples in simple and complex organoids.

B: Expression of three representative up-regulated genes in D4 complex organoid ncEEC across the menstrual cycle, across the proliferative phase and early, mid. and late secretory phase as seen in colour key. Each bar represents relative expression data from an individual biopsy. *SPP1* encodes osteopontin, *IGFBP3* encodes insulin like growth factor binding protein 3, and *TIMP3* encodes tissue inhibitor of metalloproteinase 3. The data were retrieved from microarray data deposited in the Gene Expression Omnibus (GEO Profiles, GDS2052)

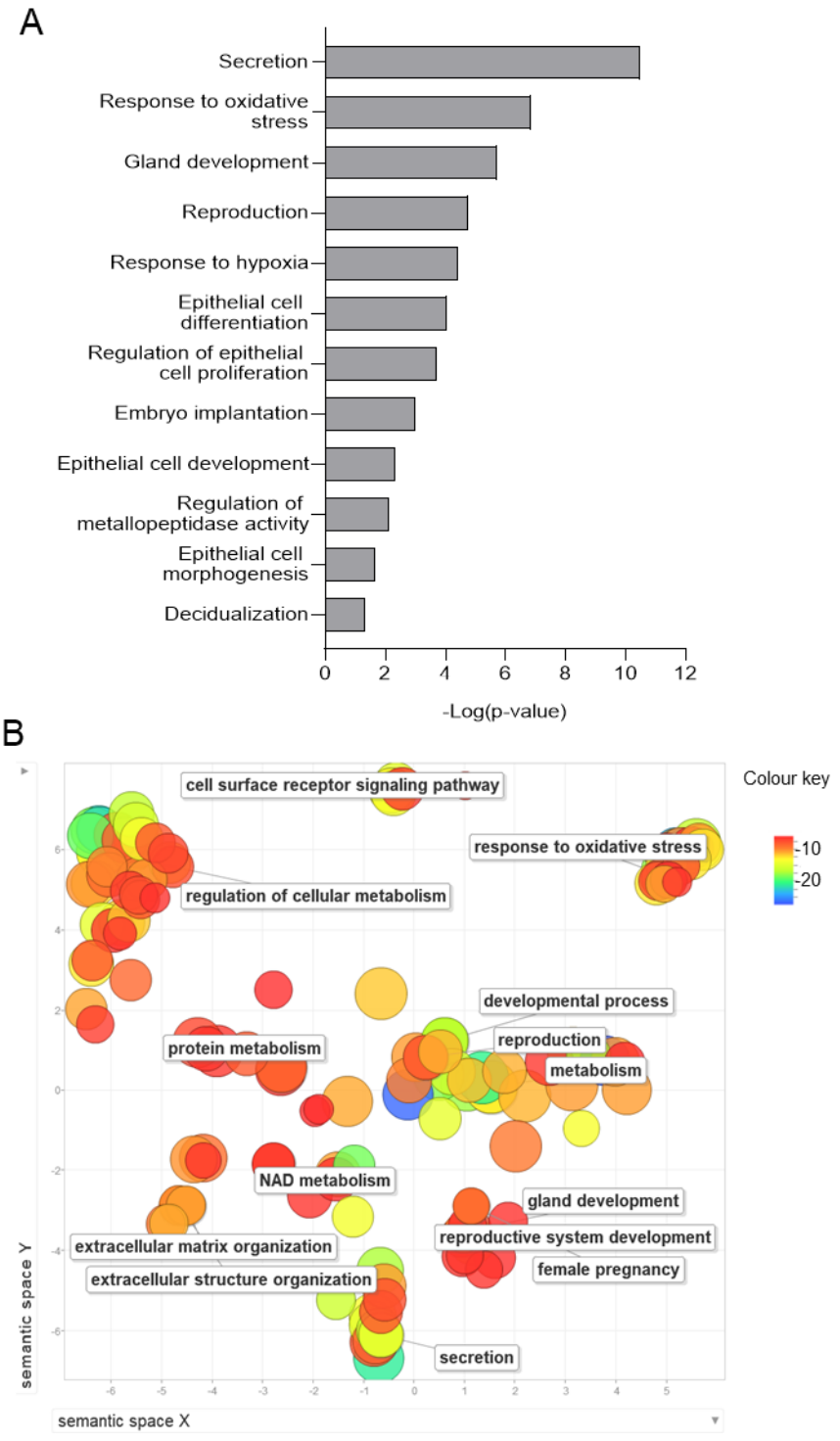

Figure 5.15: Gene ontology analysis of differentially expressed genes in D4 complex organoid ncEEC when compared to ncEEC in simple organoids.

A: Significant GO terms ($P < 0.05$) of differentially upregulated genes in D4 complex organoid ncEEC when compared to ncEEC in simple organoids using the Gene Ontology Consortium database.

B: REVIGO visualization of semantic clustering of significant GO terms ($P < 0.05$) of differentially upregulated genes in D4 complex organoid ncEEC when compared to

ncEEC in simple organoids. The colour of the circle indicates the log10 *P* value. Colour key is present on the right. Circle size is representative of the number of genes in each GO term.

secretory gene signature present, with genes such as *LIF*, *SPP1* and *DPP4* indicating that only the complex organoid derived ncEEC attained a secretory phenotype at 4 days of $DM_{min.}$ treatment. This is further demonstrated by the GO analysis, with terms such as 'embryo implantation' and 'decidualization' (Fig. 5.15). Taken together, the data indicates that the ncEEC were able to differentiate only in the presence of EnSC demonstrating the direct impact of decidualising EnSC on gland differentiation.

Finally, the EnSC were also analysed to confirm differentiation. Unfortunately, very few EnSC were sequenced from the complex organoid samples and therefore the UMAP and heatmap of marker genes for these cells were limited (Fig. 5.16). GO analysis was performed on the most significantly different, upregulated genes at each time point (Fig. 5.17). However, Bonferroni correction was not applied to the EnSC dataset for GO analysis as the correction was too stringent to produce any significant results, due to the low cell count. Hence, the data presented here can provide only a suggestion of the upregulated biological processes of each time point. The GO terms for D0 indicated the EnSC were proliferative (Fig. 5.17A). The GO terms for D2 suggested the EnSC had begun to differentiate following cell cycle arrest (Fig 5.17B) and the GO terms for D4 involved 'embryo implantation', 'secretion' and 'angiogenesis' regulation (Fig 5.17C). Therefore, this suggests that the EnSC differentiated over 4 days of $DM_{min.}$ treatment.

However, some highly expressed genes in EnSC at D4 (Fig 5.16B) such as *IL8*, *INHBA*, *FTH1* and *STC2*, are up-regulated in acute senescent decidual cells (Lucas et al., 2019), suggesting EnSC in the complex organoid culture were stressed or had senesced at 4 days of $DM_{min.}$ treatment. Overall, the data suggest the EnSC were responsive to $DM_{min.}$ treatment.

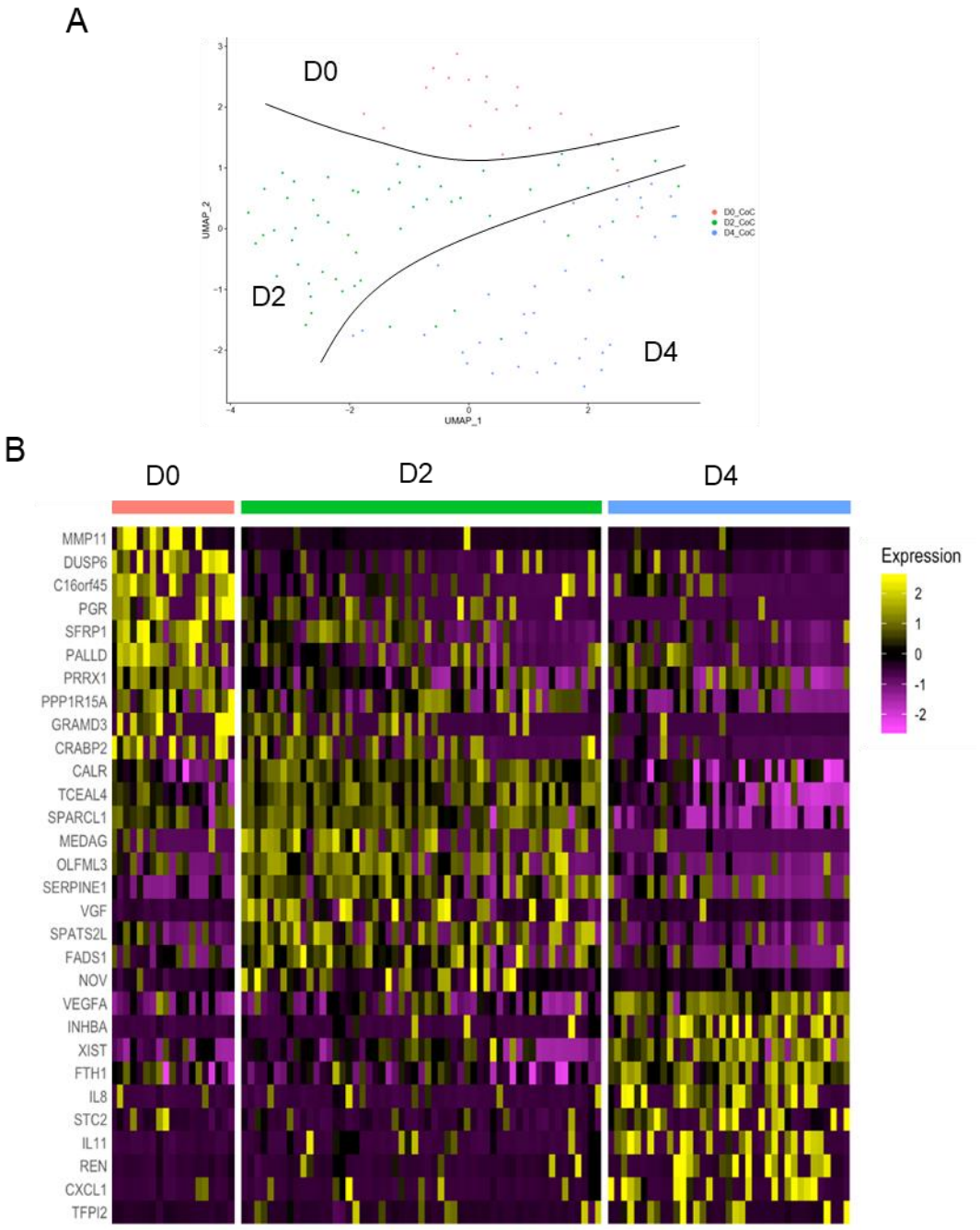

Figure 5.16: scRNA-seq analysis of EnSC only in complex organoids.

A: UMAP plot with EnSC colour-coded by complex organoid sample labelled by day. B A heat map of complex organoid EnSC marker genes per day of the decidual time course.

All panels produced in collaboration with Dr Emma Lucas and Dr Pavle Vrljicak. Panel figures produced by Dr Pavle Vrljicak.

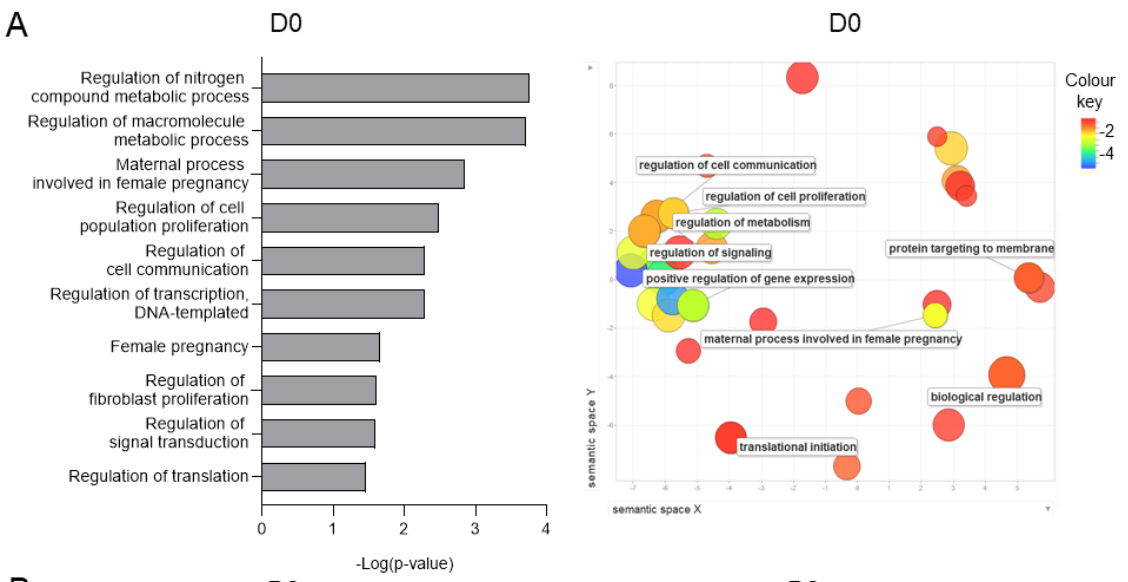
A
D0
Regulation of nitrogen compound metabolic process
Regulation of macromolecule metabolic process
Maternal process involved in female pregnancy
Regulation of cell population proliferation
Regulation of cell communication
Regulation of transcription, DNA-templated
Female pregnancy
Regulation of fibroblast proliferation
Regulation of signal transduction
Regulation of translation
0
1
2
3
4
-Log(p-value)
D0
Colour key
-2
-4
regulation of cell communication
regulation of cell proliferation
regulation of metabolism
regulation of signaling
positive regulation of gene expression
protein targeting to membrane
maternal process involved in female pregnancy
biological regulation
translational initiation
semantic space Y
semantic space X

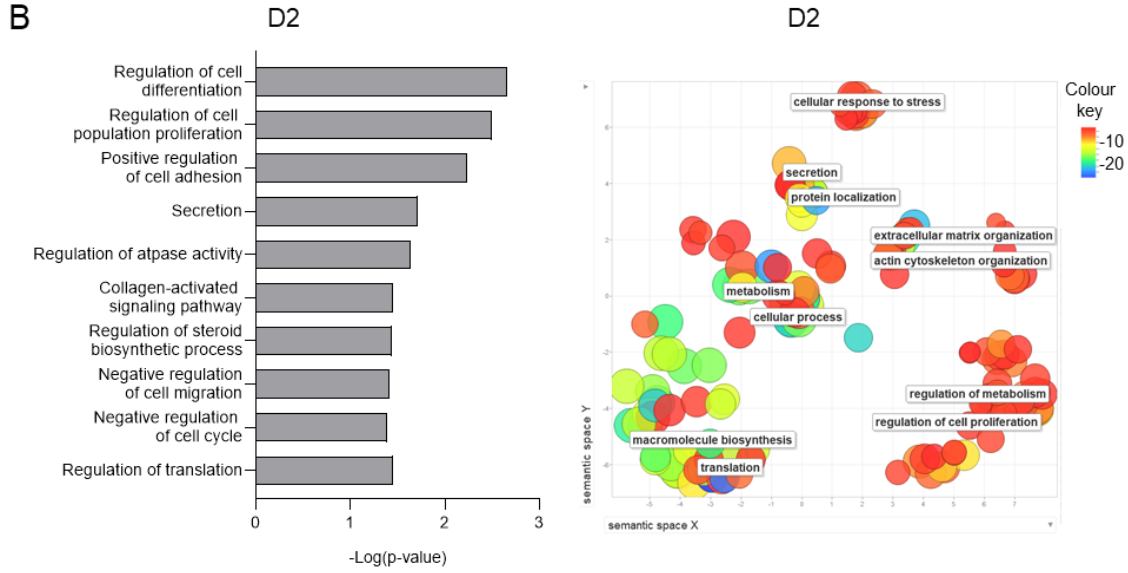
B
D2
Regulation of cell differentiation
Regulation of cell population proliferation
Positive regulation of cell adhesion
Secretion
Regulation of atpase activity
Collagen-activated signaling pathway
Regulation of steroid biosynthetic process
Negative regulation of cell migration
Negative regulation of cell cycle
Regulation of translation
0
1
2
3
-Log(p-value)
D2
Colour key
-10
-20
cellular response to stress
secretion
protein localization
extracellular matrix organization
actin cytoskeleton organization
metabolism
cellular process
regulation of metabolism
regulation of cell proliferation
macromolecule biosynthesis
translation
semantic space Y
semantic space X

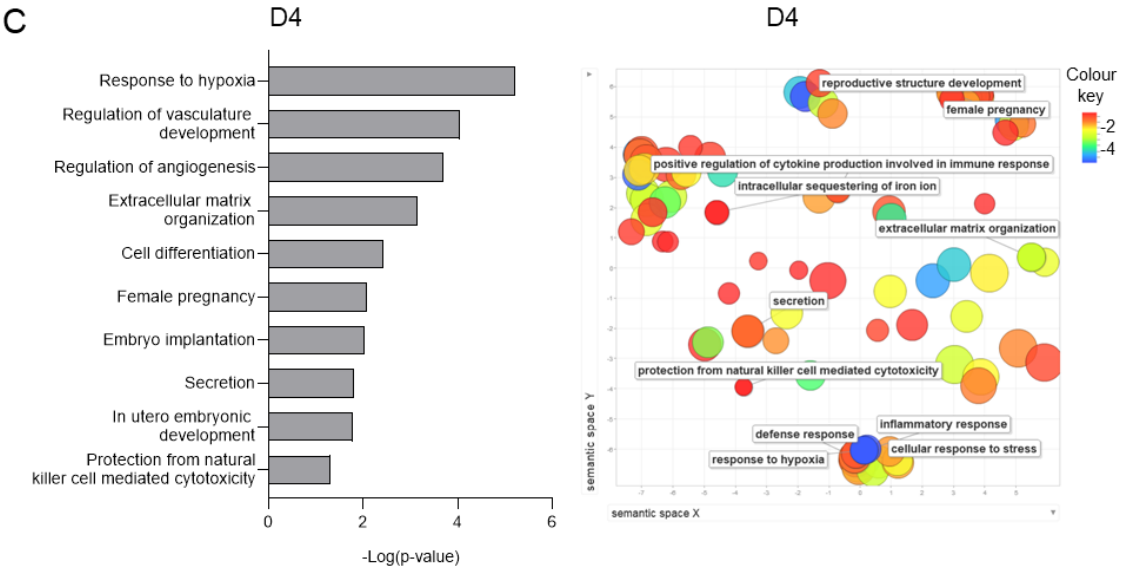
C
D4
Response to hypoxia
Regulation of vasculature development
Regulation of angiogenesis
Extracellular matrix organization
Cell differentiation
Female pregnancy
Embryo implantation
Secretion
In utero embryonic development
Protection from natural killer cell mediated cytotoxicity
0
2
4
6
-Log(p-value)
D4
Colour key
-2
-4
reproductive structure development
female pregnancy
positive regulation of cytokine production involved in immune response
intracellular sequestering of iron ion
extracellular matrix organization
secretion
protection from natural killer cell mediated cytotoxicity
inflammatory response
defense response
cellular response to stress
response to hypoxia
semantic space Y
semantic space X

Figure 5.17: Gene ontology analysis of differentially expressed genes in EnSC in complex organoids across the four-day decidual time course.

A: Left: Significant GO terms ($P < 0.05$) of differentially expressed genes in D0 complex organoid EnSC using the Gene Ontology Consortium database. Right: REVIGO visualization of semantic clustering of significant GO terms ($P < 0.05$) of differentially upregulated genes in D0 complex organoid EnSC. The colour of the circle indicates the log10 *P* value. Colour key is present on the right. Circle size is representative of the number of genes in each GO term.

B: Left: Significant GO terms ($P < 0.05$) of differentially expressed genes in D2 complex organoid EnSC using the Gene Ontology Consortium database. Right: REVIGO visualization of semantic clustering of significant GO terms ($P < 0.05$) of differentially upregulated genes in D2 complex organoid EnSC. The colour of the circle indicates the log10 *P* value. Colour key is present on the right. Circle size is representative of the number of genes in each GO term.

C: Left: Significant GO terms ($P < 0.05$) of differentially expressed genes in D4 complex organoid EnSC using the Gene Ontology Consortium database. Right: REVIGO visualization of semantic clustering of significant GO terms ($P < 0.05$) of differentially upregulated genes in D4 complex organoid EnSC. The colour of the circle indicates the log10 *P* value. Colour key is present on the right. Circle size is representative of the number of genes in each GO term.

5.3 Discussion

Investigating the EnSC-EEC interactions in complex organoid culture.

In this study, I investigated and optimised the culture conditions to enable EnSC-EEC interactions in complex organoids. First, each component of the medium was removed systematically to determine if any singular component had a major effect on organoid differentiation. RT-qPCR analysis demonstrated that the simple organoids expressed higher levels of differentiation genes *PAEP* and *SPP1* than in complex organoids. However, this is possibly due to housekeeping gene used as an internal control to normalise the data. A housekeeping gene is a gene that should maintain constant expression in all cells and experimental conditions which allows direct comparison of genes of interest between different samples (Thellin et al., 1999, Robinson and Oshlack, 2010). In this study, all RT-qPCR data were normalised by *L19*, that encodes ribosomal protein 60S L19, which is ubiquitously expressed in all cell types of the endometrium (Ayakannu et al., 2015).

This is problematic because in this present study I compared simple and complex organoids for expression of EEC-specific differentiation genes. In simple organoid cultures, the total RNA would originate from EEC only; however, in complex organoid cultures, the total RNA harvested would originate from both EEC and EnSC, diluting the number of EEC RNA molecules in the samples. This dilution would lead to lower amplification of EEC genes and a lower CT value. However, *L19* would not be diluted as it is expressed in both cell types, and therefore when normalising the diluted EEC gene expression data to *L19*, the perceived relative expression would be lower than expected. This dilution effect is less apparent in *CXCL14* likely because it is also expressed in the EnSC (See Chapter 4). Moreover, as *L19* encodes a ribosomal protein, and the relative level of expression may differ between cell types depending on their protein synthesis requirements. Overall, it is difficult to interpret the data from

this experiment as it is unclear if the normalisation process had a confounding effect on the data presented. Future work should be to develop cell type-specific housekeeping genes to circumnavigate the issue of comparing normalised RT-qPCR data from both simple and complex organoid cultures.

In the opposite experiment, all ExM factors were removed and then added back systematically one factor at a time. The complex organoids attained higher expression of the differentiation genes than simple organoid cultures in some DM formulations, even after *L19* normalisation. This indicates the inductions may well have been higher than reported in this study. The minimal differentiation medium chosen contained no growth factors or inhibitors other than NAC (N-acetyl-L-cysteine). The presence of NAC had the most significant induction of differentiation genes in complex organoids when compared to the matched simple organoid cultures. This indicated that DM with NAC and EnSC together were sufficient to induce organoid differentiation, but not in the absence of EnSC. Furthermore, the expression of *PRL* was highest from EnSC differentiated in this medium.

NAC is a prodrug for L-cysteine, which can be metabolised into glutathione, an antioxidant that has thiol groups that bind free radicals (Terada, 2006, Zafarullah et al., 2003, Circu and Aw, 2008). Free radicals are reactive molecules possessing unpaired electrons, such as reactive oxygen species (ROS). An imbalance in ROS leads to oxidative stress in cells, which can lead to cellular damage, such as DNA strand breaks and mutations, leading to apoptosis (Ott et al., 2007, Ozben, 2007). However, in EnSC, it has been previously demonstrated that rising cellular cAMP levels induces a burst of endogenous ROS through NADPH oxidase (NOX)-4. This burst of endogenous NOX-4-dependent ROS products during the initial decidual phase has been shown to be essential for subsequent differentiation of EnSC into stress resistant decidual cells (Al-Sabbagh et al., 2011). Decidual cells also confer

resistance to oxidative cell death upon decidualisation (Kajihara et al., 2006). Hence, it is unclear why using an antioxidant would not only improve EEC differentiation in complex organoid culture but also not inhibit EnSC decidualisation. However, it could possibly be required to maintain homeostasis during this period of high oxidative stress, protecting both EEC and EnSC from damage. In addition to NAC, the DM supplemented with HGF was also a valid potential candidate for the minimal differentiation medium. However it was less significant than the DM containing NAC, and EnSC produce HGF endogenously (Sugawara et al., 1997) and therefore HGF was discounted and DM supplemented with NAC was chosen for the DM_{min}.

ScRNA-seq of decidualised simple and complex organoid cultures.

Using the established $DM_{min.}$, high-throughput scRNA-seq was performed on patient-matched simple and complex organoid cultures in order to further characterise EnSC regulation of EEC differentiation observed in the preliminary RT-qPCR data. The scRNA-seq data demonstrated the divergent response in EEC from simple or complex organoid cultures to DM_{min}, as illustrated by the segregation in clustering in the UMAP single cell aggregation analysis. Divergence between simple and complex organoids was conspicuous on day 4. Several canonical differentiation genes, including *PAEP*, *DPP4* and *HSD17B2* were the most significantly different upregulated genes in EEC from complex organoids when compared to simple organoids. Furthermore, decidualising complex organoids expressed genes strongly implicated in embryo implantation, including *LIF* and *SPP1* (Aghajanova, 2004, Salleh and Giribabu, 2014, von Wolff et al., 2001) suggesting that D4 complex organoids were in a secretory state. These findings hold promise of the complex organoid system becoming a novel patient specific *in vitro* model for human embryo implantation studies.

However, the scRNA-seq data also revealed that EEC of simple and complex organoid cultures at D0 are transcriptionally similar with a gene signature mapped to the proliferative phase *in vivo*. For example, *PGR1*, encoding the progesterone receptor, is known to be downregulated when exposed to progesterone, and is highly expressed in the proliferative phase (Mote et al., 1999, Mangal et al., 1997, Kaya et al., 2015). The similarity of gene expression indicates that EnSC do not have a significant effect on proliferating EEC, at least not in co-ExM. This is likely due to co-ExM containing growth factors and inhibitors which promote organoid growth, regardless of EnSC intervention. Future work could investigate the EnSC regulation of gland organoid expansion as previous literature has shown that stromal induced gland development occurs *in vivo (Cooke et al., 1986, Cunha et al., 1985)*.

Recently, scRNA-seq performed on endometrial gland organoids has been published (Fitzgerald et al., 2019). In this study, the endometrial gland organoids were grown and differentiated in 'organoid medium', containing the same components as ExM (Turco et al., 2017). The organoids were expanded for 4 days without E2, then primed in E2 for 2 days prior to differentiation by E2 and MPA and cAMP for a further 6 days. Despite the differences in protocol, upon differentiation, this group yielded similar observations with the induction of gland differentiation genes *HSD17B2, LIF, PAEP, and SPP1 (Fitzgerald et al., 2019)*. This substantiates that replacing ExM with EnSC induces a comparable differentiation response in endometrial gland organoids.

However, Fitzgerald, et al., were able to identify 6 organoid cell types (ciliated, epithelial, secretory, proliferative, stem, and unciliated) in comparison to the 2 presented in this study (ncEEC, cEEC) (Fitzgerald et al., 2019). In addition, the group performed ligand-receptor prediction and analysis on the scRNA-seq data, in which they predicted EnSC receptors, which could have been confirmed by the data presented in this study. Unfortunately, the number of cells sequenced in this study

were much lower than expected. This therefore reduced the information available in this data set. This was particularly impactful on the analysis of the EnSC and cEEC of the organoids. This was unexpected as the proportion of EnSC and EEC were equal at the time of plating. Despite the low numbers, some analysis was performed on the EnSC and the GO analysis suggested that the EnSC decidualised by D4. However, due to low cell numbers, GO terms were presented using unadjusted p-values (without Bonferroni correction) to give only a preliminary indication of the biological processes occurring at each time point. Therefore, it is essential to repeat this experiment to ensure that more EnSC are sequenced.

The reason for the low recovery of EnSC in the scRNA-seq analysis could have been due to several reasons. The first reason is that there was an issue in the protocol. For example, the single cell digestion protocol may have favoured the digestion of the EEC over the EnSC. At the point of harvest, both cell types were visibly abundant by microscopy. The digestion protocol could be further optimised to ensure both cell types are harvested. For example, the proportion of EEC and EnSC in the single cell suspension could be determined by staining to ensure good recovery of both cell types.

However, it has been recently reported that during decidualisation, EnSC diverge into two sub-populations: acutely senescent decidual cells and decidual cells. Senescent cells can induce neighbouring decidual cells to senesce in a phenomenon called bystander senescence (Brighton et al., 2017, Lucas et al., 2018, Tewary et al., 2019, Nelson et al., 2012), which increases the proportion of these cells through the secretory phase. However, an influx of uNK cells clears the acute senescent cells *in vivo* (Brighton et al., 2017). In this complex organoid system, there is currently no senescent cell clearance system in place and therefore this could also explain their accumulation. Future experiments should focus on reducing the senescent cell

population in the complex organoid co-culture to mimic the *in vivo* environment. This could be achieved by senolytic small molecules such as dasatinib (Brighton et al., 2017, Childs et al., 2017, Zhu et al., 2015) or by introducing uNK cells into the complex organoid system.

Conclusion

In conclusion, in this study I have demonstrated that in a complex organoid system, decidualising EnSC can replace ExM in culture and induce EEC differentiation. The use of the $DM_{min.}$ and EnSC instead of the artificial environment produced by $DM_{std.}$ presents an improved, more physiological complex organoid system in which the two cell types are able to directly impact upon and influence each other, instead of being dependent on a complex medium. Therefore, in the future, this model could be used to functionally study EnSC-EEC interactions in endometrial physiology, human embryo implantation, and implantation pathologies. Complex organoids grown from biopsies of patients suffering from RPL could be compared to control patients to determine aberrations in endometrial stromal-gland interactions. Furthermore, the observations presented in this study provide evidence that cross-over experiments could bring useful insight into endometrial pathology. However. The data of the initial scRNA-seq analysis should be considered as preliminary and repeat experiments are warranted for the reasons discussed.

Chapter 6:
General Discussion

6. General Discussion

Introduction

Human embryo implantation is the rate limiting step in ART with only 25% of embryo transfers implanting successfully (Boomsma et al., 2009, Edwards, 2006, Ferraretti et al., 2012). Lack of endometrial bio-sensing of pre-implantation embryos is thought to be a cause of RPL (Quenby et al., 2002, Teklenburg et al., 2010a, Lucas et al., 2013, Lucas et al., 2016). Elucidating the mechanisms underpinning the peri-implantation endometrium would engender the discovery of novel treatments to inhibit inappropriate endometrial responses. However, human embryo implantation is exceptionally difficult to study. Animal models have been utilised, but most readily accessible animal models do not fully recapitulate human implantation physiology (Lee and DeMayo, 2004).

An alternative approach uses primary endometrial cells from biopsies, sidestepping the issue of inter-species variability. *In vitro* models have vastly developed over the years from simple 2D monolayers through to 3D layered co-culture approaches, to most recently the endometrial gland organoids (Weimar et al., 2013, Deane et al., 2017). The endometrium is a complex tissue made up of EnSC, epithelial glands, as well as a vasculature and a resident immune cell population including uNK cells. Hence, a complex co-culture system is required to closely recapitulate the *in vivo* human peri-implantation endometrium (Weimar et al., 2013). Furthermore, the endometrial gland organoids have enabled the modelling of endometrial glandular epithelium, an essential component of the peri-implantation endometrium and in embryo implantation (Turco et al., 2017, Boretto et al., 2017). Therefore, the next logical step is to develop a complex organoid-based co-culture system to improve upon previous *in vitro* models.

In this thesis, I aimed to develop a novel 3D *in vitro* model of the human endometrium to study the peri-implantation environment for embryo implantation by co-culturing EnSC and EEC. Here, two strategies were attempted:

1. The first strategy was to use the tissue-like MSC-derived ERB model. The initial conclusions were found to be erroneous upon further investigation. However, the renamed EFAM did provide insight into EFA and the silencing of the ROCK pathway upon decidualisation.
2. The second strategy was to establish a protocol for co-culturing endometrial gland organoids with EnSC. This strategy was successful, and I established and optimised a working protocol for a complex organoid culture consisting of EnSC and EEC.
3. Following this, the impact of the EnSC on the endometrial glands was investigated. I confirmed that the EnSC could replace $DM_{std.}$ to induce EEC differentiation. This was achieved by optimising a $DM_{min.}$ and performing scRNA-seq on matched simple and complex organoid cultures. Thus, these experiments demonstrated that EnSC interact with the gland organoid EEC in complex organoid culture.

The first strategy: ERB and EFAM

MSC reside in the perivasculature of the endometrium (Gargett, 2006, Gargett et al., 2015). In culture, PVC can be isolated from an endometrial biopsy by separation techniques such as MACS, followed by a CFU assay to enrich for the clonal MSC (Sivasubramaniyan et al., 2013, Masuda et al., 2012). MSC have been demonstrated to have high regenerative potential and are the drivers of endometrial regrowth following menses (Gargett, 2006, Gargett et al., 2015).

When seeded on Matrigel and cultured overnight, MSC formed a tissue-like mass the next day. It was erroneously assumed that this was endometrial regeneration enacted

by the MSC (Peter Durairaj, 2017). However, when cultured for more than 24 hours, I observed further contraction of the ERB. Therefore, I performed further time-lapse microscopy studies and hypothesised that ERB were formed by cellular contraction through fibroblast activation, not by stem cell-related tissue regeneration. Further *in silico* analyses of *in vivo* scRNA-seq in parallel with *in vitro* experimentation confirmed that the ROCK pathway and cell-matrix adhesions are implicated in the observed contraction of the EnSC (Lucas et al., 2018). Therefore, the ERB was renamed to EFAM. However, pre-decidualising EnSC for 4 days prior to performing the EFAM protocol abrogated contraction. Data mining of the scRNA-seq dataset revealed that the ROCK pathway is silenced upon decidualisation, therefore explaining the incapacitated activation when challenged with Matrigel. Furthermore, the inhibition of FAK by Y15 inhibited contraction. Overall, in this study I have described multiple mechanisms that disable EFA upon decidualisation: upstream mechanosensing, ROCK signalling and downstream contractile machinery.

Despite this model not working for the purpose intended, the implication of these observations was important for my *in vitro* model development. Studies have indicated that the contractile phenotype is due to the relative stiffness of Matrigel, which causes activation of fibroblastic cells (Balestrini et al., 2012, Heck et al., 2012, Lo et al., 2000). Matrigel is a BM-derived hydrogel and therefore is much denser than the physiological ECM (Kleinman and Martin, 2005, Iwahashi et al., 1997). Collagen hydrogels have been used previously in EnSC 3D culture (Bentin-Ley et al., 1994). Therefore, I hypothesised that other gels, such as collagen hydrogels, would be more compatible with the *in vivo* human stromal ECM and thus not induce EFA.

However, the EFAM may be useful for modelling other aspects of endometrial biology. Endometriosis is a disorder characterised by the seeding of endometrial cells in the peritoneal cavity. These can develop into painful fibrotic lesions. Previous studies

have suggested that retrograde breakthrough bleeding before adolescence is a potential source of endometrial cell seeding in the peritoneum (Brosens et al., 2013b, Brosens et al., 2013a, Brosens and Benagiano, 2016, Brosens et al., 2016, Gargett et al., 2014). Therefore, as these cells are undecidualised, it could be speculated that these cells are more likely to form a lesion as they maintain their potential for EFA. EFA is characterised by a wound healing response of depositing ECM, which if left unresolved leads to fibrosis (Kalluri, 2016). Further studies using this model to elucidate the lesion formation in endometriosis could lead to better understanding the disease.

The second strategy: co-culturing endometrial gland organoids with EnSC

The failure of the ERB necessitated a different approach. Fortuitously, a protocol for endometrial gland organoids was published at this time and therefore I decided to explore this as a different avenue for 3D endometrial modelling (Boretto et al., 2017, Turco et al., 2017). However, co-culturing gland organoids with EnSC to form complex organoids required the system to be optimised to benefit both cell populations at the same time. This involved investigating the hydrogel and medium composition to support optimal growth of both cell types.

The first issue was to optimise the hydrogel composition as the organoids had been established in Matrigel. Matrigel contains proteins such as laminins, entactin and collagen IV, all of which are major constituents of the BM (Aplin et al., 1988, Timpl, 1996, Wewer et al., 1986, Yelian et al., 1993). Therefore, Matrigel was not a suitable ECM substitute for the in *vivo* endometrial stroma, as this instead largely consists of collagens type I, III and V (Aplin et al., 1988, Aplin and Jones, 1989, Iwahashi et al., 1996). Therefore, a purified type I collagen hydrogel was considered as an alternative to Matrigel. This collagen hydrogel was chosen because collagen type I is the most abundant collagen in the endometrial stromal ECM (Iwahashi et al., 1996, Aplin et al.,

1988, Aplin and Jones, 1989). Additionally, previous literature had indicated that a collagen type I hydrogel was suitable for 3D EnSC culture *in vitro* (Bentin-Ley et al., 1994).

In the present study, when grown in the collagen hydrogel, EFA was abolished, and the EnSC appeared to form a well distributed matrix. In addition, the epithelial gland organoids were able to form in collagen hydrogel in complex organoid culture, suggesting that the missing BM proteins in the purified collagen hydrogel were secreted by the cells in culture. This was evidenced by the IHC immunostaining produced demonstrating laminin localised basally to the organoid EEC in both undifferentiated and decidualising complex organoid cultures, and around decidualising EnSC following treatment with DM. These observations are representative of the *in vivo* laminin distribution through the menstrual cycle (Aplin et al., 1995, Church et al., 1996) indicating the complex organoids were able to recapitulate ECM remodelling *in vitro*. Overall, the improved EnSC morphology in collagen hydrogel is likely due to the hydrogel being a more physiological model of the stromal ECM, therefore providing it the appropriate matrix for growth and differentiation.

However, the purified collagen hydrogel remains a basic approach to establishing complex endometrial organoids. Many studies have focused producing more complex ECM hydrogels by developing using tissue-specific ECM (Skardal et al., 2012, Bryant et al., 2005, Chan and Leong, 2008, Wolf et al., 2012). Tissue specific gels are believed to recapitulate the extracellular environment better than standard hydrogels. The hydrogel used for complex organoid culture was made of purified collagen I, which although is a major constituent of the endometrial ECM, it is not the only component (Iwahashi et al., 1997, Aplin et al., 1988, Aplin and Jones, 1989). Other collagens such as collagen III and VI are present in the endometrium throughout the

menstrual cycle, as well as many other ECM proteins and constituents. Therefore, porcine-extracted tissue, such as endometrium, has been utilised to make novel hydrogels (unpublished work, Prof. Molly Stevens group, Imperial College London). In collaboration, simple endometrial gland organoid cultures have been successfully grown in porcine endometrial ECM hydrogels. To produce a porcine endometrial hydrogel, the tissue is extracted and decellularized, lyophilised, and then reconstituted as a gel for 3D culture. However, to develop a defined tissue specific hydrogel, the protein composition of these gels needs to be characterised and quantified by proteomic analysis.

The second issue to be resolved was the medium. ExM is a highly complex medium established for endometrial gland organoid expansion (Turco et al., 2017). This medium does not contain E2 or serum, which are both routinely added to EnSC culture medium (Barros et al., 2016). Therefore, the discrepancy in media conditions needed to be ameliorated. Investigation of the medium concluded that E2 was essential for EnSC proliferation in complex organoids. The 1 nM concentration of E2 was chosen as it is standard in many previous EnSC culture studies (Lucas et al., 2016, Lucas et al., 2019, Murakami et al., 2013, Muter et al., 2015, Muter et al., 2016). However, proliferation may be improved by an increase in the E2 concentration to 10 nM as used in other studies (Greaves et al., 2015). However, additional serum replacement supplements were unnecessary. ExM does contain some serum replacing components such as N2 and B27, possibly providing the growth support required for both organoids and EnSC (Brewer et al., 1993).

In this study, I have resolved two key issues for optimising complex endometrial organoids. These complex organoids were then morphologically examined and functionally tested to determine if they can serve as a suitable model of the human peri-implantation endometrium. Morphologically, the complex organoids were similar

to the *in vivo* endometrium. The complex endometrial organoids present a step forward in modelling the peri-implantation human endometrium.

Mapping stromal-gland interactions using the complex organoids

As I had formed a functioning 3D model of the endometrium, the next step was to further develop it by investigating the interactions between the two cell types. However, to be able to unpick the impact of the EnSC on the EEC of the complex organoids from the medium was impossible. In ExM, the EEC of the gland organoids could differentiate regardless of co-culture with EnSC. Therefore, I proposed a minimal medium would be required in which only in the presence of EnSC would the EEC differentiate, therefore demonstrating the impact of the EnSC directly on the organoids without the confounding medium. This medium was produced by removing components of the ExM systematically. The final composition was the base medium with supplements plus NAC. All other inhibitors and growth factors were unnecessary when EnSC were present for EEC differentiation.

ScRNA-seq was performed to fully characterise the interactions between the EnSC and EEC. Simple and complex organoids were differentiated in $DM_{min.}$, dissociated and the single cell suspension was subjected to high-throughput scRNA-seq. The scRNA-seq allowed for the discrimination of cell types so that the organoid EEC mRNA profiles could be compared directly without EnSC contamination. The sequencing revealed that undifferentiated organoids were transcriptionally indistinguishable in both simple and complex organoid cultures. This observation was most likely due to the expansion of the gland organoids in ExM, masking putative EnSC signals. However, upon differentiation by $DM_{min.}$, the EEC of the simple and complex organoids diverged transcriptionally. Analysis of the most highly differentially upregulated genes in the complex organoid EEC demonstrated that only complex organoid EEC attain a secretory gene signature after four days of differentiation. The

secretory phenotype of the complex organoids indicates that this 3D *in vitro* model of the endometrium was successful in the primary thesis aim of modelling the implantation window. This suggests that this model could be useful to model implantation of human embryos.

Furthermore, the ability for the two cell types to cross talk opens the possibility of cross over experiments. For example, the EEC derived from a patient with implantation failure or RPL could be co-cultured with EnSC derived a control patient. This would further our understanding of how the two cell types interact in reproductive pathology and pinpoint if there is a cell type that drives a specific pathology. In addition, previously, EnSC and EEC have been manipulated by techniques such siRNA knockdowns in isolation. This complex organoid culture presents an opportunity to investigate the impact of gene knockdown in the presence of other cell types. In addition, as the endometrial glands are clonal and can be passaged, these provide the additional opportunity of producing CRISPR lines for different gene knock outs. In addition, CRISPR reporter lines could be developed to see in real time the effect of the EnSC in complex organoid culture.

Acute senescence in decidualising EnSC in complex organoids

Decidualising EnSC of the complex organoids gave an unexpected gene signature. By four days in $DM_{min.}$, the most differentially expressed genes in the EnSC population were genes relating to acute senescence. Previous studies have demonstrated that during decidualisation there is a fate decision made in which EnSC either differentiate into mature decidual cells, or into acutely senescent cells. The acute senescent cells are P4 resistant and produce inflammatory mediators (Brighton et al., 2017, Lucas et al., 2018, Salker et al., 2012b). However, in the absence of cell clearance by immune cells, acute senescent cells can induce neighbouring cells undergo ‘bystander’ or secondary senescence (Nelson et al., 2012, Brighton et al., 2017). Successful

transition of the cycling endometrium into the decidua of pregnancy has been attributed to the timely clearance of acute senescent cells by uNK cells by perforin- and granzyme-containing granule exocytosis (Brighton et al., 2017). Further, perturbations in decidualisation have been associated with RPL. The decreased clearance possibly destabilises the endometrium matrix, increasing the risk of breakdown and, later, miscarriage (Brighton et al., 2017).

Balancing the decidual and acute senescent cell populations will be essential for developing the embryo implantation model. Therefore, it is important to develop a method of controlling the acute senescence and inhibiting bystander senescence. One method is to use a senolytic drug such as dasatinib (Zhu et al., 2015, Brighton et al., 2017, Lucas et al., 2019). This could be titrated to determine the optimal concentration for controlled clearance of acute senescent cells. Dasatinib significantly switches the preponderance of senescent marker genes, such as DIO2, to the expression of decidual marker genes such as SCARA5 (Lucas et al., 2019).

In a more physiological model, senolytics could be replaced by primary uNK cells. The uNK cells could be introduced to the complex organoids in a similar manner to established protocols with monolayer EnSC. In these assays, senescence-associated beta-galactosidase (SA-β-gal) is used as a proxy measure of acute senescence (Brighton et al., 2017). When uNK cells are co-cultured with decidualised EnSC, the SA-β-gal is reduced, indicating killing of acute senescent cells (Brighton et al., 2017). In a preliminary experiment, I showed that the uNK cell killing assay works in EnSC in collagen hydrogel, indicating that there is scope for introducing uNK cells into the co-culture to form a 3D *in vitro* human endometrial multi-culture system (unpublished work).

Further model development

In addition to glandular EEC, EnSC and possibly uNK cells, luminal epithelium and endothelial cells could possibly be incorporated into the complex organoid culture. First, luminal epithelial cells could be cultured as a monolayer on top of the hydrogel droplet, as seen previously in layered co-culture systems (Bentin-Ley et al., 1994). Furthermore, the Brosens group have recently developed a protocol for isolating endothelial cells by MACS (unpublished work). The vasculature of the endometrium is of high importance for directing embryonic trophoblast invasion upon implantation for the beginning of placentation (Gellersen and Brosens, 2014, Meekins et al., 1994). Furthermore, in a 3D context, trophoblast invasion could be investigated in a way previously impossible. Upon differentiation the endometrial spiral arteries change morphology and begin to form the characteristic spirals they are named after (Farrer-Brown et al., 1970).

However, the endothelial cells require a specific endothelial medium in order to proliferate, and therefore medium optimisation would be required. In addition, functional differentiation of endothelial cells requires exposure to sheer stress as it is the case in the vasculature (Dewey et al., 1981, Yamamoto et al., 2005, Davies et al., 1986). This therefore suggests a multi-channel microfluidic approach may be more suitable for a more complex set up. There are a number of 'organoid on a chip' models already published for other tissues (Park et al., 2019, Zhang et al., 2018). For instance, in order to co-culture the complex organoids with endothelial cells, a two channel microfluidic chip could be engineered. One channel could be coated with a monolayer of endothelial cells to model a vessel. This channel would have endothelial cell medium flowed through at a rate that would cause shear stress on the cells, inducing endothelial maturation. This channel could be connected to another channel or chamber containing the EnSC and EEC in hydrogel in slow flowing or stagnant co-ExM. A fine grating between the chambers would allow for diffusion of cytokines and

chemokines without the invasion of cell types. This proposed model would recapitulate a vascularised endometrium. The embryo could be introduced to the complex organoid for implantation, and then it could be visualised by time lapse microscopy to determine whether the trophoblasts invade toward the underlying endothelial 'vessel'.

Conclusion

In summary, this thesis presents the development of a novel *in vitro* 3D model of the human endometrium. The first attempt was a misstep in achieving this aim, but the underlying biology of the EFAM gave interesting insight into the fibroblast activation potential of EnSC, silencing of the ROCK pathway in decidualising EnSC, and the potential impact of this in the initial development of endometriotic lesions. However, by exploiting the gland organoids, I was able to establish a complex organoid model consisting of EEC and EnSC. I established the growth conditions by optimising the appropriate hydrogel and ExM composition. I then confirmed direct interaction between the EnSC and gland organoids through the establishment of a $DM_{min.}$ followed by scRNA-seq of a decidual time course of simple and complex organoid cultures. In complex organoid culture, the EnSC were able to induce endometrial gland organoid differentiation and attain a secretory phenotype.

The next stage for this work is to study embryo implantation. In this thesis, I have presented evidence when differentiated in $DM_{min.}$ the complex organoids attain a secretory phenotype indicating that the embryos could be implanted. Overall, the development of complex organoid itself is a continued ongoing iterative process with each improvement requiring protocol optimisation before progression and study. The manipulation of the acute senescent cells of the decidualising culture by dasatinib will require optimisation. Moreover, the introduction of uNK or endothelial cells will be a great challenge to balance the needs of each cell type without the detriment of the

others, as seen with only the organoids and EnSC seen in this thesis. However, if proven successful, long-term this model will provide potentially the most faithful *in vitro* reconstruction of the endometrium to date and a useful tool for future study of human endometrial physiology and embryo implantation.

Finally, currently, the complex organoids have not yet been published, highlighting the importance and timeliness of this research. Globally, many groups are using the endometrial gland organoids for study and the complex organoid protocol will hopefully benefit the collective effort to produce the most faithful *in vitro* models of the human endometrium. This will in turn enable the community to study female reproductive physiology and its related pathologies in ways previously impossible. The long-term aim of this research is to develop a patient specific implantation model that could be used for drug screens for treatments for reproductive pathologies such as RPL and implantation failure.

References

ABOUSSAHOUD, W., BRUCE, C., ELLIOTT, S. & FAZELI, A. 2010. Activation of Toll-like receptor 5 decreases the attachment of human trophoblast cells to endometrial cells in vitro. *Human Reproduction,* 25**,** 2217-2228.

ABRAMSON, S. R., CONNER, G. E., NAGASE, H., NEUHAUS, I. & WOESSNER, J. F. 1995. Characterization of Rat Uterine Matrilysin and Its cDNA: RELATIONSHIP TO HUMAN PUMP-1 AND ACTIVATION OF PROCOLLAGENASES. *Journal of Biological Chemistry,* 270**,** 16016-16022.

ABUD, H. E., WATSON, N. & HEATH, J. K. 2005. Growth of intestinal epithelium in organ culture is dependent on EGF signalling. *Experimental Cell Research,* 303**,** 252-262.

AFSHAR, Y., JEONG, J.-W., ROQUEIRO, D., DEMAYO, F., LYDON, J., RADTKE, F., RADNOR, R., MIELE, L. & FAZLEABAS, A. 2011. Notch1 mediates uterine stromal differentiation and is critical for complete decidualization in the mouse. *The FASEB Journal,* 26**,** 282-294.

AGHAJANOVA, L. 2004. Leukemia inhibitory factor and human embryo implantation. *Ann N Y Acad Sci,* 1034**,** 176-83.

AGHAJANOVA, L., TATSUMI, K., HORCAJADAS, J. A., ZAMAH, A. M., ESTEBAN, F. J., HERNDON, C. N., CONTI, M. & GIUDICE, L. C. 2010. Unique Transcriptome, Pathways, and Networks in the Human Endometrial Fibroblast Response to Progesterone in Endometriosis1. *Biology of Reproduction,* 84**,** 801-815.

AIN, R., TRINH, M.-L. & SOARES, M. J. 2004. Interleukin-11 signaling is required for the differentiation of natural killer cells at the maternal–fetal interface. *Developmental Dynamics,* 231**,** 700-708.

AL-SABBAGH, M., FUSI, L., HIGHAM, J., LEE, Y., LEI, K., HANYALOGLU, A. C., LAM, E. W., CHRISTIAN, M. & BROSENS, J. J. 2011. NADPH oxidase-derived reactive oxygen species mediate decidualization of human endometrial stromal cells in response to cyclic AMP signaling. *Endocrinology,* 152**,** 730-40.

AMANO, M., NAKAYAMA, M. & KAIBUCHI, K. 2010. Rho-kinase/ROCK: A key regulator of the cytoskeleton and cell polarity. *Cytoskeleton (Hoboken, N.J.),* 67**,** 545-554.

ANACKER, J., SEGERER, S. E., HAGEMANN, C., FEIX, S., KAPP, M., BAUSCH, R. & KÄMMERER, U. 2011. Human decidua and invasive trophoblasts are rich sources of nearly all human matrix metalloproteinases. *Molecular Human Reproduction,* 17**,** 637-652.

ANGUIANO, M., CASTILLA, C., MAŠKA, M., EDERRA, C., PELÁEZ, R., MORALES, X., MUÑOZ-ARRIETA, G., MUJIKA, M., KOZUBEK, M., MUÑOZ-BARRUTIA, A., ROUZAUT, A., ARANA, S., GARCIA-AZNAR, J. M. & ORTIZ-DE-SOLORZANO, C. 2017. Characterization

of three-dimensional cancer cell migration in mixed collagen-Matrigel scaffolds using microfluidics and image analysis. *PLoS One,* 12**,** e0171417.

APLIN, J. D. 2006. In Vitro Analysis of Trophoblast Invasion. *In:* SOARES, M. J. & HUNT, J. S. (eds.) *Placenta and Trophoblast: Methods and Protocols Volume 2.* Totowa, NJ: Humana Press.

APLIN, J. D., CHARLTON, A. K. & AYAD, S. 1988. An immunohistochemical study of human endometrial extracellular matrix during the menstrual cycle and first trimester of pregnancy. *Cell and Tissue Research,* 253**,** 231-240.

APLIN, J. D. & JONES, C. J. P. 1989. Extracellular Matrix in Endometrium and Decidua. *In:* GENBAČEV, O., KLOPPER, A. & BEACONSFIELD, R. (eds.) *Placenta as a Model and a Source.* Boston, MA: Springer US.

APLIN, J. D., MYLONA, P., KIELTY, C. M., BALL, S., WILLIAMS, J. D. L., CHURCH, H. J. & JONES, C. J. P. Collagen VI and Laminin as Markers of Differentiation of Endometrial Stroma. *In:* DEY, S. K., ed. Molecular and Cellular Aspects of Periimplantation Processes, 1995// 1995 New York, NY. Springer New York, 331-351.

ARNOLD, J. T., KAUFMAN, D. G., SEPPÄLÄ, M. & LESSEY, B. A. 2001. Endometrial stromal cells regulate epithelial cell growth in vitro: a new co-culture model. *Hum Reprod,* 16**,** 836-45.

ASHBURNER, M., BALL, C. A., BLAKE, J. A., BOTSTEIN, D., BUTLER, H., CHERRY, J. M., DAVIS, A. P., DOLINSKI, K., DWIGHT, S. S., EPPIG, J. T., HARRIS, M. A., HILL, D. P., ISSEL-TARVER, L., KASARSKIS, A., LEWIS, S., MATESE, J. C., RICHARDSON, J. E., RINGWALD, M., RUBIN, G. M. & SHERLOCK, G. 2000. Gene ontology: tool for the unification of biology. The Gene Ontology Consortium. *Nature genetics,* 25**,** 25-29.

ASHKAR, A. A., BLACK, G. P., WEI, Q., HE, H., LIANG, L., HEAD, J. R. & CROY, B. A. 2003. Assessment of Requirements for IL-15 and IFN Regulatory Factors in Uterine NK Cell Differentiation and Function During Pregnancy. *The Journal of Immunology,* 171**,** 2937.

AU - BARTFELD, S. & AU - CLEVERS, H. 2015. Organoids as Model for Infectious Diseases: Culture of Human and Murine Stomach Organoids and Microinjection of Helicobacter Pylori. *JoVE***,** e53359.

AYAKANNU, T., TAYLOR, A. H., WILLETS, J. M., BROWN, L., LAMBERT, D. G., MCDONALD, J., DAVIES, Q., MOSS, E. L. & KONJE, J. C. 2015. Validation of endogenous control reference genes for normalizing gene expression studies in endometrial carcinoma. *Mol Hum Reprod,* 21**,** 723-35.

BALESTRINI, J. L., CHAUDHRY, S., SARRAZY, V., KOEHLER, A. & HINZ, B. 2012. The mechanical memory of lung myofibroblasts. *Integrative Biology,* 4**,** 410-421.

BALL, J. M., MOLDOVEANU, Z., MELSEN, L. R., KOZLOWSKI, P. A., JACKSON, S., MULLIGAN, M. J., MESTECKY, J. F. & COMPANS, R. W. 1995. A polarized human endometrial cell line that binds and transports polymeric IgA. *In Vitro Cellular & Developmental Biology - Animal,* 31**,** 196-206.

BANERJEE, P. & FAZLEABAS, A. T. 2010. Endometrial responses to embryonic signals in the primate. *The International journal of developmental biology,* 54**,** 295-302.

BARROS, F. S. V., BROSENS, J. J. & BRIGHTON, P. J. 2016. Isolation and Primary Culture of Various Cell Types from Whole Human Endometrial Biopsies. *Bio-protocol,* 6**,** e2028.

BARTFELD, S., BAYRAM, T., VAN DE WETERING, M., HUCH, M., BEGTHEL, H., KUJALA, P., VRIES, R., PETERS, P. J. & CLEVERS, H. 2015. In vitro expansion of human gastric epithelial stem cells and their responses to bacterial infection. *Gastroenterology,* 148**,** 126-136.e6.

BARTFELD, S. & CLEVERS, H. 2015. Organoids as Model for Infectious Diseases: Culture of Human and Murine Stomach Organoids and Microinjection of Helicobacter Pylori. *JoVE***,** e53359.

BARTOL, F. F., WILEY, A. A. & GOODLETT, D. R. 1988. Ovine Uterine Morphogenesis: Histochemical Aspects of Endometrial Development in the Fetus and Neonate. *Journal of Animal Science,* 66**,** 1303-1313.

BARTOL, F. F., WILEY, A. A., SPENCER, T. E., VALLET, J. L. & CHRISTENSON, R. K. 1993. Early uterine development in pigs. *J Reprod Fertil Suppl,* 48**,** 99-116.

BARTSCH, O., BARTLICK, B. & IVELL, R. 2004. Phosphodiesterase 4 Inhibition Synergizes with Relaxin Signaling to Promote Decidualization of Human Endometrial Stromal Cells. *The Journal of Clinical Endocrinology & Metabolism,* 89**,** 324-334.

BARTSCHA, O. & IVELL, R. 2004. Relaxin and Phosphodiesterases Collaborate during Decidualization. *Annals of the New York Academy of Sciences,* 1030**,** 479-492.

BAZER, F. W. 1975. Uterine protein secretions: Relationship to development of the conceptus. *J Anim Sci,* 41**,** 1376-82.

BEATO, M. & KLUG, J. 2000. Steroid hormone receptors: an update. *Human Reproduction Update,* 6**,** 225-236.

BECHT, E., DUTERTRE, C.-A., KWOK, I. W. H., NG, L. G., GINHOUX, F. & NEWELL, E. W. 2018a. Evaluation of UMAP as an alternative to t-SNE for single-cell data. *bioRxiv***,** 298430.

BECHT, E., MCINNES, L., HEALY, J., DUTERTRE, C. A., KWOK, I. W. H., NG, L. G., GINHOUX, F. & NEWELL, E. W. 2018b. Dimensionality reduction for visualizing single-cell data using UMAP. *Nat Biotechnol*.

BELLUSCI, S., GRINDLEY, J., EMOTO, H., ITOH, N. & HOGAN, B. L. 1997. Fibroblast growth factor 10 (FGF10) and branching morphogenesis in the embryonic mouse lung. *Development,* 124**,** 4867.

BEN-JONATHAN, N., MERSHON, J. L., ALLEN, D. L. & STEINMETZ, R. W. 1996. Extrapituitary Prolactin: Distribution, Regulation, Functions, and Clinical Aspects*. *Endocrine Reviews,* 17**,** 639-669.

BENTIN-LEY, U., HORN, T., SJOGREN, A., SORENSEN, S., FALCK LARSEN, J. & HAMBERGER, L. 2000. Ultrastructure of human blastocyst-endometrial interactions in vitro. *J Reprod Fertil,* 120**,** 337-50.

BENTIN-LEY, U., PEDERSEN, B., LINDENBERG, S., LARSEN, J. F., HAMBERGER, L. & HORN, T. 1994. Isolation and culture of human endometrial cells in a three-dimensional culture system. *J Reprod Fertil,* 101**,** 327-32.

BERGAMINI, C. M., PANSINI, F., BETTOCCHI, S., SEGALA, V., DALLOCCHIO, F., BAGNI, B. & MOLLICA, G. 1985. Hormonal sensitivity of adenylate cyclase from human endometrium: Modulation by estradiol. *Journal of Steroid Biochemistry,* 22**,** 299-303.

BERNEAU, S. C., RUANE, P. T., BRISON, D. R., KIMBER, S. J., WESTWOOD, M. & APLIN, J. D. 2019. Characterisation of Osteopontin in an In Vitro Model of Embryo Implantation. *Cells,* 8**,** 432.

BERTO, A. G., OBA, S. M., MICHELACCI, Y. M. & SAMPAIO, L. O. 2001. Galactosaminoglycans from normal myometrium and leiomyoma. *Braz J Med Biol Res,* 34**,** 633-7.

BHAGWAT, S. R., CHANDRASHEKAR, D. S., KAKAR, R., DAVULURI, S., BAJPAI, A. K., NAYAK, S., BHUTADA, S., ACHARYA, K. & SACHDEVA, G. 2013. Endometrial receptivity: a revisit to functional genomics studies on human endometrium and creation of HGEx-ERdb. *PloS one,* 8**,** e58419-e58419.

BIGSBY, R. M. & CUNHA, G. R. 1986. Estrogen stimulation of deoxyribonucleic acid synthesis in uterine epithelial cells which lack estrogen receptors. *Endocrinology,* 119**,** 390-6.

BINDER, N. K., EVANS, J., GARDNER, D. K., SALAMONSEN, L. A. & HANNAN, N. J. 2014. Endometrial signals improve embryo outcome: functional role of vascular endothelial growth factor isoforms on embryo development and implantation in mice. *Hum Reprod,* 29**,** 2278-86.

BINNERTS, M. E., KIM, K.-A., BRIGHT, J. M., PATEL, S. M., TRAN, K., ZHOU, M., LEUNG, J. M., LIU, Y., LOMAS, W. E., DIXON, M., HAZELL, S. A., WAGLE, M., NIE, W.-S., TOMASEVIC, N., WILLIAMS, J., ZHAN, X., LEVY, M. D., FUNK, W. D. & ABO, A. 2007. R-Spondin1 regulates Wnt signaling by inhibiting internalization of LRP6. *Proceedings of the National Academy of Sciences,* 104**,** 14700.

BLÄUER, M., HEINONEN, P. K., MARTIKAINEN, P. M., TOMÁS, E. & YLIKOMI, T. 2005. A novel organotypic culture model for normal human endometrium: regulation of epithelial cell proliferation by estradiol and medroxyprogesterone acetate. *Human Reproduction,* 20**,** 864-871.

BOOMSMA, C. M., KAVELAARS, A., EIJKEMANS, M. J. C., LENTJES, E. G., FAUSER, B. C. J. M., HEIJNEN, C. J. & MACKLON, N. S. 2009. Endometrial secretion analysis identifies a cytokine profile predictive of pregnancy in IVF. *Human Reproduction,* 24**,** 1427-1435.

BORETTO, M., COX, B., NOBEN, M., HENDRIKS, N., FASSBENDER, A., ROOSE, H., AMANT, F., TIMMERMAN, D., TOMASSETTI, C., VANHIE, A., MEULEMAN, C., FERRANTE, M. & VANKELECOM, H. 2017. Development of organoids from mouse and human endometrium showing endometrial epithelium physiology and long-term expandability. *Development,* 144**,** 1775-1786.

BORETTO, M., MAENHOUDT, N., LUO, X., HENNES, A., BOECKX, B., BUI, B., HEREMANS, R., PERNEEL, L., KOBAYASHI, H., VAN ZUNDERT, I., BREMS, H., COX, B., FERRANTE, M., UJI-I, H., KOH, K. P., D'HOOGHE, T., VANHIE, A., VERGOTE, I., MEULEMAN, C., TOMASSETTI, C., LAMBRECHTS, D., VRIENS, J., TIMMERMAN, D. & VANKELECOM, H. 2019. Patient-derived organoids from endometrial disease capture clinical heterogeneity and are amenable to drug screening. *Nature Cell Biology,* 21**,** 1041-1051.

BOTTENSTEIN, J. E. & SATO, G. H. 1979. Growth of a rat neuroblastoma cell line in serum-free supplemented medium. *Proceedings of the National Academy of Sciences of the United States of America,* 76**,** 514-517.

BRANHAM, W. S., SHEEHAN, D. M., ZEHR, D. R., MEDLOCK, K. L., NELSON, C. J. & RIDLON, E. 1985. Inhibition of Rat Uterine Gland Genesis by Tamoxifen. *Endocrinology,* 117**,** 2238-2248.

BRAR, A. K., FRANK, G. R., KESSLER, C. A., CEDARS, M. I. & HANDWERGER, S. 1997. Progesterone-dependent decidualization of the human endometrium is mediated by cAMP. *Endocrine,* 6**,** 301-307.

BRAR, A. K., HANDWERGER, S., KESSLER, C. A. & ARONOW, B. J. 2001. Gene induction and categorical reprogramming during in vitro human endometrial fibroblast decidualization. *Physiological Genomics,* 7**,** 135-148.

BRENNER, RM, ., S, LAYDEN, OD, ., KNOBI, L., E, ., NEILL, JD & . 1994. Cyclic changes in the primate oviduct and endometrium. *The Physiology of Reproduction* Raven Press.

BREWER, G. J., TORRICELLI, J. R., EVEGE, E. K. & PRICE, P. J. 1993. Optimized survival of hippocampal neurons in B27-supplemented neurobasal™, a new serum-free medium combination. *Journal of Neuroscience Research,* 35**,** 567-576.

BRIGHTON, P. J., MARUYAMA, Y., FISHWICK, K., VRLJICAK, P., TEWARY, S., FUJIHARA, R., MUTER, J., LUCAS, E. S., YAMADA, T., WOODS, L., LUCCIOLA, R., HOU LEE, Y., TAKEDA, S., OTT, S., HEMBERGER, M., QUENBY, S. & BROSENS, J. J. 2017. Clearance of senescent decidual cells by uterine natural killer cells in cycling human endometrium. *Elife,* 6.

BROMER, J. G., ALDAD, T. S. & TAYLOR, H. S. 2009. Defining the proliferative phase endometrial defect. *Fertil Steril,* 91**,** 698-704.

BROSENS, I. & BENAGIANO, G. 2016. Clinical significance of neonatal menstruation. *European Journal of Obstetrics & Gynecology and Reproductive Biology,* 196**,** 57-59.

BROSENS, I., BROSENS, J. & BENAGIANO, G. 2013a. Neonatal uterine bleeding as antecedent of pelvic endometriosis. *Human Reproduction,* 28**,** 2893-2897.

BROSENS, I., GARGETT, C. E., GUO, S.-W., PUTTEMANS, P., GORDTS, S., BROSENS, J. J. & BENAGIANO, G. 2016. Origins and Progression of Adolescent Endometriosis. *Reproductive Sciences,* 23**,** 1282-1288.

BROSENS, I., PUTTEMANS, P. & BENAGIANO, G. 2013b. Endometriosis: a life cycle approach? *American Journal of Obstetrics and Gynecology,* 209**,** 307-316.

BROSENS, J. & GELLERSEN, B. 2010. Something new about early pregnancy: Decidual biosensoring and natural embryo selection. *Ultrasound in obstetrics & gynecology : the official journal of the International Society of Ultrasound in Obstetrics and Gynecology,* 36**,** 1-5.

BROSENS, J. J., HAYASHI, N. & WHITE, J. O. 1999. Progesterone receptor regulates decidual prolactin expression in differentiating human endometrial stromal cells. *Endocrinology,* 140**,** 4809-20.

BROSENS, J. J., PARKER, M. G., MCINDOE, A., PIJNENBORG, R. & BROSENS, I. A. 2009. A role for menstruation in preconditioning the uterus for successful pregnancy. *American Journal of Obstetrics and Gynecology,* 200**,** 615.e1-615.e6.

BROSENS, J. J., PIJNENBORG, R. & BROSENS, I. A. 2002. The myometrial junctional zone spiral arteries in normal and abnormal pregnancies: A review of the literature. *American Journal of Obstetrics and Gynecology,* 187**,** 1416-1423.

BROSENS, J. J., SALKER, M. S., TEKLENBURG, G., NAUTIYAL, J., SALTER, S., LUCAS, E. S., STEEL, J. H., CHRISTIAN, M., CHAN, Y.-W., BOOMSMA, C. M., MOORE, J. D., HARTSHORNE, G. M., ŠUĆUROVIĆ, S., MULAC-JERICEVIC, B., HEIJNEN, C. J., QUENBY, S., GROOT KOERKAMP, M. J., HOLSTEGE, F. C. P., SHMYGOL, A. & MACKLON, N. S. 2014. Uterine Selection of Human Embryos at Implantation. *Scientific Reports,* 4**,** 3894.

BROSENS, J. J., TULLET, J., VARSHOCHI, R. & LAM, E. W. F. 2004. Steroid receptor action. *Best Practice & Research Clinical Obstetrics & Gynaecology,* 18**,** 265-283.

BRYANT, S. J., ARTHUR, J. A. & ANSETH, K. S. 2005. Incorporation of tissue-specific molecules alters chondrocyte metabolism and gene expression in photocrosslinked hydrogels. *Acta Biomaterialia,* 1**,** 243-252.

BURTON, G. J., JAUNIAUX, E. & CHARNOCK-JONES, D. S. 2007. Human early placental development: potential roles of the endometrial glands. *Placenta,* 28 Suppl A**,** S64-S69.

BURTON, G. J., JAUNIAUX, E. & CHARNOCK-JONES, D. S. 2010. The influence of the intrauterine environment on human placental development. *Int J Dev Biol,* 54**,** 303-12.

BURTON, G. J., JAUNIAUX, E. & WATSON, A. L. 1999. Maternal arterial connections to the placental intervillous space during the first trimester of human pregnancy: The Boyd Collection revisited. *American Journal of Obstetrics & Gynecology,* 181**,** 718-724.

BURTON, G. J., WATSON, A. L., HEMPSTOCK, J., SKEPPER, J. N. & JAUNIAUX, E. 2002. Uterine glands provide histiotrophic nutrition for the human fetus during the first trimester of pregnancy. *J Clin Endocrinol Metab,* 87**,** 2954-9.

CABALLERO-CAMPO, P., DOMÍNGUEZ, F., COLOMA, J., MESEGUER, M., REMOHÍ, J., PELLICER, A. & SIMÓN, C. 2002. Hormonal and embryonic regulation of chemokines IL-8, MCP-1 and RANTES in the human endometrium during the window of implantation. *Molecular Human Reproduction,* 8**,** 375-384.

CARTER, A. M., HILLS, F., O'GORMAN, D. B., ROBERTS, C. T., SOORANNA, S. R., WATSON, C. S. & WESTWOOD, M. 2004. The insulin-like growth factor system in mammalian pregnancy--a workshop report. *Placenta.* Netherlands.

CARVER, J., MARTIN, K., SPYROPOULOU, I., BARLOW, D., SARGENT, I. & MARDON, H. 2003. An in-vitro model for stromal invasion during implantation of the human blastocyst. *Human Reproduction,* 18**,** 283-290.

CERVELLÓ, I., GIL-SANCHIS, C., MAS, A., FAUS, A., SANZ, J., MOSCARDÓ, F., HIGUERAS, G., SANZ, M. A., PELLICER, A. & SIMÓN, C. 2012. Bone Marrow-Derived Cells from Male Donors Do Not Contribute to the Endometrial Side Population of the Recipient. *PLOS ONE,* 7**,** e30260.

CERVERO, A., DOMÍNGUEZ, F., HORCAJADAS, J. A., QUIÑONERO, A., PELLICER, A. & SIMÓN, C. 2007. Embryonic adhesion is not affected by endometrial leptin receptor gene silencing. *Fertility and Sterility,* 88**,** 1086-1092.

CHAN, B. P. & LEONG, K. W. 2008. Scaffolding in tissue engineering: general approaches and tissue-specific considerations. *European Spine Journal,* 17**,** 467-479.

CHAN, R. W. S. & GARGETT, C. E. 2006. Identification of Label-Retaining Cells in Mouse Endometrium. *STEM CELLS,* 24**,** 1529-1538.

CHAN, R. W. S., SCHWAB, K. E. & GARGETT, C. E. 2004. Clonogenicity of Human Endometrial Epithelial and Stromal Cells1. *Biology of Reproduction,* 70**,** 1738-1750.

CHASE, L. G. & FIRPO, M. T. 2007. Development of serum-free culture systems for human embryonic stem cells. *Current Opinion in Chemical Biology,* 11**,** 367-372.

CHAZARA, O., XIONG, S. & MOFFETT, A. 2011. Maternal KIR and fetal HLA-C: a fine balance. *Journal of Leukocyte Biology,* 90**,** 703-716.

CHEN, C., SPENCER, T. E. & BAZER, F. W. 2000. Fibroblast Growth Factor-10: A Stromal Mediator of Epithelial Functionin the Ovine Uterus. *Biology of Reproduction,* 63**,** 959-966.

CHILDS, B. G., GLUSCEVIC, M., BAKER, D. J., LABERGE, R. M., MARQUESS, D., DANANBERG, J. & VAN DEURSEN, J. M. 2017. Senescent cells: an emerging target for diseases of ageing. *Nat Rev Drug Discov,* 16**,** 718-735.

CHOI, C. K., VICENTE-MANZANARES, M., ZARENO, J., WHITMORE, L. A., MOGILNER, A. & HORWITZ, A. R. 2008. Actin and alpha-actinin orchestrate the assembly and maturation of nascent adhesions in a myosin II motor-independent manner. *Nature cell biology,* 10**,** 1039-1050.

CHRISTIAN, M., ZHANG, X., SCHNEIDER-MERCK, T., UNTERMAN, T. G., GELLERSEN, B., WHITE, J. O. & BROSENS, J. J. 2002. Cyclic AMP-induced Forkhead Transcription Factor, FKHR, Cooperates with CCAAT/Enhancer-binding Protein β in Differentiating Human Endometrial Stromal Cells. *Journal of Biological Chemistry,* 277**,** 20825-20832.

CHUNG, D., GAO, F., JEGGA, A. G. & DAS, S. K. 2015. Estrogen mediated epithelial proliferation in the uterus is directed by stromal Fgf10 and Bmp8a. *Molecular and Cellular Endocrinology,* 400**,** 48-60.

CHURCH, H. J., VIĆOVAC, L. M., WILLIAMS, J. D., HEY, N. A. & APLIN, J. D. 1996. Laminins 2 and 4 are expressed by human decidual cells. *Laboratory investigation; a journal of technical methods and pathology,* 74**,** 21-32.

CIDADÃO, A. J., THORSTEINSDÓTTIR, S. & DAVID-FERREIRA, J. F. 1990. Immunocytochemical study of tissue distribution and hormonal control of chondroitin-, dermatan- and keratan sulfates from rodent uterus. *Eur J Cell Biol,* 52**,** 105-16.

CIRCU, M. L. & AW, T. Y. 2008. Glutathione and apoptosis. *Free Radic Res,* 42**,** 689-706.

CLASSEN-LINKE, I., KUSCHE, M., KNAUTHE, R. & BEIER, H. M. 1997. Establishment of a human endometrial cell culture system and characterization of its polarized hormone responsive epithelial cells. *Cell Tissue Res,* 287**,** 171-85.

CLOKE, B., HUHTINEN, K., FUSI, L., KAJIHARA, T., YLIHEIKKILÄ, M., HO, K. K., TEKLENBURG, G., LAVERY, S., JONES, M. C., TREW, G., KIM, J. J., LAM, E. W., CARTWRIGHT, J. E., POUTANEN, M. & BROSENS, J. J. 2008. The androgen and progesterone receptors regulate distinct gene networks and cellular functions in decidualizing endometrium. *Endocrinology,* 149**,** 4462-74.

COOK, C. D., HILL, A. S., GUO, M., STOCKDALE, L., PAPPS, J. P., ISAACSON, K. B., LAUFFENBURGER, D. A. & GRIFFITH, L. G. 2017. Local remodeling of synthetic extracellular matrix microenvironments by co-cultured endometrial epithelial and stromal cells enables long-term dynamic physiological function. *Integr Biol (Camb),* 9**,** 271-289.

COOKE, P. S., BUCHANAN, D. L., YOUNG, P., SETIAWAN, T., BRODY, J., KORACH, K. S., TAYLOR, J., LUBAHN, D. B. & CUNHA, G. R. 1997. Stromal estrogen receptors mediate mitogenic effects of estradiol on uterine epithelium. *Proc Natl Acad Sci U S A,* 94**,** 6535-40.

COOKE, P. S., SPENCER, T. E., BARTOL, F. F. & HAYASHI, K. 2013. Uterine glands: development, function and experimental model systems. *Molecular Human Reproduction,* 19**,** 547-558.

COOKE, P. S., UCHIMA, F. D., FUJII, D. K., BERN, H. A. & CUNHA, G. R. 1986. Restoration of normal morphology and estrogen responsiveness in cultured vaginal and uterine epithelia transplanted with stroma. *Proc Natl Acad Sci U S A,* 83**,** 2109-13.

CORNILLIE, F., LAUWERYNS, J. & BROSENS, I. 1985. Normal Human Endometrium. *Gynecologic and Obstetric Investigation,* 20**,** 113-129.

COUCHMAN, J. R. & PATAKI, C. A. 2012. An introduction to proteoglycans and their localization. *J Histochem Cytochem,* 60**,** 885-97.

COUSINS, F. L., MURRAY, A., ESNAL, A., GIBSON, D. A., CRITCHLEY, H. O. D. & SAUNDERS, P. T. K. 2014. Evidence from a Mouse Model That Epithelial Cell Migration and Mesenchymal-Epithelial Transition Contribute to Rapid Restoration of Uterine Tissue Integrity during Menstruation. *PLOS ONE,* 9**,** e86378.

CRESPO, M., VILAR, E., TSAI, S.-Y., CHANG, K., AMIN, S., SRINIVASAN, T., ZHANG, T., PIPALIA, N. H., CHEN, H. J., WITHERSPOON, M., GORDILLO, M., XIANG, J. Z., MAXFIELD, F. R., LIPKIN, S., EVANS, T. & CHEN, S. 2017. Colonic organoids derived from human induced pluripotent stem cells for modeling colorectal cancer and drug testing. *Nature Medicine,* 23**,** 878.

CROFT, C. B. & TARIN, D. 1970. Ultrastructural studies of wound healing in mouse skin. I. Epithelial behaviour. *Journal of anatomy,* 106**,** 63-77.

CROY, A., VAN DEN HEUVEL, M., BORZYCHOWSKI, A. & TAYADE, C. 2006. Uterine natural killer cells: a specialized differentiation regulated by ovarian hormones. *Immunological Reviews,* 214**,** 161-185.

CUNHA, G. R., BIGSBY, R. M., COOKE, P. S. & SUGIMURA, Y. 1985. Stromal-epithelial interactions in adult organs. *Cell Differ,* 17**,** 137-48.

CUNHA, G. R. & YOUNG, P. 1992. Role of stroma in oestrogen-induced epithelial proliferation. *Epithelial Cell Biol,* 1**,** 18-31.

DAVIES, P. F., REMUZZI, A., GORDON, E. J., DEWEY, C. F. & GIMBRONE, M. A. 1986. Turbulent fluid shear stress induces vascular endothelial cell turnover in vitro. *Proceedings of the National Academy of Sciences,* 83**,** 2114.

DEANE, J. A., COUSINS, F. L. & GARGETT, C. E. 2017. Endometrial organoids: in vitro models for endometrial research and personalized medicine†. *Biology of Reproduction,* 97**,** 781-783.

DESAI, N. N., KENNARD, E. A., KNISS, D. A. & FRIEDMAN, C. I. 1994. Novel human endometrial cell line promotes blastocyst development**Presented in part at the 48th Annual Meeting of The American Fertility Society, New Orleans, Louisiana, October 31 to November 5, 1992. *Fertility and Sterility,* 61**,** 760-766.

DEWEY, C. F., JR., BUSSOLARI, S. R., GIMBRONE, M. A., JR. & DAVIES, P. F. 1981. The Dynamic Response of Vascular Endothelial Cells to Fluid Shear Stress. *Journal of Biomechanical Engineering,* 103**,** 177-185.

DEY, S. K., LIM, H., DAS, S. K., REESE, J., PARIA, B. C., DAIKOKU, T. & WANG, H. 2004. Molecular Cues to Implantation. *Endocrine Reviews,* 25**,** 341-373.

DOCKERY, P., LI, T. C., ROGERS, A. W., COOKE, I. D. & LENTON, E. A. 1988. The ultrastructure of the glandular epithelium in the timed endometrial biopsy. *Hum Reprod,* 3**,** 826-34.

DOMINGUEZ, F., GALAN, A., MARTIN, J. J. L., REMOHI, J., PELLICER, A. & SIMÓN, C. 2003. Hormonal and embryonic regulation of chemokine receptors CXCR1, CXCR4, CCR5 and CCR2B in the human endometrium and the human blastocyst. *Molecular Human Reproduction,* 9**,** 189-198.

DONJACOUR, A. A. & CUNHA, G. R. 1991. Stromal regulation of epithelial function. *Cancer Treat Res,* 53**,** 335-64.

DRISKELL, R. R. & WATT, F. M. 2015. Understanding fibroblast heterogeneity in the skin. *Trends in Cell Biology,* 25**,** 92-99.

DÍAZ-GIMENO, P., HORCAJADAS, J. A., MARTÍNEZ-CONEJERO, J. A., ESTEBAN, F. J., ALAMÁ, P., PELLICER, A. & SIMÓN, C. 2011. A genomic diagnostic tool for human endometrial receptivity based on the transcriptomic signature. *Fertil Steril,* 95**,** 50-60, 60.e1-15.

EAGLE, H., OYAMA, V. I., LEVY, M., HORTON, C. L. & FLEISCHMAN, R. 1956. THE GROWTH RESPONSE OF MAMMALIAN CELLS IN TISSUE CULTURE TO l-GLUTAMINE AND l-GLUTAMIC ACID. *Journal of Biological Chemistry,* 218**,** 607-616.

EDWARDS, R. G. 2006. Human implantation: the last barrier in assisted reproduction technologies? *Reprod Biomed Online,* 13**,** 887-904.

EHRLICH, H. P., RAJARATNAM, J. B. M. & GRISWOLD, T. R. 1986. ATP-induced cell contraction in dermal fibroblasts: Effects of cAMP and myosin light-chain kinase. *Journal of Cellular Physiology,* 128**,** 223-230.

EMERA, D., ROMERO, R. & WAGNER, G. 2012. The evolution of menstruation: A new model for genetic assimilation. *BioEssays,* 34**,** 26-35.

ESTELLA, C., HERRER, I., ATKINSON, S. P., QUIÑONERO, A., MARTÍNEZ, S., PELLICER, A. & SIMÓN, C. 2012. Inhibition of Histone Deacetylase Activity in Human Endometrial Stromal Cells Promotes Extracellular Matrix Remodelling and Limits Embryo Invasion. *PLOS ONE,* 7**,** e30508.

EVANS, J., KAITU'U-LINO, T. U. & SALAMONSEN, L. A. 2011. Extracellular Matrix Dynamics in Scar-Free Endometrial Repair: Perspectives from Mouse In Vivo and Human In Vitro Studies1. *Biology of Reproduction,* 85**,** 511-523.

EVANS, J. & SALAMONSEN, L. A. 2014. Decidualized Human Endometrial Stromal Cells Are Sensors of Hormone Withdrawal in the Menstrual Inflammatory Cascade1. *Biology of Reproduction,* 90.

EVRON, A., GOLDMAN, S. & SHALEV, E. 2011. Effect of primary human endometrial stromal cells on epithelial cell receptivity and protein expression is dependent on menstrual cycle stage. *Hum Reprod,* 26**,** 176-90.

FABER, M., WEWER, U. M., BERTHELSEN, J. G., LIOTTA, L. A. & ALBRECHTSEN, R. 1986. Laminin production by human endometrial stromal cells relates to the cyclic and pathologic state of the endometrium. *The American journal of pathology,* 124**,** 384-391.

FARRER-BROWN, G., BEILBY, J. O. W. & TARBIT, M. H. 1970. THE BLOOD SUPPLY OF THE UTERUS. *BJOG: An International Journal of Obstetrics & Gynaecology,* 77**,** 673-681.

FEINBERG, R. F., KLIMAN, H. J. & WANG, C. L. 1994. Transforming growth factor-beta stimulates trophoblast oncofetal fibronectin synthesis in vitro: implications for trophoblast implantation in vivo. *The Journal of Clinical Endocrinology & Metabolism,* 78**,** 1241-1248.

FERENCZY, A. 1976. Studies on the cytodynamics of human endometrial regeneration: I. Scanning electron microscopy. *American Journal of Obstetrics & Gynecology,* 124**,** 64-74.

FERRARETTI, A. P., GOOSSENS, V., DE MOUZON, J., BHATTACHARYA, S., CASTILLA, J. A., KORSAK, V., KUPKA, M., NYGREN, K. G. & NYBOE ANDERSEN, A. 2012. Assisted reproductive technology in Europe, 2008: results generated from European registers by ESHRE. *Hum Reprod,* 27**,** 2571-84.

FISHMAN, R. B., BRANHAM, W. S., STRECK, R. D. & SHEEHAN, D. M. 1996. Ontogeny of Estrogen Receptor Messenger Ribonucleic Acid Expression in the Postnatal Rat Uterus1. *Biology of Reproduction,* 55**,** 1221-1230.

FITZGERALD, H. C., DHAKAL, P., BEHURA, S. K., SCHUST, D. J. & SPENCER, T. E. 2019. Self-renewing endometrial epithelial organoids of the human uterus. *Proceedings of the National Academy of Sciences***,** 201915389.

FLEMING, S. & BELL, S. C. 1997. Localization of fibrillin-1 in human endometrium and decidua during the menstrual cycle and pregnancy. *Human Reproduction,* 12**,** 2051-2056.

FREEMAN, M. E., KANYICSKA, B., LERANT, A. & NAGY, G. 2000. Prolactin: Structure, Function, and Regulation of Secretion. *Physiological Reviews,* 80**,** 1523-1631.

FRIEDRICHS, B. 1997. Th. Peters. Jr.: All about Albumin. Biochemistry, Genetics, and Medical Applications. XX and 432 pages, numerous figures and tables. Academic Press, Inc., San Diego, California, 1996. Price: 85.00 US $. *Food / Nahrung,* 41**,** 382-382.

GALÁN, A., O'CONNOR, J. E., VALBUENA, D., HERRER, R., REMOHÍ, J., PAMPFER, S., PELLICER, A. & SIMÓN, C. 2000. The Human Blastocyst Regulates Endometrial Epithelial Apoptosis in Embryonic Adhesion1. *Biology of Reproduction,* 63**,** 430-439.

GARGETT, C. E. 2006. Identification and characterisation of human endometrial stem/progenitor cells. *Australian and New Zealand Journal of Obstetrics and Gynaecology,* 46**,** 250-253.

GARGETT, C. E., SCHWAB, K. E., BROSENS, J. J., PUTTEMANS, P., BENAGIANO, G. & BROSENS, I. 2014. Potential role of endometrial stem/progenitor cells in the pathogenesis of early-onset endometriosis. *Molecular Human Reproduction,* 20**,** 591-598.

GARGETT, C. E., SCHWAB, K. E. & DEANE, J. A. 2015. Endometrial stem/progenitor cells: the first 10 years. *Human Reproduction Update,* 22**,** 137-163.

GARGETT, C. E., SCHWAB, K. E., ZILLWOOD, R. M., NGUYEN, H. P. T. & WU, D. 2009. Isolation and Culture of Epithelial Progenitors and Mesenchymal Stem Cells from Human Endometrium1. *Biology of Reproduction,* 80**,** 1136-1145.

GARGETT, C. E. & YE, L. 2012. Endometrial reconstruction from stem cells. *Fertility and Sterility,* 98**,** 11-20.

GARRIDO-GOMEZ, T., DOMINGUEZ, F., QUIÑONERO, A., DIAZ-GIMENO, P., KAPIDZIC, M., GORMLEY, M., ONA, K., PADILLA-ISERTE, P., MCMASTER, M., GENBACEV, O., PERALES, A., FISHER, S. J. & SIMÓN, C. 2017. Defective decidualization during and after severe preeclampsia reveals a possible maternal contribution to the etiology. *Proceedings of the National Academy of Sciences,* 114**,** E8468-E8477.

GARRY, R., HART, R., KARTHIGASU, K. A. & BURKE, C. 2009. A re-appraisal of the morphological changes within the endometrium during menstruation: a hysteroscopic, histological and scanning electron microscopic study. *Human Reproduction,* 24**,** 1393-1401.

GEISERT, R., FAZLEABAS, A., LUCY, M. & MATHEW, D. 2012. Interaction of the conceptus and endometrium to establish pregnancy in mammals: role of interleukin 1β. *Cell and Tissue Research,* 349**,** 825-838.

GELLERSEN, B. & BROSENS, J. 2003. Cyclic AMP and progesterone receptor cross-talk in human endometrium: a decidualizing affair. *J Endocrinol,* 178**,** 357-72.

GELLERSEN, B. & BROSENS, J. J. 2014. Cyclic decidualization of the human endometrium in reproductive health and failure. *Endocr Rev,* 35**,** 851-905.

GENBACEV, O. D., PRAKOBPHOL, A., FOULK, R. A., KRTOLICA, A. R., ILIC, D., SINGER, M. S., YANG, Z.-Q., KIESSLING, L. L., ROSEN, S. D. & FISHER, S. J. 2003. Trophoblast L-Selectin-Mediated Adhesion at the Maternal-Fetal Interface. *Science,* 299**,** 405.

GLASSER, S. R., LAMPELO, S., MUNIR, M. I. & JULIAN, J. 1987. Expression of desmin, laminin and fibronectin during in situ differentiation (decidualization) of rat uterine stromal cells. *Differentiation,* 35**,** 132-142.

GLEESON, L. M., CHAKRABORTY, C., MCKINNON, T. & LALA, P. K. 2001. Insulin-Like Growth Factor-Binding Protein 1 Stimulates Human Trophoblast Migration by Signaling through α5β1 Integrin via Mitogen-Activated Protein Kinase Pathway1. *The Journal of Clinical Endocrinology & Metabolism,* 86**,** 2484-2493.

GODBOLE, G. & MODI, D. 2010. Regulation of decidualization, interleukin-11 and interleukin-15 by homeobox A 10 in endometrial stromal cells. *Journal of Reproductive Immunology,* 85**,** 130-139.

GOLUBOVSKAYA, V. M., NYBERG, C., ZHENG, M., KWEH, F., MAGIS, A., OSTROV, D. & CANCE, W. G. 2008. A small molecule inhibitor, 1,2,4,5-benzenetetraamine tetrahydrochloride, targeting the y397 site of focal adhesion kinase decreases tumor growth. *Journal of medicinal chemistry,* 51**,** 7405-7416.

GONZALEZ, M., NEUFELD, J., REIMANN, K., WITTMANN, S., SAMALECOS, A., WOLF, A., BAMBERGER, A.-M. & GELLERSEN, B. 2011. Expansion of human trophoblastic spheroids is promoted by decidualized endometrial stromal cells and enhanced by heparin-binding epidermal growth factor-like growth factor and interleukin-1β. *Molecular Human Reproduction,* 17**,** 421-433.

GONZÁLEZ, R. N. R., CABALLERO-CAMPO, P., JASPER, M., MERCADER, A., DEVOTO, L., PELLICER, A. & SIMON, C. 2000. Leptin and Leptin Receptor Are Expressed in the Human Endometrium and Endometrial Leptin Secretion Is Regulated by the Human Blastocyst1. *The Journal of Clinical Endocrinology & Metabolism,* 85**,** 4883-4888.

GRAY, C. A., BARTOL, F. F., TARLETON, B. J., WILEY, A. A., JOHNSON, G. A., BAZER, F. W. & SPENCER, T. E. 2001a. Developmental biology of uterine glands. *Biol Reprod,* 65**,** 1311-23.

GRAY, C. A., TAYLOR, K. M., RAMSEY, W. S., HILL, J. R., BAZER, F. W., BARTOL, F. F. & SPENCER, T. E. 2001b. Endometrial glands are required for preimplantation conceptus elongation and survival. *Biol Reprod,* 64**,** 1608-13.

GREAVES, E., TEMP, J., ESNAL-ZUFIURRE, A., MECHSNER, S., HORNE, A. W. & SAUNDERS, P. T. K. 2015. Estradiol Is a Critical Mediator of Macrophage-Nerve Cross Talk in Peritoneal Endometriosis. *The American Journal of Pathology,* 185**,** 2286-2297.

GRECO, T. L., FURLOW, J. D., DUELLO, T. M. & GORSKI, J. 1991. Immunodetection of Estrogen Receptors in Fetal and Neonatal Female Mouse Reproductive Tracts*. *Endocrinology,* 129**,** 1326-1332.

GREWAL, S., CARVER, J., RIDLEY, A. J. & MARDON, H. J. 2010. Human Endometrial Stromal Cell Rho GTPases Have Opposing Roles in Regulating Focal Adhesion Turnover and Embryo Invasion In Vitro1. *Biology of Reproduction,* 83**,** 75-82.

GREWAL, S., CARVER, J. G., RIDLEY, A. J. & MARDON, H. J. 2008. Implantation of the human embryo requires Rac1-dependent endometrial stromal cell migration. *Proceedings of the National Academy of Sciences,* 105**,** 16189.

GRONTHOS, S., MANKANI, M., BRAHIM, J., ROBEY, P. G. & SHI, S. 2000. Postnatal human dental pulp stem cells (DPSCs) in vitro and in vivo. *Proceedings of the National Academy of Sciences,* 97**,** 13625.

GRÜN, D., LYUBIMOVA, A., KESTER, L., WIEBRANDS, K., BASAK, O., SASAKI, N., CLEVERS, H. & VAN OUDENAARDEN, A. 2015. Single-cell messenger RNA sequencing reveals rare intestinal cell types. *Nature,* 525**,** 251-5.

GSTRAUNTHALER, G. 2003. Alternatives to the use of fetal bovine serum: Serum-free cell culture. *ALTEX,* 20**,** 275-81.

GUILLUY, C., SWAMINATHAN, V., GARCIA-MATA, R., O'BRIEN, E. T., SUPERFINE, R. & BURRIDGE, K. 2011. The Rho GEFs LARG and GEF-H1 regulate the mechanical response to force on integrins. *Nature cell biology,* 13**,** 722-727.

GURTNER, G. C., WERNER, S., BARRANDON, Y. & LONGAKER, M. T. 2008. Wound repair and regeneration. *Nature,* 453**,** 314-321.

GURUNG, S., WERKMEISTER, J. A. & GARGETT, C. E. 2015. Inhibition of Transforming Growth Factor-β Receptor signaling promotes culture expansion of undifferentiated human Endometrial Mesenchymal Stem/stromal Cells. *Scientific Reports,* 5**,** 15042.

HAIDER, S., GAMPERL, M., BURKARD, T. R., KUNIHS, V., KAINDL, U., JUNTTILA, S., FIALA, C., SCHMIDT, K., MENDJAN, S., KNÖFLER, M. & LATOS, P. A. 2019. Estrogen Signaling

Drives Ciliogenesis in Human Endometrial Organoids. *Endocrinology,* 160**,** 2282-2297.

HALLAST, P., NAGIRNAJA, L., MARGUS, T. & LAAN, M. 2005. Segmental duplications and gene conversion: Human luteinizing hormone/chorionic gonadotropin β gene cluster. *Genome Research,* 15**,** 1535-1546.

HANASHI, H., SHIOKAWA, S., AKIMOTO, Y., SAKAI, K. E. N., SAKAI, K., SUZUKI, N., KABIR-SALMANI, M., NAGAMATSU, S., IWASHITA, M. & NAKAMURA, Y. 2003. Physiologic Role of Decidual β₁ Integrin and Focal Adhesion Kinase in Embryonic Implantation. *Endocrine Journal,* 50**,** 189-198.

HANNAN, N. J., PAIVA, P., DIMITRIADIS, E. & SALAMONSEN, L. A. 2010a. Models for Study of Human Embryo Implantation: Choice of Cell Lines?1. *Biology of Reproduction,* 82**,** 235-245.

HANNAN, N. J., STEPHENS, A. N., RAINCZUK, A., HINCKS, C., ROMBAUTS, L. J. F. & SALAMONSEN, L. A. 2010b. 2D-DiGE Analysis of the Human Endometrial Secretome Reveals Differences between Receptive and Nonreceptive States in Fertile and Infertile Women. *Journal of Proteome Research,* 9**,** 6256-6264.

HARTMANN, S., RIDLEY, A. J. & LUTZ, S. 2015. The Function of Rho-Associated Kinases ROCK1 and ROCK2 in the Pathogenesis of Cardiovascular Disease. *Frontiers in pharmacology,* 6**,** 276-276.

HARUN, R., RUBAN, L., MATIN, M., DRAPER, J., JENKINS, N. M., LIEW, G. C., ANDREWS, P. W., LI, T. C., LAIRD, S. M. & MOORE, H. D. M. 2006. Cytotrophoblast stem cell lines derived from human embryonic stem cells and their capacity to mimic invasive implantation events. *Human Reproduction,* 21**,** 1349-1358.

HAUSERMANN, H. M., DONNELLY, K. M., BELL, S. C., VERHAGE, H. G. & FAZLEABAS, A. T. 1998. Regulation of the Glycosylated β-Lactoglobulin Homolog, Glycodelin [Placental Protein 14:(PP14)] in the Baboon (Papio anubis) Uterus1. *The Journal of Clinical Endocrinology & Metabolism,* 83**,** 1226-1233.

HECK, J. N., PONIK, S. M., GARCIA-MENDOZA, M. G., PEHLKE, C. A., INMAN, D. R., ELICEIRI, K. W. & KEELY, P. J. 2012. Microtubules regulate GEF-H1 in response to extracellular matrix stiffness. *Molecular biology of the cell,* 23**,** 2583-2592.

HEMPSTOCK, J., CINDROVA-DAVIES, T., JAUNIAUX, E. & BURTON, G. J. 2004a. Endometrial glands as a source of nutrients, growth factors and cytokines during the first trimester of human pregnancy: a morphological and immunohistochemical study. *Reprod Biol Endocrinol,* 2**,** 58.

HEMPSTOCK, J., CINDROVA-DAVIES, T., JAUNIAUX, E. & BURTON, G. J. 2004b. Endometrial glands as a source of nutrients, growth factors and cytokines during the first trimester of human pregnancy: A morphological and immunohistochemical study. *Reproductive Biology and Endocrinology,* 2**,** 58.

HENEWEER, C., ADELMANN, H. G., KRUSE, L. H., DENKER, H. W. & THIE, M. 2003. Human Uterine Epithelial RL95-2 Cells Reorganize Their Cytoplasmic Architecture with Respect to Rho Protein and F-Actin in Response to Trophoblast Binding. *Cells Tissues Organs,* 175**,** 1-8.

HENEWEER, C., SCHMIDT, M., DENKER, H.-W. & THIE, M. 2005. Molecular mechanisms in uterine epithelium during trophoblast binding: the role of small GTPase RhoA in human uterine Ishikawa cells. *Journal of Experimental & Clinical Assisted Reproduction,* 2**,** 4.

HO, H., SINGH, H., ALJOFAN, M. & NIE, G. 2012. A high-throughput in vitro model of human embryo attachment. *Fertility and Sterility,* 97**,** 974-978.

HOHN, H.-P., LINKE, M. & DENKER, H.-W. 2000. Adhesion of trophoblast to uterine epithelium as related to the state of trophoblast differentiation: In vitro studies using cell lines. *Molecular Reproduction and Development,* 57**,** 135-145.

HOLMBERG, J. C., HADDAD, S., WÜNSCHE, V., YANG, Y., ALDO, P. B., GNAINSKY, Y., GRANOT, I., DEKEL, N. & MOR, G. 2012. An In Vitro Model for the Study of Human Implantation. *American Journal of Reproductive Immunology,* 67**,** 169-178.

HUANG, C.-C., ORVIS, G. D., WANG, Y. & BEHRINGER, R. R. 2012. Stromal-to-Epithelial Transition during Postpartum Endometrial Regeneration. *PLOS ONE,* 7**,** e44285.

HUDSON, D. L., O'HARE, M., WATT, F. M. & MASTERS, J. R. W. 2000. Proliferative Heterogeneity in the Human Prostate: Evidence for Epithelial Stem Cells. *Laboratory Investigation,* 80**,** 1243-1250.

HUHTINEN, K., DESAI, R., STÅHLE, M., SALMINEN, A., HANDELSMAN, D. J., PERHEENTUPA, A. & POUTANEN, M. 2012. Endometrial and Endometriotic Concentrations of Estrone and Estradiol Are Determined by Local Metabolism Rather than Circulating Levels. *The Journal of Clinical Endocrinology & Metabolism,* 97**,** 4228-4235.

HWANG, J. H., PARK, M. I., HWANG, Y. Y., YOO, H. J. & MARDON, H. J. 2002. The characteristics of integrins expression in decidualized human endometrial stromal cell induced by 8-Br-cAMP in in vitro. *Experimental & Molecular Medicine,* 34**,** 194-200.

HYNES, R. O. 2002. Integrins: Bidirectional, Allosteric Signaling Machines. *Cell,* 110**,** 673-687.

ICHIKAWA, J. 2010. Serum-free medium with osteogenic supplements induces adipogenesis in rat bone marrow stromal cells. *Cell Biology International,* 34**,** 615-620.

ILLERA, M. J., JUAN, L., STEWART, C. L., CULLINAN, E., RUMAN, J. & LESSEY, B. A. 2000. Effect of peritoneal fluid from women with endometriosis on implantation in the mouse model. *Fertility and Sterility,* 74**,** 41-48.

INOUE, C., YAMAMOTO, H., NAKAMURA, T., ICHIHARA, A. & OKAMOTO, H. 1989. Nicotinamide prolongs survival of primary cultured hepatocytes without involving loss of hepatocyte-specific functions. *Journal of Biological Chemistry,* 264**,** 4747-4750.

IRUELA-ARISPE, M. L., PORTER, P., BORNSTEIN, P. & SAGE, E. H. 1996. Thrombospondin-1, an inhibitor of angiogenesis, is regulated by progesterone in the human endometrium. *J Clin Invest,* 97**,** 403-12.

IRWIN, J. C., KIRK, D., KING, R. J., QUIGLEY, M. M. & GWATKIN, R. B. 1989. Hormonal regulation of human endometrial stromal cells in culture: an in vitro model for decidualization. *Fertil Steril,* 52**,** 761-8.

ISHIZAKI, T., UEHATA, M., TAMECHIKA, I., KEEL, J., NONOMURA, K., MAEKAWA, M. & NARUMIYA, S. 2000. Pharmacological Properties of Y-27632, a Specific Inhibitor of Rho-Associated Kinases. *Molecular Pharmacology,* 57**,** 976.

IVELL, R., BALVERS, M., POHNKE, Y., TELGMANN, R., BARTSCH, O., MILDE-LANGOSCH, K., BAMBERGER, A.-M. & EINSPANIER, A. 2003. Immunoexpression of the relaxin receptor LGR7 in breast and uterine tissues of humans and primates. *Reproductive Biology and Endocrinology,* 1**,** 114.

IWAHASHI, M., MURAGAKI, Y., OOSHIMA, A., YAMOTO, M. & NAKANO, R. 1996. Alterations in distribution and composition of the extracellular matrix during decidualization of the human endometrium. *J Reprod Fertil,* 108**,** 147-55.

IWAHASHI, M., MURAGAKI, Y., OOSHIMA, A., YAMOTO, M. & NAKANO, R. 1997. Alterations in distribution and composition of the extracellular matrix during decidualization of the human endometrium. *International Journal of Gynecology & Obstetrics,* 56**,** 307-307.

JABBOUR, H. N. & CRITCHLEY, H. O. 2001. Potential roles of decidual prolactin in early pregnancy. *Reproduction,* 121**,** 197-205.

JABBOUR, H. N., GUBBAY, O. & CRITCHLEY, H. O. D. 2002. Prolactin action and signalling in the human endometrium. *Reproductive Medicine Review,* 10**,** 117-132.

JERRELL, R. J. & PAREKH, A. 2016. Matrix rigidity differentially regulates invadopodia activity through ROCK1 and ROCK2. *Biomaterials,* 84**,** 119-129.

JOHANSSON, E. & WIDE, L. 1969. PERIOVULATORY LEVELS OF PLASMA PROGESTERONE AND LUTEINIZING HORMONE IN WOMEN. *Acta Endocrinologica,* 62**,** 82-88.

JONES, M. C., FUSI, L., HIGHAM, J. H., ABDEL-HAFIZ, H., HORWITZ, K. B., LAM, E. W. F. & BROSENS, J. J. 2006. Regulation of the SUMO pathway sensitizes differentiating human endometrial stromal cells to progesterone. *Proceedings of the National Academy of Sciences of the United States of America,* 103**,** 16272-16277.

JONES, R. L., CRITCHLEY, H. O. D., BROOKS, J., JABBOUR, H. N. & MCNEILLY, A. S. 1998. Localization and Temporal Expression of Prolactin Receptor in Human Endometrium. *The Journal of Clinical Endocrinology & Metabolism,* 83**,** 258-262.

JONES, R. L., SALAMONSEN, L. A. & FINDLAY, J. K. 2002. Potential roles for endometrial inhibins, activins and follistatin during human embryo implantation and early pregnancy. *Trends in Endocrinology & Metabolism,* 13**,** 144-150.

KAJIHARA, T., JONES, M., FUSI, L., TAKANO, M., FEROZE-ZAIDI, F., PIRIANOV, G., MEHMET, H., ISHIHARA, O., HIGHAM, J. M., LAM, E. W. & BROSENS, J. J. 2006. Differential expression of FOXO1 and FOXO3a confers resistance to oxidative cell death upon endometrial decidualization. *Mol Endocrinol,* 20**,** 2444-55.

KAJIHARA, T., TANAKA, K., OGURO, T., TOCHIGI, H., PRECHAPANICH, J., UCHINO, S., ITAKURA, A., SUCUROVIC, S., MURAKAMI, K., BROSENS, J. J. & ISHIHARA, O. 2014. Androgens modulate the morphological characteristics of human endometrial stromal cells decidualized in vitro. *Reprod Sci,* 21**,** 372-80.

KALLURI, R. 2016. The biology and function of fibroblasts in cancer. *Nature Reviews Cancer,* 16**,** 582.

KAMIO, K., LIU, X., SUGIURA, H., TOGO, S., KOBAYASHI, T., KAWASAKI, S., WANG, X., MAO, L., AHN, Y., HOGABOAM, C., TOEWS, M. L. & RENNARD, S. I. 2007. Prostacyclin Analogs Inhibit Fibroblast Contraction of Collagen Gels through the cAMP-PKA Pathway. *American Journal of Respiratory Cell and Molecular Biology,* 37**,** 113-120.

KAMM, K. E. & STULL, J. T. 1985. The Function of Myosin and Myosin Light Chain Kinase Phosphorylation in Smooth Muscle. *Annual Review of Pharmacology and Toxicology,* 25**,** 593-620.

KANE, M. T., MORGAN, P. M. & COONAN, C. 1997. Peptide growth factors and preimplantation development. *Hum Reprod Update,* 3**,** 137-57.

KANEMATSU, D., SHOFUDA, T., YAMAMOTO, A., BAN, C., UEDA, T., YAMASAKI, M. & KANEMURA, Y. 2011. Isolation and cellular properties of mesenchymal cells derived from the decidua of human term placenta. *Differentiation,* 82**,** 77-88.

KARPOVICH, N., KLEMMT, P., HWANG, J. H., MCVEIGH, J. E., HEATH, J. K., BARLOW, D. H. & MARDON, H. J. 2005. The Production of Interleukin-11 and Decidualization Are Compromised in Endometrial Stromal Cells Derived from Patients with Infertility. *The Journal of Clinical Endocrinology & Metabolism,* 90**,** 1607-1612.

KARTHAUS, W. R., IAQUINTA, P. J., DROST, J., GRACANIN, A., VAN BOXTEL, R., WONGVIPAT, J., DOWLING, C. M., GAO, D., BEGTHEL, H., SACHS, N., VRIES, R. G. J., CUPPEN, E., CHEN, Y., SAWYERS, C. L. & CLEVERS, H. C. 2014. Identification of multipotent luminal progenitor cells in human prostate organoid cultures. *Cell,* 159**,** 163-175.

KASTNER, P., KRUST, A., TURCOTTE, B., STROPP, U., TORA, L., GRONEMEYER, H. & CHAMBON, P. 1990. Two distinct estrogen-regulated promoters generate transcripts encoding the two functionally different human progesterone receptor forms A and B. *The EMBO Journal,* 9**,** 1603-1614.

KAYA, H. S., HANTAK, A. M., STUBBS, L. J., TAYLOR, R. N., BAGCHI, I. C. & BAGCHI, M. K. 2015. Roles of progesterone receptor A and B isoforms during human endometrial decidualization. *Mol Endocrinol,* 29**,** 882-95.

KELLEHER, A. M., BURNS, G. W., BEHURA, S., WU, G. & SPENCER, T. E. 2016. Uterine glands impact uterine receptivity, luminal fluid homeostasis and blastocyst implantation. *Scientific reports,* 6**,** 38078-38078.

KELLEHER, A. M., DEMAYO, F. J. & SPENCER, T. E. 2019. Uterine Glands: Developmental Biology and Functional Roles in Pregnancy. *Endocrine Reviews,* 40**,** 1424-1445.

KISALUS, L. L., HERR, J. C. & LITTLE, C. D. 1987. Immunolocalization of extracellular matrix proteins and collagen synthesis in first-trimester human decidua. *The Anatomical Record,* 218**,** 402-415.

KLEINMAN, H. K. & MARTIN, G. R. 2005. Matrigel: Basement membrane matrix with biological activity. *Seminars in Cancer Biology,* 15**,** 378-386.

KLETZKY, O. A., ROSSMAN, F., BERTOLLI, S. I., PLATT, L. D. & MISHELL, D. R. 1985. Dynamics of human chorionic gonadotropin, prolactin, and growth hormone in serum and amniotic fluid throughout normal human pregnancy. *American Journal of Obstetrics and Gynecology,* 151**,** 878-884.

KOBAK, D. & BERENS, P. 2018. The art of using t-SNE for single-cell transcriptomics. *bioRxiv***,** 453449.

KOO, B.-K., STANGE, D. E., SATO, T., KARTHAUS, W., FARIN, H. F., HUCH, M., VAN ES, J. H. & CLEVERS, H. 2012. Controlled gene expression in primary Lgr5 organoid cultures. *Nature Methods,* 9**,** 81-83.

KOPPERUD, R., KRAKSTAD, C., SELHEIM, F. & DØSKELAND, S. O. 2003. cAMP effector mechanisms. Novel twists for an 'old' signaling system. *FEBS Letters,* 546**,** 121-126.

KORCH, C., SPILLMAN, M. A., JACKSON, T. A., JACOBSEN, B. M., MURPHY, S. K., LESSEY, B. A., JORDAN, V. C. & BRADFORD, A. P. 2012. DNA profiling analysis of endometrial and ovarian cell lines reveals misidentification, redundancy and contamination. *Gynecologic Oncology,* 127**,** 241-248.

KOTHAPALLI, R., BUYUKSAL, I., WU, S. Q., CHEGINI, N. & TABIBZADEH, S. 1997. Detection of ebaf, a novel human gene of the transforming growth factor beta superfamily association of gene expression with endometrial bleeding. *The Journal of Clinical Investigation,* 99**,** 2342-2350.

KRAGH-HANSEN, U. 1981. Molecular aspects of ligand binding to serum albumin. *Pharmacol Rev,* 33**,** 17-53.

KRAUSE, C., GUZMAN, A. & KNAUS, P. 2011. Noggin. *The International Journal of Biochemistry & Cell Biology,* 43**,** 478-481.

KRESSE, H. & SCHÖNHERR, E. 2001. Proteoglycans of the extracellular matrix and growth control. *J Cell Physiol,* 189**,** 266-74.

KURAMOTO, H., TAMURA, S. & NOTAKE, Y. 1972. Establishment of a cell line of human endometrial adenocarcinoma in vitro. *American Journal of Obstetrics and Gynecology,* 114**,** 1012-1019.

KURITA, T., YOUNG, P., BRODY, J. R., LYDON, J. P., O'MALLEY, B. W. & CUNHA, G. R. 1998. Stromal progesterone receptors mediate the inhibitory effects of progesterone on estrogen-induced uterine epithelial cell deoxyribonucleic acid synthesis. *Endocrinology,* 139**,** 4708-13.

LADINES-LLAVE, C. A., MARUO, T., MANALO, A. S. & MOCHIZUKI, M. 1991. Cytologic localization of epidermal growth factor and its receptor in developing human placenta varies over the course of pregnancy. *American Journal of Obstetrics & Gynecology,* 165**,** 1377-1382.

LAMAS, M., MONACO, L., ZAZOPOULOS, E., LALLI, E., TAMAI, K., PENNA, L., MAZZUCCHELLI, C., NANTEL, F., FOULKES, N. S., SASSONE-CORSI, P., BUSBY, S. J. W., GROSVELD, F. G. & LATCHMAN, D. S. 1996. CREM: a master-switch in the transcriptional response to

cAMP. *Philosophical Transactions of the Royal Society of London. Series B: Biological Sciences,* 351**,** 561-567.

LAMBRICHT, L., DE BERDT, P., VANACKER, J., LEPRINCE, J., DIOGENES, A., GOLDANSAZ, H., BOUZIN, C., PRÉAT, V., DUPONT-GILLAIN, C. & DES RIEUX, A. 2014. The type and composition of alginate and hyaluronic-based hydrogels influence the viability of stem cells of the apical papilla. *Dent Mater,* 30**,** e349-61.

LANCASTER, M. A. & KNOBLICH, J. A. 2014a. Generation of cerebral organoids from human pluripotent stem cells. *Nat Protoc,* 9**,** 2329-40.

LANCASTER, M. A. & KNOBLICH, J. A. 2014b. Organogenesis in a dish: modeling development and disease using organoid technologies. *Science,* 345**,** 1247125.

LASH, G. E., HORNBUCKLE, J., BRUNT, A., KIRKLEY, M., SEARLE, R. F., ROBSON, S. C. & BULMER, J. N. 2007. Effect of Low Oxygen Concentrations on Trophoblast-Like Cell Line Invasion. *Placenta,* 28**,** 390-398.

LAWN, A., WILSON, E. & FINN, C. 1971. THE ULTRASTRUCTURE OF HUMAN DECIDUAL AND PREDECIDUAL CELLS. *Reproduction,* 26**,** 85-90.

LEE, K. & DEMAYO, F. 2004. Animal models of implantation. *Reproduction,* 128**,** 679-695.

LEITAO, B. B., JONES, M. C. & BROSENS, J. J. 2011. The SUMO E3-ligase PIAS1 couples reactive oxygen species-dependent JNK activation to oxidative cell death. *FASEB journal : official publication of the Federation of American Societies for Experimental Biology,* 25**,** 3416-3425.

LEJEUNE, B., HOECK, J. V. & LEROY, F. 1981. Transmitter role of the luminal uterine epithelium in the induction of decidualization in rats. *Reproduction,* 61**,** 235-240.

LI, Q., KANNAN, A., WANG, W., DEMAYO, F. J., TAYLOR, R. N., BAGCHI, M. K. & BAGCHI, I. C. 2007. Bone Morphogenetic Protein 2 Functions via a Conserved Signaling Pathway Involving Wnt4 to Regulate Uterine Decidualization in the Mouse and the Human. *Journal of Biological Chemistry,* 282**,** 31725-31732.

LINDENBERG, S., NIELSEN, M. H. & LENZ, S. 1985. In Vitro Studies of Human Blastocyst Implantationa. *Annals of the New York Academy of Sciences,* 442**,** 368-374.

LIU, S., YANG, X., LIU, Y., WANG, X. & YAN, Q. 2011. sLeX/L-selectin mediates adhesion in vitro implantation model. *Molecular and Cellular Biochemistry,* 350**,** 185-192.

LO, C. M., WANG, H. B., DEMBO, M. & WANG, Y. L. 2000. Cell movement is guided by the rigidity of the substrate. *Biophysical journal,* 79**,** 144-152.

LOPES, F., DESMARAIS, J. & MURPHY, B. 2004. Embryonic diapause and its regulation. *Reproduction,* 128**,** 669-678.

LUCAS, E. S., DYER, N. P., MURAKAMI, K., LEE, Y. H., CHAN, Y. W., GRIMALDI, G., MUTER, J., BRIGHTON, P. J., MOORE, J. D., PATEL, G., CHAN, J. K., TAKEDA, S., LAM, E. W., QUENBY, S., OTT, S. & BROSENS, J. J. 2016. Loss of Endometrial Plasticity in Recurrent Pregnancy Loss. *Stem Cells,* 34**,** 346-56.

LUCAS, E. S., SALKER, M. S. & BROSENS, J. J. 2013. Uterine plasticity and reproductive fitness. *Reprod Biomed Online,* 27**,** 506-14.

LUCAS, E. S., VRLJICAK, P., DINIZ-DA-COSTA, M. M., BRIGHTON, P. J., KONG, C. S., LIPECKI, J., FISHWICK, K., MUTER, J., OTT, S. & BROSENS, J. J. 2018. Reconstruction of the Decidual Pathways in Human Endometrial Cells Using Single-Cell RNA-Seq. *bioRxiv***,** 368829.

LUCAS, E. S., VRLJICAK, P., MUTER, J., DINIZ-DA-COSTA, M. M., BRIGHTON, P. J., KONG, C.-S., LIPECKI, J., FISHWICK, K., ODENDAAL, J., EWINGTON, L. J., QUENBY, S., OTT, S. & BROSENS, J. J. 2019. Recurrent pregnancy loss is associated with a pro-senescent decidual response during the peri-implantation window. *bioRxiv***,** 368829.

LUNI, C., SERENA, E. & ELVASSORE, N. 2014. Human-on-chip for therapy development and fundamental science. *Curr Opin Biotechnol,* 25**,** 45-50.

LUSCOMBE, NM, ., AUSTIN, SE, ., BERMAN, HM, ., THORNTON, JM & . 2000. An overview of the structures of protein-DNA complexes.

MACOSKO, E. Z., BASU, A., SATIJA, R., NEMESH, J., SHEKHAR, K., GOLDMAN, M., TIROSH, I., BIALAS, A. R., KAMITAKI, N., MARTERSTECK, E. M., TROMBETTA, J. J., WEITZ, D. A., SANES, J. R., SHALEK, A. K., REGEV, A. & MCCARROLL, S. A. 2015. Highly Parallel Genome-wide Expression Profiling of Individual Cells Using Nanoliter Droplets. *Cell,* 161**,** 1202-1214.

MAHFOUDI, A., FAUCONNET, S., BRIDE, J., BECK, L., REMY-MARTIN, J.-P., NICOLLIER, M. & ADESSI, G. L. 1992. Serum-free culture of stromal and functionally polarized epithelial cells of guinea-pig endometrium: a potential model for the study of epithelial-stromal paracrine interactions. *Biology of the Cell,* 74**,** 255-265.

MANGAL, R. K., WIEHLE, R. D., POINDEXTER, A. N. & WEIGEL, N. L. 1997. Differential expression of uterine progesterone receptor forms A and B during the menstrual cycle. *J Steroid Biochem Mol Biol,* 63**,** 195-202.

MARDON, H., GREWAL, S. & MILLS, K. 2007. Experimental Models for Investigating Implantation of the Human Embryo. *Semin Reprod Med,* 25**,** 410-417.

MARJORAM, R. J., LESSEY, E. C. & BURRIDGE, K. 2014. Regulation of RhoA activity by adhesion molecules and mechanotransduction. *Current molecular medicine,* 14**,** 199-208.

MARUO, T., MATSUO, H., OTANI, T. & MOCHIZUKI, M. 1997. Epidermal growth factor (EGF) regulates trophoblast proliferation and endocrine function in synergy with thyroid hormone: A review. *Placenta,* 18**,** 27-39.

MASLAR, I. A. & RIDDICK, D. H. 1979. Prolactin production by human endometrium during the normal menstrual cycle. *American Journal of Obstetrics and Gynecology,* 135**,** 751-754.

MASUDA, H., ANWAR, S. S., BÜHRING, H.-J., RAO, J. R. & GARGETT, C. E. 2012. A Novel Marker of Human Endometrial Mesenchymal Stem-Like Cells. *Cell Transplantation,* 21**,** 2201-2214.

MATSUOKA, A., KIZUKA, F., LEE, L., TAMURA, I., TANIGUCHI, K., ASADA, H., TAKETANI, T., TAMURA, H. & SUGINO, N. 2010. Progesterone Increases Manganese Superoxide Dismutase Expression via a cAMP-Dependent Signaling Mediated by Noncanonical Wnt5a Pathway in Human Endometrial Stromal Cells. *The Journal of Clinical Endocrinology & Metabolism,* 95**,** E291-E299.

MAYR, B. & MONTMINY, M. 2001. Transcriptional regulation by the phosphorylation-dependent factor CREB. *Nature Reviews Molecular Cell Biology,* 2**,** 599-609.

MCINNES, L., HEALY, J., SAUL, N. & GROSSBERGER, L. 2018. UMAP: Uniform Manifold Approximation and Projection. *Journal of Open Source Software,* 3**,** 861.

MEEKINS, J. W., PIJNENBORG, R., HANSSENS, M., MCFADYEN, I. R. & VAN ASSHE, A. 1994. A study of placental bed spiral arteries and trophoblast invasion in normal and severe pre-eclamptic pregnancies. *BJOG: An International Journal of Obstetrics & Gynaecology,* 101**,** 669-674.

MERLE, B., DURUSSEL, L., DELMAS, P. & CLÉZARDIN, P. 2000. Decorin inhibits cell migration through a process requiring its glycosaminoglycan side chain. *Journal of cellular biochemistry,* 75**,** 538-46.

MERLOT, A. M., KALINOWSKI, D. S. & RICHARDSON, D. R. 2014. Unraveling the mysteries of serum albumin-more than just a serum protein. *Front Physiol,* 5**,** 299.

MERTENS, H. J., HEINEMAN, M. J. & EVERS, J. L. 2002. The expression of apoptosis-related proteins Bcl-2 and Ki67 in endometrium of ovulatory menstrual cycles. *Gynecol Obstet Invest,* 53**,** 224-30.

MESEGUER, M., APLIN, J. D., CABALLERO-CAMPO, P., O'CONNOR, J. E., MARTÍN, J. C., REMOHÍ, J., PELLICER, A. & SIMÓN, C. 2001. Human Endometrial Mucin MUC1 Is Up-Regulated by Progesterone and Down-Regulated In Vitro by the Human Blastocyst1. *Biology of Reproduction,* 64**,** 590-601.

MI, H., MURUGANUJAN, A., CASAGRANDE, J. T. & THOMAS, P. D. 2013. Large-scale gene function analysis with the PANTHER classification system. *Nat Protoc,* 8**,** 1551-66.

MICALLEF, L., VEDRENNE, N., BILLET, F., COULOMB, B., DARBY, I. A. & DESMOULIÈRE, A. 2012. The myofibroblast, multiple origins for major roles in normal and pathological tissue repair. *Fibrogenesis & tissue repair,* 5**,** S5-S5.

MIKHAILIK, A., MAZELLA, J., LIANG, S. & TSENG, L. 2009. Notch ligand-dependent gene expression in human endometrial stromal cells. *Biochemical and Biophysical Research Communications,* 388**,** 479-482.

MILNE, S. A., PERCHICK, G. B., BODDY, S. C. & JABBOUR, H. N. 2001. Expression, Localization, and Signaling of PGE2 and EP2/EP4 Receptors in Human Nonpregnant Endometrium across the Menstrual Cycle. *The Journal of Clinical Endocrinology & Metabolism,* 86**,** 4453-4459.

MITAKA, T., SATTLER, C. A., SATTLER, G. L., SARGENT, L. M. & PITOT, H. C. 1991. Multiple cell cycles occur in rat hepatocytes cultured in the presence of nicotinamide and epidermal growth factor. *Hepatology,* 13**,** 21-30.

MITRA, S. K., HANSON, D. A. & SCHLAEPFER, D. D. 2005. Focal adhesion kinase: in command and control of cell motility. *Nature Reviews Molecular Cell Biology,* 6**,** 56-68.

MO, B., VENDROV, A. E., PALOMINO, W. A., DUPONT, B. R., APPARAO, K. B. C. & LESSEY, B. A. 2006. ECC-1 Cells: A Well-Differentiated Steroid-Responsive Endometrial Cell Line with Characteristics of Luminal Epithelium1. *Biology of Reproduction,* 75**,** 387-394.

MONACO, J. L. & LAWRENCE, W. T. 2003. Acute wound healing: An overview. *Clinics in Plastic Surgery,* 30**,** 1-12.

MOORE, S. W., ROCA-CUSACHS, P. & SHEETZ, M. P. 2010. Stretchy proteins on stretchy substrates: the important elements of integrin-mediated rigidity sensing. *Developmental cell,* 19**,** 194-206.

MORELLI, S. S., RAMESHWAR, P. & GOLDSMITH, L. T. 2013. Experimental Evidence for Bone Marrow as a Source of Nonhematopoietic Endometrial Stromal and Epithelial Compartment Cells in a Murine Model1. *Biology of Reproduction,* 89.

MOTE, P. A., BALLEINE, R. L., MCGOWAN, E. M. & CLARKE, C. L. 1999. Colocalization of progesterone receptors A and B by dual immunofluorescent histochemistry in human endometrium during the menstrual cycle. *J Clin Endocrinol Metab,* 84**,** 2963-71.

MOTTE, S. & KAUFMAN, L. J. 2013. Strain stiffening in collagen I networks. *Biopolymers,* 99**,** 35-46.

MUNNE, S. & WELLS, D. 2017. Detection of mosaicism at blastocyst stage with the use of high-resolution next-generation sequencing. *Fertil Steril,* 107**,** 1085-1091.

MURAKAMI, K., BHANDARI, H., LUCAS, E. S., TAKEDA, S., GARGETT, C. E., QUENBY, S., BROSENS, J. J. & TAN, B. K. 2013. Deficiency in Clonogenic Endometrial Mesenchymal Stem Cells in Obese Women with Reproductive Failure – a Pilot Study. *PLOS ONE,* 8**,** e82582.

MUTER, J., ALAM, M. T., VRLJICAK, P., BARROS, F. S. V., RUANE, P. T., EWINGTON, L. J., APLIN, J. D., WESTWOOD, M. & BROSENS, J. J. 2017. The Glycosyltransferase EOGT Regulates Adropin Expression in Decidualizing Human Endometrium. *Endocrinology,* 159**,** 994-1004.

MUTER, J., BRIGHTON, P. J., LUCAS, E. S., LACEY, L., SHMYGOL, A., QUENBY, S., BLANKS, A. M. & BROSENS, J. J. 2016. Progesterone-Dependent Induction of Phospholipase C-Related Catalytically Inactive Protein 1 (PRIP-1) in Decidualizing Human Endometrial Stromal Cells. *Endocrinology,* 157**,** 2883-2893.

MUTER, J., LUCAS, E. S., CHAN, Y.-W., BRIGHTON, P. J., MOORE, J. D., LACEY, L., QUENBY, S., LAM, E. W. F. & BROSENS, J. J. 2015. The clock protein period 2 synchronizes mitotic expansion and decidual transformation of human endometrial stromal cells. *FASEB journal : official publication of the Federation of American Societies for Experimental Biology,* 29**,** 1603-1614.

NARAYANAN, K. L., CHOPRA, V., ROSAS, H. D., MALARICK, K. & HERSCH, S. 2016. Rho Kinase Pathway Alterations in the Brain and Leukocytes in Huntington's Disease. *Molecular Neurobiology,* 53**,** 2132-2140.

NARUMIYA, S., ISHIZAKI, T. & UFHATA, M. 2000. Use and properties of ROCK-specific inhibitor Y-27632. *In:* BALCH, W. E., DER, C. J. & HALL, A. (eds.) *Methods in Enzymology.* Academic Press.

NEEDHAM, L. K., TENNEKOON, G. I. & MCKHANN, G. M. 1987. Selective growth of rat Schwann cells in neuron- and serum-free primary culture. *The Journal of Neuroscience,* 7**,** 1.

NELSON, G., WORDSWORTH, J., WANG, C., JURK, D., LAWLESS, C., MARTIN-RUIZ, C. & VON ZGLINICKI, T. 2012. A senescent cell bystander effect: senescence-induced senescence. *Aging Cell,* 11**,** 345-349.

NHS MATERNITY STATISTICS, N. December 5 , 2013. *NHS Maternity Statistics - England, 2012-13* [Online]. Health and Social Care Information Centre website . http://www.hscic.gov.uk/catalogue/PUB12744 . NHS. [Accessed 12/12/2019 2019].

NISHIDA, M., KASAHARA, K., KANEKO, M., IWASAKI, H. & HAYASHI, K. 1985. [Establishment of a new human endometrial adenocarcinoma cell line, Ishikawa cells, containing estrogen and progesterone receptors]. *Nihon Sanka Fujinka Gakkai zasshi,* 37**,** 1103-1111.

NOEL, S., HERMAN, A., JOHNSON, G., GRAY, C., STEWART, M. D., BAZER, F., GERTLER, A. & SPENCER, T. 2003. Ovine placental lactogen specifically binds endometrial glands of the ovine uterus. *Biology of reproduction,* 68**,** 772-80.

NYACHIEO, A., CHAI, D. C., DEPREST, J., MWENDA, J. M. & D'HOOGHE, T. M. 2007. The Baboon as a Research Model for the Study of Endometrial Biology, Uterine Receptivity and Embryo Implantation. *Gynecologic and Obstetric Investigation,* 64**,** 149-155.

OHMICHI, H., KOSHIMIZU, U., MATSUMOTO, K. & NAKAMURA, T. 1998. Hepatocyte growth factor (HGF) acts as a mesenchyme-derived morphogenic factor during fetal lung development. *Development,* 125**,** 1315.

OKULICZ, W. C., ACE, C. I. & SCARRELL, R. 1997. Zonal Changes in Proliferation in the Rhesus Endometrium During the Late Secretory Phase and Menses. *Proceedings of the Society for Experimental Biology and Medicine,* 214**,** 132-138.

OLIVEIRA, G. B. D., VALE, A. M. D., SANTOS, A. C. D., MOURA, C. E. B. D., ROCHA, H. A. D. O. & OLIVEIRA, M. F. D. 2015. Composition and significance of glycosaminoglycans in the uterus and placenta of mammals. *Brazilian Archives of Biology and Technology,* 58**,** 512-520.

OSINKA, A., POPRZECZKO, M., ZIELINSKA, M. M., FABCZAK, H., JOACHIMIAK, E. & WLOGA, D. 2019. Ciliary Proteins: Filling the Gaps. Recent Advances in Deciphering the Protein Composition of Motile Ciliary Complexes. *Cells,* 8.

OTT, M., GOGVADZE, V., ORRENIUS, S. & ZHIVOTOVSKY, B. 2007. Mitochondria, oxidative stress and cell death. *Apoptosis,* 12**,** 913-22.

OZBEN, T. 2007. Oxidative stress and apoptosis: impact on cancer therapy. *J Pharm Sci,* 96**,** 2181-96.

O'RAHILLY, R & . 1973. The embryology and anatomy of the uterus. Th*e Uterus*: Baltimore, MD : Williams & Wilkins.

PADYKULA, H. 1991. Regeneration in the primate uterus: the role of stem cells. *Ann N Y Acad Sci*: Plenum Medical Book Company.

PADYKULA, H. A., COLES, L. G., OKULICZ, W. C., RAPAPORT, S. I., MCCRACKEN, J. A., KING, N. W., JR., LONGCOPE, C. & KAISERMAN-ABRAMOF, I. R. 1989. The Basalis of the

Primate Endometrium: A Bifunctional Germinal Compartment1. *Biology of Reproduction,* 40**,** 681-690.

PALEJWALA, S., TSENG, L., WOJTCZUK, A., WEISS, G. & GOLDSMITH, L. T. 2002. Relaxin Gene and Protein Expression and Its Regulation of Procollagenase and Vascular Endothelial Growth Factor in Human Endometrial Cells1. *Biology of Reproduction,* 66**,** 1743-1748.

PARIA, B. C., SONG, H. & DEY, S. K. 2001. Implantation: molecular basis of embryo-uterine dialogue. *Int J Dev Biol,* 45**,** 597-605.

PARK, D. W., CHOI, D. S., RYU, H.-S., KWON, H. C., JOO, H. & MIN, C. K. 2003. A well-defined in vitro three-dimensional culture of human endometrium and its applicability to endometrial cancer invasion. *Cancer Letters,* 195**,** 185-192.

PARK, S. E., GEORGESCU, A. & HUH, D. 2019. Organoids-on-a-chip. *Science.* United States: some rights reserved; exclusive licensee American Association for the Advancement of Science. No claim to original U.S. Government Works.

PATTERSON, A. L., ZHANG, L., ARANGO, N. A., TEIXEIRA, J. & PRU, J. K. 2012. Mesenchymal-to-Epithelial Transition Contributes to Endometrial Regeneration Following Natural and Artificial Decidualization. *Stem Cells and Development,* 22**,** 964-974.

PELLEGRINI, G., GOLISANO, O., PATERNA, P., LAMBIASE, A., BONINI, S., RAMA, P. & DE LUCA, M. 1999. Location and Clonal Analysis of Stem Cells and Their Differentiated Progeny in the Human Ocular Surface. *The Journal of Cell Biology,* 145**,** 769-782.

PETER DURAIRAJ, R. R. 2017. *Characterization of clonal and regenerative perivascular stem cells in human endometrium.* PhD, University of Warwick.

PETERSEN, A., BENTIN-LEY, U., RAVN, V., QVORTRUP, K., SØRENSEN, S., ISLIN, H., SJÖGREN, A., MOSSELMANN, S. & HAMBERGER, L. 2005. The antiprogesterone Org 31710 inhibits human blastocyst-endometrial interactions in vitro. *Fertility and Sterility,* 83**,** 1255-1263.

PETRIE, R. J. & YAMADA, K. M. 2012. At the leading edge of three-dimensional cell migration. *Journal of cell science,* 125**,** 5917-5926.

PIERRO, E., MINICI, F., ALESIANI, O., MICELI, F., PROTO, C., SCREPANTI, I., MANCUSO, S. & LANZONE, A. 2001. Stromal-Epithelial Interactions Modulate Estrogen Responsiveness in Normal Human Endometrium1. *Biology of Reproduction,* 64**,** 831-838.

QUENBY, S., VINCE, G., FARQUHARSON, R. & APLIN, J. 2002. Recurrent miscarriage: a defect in nature's quality control? *Hum Reprod,* 17**,** 1959-63.

RAMSDEN, C. M., POWNER, M. B., CARR, A.-J. F., SMART, M. J. K., DA CRUZ, L. & COFFEY, P. J. 2013. Stem cells in retinal regeneration: past, present and future. *Development (Cambridge, England),* 140**,** 2576-2585.

RESHEF, E., LEI, Z. M., RAO, C. V., PRIDHAM, D. D., CHEGINI, N. & LUBORSKY, J. L. 1990. The presence of gonadotropin receptors in nonpregnant human uterus, human placenta, fetal membranes, and decidua. *J Clin Endocrinol Metab,* 70**,** 421-30.

RIDER, V., CARLONE, D. L., WITROCK, D., CAI, C. & OLIVER, N. 1992. Uterine fibronectin mRNA content and localization are modulated during implantation. *Developmental Dynamics,* 195**,** 1-14.

ROBEY, P. G. 2000. Series Introduction: Stem cells near the century mark. *The Journal of Clinical Investigation,* 105**,** 1489-1491.

ROBINSON, M. D. & OSHLACK, A. 2010. A scaling normalization method for differential expression analysis of RNA-seq data. *Genome Biol,* 11**,** R25.

ROCK, J. & BARTLETT, M. K. 1937. BIOPSY STUDIES OF HUMAN ENDOMETRIUM: CRITERIA OF DATING AND INFORMATION ABOUT AMENORRHEA, MENORRHAGIA AND TIME OF OVULATION. *Journal of the American Medical Association,* 108**,** 2022-2028.

RODGERS, W. H., MATRISIAN, L. M., GIUDICE, L. C., DSUPIN, B., CANNON, P., SVITEK, C., GORSTEIN, F. & OSTEEN, K. G. 1994. Patterns of matrix metalloproteinase expression in cycling endometrium imply differential functions and regulation by steroid hormones. *The Journal of Clinical Investigation,* 94**,** 946-953.

ROGERS, P. A. 1996. Endometrial vasculature in Norplant users. *Hum Reprod,* 11 Suppl 2**,** 45-50.

ROMIJN, H. J. 1988. Development and advantages of serum-free, chemically defined nutrient media for culturing of nerve tissue. *Biology of the Cell,* 63**,** 253-268.

RUBIN, J. S., BOTTARO, D. P., CHEDID, M., MIKI, T., RON, D., CHEON, H.-G., TAYLOR, W. G., FORTNEY, E., SAKATA, H., FINCH, P. W. & LAROCHELLE, W. J. 1995. Keratinocyte growth factor. *Cell Biology International,* 19**,** 399-412.

RUTANEN, E.-M., KOISTINEN, R., WAHLSTROM, T., BOHN, H., RANTA, T. & SEPPALA, M. 1985. Synthesis of Placental Protein 12 by Human Decidua. *Endocrinology,* 116**,** 1304-1309.

RØNNOV-JESSEN, L. P., OLE WILLIAM. 1993. Induction of alpha-smooth muscle actin by transforming growth factor-beta1 in quiescent human breast gland fibroblasts. Implications for myofibroblast generation in breast neoplasia. *Lab Invest,* 68**,** 696-707.

SALAMONSEN, L. A. 2003. Tissue injury and repair in the female human reproductive tract. *Reproduction,* 125**,** 301-311.

SALAMONSEN, L. A., EVANS, J., NGUYEN, H. P. T. & EDGELL, T. A. 2016. The Microenvironment of Human Implantation: Determinant of Reproductive Success. *American Journal of Reproductive Immunology,* 75**,** 218-225.

SALAMONSEN, L. A. & WOOLLEY, D. E. 1996. Matrix metalloproteinases in normal menstruation. *Human Reproduction,* 11**,** 124-133.

SALKER, M. S., NAUTIYAL, J., STEEL, J. H., WEBSTER, Z., SUĆUROVIĆ, S., NICOU, M., SINGH, Y., LUCAS, E. S., MURAKAMI, K., CHAN, Y. W., JAMES, S., ABDALLAH, Y., CHRISTIAN, M., CROY, B. A., MULAC-JERICEVIC, B., QUENBY, S. & BROSENS, J. J. 2012a. Disordered IL-33/ST2 activation in decidualizing stromal cells prolongs uterine receptivity in women with recurrent pregnancy loss. *PLoS One,* 7**,** e52252.

SALKER, M. S., NAUTIYAL, J., STEEL, J. H., WEBSTER, Z., ŠUĆUROVIĆ, S., NICOU, M., SINGH, Y., LUCAS, E. S., MURAKAMI, K., CHAN, Y.-W., JAMES, S., ABDALLAH, Y., CHRISTIAN, M., CROY, B. A., MULAC-JERICEVIC, B., QUENBY, S. & BROSENS, J. J. 2012b. Disordered IL-33/ST2 Activation in Decidualizing Stromal Cells Prolongs Uterine Receptivity in Women with Recurrent Pregnancy Loss. *PLOS ONE,* 7**,** e52252.

SALLEH, N. & GIRIBABU, N. 2014. Leukemia inhibitory factor: roles in embryo implantation and in nonhormonal contraception. *ScientificWorldJournal,* 2014**,** 201514.

SATO, T., STANGE, D. E., FERRANTE, M., VRIES, R. G. J., VAN ES, J. H., VAN DEN BRINK, S., VAN HOUDT, W. J., PRONK, A., VAN GORP, J., SIERSEMA, P. D. & CLEVERS, H. 2011. Long-term Expansion of Epithelial Organoids From Human Colon, Adenoma, Adenocarcinoma, and Barrett's Epithelium. *Gastroenterology,* 141**,** 1762-1772.

SATO, T., VRIES, R. G., SNIPPERT, H. J., VAN DE WETERING, M., BARKER, N., STANGE, D. E., VAN ES, J. H., ABO, A., KUJALA, P., PETERS, P. J. & CLEVERS, H. 2009. Single Lgr5 stem cells build crypt-villus structures in vitro without a mesenchymal niche. *Nature,* 459**,** 262-265.

SATOH, K., KIKUCHI, N., SATOH, T., KUROSAWA, R., SUNAMURA, S., SIDDIQUE, M. A. H., OMURA, J., YAOITA, N. & SHIMOKAWA, H. 2018. Identification of Novel Therapeutic Targets for Pulmonary Arterial Hypertension. *International journal of molecular sciences,* 19**,** 4081.

SATYASWAROOP, P. G. & TABIBZADEH, S. S. 1991. Extracellular Matrix and the Patterns of Differentiation of Human Endometrial Carcinomas in Vitro and in Vivo. *Cancer Research,* 51**,** 5661.

SCHAEFER, L. & SCHAEFER, R. M. 2010. Proteoglycans: from structural compounds to signaling molecules. *Cell Tissue Res,* 339**,** 237-46.

SCHILLER, M., DENNLER, S., ANDEREGG, U., KOKOT, A., SIMON, J. C., LUGER, T. A., MAUVIEL, A. & BÖHM, M. 2010. Increased cAMP Levels Modulate Transforming Growth Factor-β/Smad-induced Expression of Extracellular Matrix Components and Other Key Fibroblast Effector Functions. *Journal of Biological Chemistry,* 285**,** 409-421.

SCHWAB, K. E., CHAN, R. W. S. & GARGETT, C. E. 2005. Putative stem cell activity of human endometrial epithelial and stromal cells during the menstrual cycle. *Fertility and Sterility,* 84**,** 1124-1130.

SCHWAB, K. E. & GARGETT, C. E. 2007. Co-expression of two perivascular cell markers isolates mesenchymal stem-like cells from human endometrium. *Human Reproduction,* 22**,** 2903-2911.

SHAH, K. M., WEBBER, J., CARZANIGA, R., TAYLOR, D. M., FUSI, L., CLAYTON, A., BROSENS, J. J., HARTSHORNE, G. & CHRISTIAN, M. 2013. Induction of microRNA resistance and secretion in differentiating human endometrial stromal cells. *Journal of molecular cell biology,* 5**,** 67-70.

SHI, J., WU, X., SURMA, M., VEMULA, S., ZHANG, L., YANG, Y., KAPUR, R. & WEI, L. 2013. Distinct roles for ROCK1 and ROCK2 in the regulation of cell detachment. *Cell death & disease,* 4**,** e483-e483.

SHIOKAWA, S., YOSHIMURA, Y., NAGAMATSU, S., SAWA, H., HANASHI, H., KOYAMA, N., KATSUMATA, Y., NAGAI, A. & NAKAMURA, Y. 1996. Function of β, Integrins on Human Decidual Cells during Implantation. *Biology of Reproduction,* 54**,** 745-752.

SHUYA, L. L., MENKHORST, E. M., YAP, J., LI, P., LANE, N. & DIMITRIADIS, E. 2011. Leukemia Inhibitory Factor Enhances Endometrial Stromal Cell Decidualization in Humans and Mice. *PLOS ONE,* 6**,** e25288.

SIMÓN, C., GIMENO, M. A. J., MERCADER, A., O'CONNOR, J. E., REMOHÍ, J., POLAN, M. L. & PELLICER, A. 1997. Embryonic Regulation of Integrins β3,α 4, and α1 in Human Endometrial Epithelial Cells in Vitro1. *The Journal of Clinical Endocrinology & Metabolism,* 82**,** 2607-2616.

SIMÓN, C., MERCADER, A., GARCIA-VELASCO, J., NIKAS, G., MORENO, C., REMOHÍ, J. & PELLICER, A. 1999. Coculture of Human Embryos with Autologous Human Endometrial Epithelial Cells in Patients with Implantation Failure1. *The Journal of Clinical Endocrinology & Metabolism,* 84**,** 2638-2646.

SIMÓN, C., DOMINGUEZ, F., REMOHÍ, J. & PELLICER, A. 2001. Embryo Effects in Human Implantation. *Annals of the New York Academy of Sciences,* 943**,** 1-16.

SINGH, H. & APLIN, J. D. 2009. Adhesion molecules in endometrial epithelium: tissue integrity and embryo implantation. *Journal of anatomy,* 215**,** 3-13.

SIVASUBRAMANIYAN, K., HARICHANDAN, A., SCHUMANN, S., SOBIESIAK, M., LENGERKE, C., MAURER, A., KALBACHER, H. & BÜHRING, H.-J. 2013. Prospective Isolation of Mesenchymal Stem Cells from Human Bone Marrow Using Novel Antibodies Directed Against Sushi Domain Containing 2. *Stem Cells and Development,* 22**,** 1944-1954.

SKALHEGG, B. S. & TASKEN, K. 2000. Specificity in the cAMP/PKA signaling pathway. Differential expression,regulation, and subcellular localization of subunits of PKA. *Front Biosci,* 5**,** D678-93.

SKARDAL, A., SMITH, L., BHARADWAJ, S., ATALA, A., SOKER, S. & ZHANG, Y. 2012. Tissue specific synthetic ECM hydrogels for 3-D in vitro maintenance of hepatocyte function. *Biomaterials,* 33**,** 4565-4575.

SLAYDEN, O. D. & KEATOR, C. S. 2007. Role of progesterone in nonhuman primate implantation. *Semin Reprod Med,* 25**,** 418-30.

SONG, J. 1964. The Human Uterus: Morphogenesis and Embryological Basis for Cancer. Springfield Charles C. Thomas.

SPENCER, T. E., BARTOL, F. F., WILEY, A. A., COLEMAN, D. A. & WOLFE, D. F. 1993. Neonatal Porcine Endometrial Development Involves Coordinated Changes in DNA Synthesis, Glycosaminoglycan Distribution, and 3H-Glucosamine Labeling1. *Biology of Reproduction,* 48**,** 729-740.

SPENCER, T. E., DUNLAP, K. A. & FILANT, J. 2012. Comparative developmental biology of the uterus: insights into mechanisms and developmental disruption. *Mol Cell Endocrinol,* 354**,** 34-53.

SPENCER, T. E., JOHNSON, G. A., BURGHARDT, R. C. & BAZER, F. W. 2004. Progesterone and placental hormone actions on the uterus: insights from domestic animals. *Biol Reprod,* 71**,** 2-10.

STEWART, M. D., JOHNSON, G. A., GRAY, C. A., BURGHARDT, R. C., SCHULER, L. A., JOYCE, M. M., BAZER, F. W. & SPENCER, T. E. 2000. Prolactin Receptor and Uterine Milk Protein Expression in the Ovine Endometrium During the Estrous Cycle and Pregnancy1. *Biology of Reproduction,* 62**,** 1779-1789.

STRASSMANN, B. I. 1997. The Biology of Menstruation in Homo Sapiens: Total Lifetime Menses, Fecundity, and Nonsynchrony in a Natural-Fertility Population. *Current Anthropology,* 38**,** 123-129.

STRASSMANN, B. I. 1999. Menstrual synchrony pheromones: cause for doubt. *Human Reproduction,* 14**,** 579-580.

SUGAWARA, J., FUKAYA, T., MURAKAMI, T., YOSHIDA, H. & YAJIMA, A. 1997. Hepatocyte growth factor stimulated proliferation, migration, and lumen formation of human endometrial epithelial cells in vitro. *Biol Reprod,* 57**,** 936-42.

SUPEK, F., BOŠNJAK, M., ŠKUNCA, N. & ŠMUC, T. 2011. REVIGO summarizes and visualizes long lists of gene ontology terms. *PloS one,* 6**,** e21800-e21800.

SUZUKI, A., SEKIYA, S., GUNSHIMA, E., FUJII, S. & TANIGUCHI, H. 2010. EGF signaling activates proliferation and blocks apoptosis of mouse and human intestinal stem/progenitor cells in long-term monolayer cell culture. *Laboratory Investigation,* 90**,** 1425-1436.

TABANELLI, S., TANG, B. & GURPIDE, E. 1992. In vitro decidualization of human endometrial stromal cells. *The Journal of Steroid Biochemistry and Molecular Biology,* 42**,** 337-344.

TABIBZADEH, S. 1998. Molecular control of the implantation window. *Hum Reprod Update,* 4**,** 465-71.

TALMADGE, K., BOORSTEIN, W. R. & FIDDES, J. C. 1983. The Human Genome Contains Seven Genes for the β-Subunit of Chorionic Gonadotropin but Only One Gene for the β-Subunit of Luteinizing Hormone. *DNA,* 2**,** 281-289.

TAMPE, B. & ZEISBERG, M. 2013. Contribution of genetics and epigenetics to progression of kidney fibrosis. *Nephrology Dialysis Transplantation,* 29**,** iv72-iv79.

TAMURA, M., SEBASTIAN, S., YANG, S., GURATES, B., FANG, Z. & BULUN, S. E. 2002. Interleukin-1β Elevates Cyclooxygenase-2 Protein Level and Enzyme Activity via Increasing Its mRNA Stability in Human Endometrial Stromal Cells: An Effect Mediated by Extracellularly Regulated Kinases 1 and 2. *The Journal of Clinical Endocrinology & Metabolism,* 87**,** 3263-3273.

TANAKA, N., MIYAZAKI, K., TASHIRO, H., MIZUTANI, H. & OKAMURA, H. 1993. Changes in adenylyl cyclase activity in human endometrium during the menstrual cycle and in human decidua during pregnancy. *Reproduction,* 98**,** 33-39.

TEILMANN, S., CLEMENT, C., THORUP, J., BYSKOV, A. & CHRISTENSEN, S. 2006. Expression and localization of the progesterone receptor in mouse and human reproductive organs. *Journal of Endocrinology,* 191**,** 525-535.

TEKLENBURG, G., SALKER, M., HEIJNEN, C., MACKLON, N. S. & BROSENS, J. J. 2010a. The molecular basis of recurrent pregnancy loss: impaired natural embryo selection. *Mol Hum Reprod,* 16**,** 886-95.

TEKLENBURG, G., SALKER, M., MOLOKHIA, M., LAVERY, S., TREW, G., AOJANEPONG, T., MARDON, H. J., LOKUGAMAGE, A. U., RAI, R., LANDLES, C., ROELEN, B. A. J., QUENBY, S., KUIJK, E. W., KAVELAARS, A., HEIJNEN, C. J., REGAN, L., BROSENS, J. J. & MACKLON, N. S. 2010b. Natural Selection of Human Embryos: Decidualizing Endometrial Stromal Cells Serve as Sensors of Embryo Quality upon Implantation. *PLOS ONE,* 5**,** e10258.

TEKLENBURG, G., WEIMAR, C. H. E., FAUSER, B. C. J. M., MACKLON, N., GEIJSEN, N., HEIJNEN, C. J., CHUVA DE SOUSA LOPES, S. M. & KUIJK, E. W. 2012. Cell Lineage Specific Distribution of H3K27 Trimethylation Accumulation in an In Vitro Model for Human Implantation. *PLOS ONE,* 7**,** e32701.

TELGMANN, R. & GELLERSEN, B. 1998. Marker genes of decidualization: activation of the decidual prolactin gene. *Hum Reprod Update,* 4**,** 472-9.

TELLERIA, C. M., ZHONG, L., DEB, S., SRIVASTAVA, R. K., PARK, K. S., SUGINO, N., PARK-SARGE, O. K. & GIBORI, G. 1998. Differential expression of the estrogen receptors alpha and beta in the rat corpus luteum of pregnancy: regulation by prolactin and placental lactogens. *Endocrinology,* 139**,** 2432-42.

TERADA, L. S. 2006. Specificity in reactive oxidant signaling: think globally, act locally. *J Cell Biol,* 174**,** 615-23.

TEVES, M. E., ZHANG, Z., COSTANZO, R. M., HENDERSON, S. C., CORWIN, F. D., ZWEIT, J., SUNDARESAN, G., SUBLER, M., SALLOUM, F. N., RUBIN, B. K. & STRAUSS, J. F. 2013. Sperm-Associated Antigen–17 Gene Is Essential for Motile Cilia Function and Neonatal Survival. *American Journal of Respiratory Cell and Molecular Biology,* 48**,** 765-772.

TEWARY, S., LUCAS, E. S., FUJIHARA, R., KIMANI, P. K., POLANCO, A., BRIGHTON, P. J., MUTER, J., FISHWICK, K. J., DINIZ DA COSTA, M. J. M., EWINGTON, L. J., LACEY, L., TAKEDA, S., BROSENS, J. & QUENBY, S. 2019. Impact of Sitagliptin on Endometrial Mesenchymal Stem-Like Progenitor Cells: A Randomised, Double-Blind Placebo-Controlled Feasibility Trial. *reprints with The Lancet, SSRN*.

THE, E. G. G. O. R. P. L., BENDER ATIK, R., CHRISTIANSEN, O. B., ELSON, J., KOLTE, A. M., LEWIS, S., MIDDELDORP, S., NELEN, W., PERAMO, B., QUENBY, S., VERMEULEN, N. &

GODDIJN, M. 2018. ESHRE guideline: recurrent pregnancy loss. *Human Reproduction Open,* 2018.

THELLIN, O., ZORZI, W., LAKAYE, B., DE BORMAN, B., COUMANS, B., HENNEN, G., GRISAR, T., IGOUT, A. & HEINEN, E. 1999. Housekeeping genes as internal standards: use and limits. *J Biotechnol,* 75**,** 291-5.

THE GENE ONTOLOGY CONSORTIUM 2018. The Gene Ontology Resource: 20 years and still GOing strong. *Nucleic Acids Research,* 47**,** D330-D338.

THIET, M.-P., OSATHANONDH, R. & YEH, J. 1994. Localization and timing of appearance of insulin, insulin-like growth factor-I, and their receptors in the human fetal müllerian tract. *American Journal of Obstetrics and Gynecology,* 170**,** 152-156.

TIMPL, R. 1996. Macromolecular organization of basement membranes. *Current Opinion in Cell Biology,* 8**,** 618-624.

TOJO, M., HAMASHIMA, Y., HANYU, A., KAJIMOTO, T., SAITOH, M., MIYAZONO, K., NODE, M. & IMAMURA, T. 2005a. The ALK-5 inhibitor A-83-01 inhibits Smad signaling and epithelial-to-mesenchymal transition by transforming growth factor-beta. *Cancer Sci,* 96**,** 791-800.

TOJO, M., HAMASHIMA, Y., HANYU, A., KAJIMOTO, T., SAITOH, M., MIYAZONO, K., NODE, M. & IMAMURA, T. 2005b. The ALK-5 inhibitor A-83-01 inhibits Smad signaling and epithelial-to-mesenchymal transition by transforming growth factor-β. *Cancer Science,* 96**,** 791-800.

TOMASEK, J. J., GABBIANI, G., HINZ, B., CHAPONNIER, C. & BROWN, R. A. 2002. Myofibroblasts and mechano-regulation of connective tissue remodelling. *Nature Reviews Molecular Cell Biology,* 3**,** 349-363.

TOTSUKAWA, G., YAMAKITA, Y., YAMASHIRO, S., HARTSHORNE, D. J., SASAKI, Y. & MATSUMURA, F. 2000. Distinct roles of ROCK (Rho-kinase) and MLCK in spatial regulation of MLC phosphorylation for assembly of stress fibers and focal adhesions in 3T3 fibroblasts. *The Journal of cell biology,* 150**,** 797-806.

TSUNO, A., NASU, K., YUGE, A., MATSUMOTO, H., NISHIDA, M. & NARAHARA, H. 2009. Decidualization Attenuates the Contractility of Eutopic and Ectopic Endometrial Stromal Cells: Implications for Hormone Therapy of Endometriosis. *The Journal of Clinical Endocrinology & Metabolism,* 94**,** 2516-2523.

TURCO, M. Y., GARDNER, L., HUGHES, J., CINDROVA-DAVIES, T., GOMEZ, M. J., FARRELL, L., HOLLINSHEAD, M., MARSH, S. G. E., BROSENS, J. J., CRITCHLEY, H. O., SIMONS, B. D., HEMBERGER, M., KOO, B. K., MOFFETT, A. & BURTON, G. J. 2017. Long-term,

hormone-responsive organoid cultures of human endometrium in a chemically defined medium. *Nat Cell Biol,* 19**,** 568-577.

UCHIDA, H., MARUYAMA, T., ONO, M., OHTA, K., KAJITANI, T., MASUDA, H., NAGASHIMA, T., ARASE, T., ASADA, H. & YOSHIMURA, Y. 2007. Histone Deacetylase Inhibitors Stimulate Cell Migration in Human Endometrial Adenocarcinoma Cells through Up-Regulation of Glycodelin. *Endocrinology,* 148**,** 896-902.

UHLÉN, M., FAGERBERG, L., HALLSTRÖM, B. M., LINDSKOG, C., OKSVOLD, P., MARDINOGLU, A., SIVERTSSON, Å., KAMPF, C., SJÖSTEDT, E., ASPLUND, A., OLSSON, I., EDLUND, K., LUNDBERG, E., NAVANI, S., SZIGYARTO, C. A., ODEBERG, J., DJUREINOVIC, D., TAKANEN, J. O., HOBER, S., ALM, T., EDQVIST, P. H., BERLING, H., TEGEL, H., MULDER, J., ROCKBERG, J., NILSSON, P., SCHWENK, J. M., HAMSTEN, M., VON FEILITZEN, K., FORSBERG, M., PERSSON, L., JOHANSSON, F., ZWAHLEN, M., VON HEIJNE, G., NIELSEN, J. & PONTÉN, F. 2015. Proteomics. Tissue-based map of the human proteome. *Science,* 347**,** 1260419.

VALDES-DAPENA, M., NORRIS, H., HERTIG, A. & ABELL, M. 1973. The development of the uterus in late fetal life, infancy, and childhood, The Uterus. Baltimore Williams and Wilkins.

VAN DER MAATEN, L. & HINTON, G. 2008. Viualizing data using t-SNE. *Journal of Machine Learning Research,* 9**,** 2579-2605.

VAN DEURSEN, J. M. 2014. The role of senescent cells in ageing. *Nature,* 509**,** 439-446.

VAN MOURIK, M. S. M., MACKLON, N. S. & HEIJNEN, C. J. 2009. Embryonic implantation: cytokines, adhesion molecules, and immune cells in establishing an implantation environment. *Journal of Leukocyte Biology,* 85**,** 4-19.

VEGETO, E., SHAHBAZ, M. M., WEN, D. X., GOLDMAN, M. E., O'MALLEY, B. W. & MCDONNELL, D. P. 1993. Human progesterone receptor A form is a cell- and promoter-specific repressor of human progesterone receptor B function. *Molecular Endocrinology,* 7**,** 1244-1255.

VICENTE-MANZANARES, M., WEBB, D. J. & HORWITZ, A. R. 2005. Cell migration at a glance. *Journal of Cell Science,* 118**,** 4917.

VILELLA, F., RAMIREZ, L., BERLANGA, O., MARTINEZ, S., ALAMA, P., MESEGUER, M., PELLICER, A. & SIMON, C. 2013. PGE2 and PGF2alpha concentrations in human endometrial fluid as biomarkers for embryonic implantation. *J Clin Endocrinol Metab,* 98**,** 4123-32.

VOLLMER, G., SIEGAL, G. P., CHIQUET-EHRISMANN, R., LIGHTNER, V. A., ARNHOLDT, H. & KNUPPEN, R. 1990. Tenascin expression in the human endometrium and in endometrial adenocarcinomas. *Laboratory investigation; a journal of technical methods and pathology,* 62**,** 725-730.

VON ARNIM, A. G. & DENG, X.-W. 1994. Light inactivation of Arabidopsis photomorphogenic repressor COP1 involves a cell-specific regulation of its nucleocytoplasmic partitioning. *Cell,* 79**,** 1035-1045.

VON WOLFF, M., STROWITZKI, T., BECKER, V., ZEPF, C., TABIBZADEH, S. & THALER, C. J. 2001. Endometrial osteopontin, a ligand of beta3-integrin, is maximally expressed around the time of the "implantation window". *Fertil Steril,* 76**,** 775-81.

WANG, H., CRITCHLEY, H. O., KELLY, R. W., SHEN, D. & BAIRD, D. T. 1998. Progesterone receptor subtype B is differentially regulated in human endometrial stroma. *Mol Hum Reprod,* 4**,** 407-12.

WANG, H. & DEY, S. K. 2006. Roadmap to embryo implantation: clues from mouse models. *Nature Reviews Genetics,* 7**,** 185-199.

WANG, H., PILLA, F., ANDERSON, S., MARTÍNEZ-ESCRIBANO, S., HERRER, I., MORENO-MOYA, J. M., MUSTI, S., BOCCA, S., OEHNINGER, S. & HORCAJADAS, J. A. 2011. A novel model of human implantation: 3D endometrium-like culture system to study attachment of human trophoblast (Jar) cell spheroids. *Molecular Human Reproduction,* 18**,** 33-43.

WANG, H. S. & CHARD, T. 1999. IGFs and IGF-binding proteins in the regulation of human ovarian and endometrial function. *J Endocrinol,* 161**,** 1-13.

WATHEN, N. C., CAMPBELL, D. J., PATEL, B., TOUZEL, R. & CHARD, T. 1993. Dynamics of prolactin in amniotic fluid and extraembryonic coelomic fluid in early human pregnancy. *Early Human Development,* 35**,** 167-172.

WAY, D. L., GROSSO, D. S., DAVIS, J. R., SURWIT, E. A. & CHRISTIAN, C. D. 1983. Characterization of a new human endometrial carcinoma (RL95-2) established in tissue culture. *In Vitro,* 19**,** 147-158.

WEIDNER, K. M., SACHS, M. & BIRCHMEIER, W. 1993. The Met receptor tyrosine kinase transduces motility, proliferation, and morphogenic signals of scatter factor/hepatocyte growth factor in epithelial cells. *The Journal of Cell Biology,* 121**,** 145-154.

WEIMAR, C. H. E., KAVELAARS, A., BROSENS, J. J., GELLERSEN, B., DE VREEDEN-ELBERTSE, J. M. T., HEIJNEN, C. J. & MACKLON, N. S. 2012. Endometrial Stromal Cells of Women

with Recurrent Miscarriage Fail to Discriminate between High- and Low-Quality Human Embryos. *PLOS ONE,* 7**,** e41424.

WEIMAR, C. H. E., POST UITERWEER, E. D., TEKLENBURG, G., HEIJNEN, C. J. & MACKLON, N. S. 2013. In-vitro model systems for the study of human embryo–endometrium interactions. *Reproductive BioMedicine Online,* 27**,** 461-476.

WEISSMAN, I. L. 2000. Stem cells: units of development, units of regeneration, and units in evolution. *Cell,* 100**,** 157-68.

WERB, Z., SYMPSON, C. J., ALEXANDER, C. M., THOMASSET, N., LUND, L. R., MACAULEY, A., ASHKENAS, J. & BISSELL, M. J. 1996. Extracellular matrix remodeling and the regulation of epithelial-stromal interactions during differentiation and involution. *Kidney international. Supplement,* 54**,** S68-S74.

WEWER, U. M., DAMJANOV, A., WEISS, J., LIOTTA, L. A. & DAMJANOV, I. 1986. Mouse endometrial stromal cells produce basement-membrane components. *Differentiation,* 32**,** 49-58.

WEWER, U. M., FABER, M., LIOTTA, L. A. & ALBRECHTSEN, R. 1985. Immunochemical and ultrastructural assessment of the nature of the pericellular basement membrane of human decidual cells. *Laboratory investigation; a journal of technical methods and pathology,* 53**,** 624-633.

WOLF, M. T., DALY, K. A., BRENNAN-PIERCE, E. P., JOHNSON, S. A., CARRUTHERS, C. A., D'AMORE, A., NAGARKAR, S. P., VELANKAR, S. S. & BADYLAK, S. F. 2012. A hydrogel derived from decellularized dermal extracellular matrix. *Biomaterials,* 33**,** 7028-7038.

XIA, Y., NIVET, E., SANCHO-MARTINEZ, I., GALLEGOS, T., SUZUKI, K., OKAMURA, D., WU, M. Z., DUBOVA, I., ESTEBAN, C. R., MONTSERRAT, N., CAMPISTOL, J. M. & IZPISUA BELMONTE, J. C. 2013. Directed differentiation of human pluripotent cells to ureteric bud kidney progenitor-like cells. *Nat Cell Biol,* 15**,** 1507-15.

XINARIS, C., BENEDETTI, V., RIZZO, P., ABBATE, M., CORNA, D., AZZOLLINI, N., CONTI, S., UNBEKANDT, M., DAVIES, J. A., MORIGI, M., BENIGNI, A. & REMUZZI, G. 2012. In vivo maturation of functional renal organoids formed from embryonic cell suspensions. *J Am Soc Nephrol,* 23**,** 1857-68.

XIONG, S., SHARKEY, A. M., KENNEDY, P. R., GARDNER, L., FARRELL, L. E., CHAZARA, O., BAUER, J., HIBY, S. E., COLUCCI, F. & MOFFETT, A. 2013. Maternal uterine NK cell–activating receptor KIR2DS1 enhances placentation. *The Journal of Clinical Investigation,* 123**,** 4264-4272.

XU, C. & SU, Z. 2015. Identification of cell types from single-cell transcriptomes using a novel clustering method. *Bioinformatics,* 31**,** 1974-80.

YAHIA, L., CHIRANI, N., GRITSCH, L., MOTTA, F., CHIRANI , S. & FARE, S. 2015. History and Applications of Hydrogels. *J Biomedical Sci,* 4.

YAMAMOTO, K., SOKABE, T., WATABE, T., MIYAZONO, K., YAMASHITA, J. K., OBI, S., OHURA, N., MATSUSHITA, A., KAMIYA, A. & ANDO, J. 2005. Fluid shear stress induces differentiation of Flk-1-positive embryonic stem cells into vascular endothelial cells in vitro. *American Journal of Physiology-Heart and Circulatory Physiology,* 288**,** H1915-H1924.

YAMASAKI, M., MIYAKE, A., TAGASHIRA, S. & ITOH, N. 1996. Structure and Expression of the Rat mRNA Encoding a Novel Member of the Fibroblast Growth Factor Family. *Journal of Biological Chemistry,* 271**,** 15918-15921.

YELIAN, F. D., EDGEWORTH, N. A., DONG, L. J., CHUNG, A. E. & ARMANT, D. R. 1993. Recombinant entactin promotes mouse primary trophoblast cell adhesion and migration through the Arg-Gly-Asp (RGD) recognition sequence. *Journal of Cell Biology,* 121**,** 923-929.

YONEDA, A., MULTHAUPT, H. A. B. & COUCHMAN, J. R. 2005. The Rho kinases I and II regulate different aspects of myosin II activity. *The Journal of Cell Biology,* 170**,** 443.

YOSHINO, O., OSUGA, Y., HIROTA, Y., KOGA, K., YANO, T., TSUTSUMI, O. & TAKETANI, Y. 2003. Akt as a possible intracellular mediator for decidualization in human endometrial stromal cells. *Molecular Human Reproduction,* 9**,** 265-269.

YU, D., WONG, Y.-M., CHEONG, Y., XIA, E. & LI, T.-C. 2008. Asherman syndrome—one century later. *Fertility and Sterility,* 89**,** 759-779.

ZAFARULLAH, M., LI, W. Q., SYLVESTER, J. & AHMAD, M. 2003. Molecular mechanisms of N-acetylcysteine actions. *Cell Mol Life Sci,* 60**,** 6-20.

ZEISBERG, E. M. & ZEISBERG, M. 2013. The role of promoter hypermethylation in fibroblast activation and fibrogenesis. *The Journal of Pathology,* 229**,** 264-273.

ZHANG, B., KOROLJ, A., LAI, B. F. L. & RADISIC, M. 2018. Advances in organ-on-a-chip engineering. *Nature Reviews Materials,* 3**,** 257-278.

ZHANG, J. & SALAMONSEN, L. A. 1997. Tissue inhibitor of metalloproteinases (TIMP)-1, -2 and -3 in human endometrium during the menstrual cycle. *Molecular Human Reproduction,* 3**,** 735-741.

ZHOU, J., YANG, F., LEU, N. A. & WANG, P. J. 2012. MNS1 Is Essential for Spermiogenesis and Motile Ciliary Functions in Mice. *PLOS Genetics,* 8**,** e1002516.

ZHU, Y., TCHKONIA, T., PIRTSKHALAVA, T., GOWER, A. C., DING, H., GIORGADZE, N., PALMER, A. K., IKENO, Y., HUBBARD, G. B., LENBURG, M., O'HARA, S. P., LARUSSO, N. F., MILLER, J. D., ROOS, C. M., VERZOSA, G. C., LEBRASSEUR, N. K., WREN, J. D., FARR, J. N., KHOSLA, S., STOUT, M. B., MCGOWAN, S. J., FUHRMANN-STROISSNIGG, H., GURKAR, A. U., ZHAO, J., COLANGELO, D., DORRONSORO, A., LING, Y. Y., BARGHOUTHY, A. S., NAVARRO, D. C., SANO, T., ROBBINS, P. D., NIEDERNHOFER, L. J. & KIRKLAND, J. L. 2015. The Achilles' heel of senescent cells: from transcriptome to senolytic drugs. *Aging Cell,* 14**,** 644-58.

ZIMMERMANN, B. 1987. Lung organoid culture. *Differentiation,* 36**,** 86-109.